



Nouveaux hydrogels à liaison imine double préparés à partir d'O-carboxyméthyl chitosane et de Jeffamine par chimie covalente dynamique pour applications biomédicales

Rui Yu

► To cite this version:

Rui Yu. Nouveaux hydrogels à liaison imine double préparés à partir d'O-carboxyméthyl chitosane et de Jeffamine par chimie covalente dynamique pour applications biomédicales. Autre. Université Montpellier, 2021. Français. NNT : 2021MONT011 . tel-03346833

HAL Id: tel-03346833

<https://theses.hal.science/tel-03346833>

Submitted on 16 Sep 2021

HAL is a multi-disciplinary open access archive for the deposit and dissemination of scientific research documents, whether they are published or not. The documents may come from teaching and research institutions in France or abroad, or from public or private research centers.

L'archive ouverte pluridisciplinaire **HAL**, est destinée au dépôt et à la diffusion de documents scientifiques de niveau recherche, publiés ou non, émanant des établissements d'enseignement et de recherche français ou étrangers, des laboratoires publics ou privés.

THÈSE

Pour obtenir le grade de
Docteur

Délivré par **Université de Montpellier**

Préparée au sein de l'**Ecole Doctorale Sciences Chimiques Balard**
ED 459

Et de l'unité de recherche **Institut Européen des Membranes**
(UMR 5635)

Spécialité : **Chimie et Physicochimie des Matériaux**

Présentée par **Rui YU**

**Nouveaux hydrogels à liaison imine double préparés à partir
d'O-carboxyméthyl chitosane et de Jeffamine
par chimie covalente dynamique pour applications biomédicales**

**Novel dual imine bonding hydrogels prepared from
O-carboxymethyl chitosan and Jeffamine
by dynamic covalent chemistry for biomedical applications**

Soutenue le 26 mars, 2021 devant le jury composé de

M. DELAIR Thierry, Professeur, Université Lyon 1	Rapporteur
M. SCHATZ Christophe, MCU, Bordeaux INP	Rapporteur
Mme. MINGOTAUD Anne-Françoise, CR CNRS, IMRCP, UMR 5623	Examinatrice
Mme. NOËL Danièle, DR INSERM, IRMB, U 1183	Présidente
M. BARBOIU Mihail, DR CNRS, IEM, UMR 5635	Co-directeur de thèse
M. LI Suming, DR CNRS, IEM, UMR 5635	Directeur de thèse

Résumé	I
Abstract	VII
List of Tables	XIII
List of Schemes	XV
List of Figures	XVII
List of Figures Supplementary	XXIII
List of Abbreviations	XXV
Chapter 1 Introduction	1
1.1 Hydrogels	1
1.1.1 Physical hydrogels.....	2
1.1.1.1 Physical hydrogels by hydrogen bonds.....	2
1.1.1.2 Physical hydrogels by crystallization cross-linking	3
1.1.1.3 Physical hydrogels by stereo-complexation	4
1.1.1.4 Physical hydrogels by electrostatic interactions	4
1.1.1.5 Physical hydrogels by ionic cross-linking	5
1.1.1.6 Physical hydrogels by hydrophobic association	6
1.1.2 Chemical hydrogels	6
1.1.2.1 Chemical hydrogels by grafting.....	7
1.1.2.2 Chemical hydrogels by radical polymerization	7
1.1.2.3 Chemical hydrogels by condensation reaction.....	8
1.1.2.4 Chemical hydrogels by enzymatic reaction	8
1.1.2.5 Chemical hydrogels by high-energy radiation	10
1.2 Dynamic hydrogels	10
1.2.1 Dynamic hydrogels linked by boronate ester.....	11
1.2.2 Dynamic hydrogels linked by acylhydrazone bonds	11

1.2.3	Dynamic hydrogels linked by disulfide bonds	13
1.2.4	Dynamic hydrogels synthesized by Diels-Alder (DA) reaction..	14
1.2.5	Dynamic hydrogels linked by imine bonds.....	15
1.3	Raw materials for preparation of hydrogels	21
1.3.1	Natural polymers	21
1.3.1.1	Alginate.....	21
1.3.1.2	Dextran	22
1.3.1.3	Cellulose	23
1.3.1.4	Hyaluronic acid	24
1.3.1.5	Gelatin	25
1.3.1.6	Chitosan.....	26
1.3.2	Synthetic polymers	29
1.3.2.1	Poly(vinyl alcohol) (PVA).....	30
1.3.2.2	Poly(N-isopropylacrylamide) (PNIPAAm).....	31
1.3.2.3	Poly(ethylene glycol) (PEG).....	31
1.3.2.4	Jeffamine	33
1.4	Biomedical applications of hydrogels.....	34
1.4.1	Cartilage engineering	34
1.4.2	Drug delivery	36
1.4.2.1	Hydrogel drug delivery systems.....	37
1.4.2.2	Anti-cancer drugs.....	39
1.5	Summary and work plan	40
	References.....	42

Chapter 2	Biobased pH-responsive and self-healing hydrogels prepared from O-carboxymethyl chitosan and a 3-dimensional dynamer as cartilage engineering scaffold	65
2.1	Introduction.....	65

2.2	Experimental section	68
2.2.1	Materials.....	68
2.2.2	Synthesis of dynamer Dy.....	68
2.2.3	Preparation of CMCS-Dy hydrogels	68
2.2.4	Characterization	69
2.2.5	Structural stability of Dy.....	69
2.2.6	Rheology	69
2.2.7	Swelling	70
2.2.8	Self-healing experiments	70
2.2.9	Cell cultures and cytotoxicity	71
2.3	Results and discussion	71
2.3.1	Synthesis of dynamer	71
2.3.2	Synthesis of CMCS-Dy hydrogels	74
2.3.3	Rheological studies	76
2.3.4	Morphology and swelling studies.....	78
2.3.5	Self-healing	83
2.3.6	Cytocompatibility of hydrogels.....	86
2.4	Conclusions	87
	Supporting information	88
	References	92

Chapter 3 Anti-bacterial dynamic hydrogels prepared from O-carboxymethyl chitosan by dual imine bond crosslinking for biomedical applications97

3.1	Introduction.....	98
3.2	Experimental section	100
3.2.1	Materials.....	100
3.2.2	Synthesis of dynamers Dy500, Dy800 and Dy1900	101

3.2.3	Synthesis of hydrogels	101
3.2.4	Preparation of H1900 membranes.....	102
3.2.5	Characterization	102
3.2.6	Swelling of freeze-dried gels	103
3.2.7	Self-healing properties of hydrogels	103
3.2.8	Antibacterial activity of membranes	104
3.2.8.1	Bacterium and preparation of the bacterial suspension	104
3.2.8.2	Antibacterial tests.....	104
3.2.8.3	Counting of viable cells	105
3.3	Results and discussion	106
3.3.1	Preparation of hydrogels	106
3.3.2	FT-IR	109
3.3.3	Rheology	110
3.3.4	Morphology and swelling performance	111
3.3.5	Self-healing	115
3.3.6	<i>In vitro</i> antibacterial assay	116
3.4	Conclusions	120
	Supporting information	121
	References	121

Chapter 4 Biobased dynamic hydrogels by reversible imine bonding for controlled release of thymopentin.....127

4.1	Introduction.....	128
4.2	Experimental section	131
4.2.1	Materials.....	131
4.2.2	Synthesis of dynamer	131
4.2.3	Depolymerization of CMCS	131
4.2.4	Preparation of dynamic hydrogels	132

4.2.5	Preparation of TP5 loaded hydrogels	132
4.2.6	Characterization	133
4.2.7	Swelling of freeze-dried hydrogels.....	133
4.2.8	<i>In-vitro</i> release of TP5	134
4.2.9	The release kinetics model.....	135
4.2.10	Density functional theory (DFT) computation	135
4.3	Results and discussion.....	136
4.3.1	Preparation of hydrogels	136
4.3.2	FT-IR and NMR	138
4.3.3	Rheology	140
4.3.4	Morphology and swelling.....	143
4.3.5	<i>In vitro</i> release of the TP5	146
4.3.6	Drug release kinetics	150
4.3.7	Density functional theory (DFT) insights.....	151
4.4	Conclusion.....	155
	Supporting materials	156
	References.....	161
	Conclusion	169
	Publications	173
	Communications.....	175
	Acknowledgements	177

Résumé

Les liaisons covalentes dynamiques (LCD) dans les réseaux polymères peuvent s'associer et se dissocier dans des conditions destructives, et ainsi donner lieu à des matériaux « récupérateurs » aux propriétés inchangées / stables. En général, les LCD sont statiques dans les conditions ambiantes, mais dynamiques sous l'effet des déclencheurs (par exemple, la lumière, la température et le pH). Par conséquent, les matériaux polymères reliés par des LCD sont à la fois robustes et adaptatifs. La liaison imine est l'une des LCD les plus fréquemment utilisées dans la construction de matériaux dynamiques en raison des caractéristiques intrinsèques de « relecture » et de « vérification d'erreurs » associées à ces liaisons réversibles. Généralement, la formation d'une liaison imine se produit entre une amine et un aldéhyde, une réaction réversible qui se déroule sous contrôle thermodynamique.

O-carboxyméthyl chitosane (O-CMCS) est un dérivé hydrosoluble du chitosane (CS), le deuxième biopolymère le plus abondant dans la nature. Le CMCS présente une très bonne biocompatibilité, une bonne activité antibactérienne et une excellente biodégradabilité. Il est une matière première de choix pour la construction d'hydrogels par des LCD capables d'encapsuler des principes actifs, des facteurs de croissance et des cellules à des fins d'ingénierie du cartilage ou de délivrance de principes actifs. La réticulation de CS ou de CMCS avec différents aldéhydes par réaction de base de Schiff a été rapportée dans la littérature pour préparer des hydrogels dynamiques, y compris des monoaldéhydes, des dialdéhydes et des dérivés d'aldéhydes. Néanmoins, les hydrogels résultants présentent certains inconvénients tels qu'un faible taux de gonflement, une procédure de préparation fastidieuse, une micro-structure désordonnée, etc.

Jeffamine ED est une série de polyétheramines biocompatibles constituées de

blocs poly(oxyde de propylène) (POP) hydrophobes et de blocs poly(oxyde d'éthylène) (POE) hydrophiles terminés par deux groupements amine primaires. Les trois membres de la série Jeffamine ED, à savoir Jeffamine ED600, Jeffamine ED900 et Jeffamine ED2003 ont un rapport molaire POP/POE de 3,6/9, 6/12,5 et 6/39, respectivement. Ils sont solubles dans l'eau en raison de la présence d'un segment POE prédominant, et peuvent donc être utilisés comme composant hydrophile pour la fabrication de matériaux hydrophiles ou amphiphiles. Le benzène-1,3,5-tricarbaldéhyde (BTA) est un agent de réticulation prometteur pour la formulation d'hydrogels dynamiques basés sur la liaison imine car il peut agir comme un centre tri-fonctionnel pour la réticulation tridimensionnelle avec des polymères comportant des groupements amine. Comme le BTA est insoluble dans l'eau, une réaction de base de Schiff de BTA avec une Jeffamine ED est effectuée pour produire un dynamère 3D hydrosoluble qui peut être utilisé pour synthétiser des hydrogels dynamiques par une réaction similaire de Base de Schiff avec le CMCS.

Dans ce travail, une série d'hydrogels dynamiques basés sur la double liaison imine entre CMCS et Jeffamine avec BTA a été synthétisée. L'effet du rapport molaire du CMCS/Dy, de la masse molaire de la Jeffamine et de la masse molaire du CMCS sur les propriétés physico-chimiques des hydrogels dynamiques résultants a été étudié. Les divers hydrogels peuvent servir de matrice pour l'encapsulation cellulaire, de membrane antibactérienne et de support de principes actifs hydrophiles. Les propriétés de gonflement sensibles au pH, les performances d'auto-guérison, les propriétés rhéologiques, la cytocompatibilité, l'activité antibactérienne, l'immobilisation et la libération de principes actifs des hydrogels ont été étudiées en détail et discutées en comparaison avec la littérature. Le contenu principal de la thèse est présenté ci-dessous:

- a) Une série d'hydrogels dynamiques à base d'O-CMCS (Gel1-1, Gel2-1, Gel4-1, Gel6-1 et Gel8-1) avec différents rapports molaires D-

glucosamine/dynamer (1/1, 2/1, 4/1, 6/1, et 8/1) a été synthétisée via réaction de base de Schiff à 37 °C. Typiquement, un dynamère (Dy) a d'abord été préparé par réaction de base de Schiff entre BTA et Jeffamine dans du méthanol dans des conditions de reflux à 70 °C. Après évaporation du méthanol, de l'eau Milli-Q a été ajoutée pour donner une solution aqueuse de Dy. Par la suite, des hydrogels dynamiques ont été préparés par réaction de Base de Schiff en mélangeant des solutions aqueuses de CMCS et de Dy à 37 °C pendant 24 h.

Ces hydrogels résultants et leurs précurseurs ont été caractérisés en utilisant diverses techniques analytiques, y compris la spectroscopie infrarouge à transformée de Fourier (FT-IR), la résonance magnétique nucléaire (RMN) du proton, la microscopie électronique à balayage (MEB) et des mesures rhéologiques. L'analyse RMN a montré que le dynamère est stable en milieu neutre et légèrement acide ($> \text{pH } 3$), mais est rapidement hydrolysé en milieu fortement acide ($\text{pH} = 1$). L'hydrogel Gel4-1 présente le temps de gélification le plus court et le module de conservation le plus élevé, en accord avec une réticulation ou une formation de liaison imine optimale. Les gels lyophilisés présentent des structures poreuses interconnectées et un comportement de gonflement dépendant du pH. Le taux de gonflement est relativement faible à pH acide en raison de l'attraction électrostatique, et devient très élevé, jusqu'à 7000% à pH 8 en raison de la répulsion électrostatique. Une perte de masse est observée après gonflement des hydrogels, résultant de la diffusion et la dissolution des espèces non réticulées. De plus, les hydrogels présentent des propriétés d'auto-guérison exceptionnelles, comme en témoignent la fermeture des pièces fendues et les études rhéologiques en appliquant alternativement des déformations de cisaillement oscillatoires élevées et faibles.

Des cellules stromales mésenchymateuses humaines (MSC) isolées du

tissu adipeux sous-cutané ou de la moelle osseuse ont été encapsulées dans Gel4-1 (1×10^6 cellules/mL) et cultivées jusqu'à 7 jours en milieu de prolifération à 37 °C pour évaluer la cytocompatibilité. Les deux types de cellules ont survécu pendant au moins 7 jours avec seulement 1 et 4% de cellules mortes quantifiées pour les deux types de MSC, respectivement, démontrant l'excellente cytocompatibilité de l'hydrogel dynamique. De plus, la reconstruction 3D montre clairement une distribution homogène des MSC dans tout le volume d'hydrogel, indiquant que le temps de gélification est bien compatible avec une distribution homogène des cellules sans sédimentation.

- b) Dans la deuxième partie, trois hydrogels dynamiques à base d'O-CMCS (H500, H800 et H1900) avec différentes masses molaires de Jeffamine ($M_n = 500, 800$ et 1900) ont été préparés par réaction de base de Schiff à 37 °C. Trois dynamères, à savoir Dy500, Dy800 et Dy1900 ont d'abord été préparés par réaction de base de Schiff entre BTA et Jeffamine. Ensuite, des hydrogels dynamiques ont été préparés à partir de solutions aqueuses de CMCS et de Dy dans les mêmes conditions mentionnées ci-dessus. Les hydrogels obtenus et leurs précurseurs ont été caractérisés par la FT-IR, la RMN, la MEB et des mesures rhéologiques. Les spectres FT-IR confirment la formation d'hydrogels par liaison imine. Le temps de gélification augmente avec la masse molaire de Jeffamine parce que une faible masse molaire signifie une mobilité plus élevée, ce qui favorise la réticulation. Le module de conservation des hydrogels augmente également avec l'augmentation de la masse molaire de la Jeffamine. Les images MEB montrent que H1900 présente une plus grande taille de pore par rapport à H500 et H800 en raison de la masse molaire plus élevée du réticulant Jeffamine. Un comportement de gonflement similaire est observé pour les trois hydrogels avec différentes Jeffamines dans la zone de pH de 3 à 10, c'est-à-dire un faible gonflement en milieu acide, un gonflement

relativement élevé en milieu neutre, et un gonflement extrêmement élevé en milieu alcalin. La perte de masse montre que H1900 présente la perte de masse la plus élevée dans toute la gamme de pH en raison de la masse molaire plus élevée de Jeffamine ED2003. Un comportement d'auto-guérison similaire a été observé pour tous les hydrogels.

Les membranes ont été préparées à partir d'hydrogel H1900. Les propriétés antibactériennes des membranes H1900 exposées uniquement à un traitement thermique (H1900^a) et à un traitement thermique suivi d'une exposition aux UVc (H1900^b) ont été évaluées par le test liquide et le test agar mou. Environ 97% et 100% des bactéries ont été éliminées par H1900^a et H1900^b, respectivement. Des tests sur agar mou ont confirmé les excellentes propriétés antibactériennes contre *E. coli* (bactérie à Gram négatif), en particulier dans le cas du H1900^b car aucune colonie ne s'est développée sur la membrane.

- c) Dans la troisième partie, trois hydrogels dynamiques, à savoir Gel80K, Gel30K et Gel25K ont été préparés à partir de CMCS de différentes masses molaires ($M_n = 80K, 30K$ et $25K$) via une réaction de base de Schiff dans des conditions similaires mentionnées ci-dessus. Les oligomères de CMCS ($M_n = 30K$ et $25K$) ont été obtenus par dépolymérisation du CMCS d'origine ($M_n = 80K$) pendant 30 et 60 minutes en présence de H_2O_2 . La thymopentine (TP5), un immunostimulant hydrophile, a été encapsulée dans des hydrogels dynamiques pour former une série d'hydrogels chargés de TP5, à savoir Gel80k-TP5-X, Gel30k-TP5-X et Gel25k-TP5-X avec X représentant la concentration de la TP5.

Les hydrogels seuls (Gel80K, Gel30K et Gel25K) et les hydrogels chargés de TP5 (Gel80K-TP5, Gel30K-TP5 et Gel25K-TP5) ont été analysés par la FT-IR, la RMN, la MEB et des mesures rhéologiques. Divers facteurs, y compris la masse molaire du CMCS, les conditions d'encapsulation et la teneur en TP5, ont été pris en compte pour déterminer leurs effets sur les

propriétés de l'hydrogel et les comportements de libération de TP5. Les caractéristiques structurales, rhéologiques, morphologiques et de gonflement des hydrogels ont été étudiées. Tous les hydrogels présentent une architecture poreuse régulière et interpénétrante, et un gonflement extraordinaire sensible au pH qui peut atteindre plus de 10 000% à pH 8. La nature dynamique des liaisons imine confère aux hydrogels une bonne stabilité rhéologique dans la zone de déformation de 0,1 à 20% ou la zone de fréquence de 0,1 à 50 Hz. L'encapsulation de TP5 affecte les propriétés rhéologiques des hydrogels car TP5 est partiellement attaché au réseau via des liaisons imine entre les groupements amine de TP5 et les groupements aldéhyde du dynamère.

La libération in vitro de TP5 a été réalisée dans un milieu salin tamponné au phosphate à 37 °C. Dans tous les cas, une libération rapide est observée dans les premières heures, suivie d'une libération plus lente pour atteindre un plateau. Une teneur en TP5 plus élevée conduit à des taux de libération initiale et finale plus élevés. La TP5 n'est pas totalement libérée en raison de son attachement au réseau d'hydrogel via des liaisons imine. Une libération plus rapide est observée à pH 5,5 qu'à pH 7,4 en raison de la stabilité plus faible des liaisons imine dans les milieux acides. L'ajustement des données de libération à l'aide du modèle Higuchi montre que la libération initiale de la TP5 est essentiellement contrôlée par la diffusion. La théorie fonctionnelle de la densité a été appliquée pour confirmer théoriquement les connexions chimiques entre TP5 et CMCS avec Dy. Toutes ces découvertes prouvent que les hydrogels dynamiques à base de CMCS sont des vecteurs prometteurs pour l'administration contrôlée de principes actifs hydrophiles, ainsi jettent une nouvelle base sur la conception de systèmes de libération de principes actifs à la fois par mélange physique et par liaison covalente réversible.

Abstract

Dynamic covalent bonds (DCBs) in polymeric networks can disassociate and associate under destructive conditions, and thus result in recuperative materials with unchanged/stable properties. In general, DCBs are static at ambient conditions, while dynamic under triggers (e.g., light, temperature, and pH). Consequently, polymeric materials connected by DCBs are both robust and adaptive. Imine bond is one of the most frequently used DCBs in the construction of dynamic materials owing to the intrinsic 'proof-reading' and 'error-checking' characteristics associated with these reversible bonds. Generally, the formation of an imine bond occurs between an amine and an aldehyde, which is a reversible reaction which proceeds under thermodynamic control.

O-carboxymethyl chitosan (O-CMCS) a water-soluble derivative of chitosan (CS), the second most abundant biopolymer in nature. CMCS presents outstanding biocompatibility, antibacterial activity and biodegradability, and thus is a raw material of choice for the construction of hydrogels by DCBs which are able to encapsulate drugs, growth factors, and cells for cartilage engineering or drug delivery purposes. Crosslinking of CS or CMCS with different aldehydes by Schiff-base reaction has been reported to prepare hydrogels, including monoaldehydes, dialdehydes, and derivatives of aldehydes. Nevertheless, the resulting hydrogels present some disadvantages such as low swelling ratio, tedious preparation procedure, disordered micro-structure, etc. Jeffamine ED series are biocompatible polyetheramines consisting of hydrophobic poly(propylene oxide) (PPO) and hydrophilic poly(ethylene oxide) (PEO) blocks terminated with two primary amino groups. The three members of the Jeffamine ED series, namely Jeffamine ED600, Jeffamine ED900, and Jeffamine ED2003 have a PPO/PEO molar ratio of 3.6/9, 6/12.5, and 6/39, respectively. They are water soluble because of the presence of a predominant PEG backbone, and

thus can be used as a hydrophilic component for manufacturing hydrophilic or amphiphilic materials. Benzene-1,3,5-tricarbaldehyde (BTA) is a promising crosslinker for the formulation of dynamic hydrogels based on imine bonding as it can act as a tri-topic center for three-dimensional crosslinking with di-amino polymers. As BTA is insoluble in water, Schiff-base reaction of BTA with Jeffamine ED is performed to produce a water-soluble 3D dynamer which can be further used to synthesize dynamic hydrogels by similar Schiff-base reaction with CMCS.

In this work, a series of dynamic hydrogels based on dual imine bonding between CMCS and Jeffamine with BTA were synthesized. The effect of molar ratio of CMCS/Dy, Jeffamine molar mass, and CMCS molar mass on the physico-chemical properties of resulting dynamic hydrogels was investigated. The various hydrogels can serve as scaffold for cell encapsulation, antibacterial membrane, and carrier of hydrophilic drugs. The pH sensitive swelling properties, self-healing performance, rheological properties, cytocompatibility, antibacterial activity, drug immobilizing and drug release behaviors of hydrogels were studied in detail and discussed in comparison with literature. The main contents of thesis are shown in the following:

- a) A series of O-CMCS based dynamic hydrogels (Gel1-1, Gel2-1, Gel4-1, Gel6-1, and Gel8-1) with various D-glucosamine to dynamer molar ratios (1/1, 2/1, 4/1, 6/1, 8/1) were synthesized via Schiff-base reaction at 37 °C. Typically, a 3D dynamer (Dy) was first prepared through Schiff-base reaction between BTA and Jeffamine in methanol under reflux conditions at 70 °C. After evaporation of methanol, Milli-Q water was added to yield an aqueous solution of Dy. Subsequently, dynamic hydrogels were prepared by Schiff-base reaction via mixing CMCS and Dy aqueous solutions at 37 °C for 24 h. These resultant hydrogels and precursors were characterized by using various analytical techniques, including FT-IR, ¹H NMR, SEM, and rheological measurements. NMR analysis showed that the

as-prepared dynamer is stable in neutral and slightly acidic media ($> \text{pH } 3$), but is rapidly hydrolyzed in strongly acidic medium ($\text{pH} = 1$). The hydrogel Gel4-1 exhibits the shortest gelation time and the highest storage modulus, in agreement with optimal crosslinking or imine bond formation. Freeze-dried gels exhibit interconnected porous structures and pH-dependent swelling behavior. The swelling ratio is relatively low at acidic pH 3-5 due to electrostatic attraction, and becomes very high, up to 7000 % at pH 8 due to electrostatic repulsion. Mass loss is observed after swelling of hydrogels, resulting from the diffusion and washing away of non-crosslinked species. Moreover, hydrogels present outstanding self-healing properties as evidenced by closure of split pieces and rheological studies by alternatively applying high and low oscillatory shear strains. Last but not least, human mesenchymal stromal cells (MSCs) encapsulated in hydrogels are all alive after 7 days, in agreement with the excellent cytocompatibility of hydrogels.

- b) In the second part, three O-CMCS based dynamic hydrogels (H500, H800, and H1900) with different molar masses of Jeffamine ($M_n = 500, 800, \text{ and } 1900$) were prepared by Schiff-base reaction at 37°C . Three dynamers, namely Dy500, Dy800, and Dy1900 were first prepared by Schiff-base reaction between BTA and Jeffamine. Subsequently, dynamic hydrogels were prepared from CMCS and Dy aqueous solutions under the same conditions mentioned above. The obtained hydrogels precursors were characterized by FT-IR, NMR, SEM, and rheological measurements. FT-IR spectra confirm the formation of hydrogels via imine bonding. The gelation time increases with the molar mass of Jeffamine because low molar mass has higher mobility which favors crosslinking. The storage modulus of hydrogels also increases with the increase of Jeffamine molar mass. SEM images show that H1900 presents larger pore size as compared to H500 and H800 due to the higher molar mass of Jeffamine linker. Similar swelling behavior is observed for the three hydrogels with different Jeffamines in the

pH range of 3-10, i.e., low swelling in acidic media, relatively high swelling in neutral medium and extremely high swelling in alkaline medium. Mass loss show that H1900 exhibits the highest mass loss in the whole pH range due to the higher molar mass of Jeffamine ED2003. Similar self-healing behavior was observed for all the hydrogels.

Membranes were prepared from H1900 hydrogel. The antibacterial properties of H1900 membranes exposed to thermal treatment only (H1900^a) and to thermal treatment followed by UVc exposure (H1900^b) were evaluated by liquid and agar tests. Nearly 97% and 100% of bacteria were removed by H1900^a and H1900^b, respectively. Soft agar tests confirmed the excellent antibacterial properties against *E. coli* (Gram-negative bacterium), especially in the case of the H1900^b as no colonies grew onto the membrane.

- c) In the third part, three dynamic hydrogels, namely Gel80k, Gel30k, and Gel25k were prepared from CMCS with different molar masses ($M_n = 80K$, 30K, and 25K) via Schiff-base reaction under similar conditions mentioned above. CMCS oligomers ($M_n = 30K$, and 25K) were obtained by depolymerization of original CMCS ($M_n = 80K$) for 30 and 60 min in the presence of H_2O_2 . Thymopentin (TP5), a hydrophilic immunostimulant, was loaded in dynamic hydrogels to yield a series of drug loaded hydrogels, namely Gel80k-TP5-X, Gel30k-TP5-X, and Gel25k-TP5-X with X representing the drug concentration. Blank hydrogels (Gel80k, Gel30k, and Gel25k) and TP5-loaded hydrogels (Gel80k-TP5, Gel30k-TP5, and Gel25k-TP5) were analyzed by FT-IR, NMR, SEM, and rheological measurements. Various factors, including the molar mass of CMCS, drug loading conditions, and drug content, were considered to figure out their effects on hydrogel properties and drug release behaviors. The structural, rheological, morphological and swelling characteristics of the hydrogels were investigated. All hydrogels showed regular and interpenetrating porous

architecture, and extraordinary pH-sensitive swelling which could reach over 10,000 % at pH 8. The dynamic nature of imine bonds endows hydrogels with good rheological stability in the strain range from 0.1-20 % or in the frequency change from 0.1 to 50 Hz. Importantly, TP5 encapsulation affects the rheological properties of hydrogels as TP5 is partially attached to the network via imine bonding between the amino groups of TP5 and aldehyde groups of the dynamer. *In vitro* release of TP5 was performed in phosphate buffered saline at 37 °C. In all cases, an initial burst is observed, followed by slower release to reach a plateau. Higher TP5 loading content led to higher initial and final release rates. TP5 was not totally released because of attachment to the hydrogel network via imine bonding. Faster release is observed at pH 5.5 than at pH 7.4 due to lower stability of imine bonds in acidic media. Fitting of release data by using Higuchi model showed that the initial TP5 release is essentially diffusion controlled. Density functional theory (DFT) computation was applied to theoretically confirm the chemical connections between TP5 and CMCS with Dy. All these findings proved that CMCS based dynamic hydrogels are promising carriers for controlled delivery of hydrophilic drugs, and shed new light on the design of drug release systems by both physical mixing and reversible covalent bonding

List of Tables

Table 2.1 Molar and mass composition of CMCS-Dy hydrogels ^{a)}	75
Table 3.1 Molar and mass compositions of dynamic hydrogels ^{a)}	108
Table 3.2 Antibacterial activity of H1900 membrane (entry 1-5: liquid test; entries 6-9: soft agar tests)	118
Table 4.1 Molar and mass compositions of blank and TP5 loaded hydrogels ^{a)}	137
Table 4.2 Parameters obtained from fitting of experimental data using Higuchi model ^{a)}	151

List of Schemes

Scheme 2.1 Synthesis route of CMCS-based dynamic hydrogel: a) chemical structures of BTA, CMCS and Jeffamine; b) synthesis of the dynamer Dy by reaction of equimolar BTA and Jeffamine, and synthesis of hydrogel by imine formation between Dy and CMCS; c) images of as prepared hydrogel and freeze-dried hydrogel; and d) SEM images of freeze-dried hydrogel.	72
Scheme 3.1 Synthesis route of dynamic hydrogel by imine bond formation between CMCS and a dynamer obtained from BTA and Jeffamine.	106
Scheme 4.1 Synthesis of dynamic hydrogels via Schiff-base reaction between CMCS and Dy, and in-situ loading of TP5 in hydrogels.	136

List of Figures

Figure 1.1 Double H-bonding network of physical hydrogels [10].	3
Figure 1.2 Mechanism of ion-chain binding in ionically cross-linked alginate hydrogels [39].	5
Figure 1.3 Schematic illustration of synthesis of cellulose-based hydrogels by radical polymerization [50].	7
Figure 1.4 Synthesis of MF-PEG via the Ugi reaction, PEG-acid: amine: aldehyde: isocyanide = 1:6:6:10, methanol, 45 °C, 12 h [53].	8
Figure 1.5 (A) Synthesis of CMC-DA hydrogels by enzymatic crosslinking in the present of HRP and H ₂ O ₂ . (B) Photographs of the CMC-DA solution before and after gelation [55].	9
Figure 1.6 Representation of (a) a model and (b) a randomly crosslinked dynamic covalent polymer network crosslinked via acylhydrazone bonds [66].	12
Figure 1.7 Mechanism of the photoinduced radical disulfide exchange [70].	13
Figure 1.8 Diels-Alder and retro-Diels-Alder reactions [79].	14
Figure 1.9 Three types of imine reactions (a) imine condensation, (b) exchange, and (c) metathesis [84].	16
Figure 1.10 Schematic representation of water-disintegration, self-healing and biodegradation processes of a green dynamer [86].	16
Figure 1.11 Synthesis of DF-PEGs and their coupling with chitosan to form dynamic hydrogels.	17
Figure 1.12 Schematic illustration of forming the dynamic covalent network based on imine bonds [85].	18
Figure 1.13 Synthesis scheme of the CEC-I-OSA-I-ADH hydrogels. a) Photographs before and after gelation of CEC-I-OSA-I-ADH hydrogel (R = 0.5) in PBS (pH 7.0). b) Schematic presentation and chemical structures of the CEC-I-OSA-I-ADH hydrogel obtained by condensation reaction of the aldehyde	

groups (from OSA) with the amino groups (from CEC) and hydrazides (from ADH), resulting in dynamic imine and acylhydrazone bonds, respectively [88].	19
Figure 1.14 Schematic illustration of a DDN hydrogel with imine and borate ester linkages [89].	20
Figure 1.15 Chemical structure of G-block, M-block, and alternating block in alginate [104].	22
Figure 1.16 Part of the α -(1 6)-linked glucose main chain of dextran with branching points in 2-, 3- and 4-positions [110].	23
Figure 1.17 Chemical structure of native cellulose.	24
Figure 1.18 Chemical structure of hyaluronic acid (HA) [123].	25
Figure 1.19 Representation of gelatin chemical structure [129].	25
Figure 1.20 Preparation of chitosan by deacetylation of chitin [130].	26
Figure 1.21 Chemical structure of chitosan [130].	26
Figure 1.22 Synthetic routes of chitosan derivatives containing alkyl, aminoalkyl, aromatic, carboxyalkyl, and guanidiny l Groups [130].	27
Figure 1.23 Carboxymethylation and carboxyethylation of chitosan [135].	28
Figure 1.24 Conventional synthesis route of poly(vinyl alcohol) (PVA) [145].	30
Figure 1.25 Chemical structure of PEG and its derivatives [160].	32
Figure 1.26 Chemical structure of Jeffamine ED series.	33
Figure 1.27 Schematic illustration of cartilage and bone tissue engineering using hydrogel scaffold [171].	36
Figure 1.28 Macroscopic design determines the delivery route [182].	38
Figure 1.29 Structural formula of thymopentin (TP5).	39
Figure 2.1 ^1H NMR spectrum of the dynamer Dy obtained by reaction of BTA and Jeffamine in CDCl_3 .	73
Figure 2.2 ^1H NMR spectra of the dynamer Dy in pure D_2O and acidic D_2O at pH = 1, 3, and 5.	74
Figure 2.3 a) FT-IR spectra and b) enlarged view of the $1550\text{-}1750\text{ cm}^{-1}$	

wavelength range of CMCS, dynamer Dy and freeze-dried CMCS-Dy hydrogels.	75
Figure 2.4 a) Storage modulus (G') and loss modulus (G'') changes as a function of time after mixing CMCS and Dy aqueous solutions at various ratios at 37 °C, strain of 1%, and frequency of 1 Hz; b) G' changes as a function of applied strain for all hydrogels at 25 °C, and frequency of 1 Hz; and c) G' and G'' changes of Gel4-1 as a function of frequency at 25 °C, and strain of 1%. All hydrogels are prepared in Milli-Q water.	77
Figure 2.5 SEM images of freeze-dried hydrogels: (a, b) Gel1-1; (c, d) Gel2-1; (e, f) Gel4-1; (g, h) Gel6-1; (i, j) Gel8-1.	79
Figure 2.6 a) Equilibrium swelling ratios, and b) Mass loss ratios of Gel1-1, Gel2-1, Gel4-1, Gel6-1, and Gel8-1 at various pH values for 24 h, c) Swelling ratios, and d) Mass loss ratios of Gel4-1 at different pH values as a function of immersion time, e) Schematic presentation of the swelling behavior of freeze-dried hydrogels immersed in buffers at various pH values.	80
Figure 2.7 a) Modulus changes as a function of strain of Gel4-1 prepared in Milli-Q water; b) Modulus changes of Gel4-1 prepared in Milli-Q water with alternatively applied high and low oscillatory shear strains at 37°C; c-f) Self-healing macroscopic approaches using hydrogel samples prepared in Milli-Q water (c-d), at pH 7 (e) and at pH 8 (f) , see text for details.	84
Figure 2.8 Cell viability of human AT-MSCs or BM-MSCs in Gel4-1, in comparison with BM-MSCs in collagen hydrogel or plated on TCPS as control. Cells were labelled using the Live/Dead assay after 1 or 7 days in culture and imaged using confocal microscopy. Viable cells were stained in green and dead cells in red. Images are maximal projections of z-axis and scale bars represent 100 μ m (TCPS: Tissue Culture Polystyrene Surface; AT-MSCs: Adipose Tissue-MSCs; BM-MSCs: Bone Marrow-MSCs).	86
Figure 3.1 ^1H NMR spectra of the dynamers Dy500, Dy800 and Dy1900 obtained by reaction of BTA and Jeffamine.	107

Figure 3.2 a) FT-IR spectra, and b) enlarged view of the 1550-1750 cm^{-1} wavenumber range of CMCS, Dy500, Dy800, Dy1900, H500, H800 and H1900.	109
Figure 3.3 a) Storage modulus (G') and loss modulus (G'') changes as a function of time after mixing CMCS with Dy solutions at 37 °C, at strain of 1% and frequency of 1 Hz; b) Storage modulus (G') and loss modulus (G'') changes of H500, H800 and H1900 as a function of strain at 25 °C and 1 Hz.	110
Figure 3.4 SEM images and pore size distributions of freeze-dried gels: (a, b) H500; (c, d) H800; (e, f) H1900.	112
Figure 3.5 a) Equilibrium swelling ratios, and b) Mass loss ratios of H500, H800 and H1900 after 24 h immersion in buffers at various pH values.	113
Figure 3.6 a) Modulus changes as a function of strain of H1900 prepared in Milli-Q water; b) Modulus changes of H1900 prepared in Milli-Q water with alternatively applied high and low oscillatory shear strains at 37 °C; c) Macroscopic observation of self-healing of H1900 at 37 °C.	115
Figure 3.7 Bacterial concentrations (CFU mL^{-1}) obtained for positive control, CMCS, H1900 ^a , and H1900 ^b in liquid tests. (H1900 ^a : dealt with only thermal treatment for sterilization; H1900 ^b : dealt with both thermal treatment and UVc exposure for sterilization)	117
Figure 3.8 Soft agar tests: a) picture of the positive control plate and b) picture of the plate with H1900 ^b membrane. (H1900 ^b : dealt with both thermal treatment and UV exposure for sterilization).	120
Figure 4.1 a) FT-IR spectra of freeze-dried CMCS, Dy, Gel80K and Gel80K-TP5-3; b) FT-IR spectra of Dy, TP5, and Dy-TP5 which is an obtained by mixing TP5 in Dy solution at a molar ratio of 1/1, reaction at 37 °C for 24h, and 24 h lyophilization.	138
Figure 4.2 ^1H NMR spectra of the Dy, TP5, and Dy-TP5 in D_2O .	139
Figure 4.3 Storage modulus (G') and loss modulus (G'') changes of Gel80K, Gel30K and Gel25K as a function of strain at 25 °C and at 1 Hz (a) and as a	

function of frequency at 25 °C and at a strain of 1 % (b); G' and G'' changes of Gel80K, , Gel80K-TP5-0.1, Gel80K-TP5-3 and Gel80K-TP5-9 as a function of strain at 25 °C and at 1 Hz (c) and as a function of frequency at 25 °C and at a strain of 1% (d); G' and G'' changes of Gel80K, Gel80K-TP5-3, and Gel80K-TP5-3B as a function of strain at 25 °C and at 1 Hz (e) and as a function of frequency at 25 °C and at a strain of 1 % (f).	141
Figure 4.4 SEM images and pore size distributions of freeze-dried gels: (a, b, c) Gel80K; (d, e, f) Gel30K; (g, h, i) Gel25K.....	144
Figure 4.5 a) Swelling ratios, and b) Mass loss ratios of Gel80K, Gel30K and Gel25K after 24 h immersion in buffers at various pH values. Data are expressed as mean \pm SD for n = 3.	145
Figure 4.6 Cumulative release of TP5 from Gel80K-TP5-3, Gel30K-TP5-3, and Gel25K-TP5-3; Values were expressed as mean \pm SD for n = 3.	148
Figure 4.7 a) Cumulative release of TP5 from Gel80K-TP5-3 synthesized at 25 °C and 37 °C, namely, Gel80K-TP5-3 (25 °C) and Gel80K-TP5-3 (37 °C); b) Cumulative release of TP5 from Gel80K-TP5-3 under PBS medium (pH 7.4, 37 °C) and acid buffer medium (pH 5.5, 37 °C), respectively; c) Cumulative release of TP5 from Gel80K loaded with various TP5 content: Gel80K-TP5-0.1, Gel80K-TP5-3, and Gel80K-TP5-9; d) Cumulative release of TP5 from Gel80K-TP5-3 with different TP5 addition sequence, namely, Gel80K-TP5-3 and Gel80K-TP5-3B. Values were expressed as mean \pm SD for n = 3.....	150
Figure 4.8 Computation by Density Functional Theory (DFT) to determine the lowest reaction pathways between : a) CMCS-I-Dy; b) TP5(1)-I-Dy (TP5 site 1); c) TP5(2)-I-Dy (TP5 site 2); and d) TP5(3)-I-Dy (TP5 site 3). The reaction energy and energy barrier are calculated by Eq. 4 and Eq. 5 in kcal/mol.	154

List of Figures Supplementary

Figure S2.1 ^1H NMR spectra of the dynamer Dy obtained After 4, 8, 24, 48 and 72 h reaction recorded in CDCl_3	88
Figure S2.2 ^1H NMR spectra of the dynamer Dy recorded after 7 days in D_2O and at pH = 1, 3, and 5.	88
Figure S2.3 Storage modulus (G') and loss modulus (G'') changes as function of frequency for samples: Gel1/1, Gel2/1, Gel6/1, Gel8/1.....	89
Figure S2.4 SEM images of freeze-dried hydrogels (a, b) Gel1-1; (c, d) Gel2-1; (e, f) Gel4-1; (g, h) Gel6-1; (i, j) Gel8-1 after 24 h swelling at pH 4.....	90
Figure S2.5 SEM images of freeze-dried hydrogels (a, b) Gel1-1; (c, d) Gel2-1; (e, f) Gel4-1; (g, h) Gel6-1; (i, j) Gel8-1 after 24 h swelling at pH=8.....	91
Figure S2.6 Modulus changes as a function of strain of Gel4-1 prepared at pH=7 (a) and pH=8 (c); modulus changes with alternatively applied low and high oscillatory shear strains at 37 °C for Gel4-1 prepared at pH=7 (b) and pH=8 (d).	92
Figure S3.1 Storage modulus (G') and loss modulus (G'') changes of H500, H800 and H1900 as a function of frequency at 25 °C and 1% strain.	121
Figure S3.2 FT-IR spectra of the pristine H1900 membrane, H1900 ^a and H1900 ^b . (H1900 ^a : dealt with only thermal treatment for sterilization; H1900 ^b : dealt with both thermal treatment and UV exposure for sterilization).	121
Figure S4.1 FT-IR spectra of freeze-dried Gel30K, Gel25K, Gel30K-TP5, and Gel25K-TP5.	156
Figure S4.2 SEM images of freeze-dried CMCS (a, b) Dy (c,d), CMCS-TP5 (e,f) and Dy-TP5 (g, h). The samples CMCS-TP5 and Dy-TP5 are obtained by mixing CMCS and TP5 or Dy and TP5 in water with a molar ratio of 1/1, and freeze dried after 24 h at 37°C.....	157
Figure S4.3 Storage modulus (G') and loss modulus (G'') changes of Gel30K, Gel30K-TP5-3, Gel25K, and Gel25K-TP5-3 as a function of strain a); or as a	

function of frequency b) at 25 °C.	158
Figure S4.4 a) Swelling ratio, and b) mass loss ratio of Gel80K <i>versus</i> immersion time in pH 7.4 PBS at 37 °C. Values were expressed as mean \pm SD for n = 3, and presented by error band.	158
Figure S4.5 SEM images of TP5-loaded hydrogels: a, b) Gel80K-TP5-0.1; c, d) Gel80K-TP5-3; e, f) Gel80K-TP5-9; g, h) Gel80K-TP5-3B; i, j) Gel30KTP5-3; and k, l) Gel25K-TP5-3.	160
Figure S4.6 Graphical representation of the model fitting on the TP5 release data using Higuchi model.....	160
Figure S4.7 Typical geometries of a) CMCS; b) Dy, and c) TP5. TP5(1), TP5(2), and TP5(3) stand for site 1, site 2, and site 3 in TP5, respectively.....	161

List of Abbreviations

A

AC: allyl cellulose

ADH: adipic acid dihydrazide

AIDS: acquired immunodeficiency syndrome

APS: ammonium persulfate

AT-MSCs: adipose tissue mesenchymal stromal cells

B

BM-MSCs: bone-marrow mesenchymal stromal cells

BSA: bovine serum albumin

BTA: benzene-1,3,5-tricarbaldehyde

C

CEC: N-carboxyethyl chitosan

CFU: colony-forming unit

CG: conjugated gradient

CMC: carboxymethyl cellulose

CMCS: carboxymethyl chitosan

CNCs: cellulose nanocrystals

COSMO: conductor-like screening model

CS: chitosan

D

DA: Diels-Alder

DCBs: dynamic covalent bonds

DCC: dynamic covalent chemistry

DCF: Dynamic Constitutional Frameworks

DCPNs: Dynamic covalent polymer networks

DDN: double dynamic network

DDSs: drug delivery systems

DEAP: 2,2-diethoxyacetophenone

Dex-TA: dextran-tyramine

DF-PEG: di-benzaldehyde-modified telechelic poly(ethylene glycol)

DFT: density functional theory

DMA: N,N-dimethylacrylamide

DNP: double numerical plus polarization

DOX: doxorubicin

DS: diclofenac sodium

Dy: dynamer

E

EC: ethyl cellulose

ECM: extracellular matrix

EPR: enhanced permeability and retention

F

FDA: Food and Drug Administration

Fer: feruloyl

FerFFK: Feruloyl-(L)-Phe-(L)-Phe-(L)-Lys

FT-IR: Fourier-transform infrared spectroscopy

G

GC: glycol chitosan

GC: glycol chitosan

GDs: green dynamers

GPC: gel permeation chromatography

H

HA: hyaluronic acid

HACC: 2-hydroxypropyltrimethyl ammonium chloride chitosan

HEA: 2-hydroxyethyl acrylate

HEC: hydroxyethyl cellulose

HPMC: hydroxypropyl methyl cellulose

HPMC: hydroxypropyl methylcellulose

HRP: horseradish peroxidase

K

KPS: potassium persulfate

L

LB: Lysogeny Broth

LCST: lower critical solution temperature

LST: linear synchronous transit

M

MC: methyl cellulose

MF-PEG: multifunctional PEG

MSCs: mesenchymal stromal cells

N

N-CMCS: N-carboxymethyl chitosan

NMR: nuclear magnetic resonance

NO-CMCS: N,O-carboxymethyl chitosan

O

O-CMCS: O-carboxymethyl chitosan

OSA: oxidized sodium alginate

P

P(NAGA-co-NBAA): poly(N-acryloyl glycinamide-co-N-benzyl acrylamide)

PAA: poly(acrylic acid)

PAAm: polyacrylamide

PANI/PSS: polyaniline/poly(4-styrenesulfonate)

PBA: poly(butylene adipate)

PBS: poly(butylene succinate)

PDLA: poly (D-lactide)

PEC: polyelectrolyte complex

PEG: poly(ethylene glycol)

PEI: polyethylenimine

PEO: poly(ethylene oxide)

PHEMA: poly(hydroxyl ethyl methacrylate)

PhP: phenolphthalein

PLA: polylactide

PLLA: poly (L-lactide)

PNIPAAm: poly(N-isopropylacrylamide)

PNIPAM: poly(N-isopropylacrylamide)

PPO: poly(propylene oxide)

PTX: paclitaxel

PVA: poly(vinyl alcohol)

PVP: polyvinyl pyrrolidone

Q

QST: quadratic synchronous transit

R

RDA: retro-Diels-Alder

RDE: Radical disulfide exchange

S

SCF: self-consistent field

SEM: scanning electron microscopy

T

TMS: tetramethylsilane

TP5: thymopentin

U

UPy: 2-ureido-4 [1*H*]-pyrimidinone

5

5-Fu: 5-Fluorouracil

Chapter 1 Introduction

1.1 Hydrogels

Hydrogel was first reported by Wichterle and Lim in 1960 [1] following their work to develop a hydrogel based on poly(hydroxyl ethyl methacrylate) (PHEMA) for biological use. PHEMA was cross-linked with ethylene glycol dimethacrylate to yield a hydrogel under the commercial name of Polymacon which is used in the manufacture of soft contact lenses since 1970. From then on, a great deal of work has been devoted and are going on to extend the potential applications of hydrogels. et al [2-4]. As time flies into the 21st century, research on hydrogels is soaring. In 2019, the number of publications under the topic “hydrogel” are dramatically high. Nearly 10000 papers were published, which is close to the number of papers published under the topic “2D-material”, another hot topic in recent years. In particular, the ever-growing hydrogel technology has led to dramatic advances in pharmaceutical and biomedical fields.

According to the definition, hydrogels are three-dimensional (3D) polymeric networks that are capable of imbibing large quantity of water or biological fluids, owing to the presence of hydrophilic groups, such as, -OH, -CONH-, -CONH₂-, -COOH and -SO₃H in polymers forming hydrogel structures. Swelling of hydrogel is an intricate process [5]. First, bound water is formed due to interactions between water and polar hydrophilic groups, as well as interactions between water and exposed hydrophobic groups. Then, additional water is absorbed owing to the resistance caused by the physical and/or chemical crosslinks in hydrogel towards infinite dilution because of the osmotic driving force of the network. At the equilibrium swelling, the water up taken into the interspaces between the network or chains and the center of the pores of hydrogels is called bulk water or free water. Nevertheless, hydrogels can keep

their integrity in spite of high swelling because of the crosslinked structure.

With the advance of materials science, various strategies emerged for the preparation of hydrogels in recent years. Through different synthesis routes, appropriate raw materials selection, composite design, double network formation, etc. Hydrogels can be categorized based on a variety of characteristics, such as hydrogel size [6] (macroscopic hydrogel, microgel (0.5-10 μm), and nanogel (< 200 nm)), preparation method [7] (physical or chemical hydrogels), mechanical properties [8] (soft hydrogel or hard hydrogel), raw material (natural hydrogel, hybrid or synthetic hydrogel), etc. However, classification based on preparation method is most frequently used, namely physical hydrogel and chemical hydrogel.

1.1.1 Physical hydrogels

Physical hydrogels attracted considerable attention for applications in food, pharmaceutical and biomedical fields due to the relatively easy synthesis protocol without any crosslinking agents. They are obtained by physical interactions between polymer chains [9], including hydrogel bonds, crystallization, stereo-complexation, etc.

1.1.1.1 Physical hydrogels based on hydrogen bonds

Physically cross-linked hydrogels can be obtained by hydrogen bonding interactions. Feng et al. [10] prepared a versatile hydrogel with two noncovalent crosslinked networks, as shown in Figure 1.1. The hydrogels are synthesized via intramolecular hydrogen bonding between the side chain amide groups of poly(N-acryloyl glycinamide-co-N-benzyl acrylamide) (P(NAGA-co-NBAA)) and intermolecular H-bonding between P(NAGA-co-NBAA) and agar. Such a double network provides the hydrogel with high self-healing, good shape memory, and high mechanical strength. But the hydrogels are disassociated upon heating.

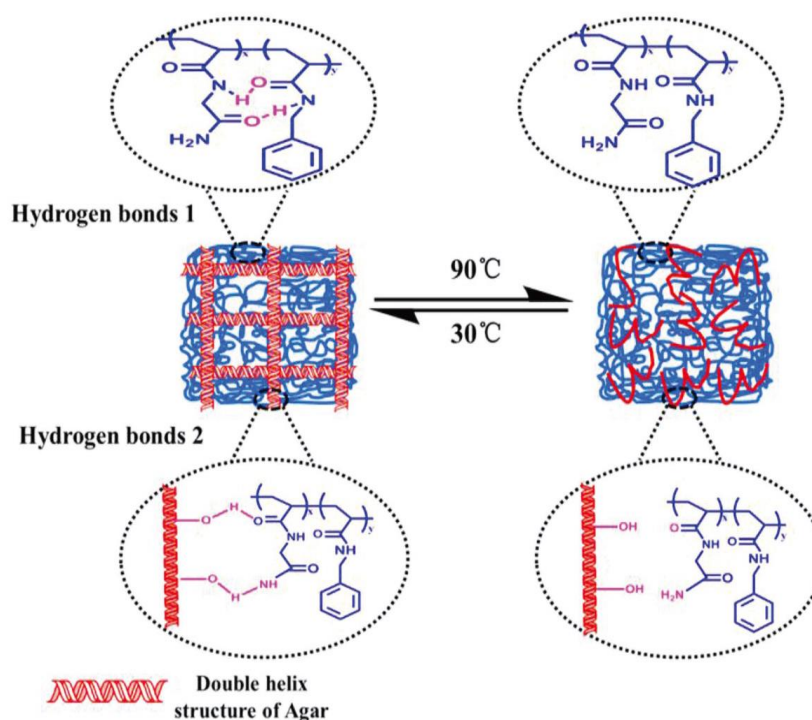


Figure 1.1 Double H-bonding network of physical hydrogels [10].

Other multiple hydrogen bonding hydrogels include polyaniline/poly(4-styrenesulfonate) (PANI/PSS), and poly(N-isopropylacrylamide) (PNIPAM). Hydrogen-bonded cross-linking points are formed in the presence of 2-ureido-4 [1*H*]-pyrimidinone (UPy) as cross-linking agent. Therefore, physical hydrogels by H-banding present great potential for applications in various fields [11-13], including cell culture, photothermal imaging, bioelectronics, supercapacitors, etc.

1.1.1.2 Physical hydrogels based on crystallization cross-linking

Crystallization induced cross-linking can be used to prepare physical hydrogels via repetitive freeze-thaw cycles [7]. The gelation mechanism, firstly described [14] by Peppas and Stauffer for PVA-based hydrogels, involves formation of microcrystals in the structure due to freezing and thawing. In fact, phase separation occurs during crystallization of water, which pushes polymer chains close to each other. The authors showed [15] that repeated cycles of freezing at -20 °C and thawing at 25 °C result in formation of crystalline regions that

remain intact when placed in contact with water or biological fluids at 37 °C, thus endowing hydrogels with enhanced mechanical strength. PVA based hydrogels have been used as soft tissue engineering scaffolds [16]. Composite hydrogels have also been reported such as PVA/hyaluronic acid (HA) hydrogel and cellulose-reinforced PVA hydrogel.

1.1.1.3 Physical hydrogels by stereo-complexation

Stereo-complexation refers to synergistic interactions between polymer chains or small molecules having the same chemical composition but opposite stereochemistry [17, 18]. Noticeably, hydrogels obtained from dextran-*graft*-PLA copolymers by stereo-complexation have been reported [17, 18]. The major advantage of physical hydrogels by stereo-complexation is the simplicity of preparation as hydrogels can be obtained by mixing aqueous solution of copolymers. The best example of this type of hydrogels is those obtained from polylactide-poly(ethylene glycol) (PLA-PEG) block copolymers. PLA is a hydrophobic biodegradable polyester widely used for biomedical applications. A stereo-complex can be obtained by mixing poly (L-lactide) (PLLA) and poly (D-lactide) (PDLA) in solution or in melt. When the PLLA-PEG and PDLA-PEG block copolymers are mixed in an aqueous solution, the interactions between PLLA and PDLA blocks can lead to stereo-complexation and the formation of a hydrogel [19].

1.1.1.4 Physical hydrogels by electrostatic interactions

Physical hydrogels can be obtained by ionic interactions between two or more polyelectrolytes with opposite charges [20]. A polyelectrolyte [21-25] is a macromolecule carrying ionizable functional groups which are converted into a charged long chain with counter ions in polar solvent. It can be a synthetic polymer such as poly(acrylic acid) (PAA) and polyethylenimine (PEI), or a biopolymer [26-28] such as chitosan, hyaluronic acid, and alginate.

Electrostatic interactions between oppositely charged PEs yield a polyelectrolyte complex (PEC) [22, 29, 30], thus resulting in phase separation in solution or gelation [21, 31].

You et al. [32] synthesized PEC hydrogels via in situ polymerization of acrylic acid in concentrated quaternized chitosan solution. The resulting hydrogels exhibit self-recovery behavior and good mechanical performance. Another example of such hydrogels was prepared from chitosan and sodium alginate by Oliveira et al [33].

1.1.1.5 Physical hydrogels by ionic cross-linking

Ionic cross-linked hydrogels are three-dimensional polymeric network cross-linked by ions which are able to form ionic interchain bridges or chelation interactions with functional groups or atoms of polymers [34, 35]. In fact, some metal ions [36-38], and especially transition metals such as Zn^{2+} , Ca^{2+} , Cu^{2+} , Ce^{3+} , and Fe^{3+} are able to interact with functional groups of polymers such as carboxyl and amino groups, leading to ionically cross-linked hydrogels.

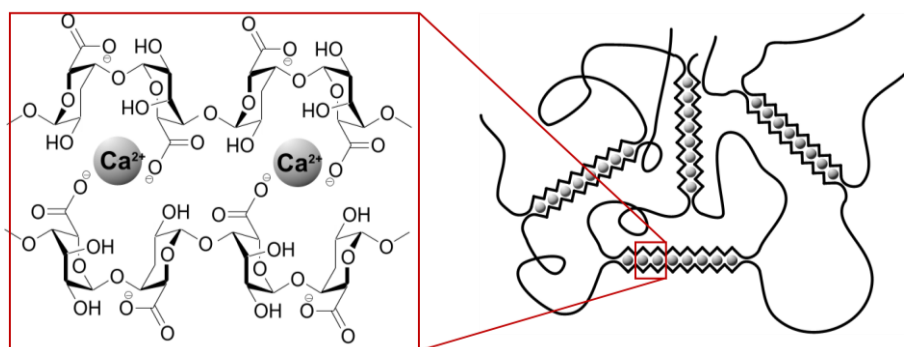


Figure 1.2 Mechanism of ion-chain binding in ionically cross-linked alginate hydrogels [39].

An “egg-box” model [39] have been proposed to illustrate the cooperative mechanism of ion-chain binding in ionically cross-linked alginate hydrogels. As shown in Figure 1.2, Li et al. [40] reported synthesis of sodium alginate/k-carrageenan double-network gel beads through a facile ionically cross-linking method. Data show that the metal ions not only play a role in crosslinking but

also allow to improve hydrogel overall performance.

The properties of ionically cross-linked hydrogels can be tuned through introduction of other metal ions [41]. Soft Ca^{2+} -alginate/polyacrylamide hydrogels become tough with addition of Fe^{3+} ions, and become soft again when Fe^{3+} ions are reduced to Fe^{2+} ones.

Fe^{3+} ions have been used for enhancing the stiffness of other hydrogels [42, 43], including 2-hydroxypropyltrimethyl ammonium chloride chitosan (HACC)/poly(acrylic acid) (PAA)- Fe^{3+} polyacrylamide (PAAm)/chitosan (CS) hybrid hydrogels. Moreover, negative ions such as Cl^- , SO_4^{2-} , and Cit^{3-} have also been used to fabricate ionically cross-linked polyacrylamide (PAAm)/chitosan hydrogels [44].

1.1.1.6 Physical hydrogels by hydrophobic association

Physical hydrogels can be obtained from amphiphilic polymers via hydrophobic association [20]. In fact, the hydrophobic groups of amphiphilic polymers will aggregate and associate with each other with increasing concentration, leading to formation of a three-dimensional framework in aqueous solution. Chitosan is widely used in hydrophobic association hydrogels. The common approach is to dissolve chitosan in acidic solution, and neutralize it with alkaline solution, resulting in the three-dimensional framework via hydrogen bonding and hydrophobic interaction between the molecular chains [45]. Cellulose and its derivatives such as hydroxypropyl methylcellulose (HPMC) have also been used to fabricate novel 'soft' materials through hydrophobic interactions [46].

1.1.2 Chemical hydrogels

Physical hydrogels present many advantages such as easy preparation and good mechanical strength, but their stability is rather low. Hence, it is of great importance to study polymer networks crosslinked by covalent bonds which ensure the system's stability [47]. Several methods are available to synthesize

chemically cross-linked hydrogels.

1.1.2.1 Chemical hydrogels by grafting

This strategy consists in grafting polymer chains on the backbone of a hydrophilic polymer, typically a polysaccharide such as chitosan or alginate. For example, Mahanta et al. [48] developed an injectable hydrogel through grafting of a hydrophobic prepolymer on chitosan chains. Firstly, a polyurethane prepolymer terminated with isocyanate groups at both ends is synthesized. The prepolymer is then grafted on the chitosan backbone via reaction of isocyanate with amino or hydroxyl groups, leading to a crosslinked network.

1.1.2.2 Chemical hydrogels by radical polymerization

Chemically cross-linked gels can also be fabricated by radical polymerization of low molar mass monomers attached to a hydrophilic biopolymer such as cellulose or chitosan in the presence of an initiator such as ammonium persulfate (APS) or potassium persulfate (KPS) [49]. This is one of the most common methods for the preparation of hydrogels due to rapid gelation and mild conditions.

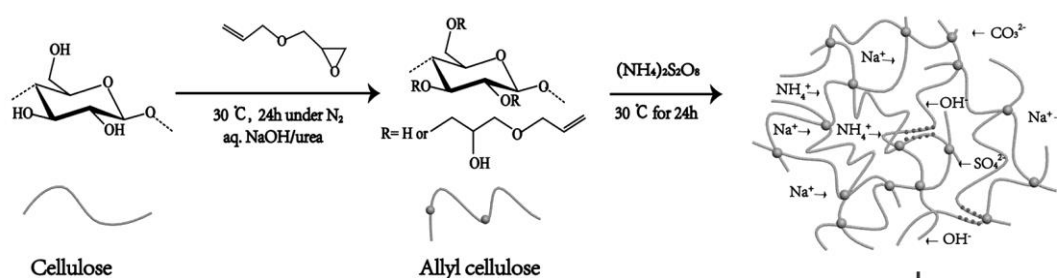


Figure 1.3 Schematic illustration of synthesis of cellulose-based hydrogels by radical polymerization [50].

Tong et al. [50] reported cellulose based ionic hydrogels via chemical cross-linking based on free radical polymerization of allyl cellulose (AC) in NaOH / urea aqueous solution, as shown in Figure 1.3. The resulted hydrogels display high stretch ability (tensile strain ~126 %) and compressibility (compression

strain ~80%), good transparency (transmittance of ~89% at 550 nm) and ionic conductivity ($\sim 0.16 \text{ mS cm}^{-1}$). Glucan / chitosan-based hydrogels have also been obtained by KPS initiated radical polymerization [51].

1.1.2.3 Chemical hydrogels by condensation reaction

Chemical hydrogels can be synthesized by condensation of polymers containing hydroxyl / amine groups with carboxylic acids or their derivatives. Owing to the presence of carboxyl, hydroxyl, or amine groups in many polysaccharides, condensation reactions can be utilized as a common approach for the synthesis of polysaccharide hydrogels, in particular, the Ugi reaction involving four components, i.e., amine (secondary or primary), aldehyde (or ketone), carboxylic acid, and isocyanide [52].

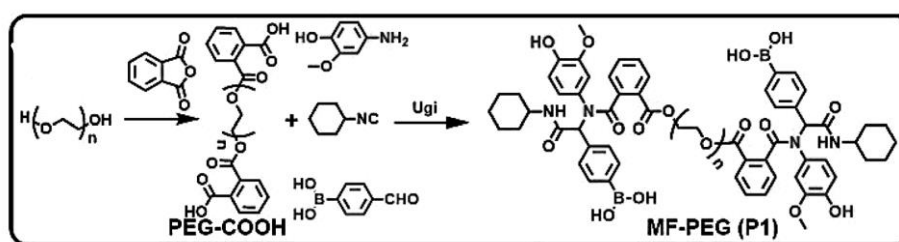


Figure 1.4 Synthesis of MF-PEG via the Ugi reaction, PEG-acid: amine: aldehyde: isocyanide = 1:6:6:10, methanol, 45 °C, 12 h [53].

Tao et al. recently reported the synthesis of an antibacterial self-healing hydrogel via the Ugi reaction [53], firstly, a multifunctional PEG (MF-PEG) containing phenylboronic acid and phenolic groups at both chain ends was prepared via the one step Ugi reaction, as shown in Figure 1.4. The as-prepared MF-PEG was then cross-linked with poly(vinyl alcohol) (PVA) via dynamic borate ester linkages to quickly generate a self-healing hydrogel under mild conditions.

1.1.2.4 Chemical hydrogels by enzymatic reaction

Another hydrogel formulation is achieved by enzymatic catalyzed reaction. Jin

et al. [54] reported an enzymatically-crosslinked biomimetic hydrogel HA-g-Dex-TA based on hyaluronic acid (HA) and dextran-tyramine (Dex-TA), by using HRP (horseradish peroxidase) as a catalyst and H_2O_2 as an oxidant. The properties of the hydrogels could be tuned by varying the degree of substitution of tyramine units and polymer concentration. Moreover, the as-prepared hydrogels induced enhanced cell proliferation and matrix deposition, which is of great importance for applications in tissue engineering.

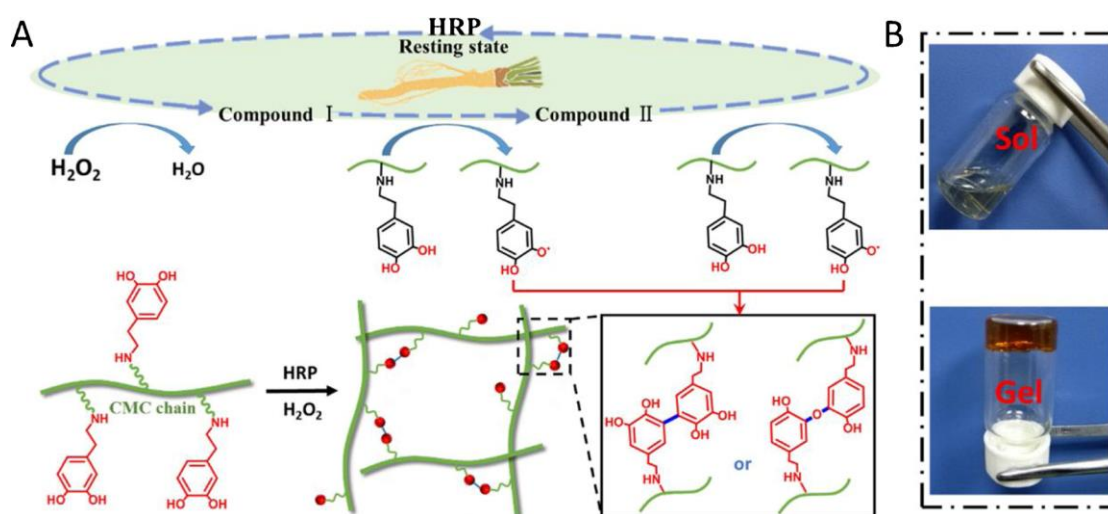


Figure 1.5 (A) Synthesis of CMC-DA hydrogels by enzymatic crosslinking in the present of HRP and H_2O_2 . (B) Photographs of the CMC-DA solution before and after gelation [55].

Guo et al. used the same procedure to synthesize dopamine (DA) modified carboxymethyl cellulose (CMC) hydrogels (CMC-DA) [55], as shown in Figure 1.5. The as-fabricated hydrogels exhibited reinforced wet tissue adhesion behavior, which is promising for health care applications such as wound dressing and drug delivery.

Another example of enzymatically crosslinked hydrogels was reported by Wei et al [56]. The authors prepared antioxidant Feruloyl-(L)-Phe-(L)-Phe-(L)-Lys(FerFFK)/glycol chitosan (GC) hydrogel based on laccase-mediated crosslinking reaction between feruloyl(Fer)-modified tripeptide and glycol chitosan. The as-made hydrogels could promote generation of mature skin

structures, including epithelium and dermis, and are thus promising for utilization in cutaneous wound healing.

1.1.2.5 Chemical hydrogels by high-energy radiation

Chemical hydrogels can be synthesized from unsaturated compounds through high-energy radiation [7], including gamma and electron beam irradiation. Typically, when subjected to gamma or electron beam radiation, radicals are formed on water-soluble polymers modified with vinyl groups via homolytic thermal scission [57], finally leading to cross-linked structures by covalent bonding. An example was given by R. Singh and D. Singh [58] who prepared polyvinyl pyrrolidone(PVP)/alginate hydrogel. PVP and alginate aqueous solutions were mixed, sealed and gamma irradiated at different doses in the absence/presence of nano-silver. Although this hydrogel could be synthesized under mild conditions and has great clinical potential as wound dressing material, irradiation could lead to formation of non-biodegradable C-C linkages, which could greatly limit its further utilization.

1.2 Dynamic hydrogels

Reversible bonds endow a better ability to biomaterials for disassociation and association upon external triggers. Compared to covalently bonding, in which there's no exchange gelation occur in the hydrogel connected by the reversible sacrificial bonds. Thus, hydrogels obtained by dynamic bonds are able to recover from a split or damaged state [59]. This property inspired researchers to design self-healing networks based on dynamic covalent chemistry (DCC) [60, 61].

Generally, DCC refers to linkage forming and breaking in the process of network formation, including boronate-diol exchange, transesterification, siloxane equilibrium, hydrazide-acylhydrazone exchange, radical disulfide exchange, transamination, transalkylation, radical thiyl-allyl sulfide exchange, Diels-Alder

(DA) reaction, imine exchange, etc.

1.2.1 Dynamic hydrogels linked by boronate ester

Boronate ester bond is formed between boronic acids and 1,2- or 1,3- diols [62]. It is increasingly utilized to design smart hydrogels.

Chen et al. [63] synthesized an elastomeric hydrogel by random copolymerization of N,N-dimethylacrylamide (DMA), 2-hydroxyethyl acrylate (HEA) and boric acid, using 2,2-diethoxyacetophenone (DEAP) as photoinitiator. These hydrogels exhibited autonomously self-healable behaviors owing to the dynamic boronate ester linkages. Besides, the dynamic boronate ester bonds were applied to fabricate smart electrochemical capacitors as well. For example, Wang et al. [64] reported a poly(vinyl alcohol)-based hydrogel electrolyte based on dynamic diol-borate ester bonding. The authors demonstrated that the dynamic bonds not only endow the self-healing property but also adequate strength for wearable and smart energy-storage devices.

1.2.2 Dynamic hydrogels linked by acylhydrazone bonds

In the past decades, hydrazone or acylhydrazone formation via condensation of carbonyl groups and hydrazines or hydrazides has been widely explored for the synthesis of biological substances or polymeric materials [65]. Dynamic covalent polymer networks (DCPNs) with acylhydrazone bonds generally consist of polymer chains with near-monodisperse molar mass distribution and evenly spaced crosslinking junctions, called model DCPNs, but also of less well-defined polymer chains and crosslinking junctions, called randomly crosslinked DCPNs [66], as shown in Figure 1.6.

Although the model DCPNs were rarely reported because of the synthetic difficulties in forming polymers, Deng and co-workers developed a kind of reversible polymer gels based acylhydrazone bonds which obtained from the condensation of acylhydrazines at the two ends of a poly(ethylene oxide) (PEO)

with aldehyde groups in tris [(4-formylphenoxy)methyl]ethane [67]. The as-prepared hydrogels displayed excellent reversibility, owing to the disassociation of framework and the association of the starting reagents under mild conditions in presence of acid catalysis. The hydrogels connected by the model DCPNs performance in a similar way as a supramolecular gel.

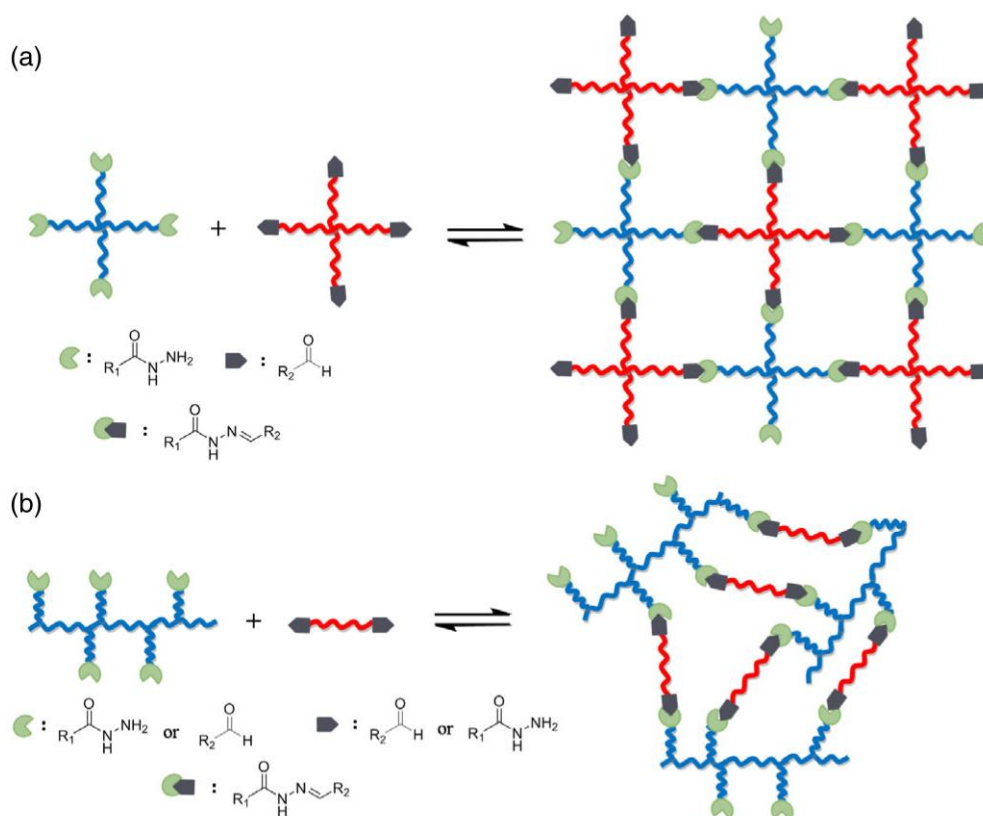


Figure 1.6 Representation of (a) a model and (b) a randomly crosslinked dynamic covalent polymer network crosslinked via acylhydrazone bonds [66].

In contrast to model DCPNs, randomly crosslinked DCPNs have been widely studied. Yang et al. [68] synthesized a self-healing and pH/temperature responsive gel from a hydrazide - modified calix [4]arene derivative and linear benzaldehyde - terminated poly(ethylene glycol) in mixed solvent (ethanol and water) involving randomly crosslinked DCPNs. Acid - degradable hydrogel can be obtained via natural drying of the mixed solvent gel first and then swelling in pure water. Zhang's group synthesized a series of cellulose-based self-healing hydrogels constructed via dynamic covalent acylhydrazone linkages [69]. The

hydrogels display attractive self-healing ability with a healing efficiency over 96 %, and excellent mechanical properties. Most interestingly, is the hydrogels also exhibit pH/redox dual responsive sol-gel transition behavior, which is promising for controlled release of doxorubicin. The formation of acylhydrazone bonds is achieved under mild conditions as it is actually a Schiff's base reaction. Therefore, the utilization of acylhydrazone exchange constitutes an attractive strategy to construct dynamic hydrogels.

1.2.3 Dynamic hydrogels linked by disulfide bonds

Radical disulfide exchange (RDE) is a classic dynamic covalent reaction that requires initiators to induce the homolysis of the disulfide bond. Therefore, the construction of dynamic covalent systems could be activated by external stimuli [70].

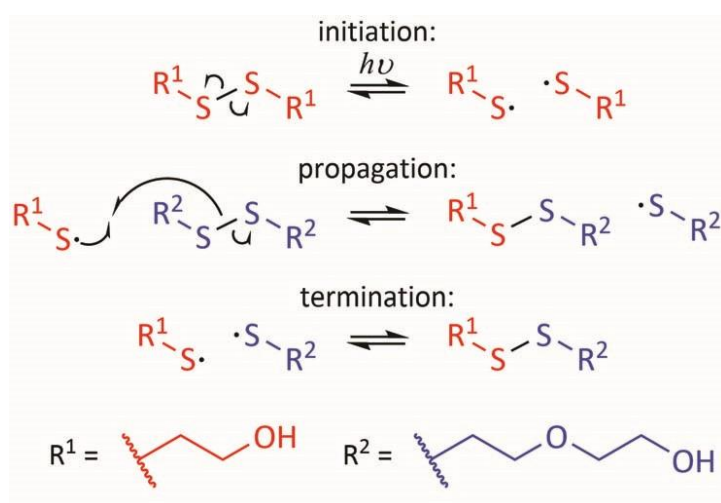


Figure 1.7 Mechanism of the photoinduced radical disulfide exchange [70].

In 1963, Tobolsky et al. suggested that disulfide exchange could be initiated by radicals generated from the thermal cleavage of the S₈ sulfur ring [71]. From then on, disulfide exchange has been widely studied in dynamic covalent chemistry. Disulfide exchange reactions generally could be initiated by sonication [72], rhodium catalyst [73], metal [74], and UV irradiation [75]. As shown in Figure 1.7, a disulfide bond is first homolytically cleaved to generate

two sulfenyl radicals when exposed to UV, followed by exchange of a sulfenyl radical with another disulfide, and finally the combination of two different free sulfenyl radicals to yield an exchanged product [70].

For example, Tran and co-workers synthesized multifunctional hydrogels by copolymerizing 2,3-dimercapto-1-propanol and meso-2,3-dimercaptosuccinic acid, yielding a dynamic poly(disulfide) backbone and numerous physical crosslinks (H-bonds and ionic interactions) [76]. The high-density disulfide bonds and physical crosslinkers synergistically provide the hydrogels with fast self-healing in air and underwater, good stretchability, and complete degradability.

1.2.4 Dynamic hydrogels synthesized by Diels-Alder (DA) reaction

The reaction of an electron-deficient dienophile with an electron-rich conjugated diene is the representative Diels-Alder (DA) reaction in which a cyclohexene adduct is formed through a [4+2] cycloaddition [77]. DA reaction is performed under mild conditions, and can be reversed at increased temperatures (110 °C) by a dissociative retro-Diels-Alder (rDA) reaction [78, 79], as shown in Figure 1.8.

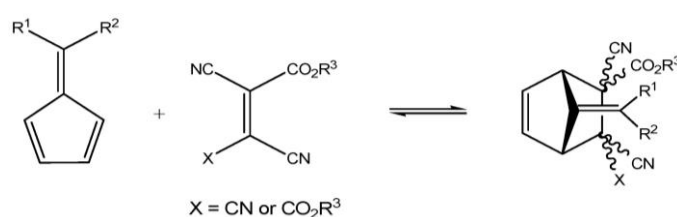


Figure 1.8 Diels-Alder and retro-Diels-Alder reactions [79].

Furthermore, the DA reaction is classified as ‘click’ reaction because the reaction occurs between azides and alkynes or nitriles [80]. It has been largely used to construct polymer networks with dynamic properties owing to its excellent selectivity and efficiency.

Yang et al. reported novel cellulose nanocrystals (CNCs)-poly(ethylene glycol)

nanocomposite hydrogels with CNCs as both reinforcing phase and chemical cross-linker in a reversible DA reaction [81]. The reversibility of the DA reaction endowed the hydrogel with outstanding self-healing property, renewability and ultrahigh tensile stiffness.

More recently, Bi et al. successfully synthesized in situ forming thermosensitive hydroxypropyl chitin-based hydrogels by applying DA reaction without using any initiator or catalyst under physiological conditions [82]. Rapid gelation was achieved at 37 °C, and the hydrogels displayed excellent mechanical strength.

1.2.5 Dynamic hydrogels linked by Imine bonds

In organic chemistry, 'Schiff-base' reaction is a reversible polycondensation between amines and aldehydes. It is a classical and omnipresent reaction discovered by the German chemist Hugo Schiff in 1864 [83]. A Schiff's base has a general formula of $R^1R^2C=NR^3$, where R^1 and R^2 represent for either i) an aryl or alkyl group ii) a mixture of the two, or iii) a hydrogen, and R^3 an aryl or alkyl group, but not a hydrogen [84].

Imine bond is a strong covalent bond with a bond dissociation energy of 147 kcal mol⁻¹. It could undergo quick degenerative bond exchange without generation of side-products [85]. In a typical imine bond formation, reaction between an amino group and a carbonyl one result in a $-C=N-$ bond plus a water.

Besides, H₂O addition would lead to the hydrolysis of an imine back to the starting materials. Therefore, it is of great importance to take into consideration the factors which can affect the equilibrium between an imine and the initial reagents, including temperature, concentration, pH, solvent, steric or electronic effect, etc. In principle, imines can undergo three kinds of equilibrium-controlled reactions [84], as shown in Figure 1.9.

i) Hydrolysis : The imine hydrolyzes back to the starting materials, amine and carbonyl-containing chemicals by adding H₂O;

ii) Exchange : by addition of a second amine, the R groups are exchanged via transimination of original imine;

iii) Metathesis : Upon introduction of a second imine, the two R groups are exchanged via a reaction of the two imines.

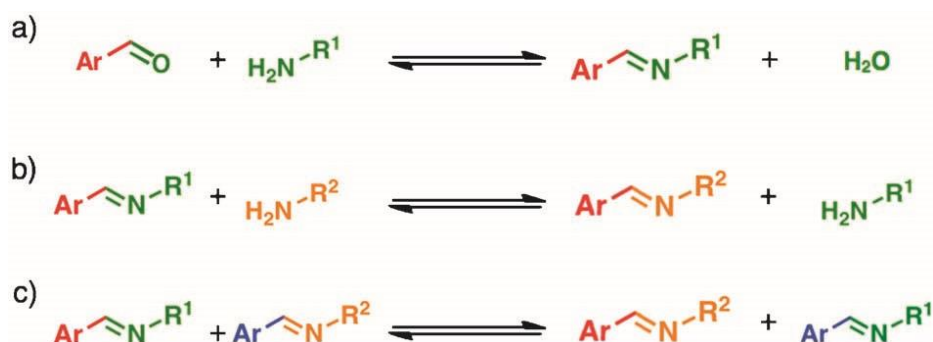


Figure 1.9 Three types of imine reactions (a) imine condensation, (b) exchange, and (c) metathesis [84].

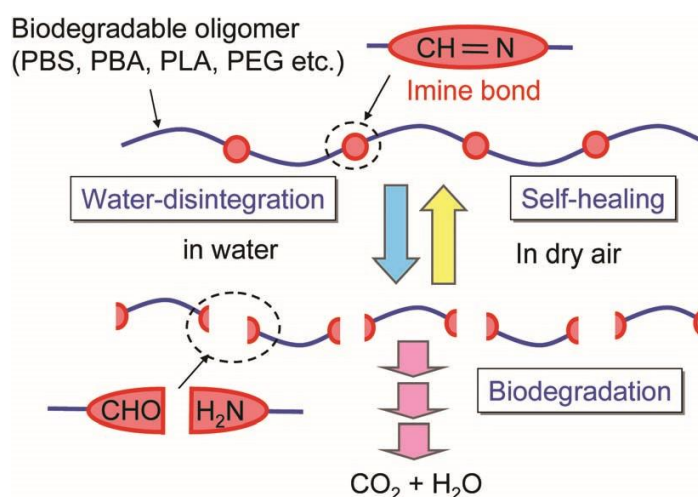


Figure 1.10 Schematic representation of water-disintegration, self-healing and biodegradation processes of a green dynamer [86].

Lehn's group developed environmentally friendly "green dynamers (GDs)" [86], namely dynamic polymers presenting sequential double-degradation features [87]. They were obtained by connecting biodegradable oligomers such as poly(butylene adipate) (PBA), PLA, and poly(butylene succinate) (PBS) through chemically degradable reversible imine bonds shown in Figure 1.10. The GDs were thermodynamically stable and maintained their molar mass and mechanical strength in the absence of water. However, when they were in

contact with water, both the imine and ester bonds were hydrolyzed, breaking up into monomers and finally into CO₂ and water.

Hence, because of the direct reversible association and disassociation of imine bonds without involving intermediates, imine chemistry has been widely adopted for constructing dynamic polymers.

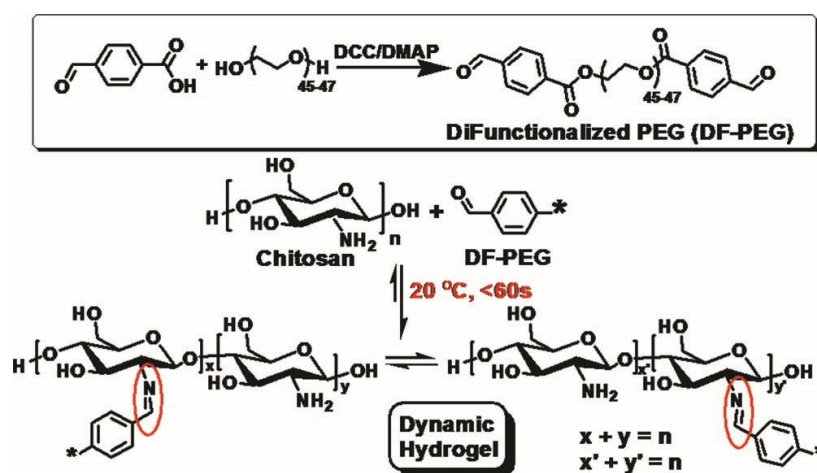


Figure 1.11 Synthesis of DF-PEGs and their coupling with chitosan to form dynamic hydrogels [88].

Zhang and co-workers reported synthesis of a dynamic chitosan based hydrogel by reaction of a di-benzaldehyde-modified telechelic poly(ethylene glycol) (DF-PEG) and chitosan [88], as shown in Figure 1.11. The hydrogels displayed excellent self-healing behaviors because of the dynamic equilibrium between the Schiff base linkage and the aldehyde and amine groups. Besides, the as-prepared hydrogel is sensitive to external biochemical-stimuli, including pH, amino acids, and vitamin B6 derivatives. Nevertheless, the ester bonds in DF-PEG is much more sensitive to hydrolysis than imine bonds, which could lead to rapid hydrogel disintegration under physiological conditions.

Zhang et al. developed a dynamic covalent polymer network by reaction of poly(ethylene glycol) bis(3-aminopropyl) (PEG-diamine) with 1,3,5-triformylbenzene [85], as shown in Figure 1.12. The effect of molar mass of PEO diamines and solvent polarity on the properties of gels was investigated. The results showed that the gelation time is molar mass dependent, and lower

molar mass of PEG is better for formulating soft ‘free-standing’ gel. The malleability of the polymer networks swollen in various solvents is greatly dependent on the solvent polarity. Higher polarity leads to more rapid imine exchange and better malleability because dynamic imine bond exchange is faster in the polar solvents than in nonpolar

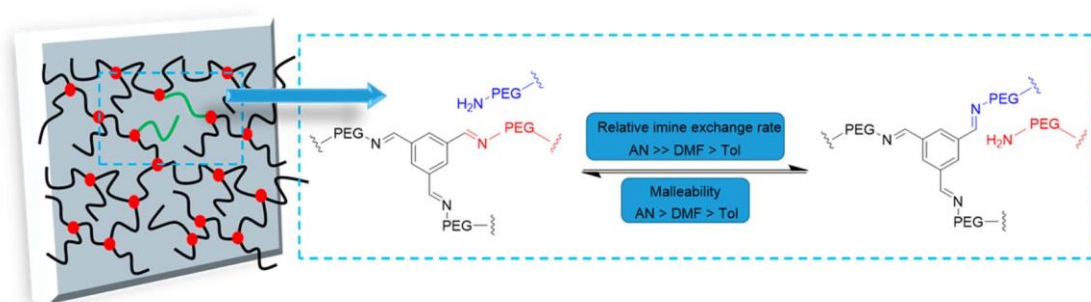


Figure 1.12 Schematic illustration of forming the dynamic covalent network based on imine bonds [85].

Chen’s group reported a polysaccharide-based self-healing hydrogel (CEC-I-OA-I-ADH, ‘I’ means “linked-by”) via dynamic reaction between N-carboxyethyl chitosan (CEC), adipic acid dihydrazide (ADH) and oxidized sodium alginate (OSA) [89]. Hydrogels were obtained through homogeneously mixing an OSA solution with a solution of CEC and ADH at room temperature (25 °C) by using phosphate buffered saline (PBS, pH 7.0 or 6.0) as solvent, as shown in Figure 1.13. The procedure appears promising for formulating novel dynamic hydrogels. Moreover, due to the coexistence of dynamic imine and acylhydrazone bonds throughout the hydrogel network, the as-prepared hydrogels not only exhibit excellent self-healing capability without any external triggers, but also high healing efficiency (around 95%) in physiological conditions.

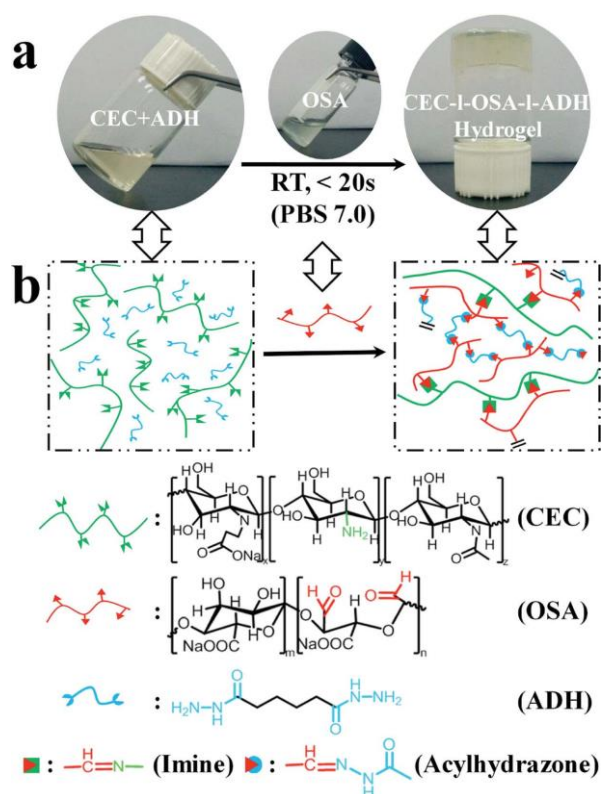


Figure 1.13 Synthesis scheme of the CEC-I-OSA-I-ADH hydrogels. a) Photographs before and after gelation of CEC-I-OSA-I-ADH hydrogel ($R = 0.5$) in PBS (pH 7.0). b) Schematic presentation and chemical structures of the CEC-I-OSA-I-ADH hydrogel obtained by condensation reaction of the aldehyde groups (from OSA) with the amino groups (from CEC) and hydrazides (from ADH), resulting in dynamic imine and acylhydrazone bonds, respectively [89].

More recently, a similar approach for constructing double dynamic networks was reported by Tao's group [90]. They used four-component Ugi reaction to form a double dynamic network (DDN) combining imine and borate ester linkages. Multifunctional poly(ethylene glycol) (MF-PEG) is simultaneously cross-linked with poly(vinyl alcohol) (PVA) and glycol chitosan (GC) by via borate ester and imine bonding, respectively, to generate a self-healing hydrogel with a unique DDN structure in seconds under mild conditions (pH \approx 7, 25 °C) (Figure 1.14). The hydrogel showed not only enhanced strength and mucoadhesive abilities because of the complimentary interpenetrating dynamic networks, but also satisfactory. However, the preparation of MF-PEG containing a benzaldehyde group and a phenylboronic acid group at each chain end is a complex procedure with a yield of x%.

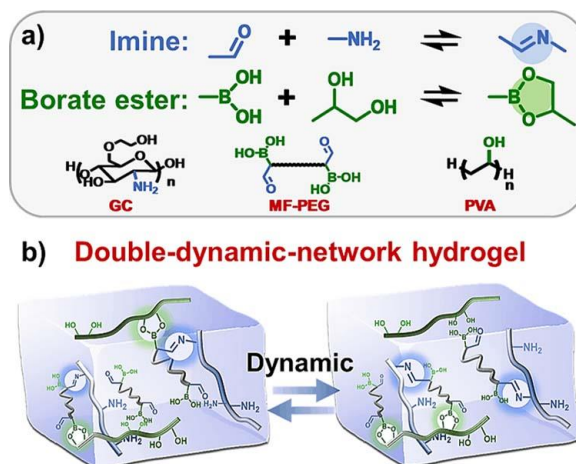


Figure 1.14 Schematic illustration of a DDN hydrogel with imine and borate ester linkages [90].

As mentioned above, dynamic covalent chemistry is largely explored in order to design self-healing hydrogels due to two major advantages, including stability of covalent bond and reversibility of noncovalent bond. The various dynamic covalent bonds could endow hydrogels with inherent dynamic equilibrium of bond association and dissociation to hydrogel network. Nevertheless, some of these reactions such as Diels-Alder reaction, hydrazide-acylhydrazone exchange, and radical disulfide exchange are quite difficult to be applied in vivo owing to their non-autonomous self-healing features [89], which greatly limits their further application. For example, the self-healing of dynamic hydrogels based on phenylboronic esters requires acid conditions (pH 4.2) [91], which is not beneficial for drug stability and cell viability. Radical bond exchanges, e.g. radical thiyl-allyl sulfide and radical disulfide exchanges, possess advantages such as thermally induction and photo-initiation, but the reversibility of hydrogel networks are limited because of the unavoidable radical termination [85]. Moreover, alkaline environment (pH 9) is needed for promoting the reversibility of dynamic linkages in hydrogel based on disulfide bonds [92]. The synthetic routes and biocompatibility of these hydrogels should also be taken into account. Although Diels-Alder reaction has been widely studied, specific diene and dienophile are required in this reaction [93], which might introduce some

toxicity. In the case of hydrogels crosslinked by dynamic acylhydrazone bonds, the reaction is quite slow in neutral conditions [94, 95]. In contrast, imine bond appears most attractive as it is more active than acylhydrazone bonds. Moreover, imine bond can be formed in mild reaction environment, and exhibit outstanding dynamic reversibility which depends on the solvent, pH, temperature, and imine structure [96, 97].

Therefore, it seems challenging to formulate autonomous self-healing hydrogels with prominent biocompatibility for biomedical and pharmaceutical applications, without requirement of external triggers. Hereby, this thesis will explore the potential of imine bond for the synthesis of dynamic hydrogels and their applications in tissue engineering and drug delivery.

1.3 Raw materials for preparation of hydrogels

The raw materials used to fabricate hydrogels are generally hydrophilic polymers, including both natural and synthetic polymers.

1.3.1 Natural polymers

Natural polymers, also called biopolymers [98] are a class of polymers from natural origins, mainly including polysaccharides (e.g., chitosan, alginate, cellulose, hyaluronic acid, etc.), and proteins (gelatin, collagen). Owing to their abundant availability, renewable resources, eco-friendly properties, low cost, and biocompatibility, a great deal of work has been done to explore the biological and chemical properties of natural polymers for applications as biomaterials [99, 100], biosensors [101], polymeric membrane [102], food packaging [103, 104], etc.

1.3.1.1 Alginate

Alginate is an anionic polysaccharide derived from brown seaweed. It belongs

to the family of linear copolymers comprising blocks of (1,4)-linked β -D-mannuronate (M) and α -L-guluronate (G) residues, including consecutive G residues (GGGGGG), consecutive M residues (MMMMMM), and alternating M and G residues (GMGMGM) [105], as shown in Figure 1.15.

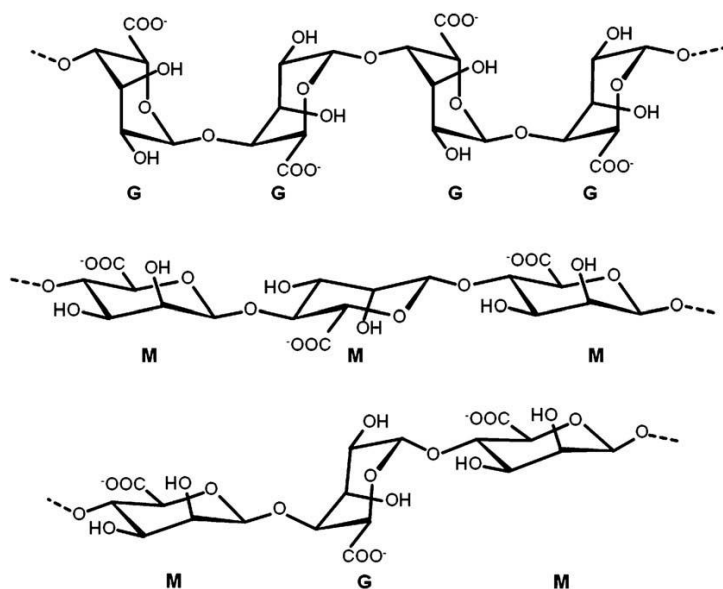


Figure 1.15 Chemical structure of G-block, M-block, and alternating block in alginate [105].

Alginate-based hydrogels can be synthesized through different cross-linking methods. The most widely used method is simply addition of divalent cations such as Ca^{2+} ion [106]. The structure of alginate-based hydrogels is similar to extracellular matrices of living tissues. As a consequence, they have been wide applied in wound healing [107], delivery of drugs or proteins [108, 109], and tissue regeneration [110] as well.

1.3.1.2 Dextran

Dextran is a polysaccharide which consists of 1,6-linked D-glucopyranose residues [112], as shown in Figure 1.16. It presents many advantages such as low tissue toxicity, degradability, etc. Therefore, dextran-based hydrogels have received much attention, and been extensively used as a prominent matrix for controlled delivery of drugs [113] or cells [114].

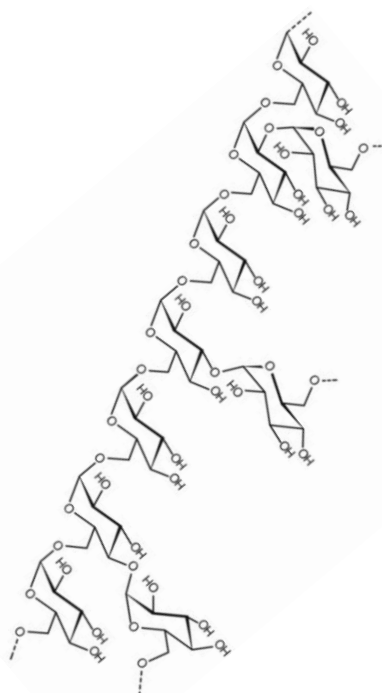


Figure 1.16 Part of the α -(1 \rightarrow 6)-linked glucose main chain of dextran with branching points in 2-, 3- and 4-positions [111].

1.3.1.3 Cellulose and carboxymethyl cellulose

Native cellulose is the naturally occurring polymer composed of 1 \rightarrow 4 linked β -D-glucose residues, as shown in Figure 1.17. It is the most abundant biopolymer and the major component of many plants. Cellulose is insoluble in water and common organic solvents due to strong intermolecular and intramolecular hydrogen bonding. Chemical modification of cellulose such as etherification or esterification leads to cellulose derivatives with improved solubility, including hydroxypropyl methyl cellulose (HPMC), methyl cellulose (MC), hydroxyethyl cellulose (HEC), ethyl cellulose (EC), and carboxymethyl cellulose (CMC). Taking CMC as example, has excellent combination capacity with metal ions due to the presence of a large number of carboxyl groups [115]. Therefore, in the presence of transition metal ions such as Fe^{3+} , the carboxyl groups in CMC side chains can coordinate with metal ions and thus form hydrogels [116]. CMC has been used for many applications, mostly as additives in food and

pharmaceutical industries [117]. Moreover, due to the natural amphoteric electric-sensitive property, CMC-based hydrogels have been used in microsensor and actuator applications [118].

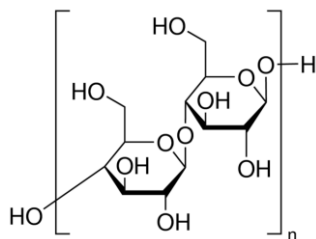


Figure 1.17 Chemical structure of native cellulose.

1.3.1.4 Hyaluronic acid

Hyaluronic acid (HA) is the most popular glycosaminoglycan which is naturally highly charged. It has a long, unbranched polysaccharide chain with repeating disaccharides of D-glucuronic and N-acetyl-D-glucosamine [119], as shown in Figure 1.18. It was first obtained from the vitreous body of the bovine eye by Karl Meyer and John Palmer in 1934 [120]. HA is biocompatible, non-toxic, non-immunogenic, non-inflammatory, and degradable by native enzymes [121]. Therefore, it has been used for various medical applications including arthritis treatment, wound dressing, ocular surgery, and tissue regeneration [122]. HA also has received much attention as a biopolymer for drug delivery system development because of its mucoadhesive property and biocompatibility. It has been used as a drug carrier in both non-parenteral and parenteral administrations. The former includes ocular and nasal delivery systems, and the latter includes sustained release formulations of protein drugs through subcutaneous injection. Furthermore, the functional groups of hyaluronic acid, including, hydroxyl, carboxyl, and N-acetyl are generally can be chemically modified for biomedical applications, especially as drug carrier for targeted drug delivery [123].

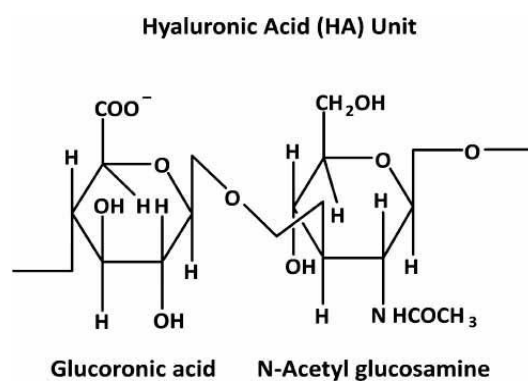


Figure 1.18 Chemical structure of hyaluronic acid (HA) [124].

1.3.1.5 Gelatin

Gelatin is obtained from thermal denaturation or from physical and chemical degradation of collagen, a protein of animal origin. Gelatin is composed of both hydrophobic (proline, leucine, etc.) and hydrophilic (serine, arginine, etc.) amino acids (Figure 1.19), which gives them an amphiphilic character [125]. It is the only protein capable of forming a thermo-reversible and elastic gel [126].

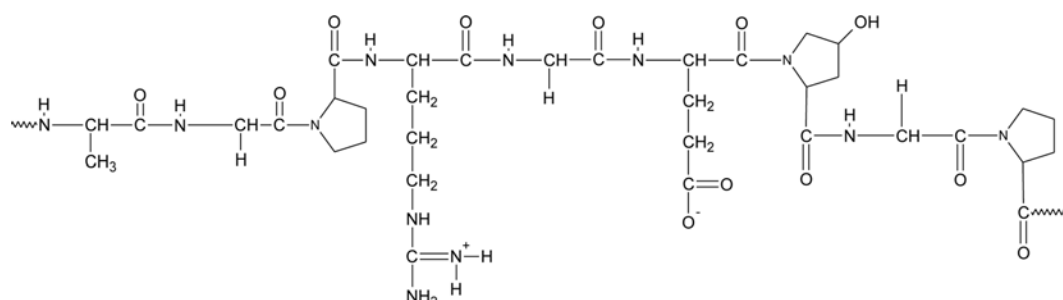


Figure 1.19 Representation of gelatin chemical structure [130].

Gelatin is considered as an excellent material in regenerative medicine because of its good biocompatibility with respect to the cellular medium, good biodegradability, and low antigenicity. It has been shown that a gelatin dressing treatment combined with injectable gelatin microcryogels loaded with cells could facilitate the wound healing process [127]. Gelatin-based hydrogels have also been used for other applications [128], especially in pharmaceutical industry due to its viscoelastic and biological properties [129].

1.3.1.6 Chitosan

Chitin is an acetylated polysaccharide made by N-acetyl-d-glucosamine groups, which are linked by a $\beta(1 \rightarrow 4)$ linkage. It is the second most abundant biopolymer produced in nature after cellulose, which ubiquitously exists in arthropod exoskeleton [132]. As chitin is insoluble in most solvents, its partial deacetylation yields a readily soluble derivative, i.e., chitosan, as shown in Figure 1.20 Chitosan is a linear polysaccharide comprising $\beta(1 \rightarrow 4)$ linked D-glucosamine residues with a variable number of randomly distributed N-acetylglucosamine groups [132], as shown in Figure 1.21.

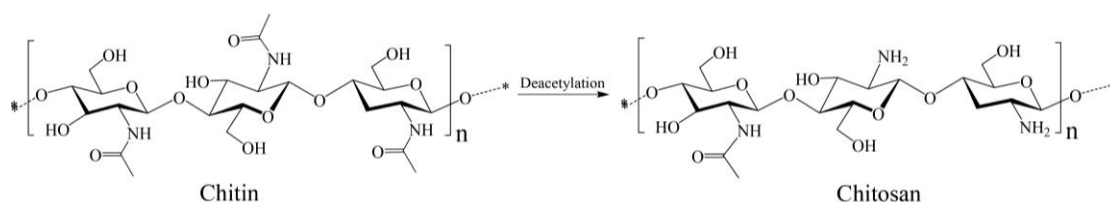


Figure 1.20 Preparation of chitosan by deacetylation of chitin [131].

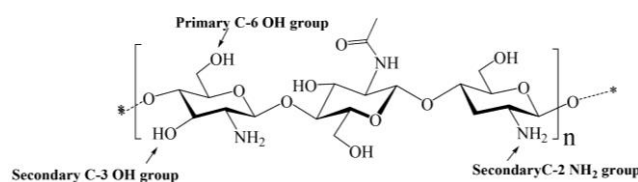


Figure 1.21 Chemical structure of chitosan [131].

Chitosan is a semi-crystalline polymer, and the degree of crystallinity is a function of the degree of deacetylation [132]. As a linear polyelectrolyte in acidic conditions, chitosan is soluble in acidic medium and can interact with polyanionic counterions [133]. Moreover, the amino groups along chitosan chains tend to react with compounds containing aldehydes. Hence, it can form gels with glutaraldehyde and even with a number of multivalent anions [134]. However, chitosan is insoluble in neutral or alkaline solutions, which considerably limits its applications in different fields.

Therefore, great efforts have been devoted to the modification of chitosan so as to enlarge the range of applications. In fact, the hydroxyl and acetyl side

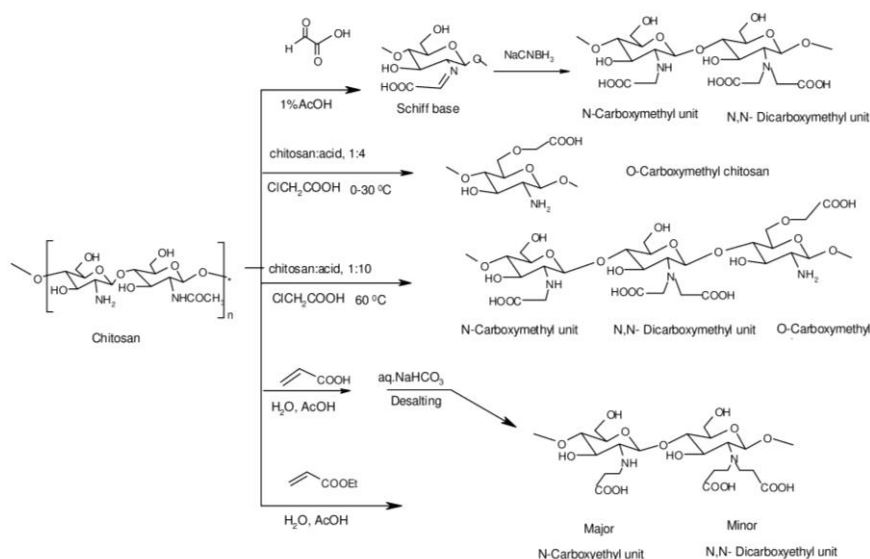


Figure 1.23 Carboxymethylation and carboxyethylation of chitosan [136].

O-CMCS exhibits excellent performance on the modulation of cell functioning. Inouye and co-workers introduced O-CMC into PDLLA films. The introduction of O-CMCS not only improved the hydrophilicity of polymer film, but also facilitated the interaction between PDLLA surface and negatively-charged cell membrane surface [137]. Moreover, the blood compatibility could be improved via introduction of O-CMCS into the Dacron vascular grafts [138].

CMCS also displays excellent antibacterial ability similar to the parent chitosan. The antibacterial activity of chitosan and CMCS is dependent on the effective number of -NH^{3+} groups [139]. Noticeably, the antibacterial activity was demonstrated to increase in the order following: NO-CMC < chitosan < O-CMCS [136]. In the case of CMCS, the substitution occurs at -OH active sites only, and thus the number of -NH_2 is the same as that in chitosan [136]. Moreover, there are intra- or intermolecular interactions between the -COOH groups and -NH_2 groups. The latter are thus charged. Therefore, in the same condition, O-CMCS has a larger number of -NH^{3+} groups than parent chitosan. Besides, NO-CMCS exhibited lower antibacterial ability due to the partial substitution of -NH_2 groups.

CMCS has also been used in drug delivery due to its good solubility and

aggregation properties. Various CMCS-based drug delivery systems have been developed to deliver anticancer, antibacterial, antifungal, anti-inflammatory drugs as well as peptides, proteins, DNAs and genes [140]. According to Donnan membrane equilibrium theory [141], the swelling performance of CMCS based hydrogel is highly dependent on osmotic pressure difference between the media inside and outside the gel. Therefore, constructing a swelling-controlled drug delivery system seems to be an attractive strategy. Vaghani et al. prepared a CMCS-based hydrogel for colon targeted delivery of ornidazole [142]. The hydrogel showed exceptional pH-dependent swelling and drug release at pH values of 6.8 and 7.4, demonstrating that such hydrogels were suitable for targeted drug delivery. More recently, Jiang's group reported a CMCS-based hydrogel for phenolphthalein (PhP) release [143]. A sustained drug delivery behavior was observed.

As discussed above, although chitosan presents interesting properties, its broad applications are greatly restrained due to its poor solubility in most solvents. Therefore, it is necessary to improve its solubility in aqueous medium by chemical modification. Carboxymethylation is an attractive method as CMCS-based materials exhibit improved properties, including moisture retention, membrane forming, flocculating, chelating and sorption properties [136], and are thus promising for uses in biomedical fields as drug carrier, antibacterial material, and tissue engineering scaffold. Moreover, CMCS has numerous functional groups which allow further modifications using various methods such as Schiff-base reaction [144]. Therefore, CMCS was selected as raw material for the conception of novel dynamic hydrogels in this thesis.

1.3.2 Synthetic polymers

Besides natural polymers, a number of synthetic polymers are also used in the preparation of hydrogels, such as poly(ethylene glycol) (PEG), poly(vinyl alcohol) (PVA), polyacrylamide (PAM), poly(N-isopropylacrylamide) (PNIPAAm),

poly(acrylic acid) (PAA), Jeffamine, and so forth. Noticeably, synthetic materials that can be used as a component of hydrogel for biomedical applications should fulfill some requirements [145], including biocompatibility, biodegradation or bio-resorption, non-toxicity, and appropriate mechanical properties.

1.3.2.1 Poly(vinyl alcohol) (PVA)

Poly(vinyl alcohol) (PVA) is a hydrophilic polymer with a simple chemical structure. It is produced by partial or full hydrolysis of poly(vinyl acetate) to remove the acetate groups [147], as shown in Figure 1.24. The basic properties of PVA depend on its degree of polymerization, degree of hydrolysis, and distribution of OH groups. PVA is used mainly in aqueous solutions. The degree of hydrolysis has the most significant effect on the solubility. Hydrogen bonding between the intra- and intermolecular hydroxyl groups decreases its solubility in water. Aqueous solutions of PVA with a high degree of hydrolysis increase in viscosity with time and concentration, and may finally gel.

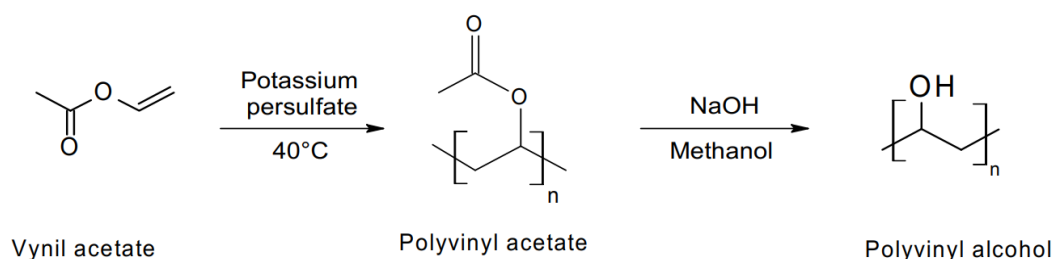


Figure 1.24 Conventional synthesis route of poly(vinyl alcohol) (PVA) [146].

The high hydroxyl group contents provide PVA and PVA-based materials many desired properties, including biocompatibility, nontoxicity, non-carcinogenicity, non-immunogenicity and inertia in body fluids [148]. Because of its high-water content, high oxygen permeability, high optical clarity, and low protein adsorption, PVA hydrogel finds new applications in the manufacturing of soft contact lenses [149]. High mechanical strength, rubber-like elasticity and no adhesion to surrounding tissue make PVA gels potential materials for soft tissue replacements, artificial cartilage, and other artificial organs [150]. PVA gels with

unique semicrystalline structure exhibited controlled dissolution behavior of drugs [151]. Non-immunogenic characteristics of PVA gels were investigated for accelerating wound healing and anti-postoperative adhesion [152].

1.3.2.2 Poly(N-isopropylacrylamide) (PNIPAAm)

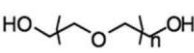
In recent decades, another synthetic polymer frequently used in hydrogel preparation is poly(N-isopropylacrylamide) (PNIPAAm) which contains both hydrophilic amide (-CONH-) groups and hydrophobic isopropyl (-CH(CH₃)₂) side chains [153]. PNIPAAm is the most studied thermo-responsive polymer with a lower critical solution temperature (LCST) at 32 °C where it exhibits a sharp phase transition from hydrophilic coils to hydrophobic globules. Hence, PNIPAAm solutions present a sol state at room temperature while transform into a gel state when the temperature increases to above the LCST or to the body temperature [154]. This attractive feature of PNIPAAm makes it a good candidate for applications in versatile biomedical domains as matrix for drug delivery [155], scaffolds for tissue engineering [156], and wound dressing [157], etc.

Nevertheless, PNIPAAm-based hydrogels also present some inherent drawbacks [158, 159], including, bad biodegradability, weak mechanical strength, low drug loading efficiency, which highly limit their further applications [160].

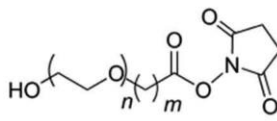
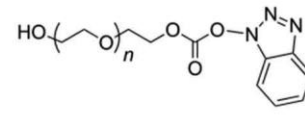
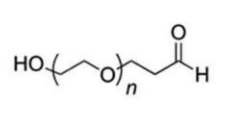
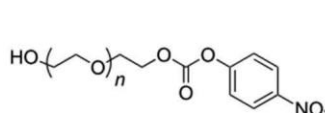
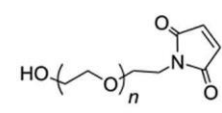
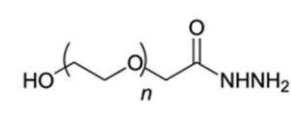
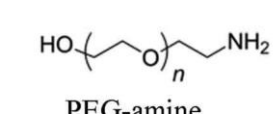
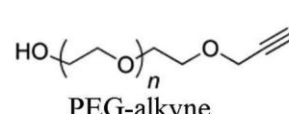
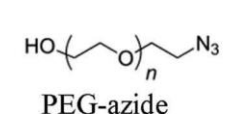
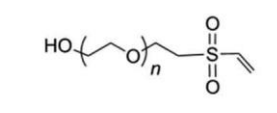
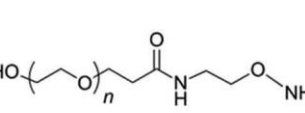
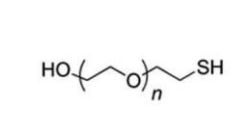
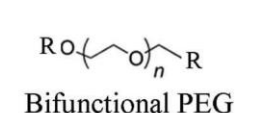
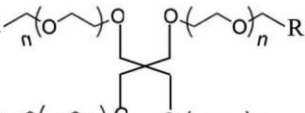
1.3.2.3 Poly(ethylene glycol) (PEG)

PEG is a polyether composed of repeated ethylene oxide units $[-(\text{CH}_2\text{CH}_2\text{O})_n]$ [161], as shown in Figure 1.25. PEG is a cheap, neutral, water soluble and biocompatible polymer with good hydrolytic resistance. The water solubility of PEG results from the strong tendency to form hydrogen bonds with water via -O- groups. The hydrophilic character with surface-wetting properties is especially important for the prevention of protein adsorption and the blood compatibility in biomedical applications.

Parent PEG

$(C_2H_4O)_{n+1}H_2O$		$CH_3O-(CH_2CH_2O)_n-R$
Chemical formula	Chemical structure	Methoxy PEG (mPEG)

PEG derivatives

		
PEG-NHS ester	PEG-Benzotriazole carbonate	PEG-aldehyde
		
PEG-p-nitrophenylcarbonate	PEG-maleimide	PEG-hydrazide
		
PEG-amine	PEG-alkyne	PEG-azide
		
PEG-vinyl sulfone	PEG-aminoxy	PEG-thiol
		
Bifunctional PEG	Tetrafunctional PEG	

n indicates number of oxyethylene groups

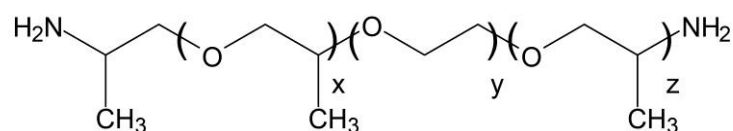
Figure 1.25 Chemical structure of PEG and its derivatives [161].

PEG has been approved by the US Food and Drug Administration (FDA), and is probably the most widely applied synthetic polymer in the domains of biotechnology, pharmacology, and medicine. As mentioned in the hydrogel section, PEG-based hydrogels are generally obtained by chemical bonding between PEG chain ends and other polymer functional groups. Due to the beneficial characteristics of PEG, such as high hydrophilicity, bio-inertness, and outstanding biocompatibility, PEG has been used in the formulation of hydrogels for drug delivery [162], gene delivery [163], tissue engineering

scaffolds [164], etc. It is also noteworthy that, in last decade, many PEG derivatives (Figure 1.25) have been synthesized for various biomedical applications [161].

1.3.2.4 Jeffamine

Historically, Jeffamine is a polyetheramine which mainly exists in the form of monoamines, diamines, and triamines, based on its core structure. Because of the particularity of its structure, hydrophilic or amphiphilic block copolymers with various geometrical structures can be obtained via combining Jeffamine with a hydrophilic block [165].



JEFFAMINE®	y	x + z
ED-600 (XTJ-500)	~9.0	~3.6
ED-900 (XTJ-501)	~12.5	~6.0
ED-2003 (XTJ-502)	~39	~6.0

Figure 1.26 Chemical structure of Jeffamine ED series.

Jeffamine ED series are biocompatible polyetheramines comprising of poly(propylene oxide) (PPO) and poly (ethylene oxide) (PEO) blocks terminated with two primary amino groups, as shown in Figure 1.26. The three members of the Jeffamine ED series, namely Jeffamine ED600, Jeffamine ED900, and Jeffamine ED2003 have a PPO/PEO molar ratio of 3.6/9, 6/12.5, and 6/39, respectively. They are water soluble because of the presence of a predominant PEG backbone, enabling them to be used as a hydrophilic component for manufacturing hydrophilic or amphiphilic materials.

Jeffamine products inherit the benefits of PEG, including low color and vapor pressure, water solubility, and good biocompatibility [166]. Moreover, the reactivity of the primary amine end groups allows reactions to yield block

copolymers or polymeric networks. In fact, Jeffamine has been reported for micelles synthesis [165], hydrophilic block copolymers [166], hydrogel [167], dendrimers [168], etc. However, Jeffamine ED series have been rarely studied for dynamic hydrogel preparation. In this thesis, Jeffamine ED600, Jeffamine ED900, and Jeffamine ED2003 are selected as one of the components in the formulation of dynamic hydrogels.

1.4 Biomedical applications of hydrogels

Hydrogels are a unique category of materials which exhibit outstanding properties [169], including, biocompatibility, free-standing ability, water up-taking capability, tissue adhesiveness, porous structure, etc. The three-dimensional viscoelastic network allows the diffusion and the attachment of molecules and cells [170]. Therefore, since the pioneering work of Wichterle and Lim in 1960 on crosslinked HEMA hydrogels for biological use [1], versatile applications of hydrogels have been booming, including injectable implants, disposable diapers, contact lenses, biosensors, wound dressing, drug vectors, and scaffolds in tissue engineering. Among these various applications, biomedical applications of hydrogels, in particular in cartilage engineering and drug delivery, have been most widely investigated in the past decades [170, 171].

1.4.1 Cartilage engineering

Hydrogels present great potential as 3D cell culture scaffolds in cartilage and tissue engineering [172] because of their excellent water maintaining ability, high similarity to natural extracellular matrix (ECM), porous architecture for cell transplantation-differentiation-proliferation, non-toxicity, and adaptability to fill irregular defects. Therefore, injectable hydrogels have been widely used in cartilage and bone tissue engineering.

Osteoarthritis is a degenerative joint disease which affects over 50% of adults

aged 65 years and older, and is characterized by progressive loss of hyaline cartilage in synovial joints. Accidental traumas induce cartilage focal lesions that can also reach the sub-chondral bone, leading to post-traumatic osteoarthritis which requires joint arthroplasty. This surgery is not proposed to young patients because of the relatively short half-life of prostheses. Cartilage and bone tissue engineering is thus considered as an alternative therapy.

In a pioneer work in 1977, Green proposed the concept of a tissue engineering approach to address the issue of articular cartilage repair [173]. The first clinical application of tissue engineering was conducted in 1994 by Mats Brittberg and co-workers who performed treatment of deep cartilage defects in the knee with autologous chondrocyte transplantation [174]. Since the early 90s of last century, tissue engineering has become one of the most frequently used strategies for cartilage and bone tissue reconstruction and regeneration [175]. In general, tissue engineering involves a scaffold, cells, and appropriate growth factors. The scaffold should be biocompatible and biodegradable, and should retain sufficient mechanical strength to support the growing tissue until it matures. With the development of materials science, numerous biomaterials have been studied in cartilage tissue engineering [176, 177]. Among them, hydrogels have attracted much attention due to their similar structure with the extracellular matrix (ECM). Furthermore, their porous framework allows cell diffusion, differentiation and proliferation [9]. Theoretically, a hydrogel scaffold mimics the ECM and matches the damaged defects, favors the migration, adhesion, proliferation, and differentiation of chondrocytes and osteoprogenitor cells to osteoblasts, efficiently delivers nutrients and growth factors, and ultimately achieve the cartilage repair [178, 179], as shown in Figure 1.27.

Therefore, seeking appropriate strategies to synthesize injectable hydrogels for cartilage engineering is attractive and promising. In this thesis, a series of dynamic, injectable and self-healing hydrogels are prepared and further applied in cell encapsulation and culture for cartilage repair.

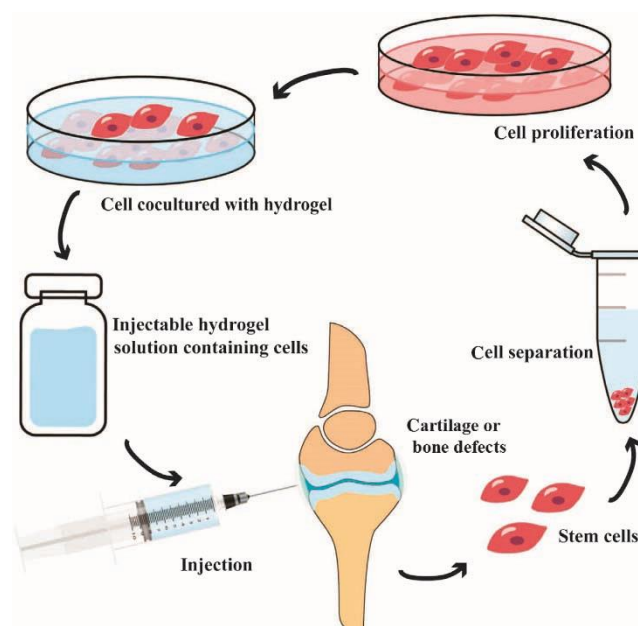


Figure 1.27 Schematic illustration of cartilage and bone tissue engineering using hydrogel scaffold [171].

1.4.2 Drug delivery

Cancer is the leading cause of death and the most important barrier to increasing life expectancy in the world [180]. Based on a status report of the International Agency for Research on Cancer, there were an estimated 18.1 million new cancer cases and 9.6 million cancer deaths in 2018. Traditional cancer treatments include surgery, chemotherapy and radiotherapy. As is well known, many traditional chemotherapeutic drugs present serious side effects, which greatly restrains their potential applications in cancer treatment. Well defined drug carriers with encapsulated or conjugated drugs present great interest as they allow to improve the therapeutic efficiency and to reduce the side effects. At the same time, drug carriers also protect the drugs from biodegradation or excretion.

Over the past decades, there has been enormous advances in cancer treatment using various drug delivery systems (DDSs) , including nanoparticles, micelles, liposomes, and hydrogels. Nano-carriers allow passive drug targeting due to the enhanced permeability and retention (EPR) effect which promotes

their accumulation in tumor tissues. Nevertheless, they also present disadvantages such as burst release, poor bio-adhesion, and irreversible deformation [181]. In contrast, hydrogels appear as an attractive alternative to nano-carriers of antitumor drugs, especially in the case of local drug delivery [182]. In this thesis, dynamic hydrogels are used for sustained drug release.

1.4.2.1 Hydrogel drug delivery systems

Hydrogels can act as a matrix on which many physiochemical interactions with the loaded drugs exist. Hydrogels can realize sustained drug release, owing to their adjustable physical properties, suitable degradability, and ability to protect labile drugs from degradation [183].

As mentioned above, hydrogel generally presents high water content (typically 70-99%), which allows to encapsulate hydrophilic drugs. Owing to the fact that the hydrogels are typically prepared in aqueous solutions, the risk of drug denaturation and aggregation upon exposure to organic solvents is minimized [183]. Furthermore, for *in situ* drug loaded hydrogel system, the drug encapsulation efficiency is very high as compared to conventional drug carriers. In addition, the crosslinked polymeric framework endows hydrogels with tunable mechanical properties, enabling their physico-chemical properties to be adapted to soft tissues in the human body [184, 185]. Apart from providing the mechanical strength, the polymeric network of hydrogel also can hinder penetration of various proteins [186], thus preventing bioactive therapeutics from immature degradation by inwards diffusing enzymes. All these properties of hydrogels make them good candidate materials for sustained release of various drugs, including both hydrophobic and hydrophilic drugs, have great potential in clinical uses [187].

As shown above, hydrogels can be categorized in macroscopic gels, microgels (0.5-10 μm), and nanogels (<200 nm), based on their size and appearance [6]. Noticeably, the size of a hydrogel determines the delivery route. In other words,

different delivery routes require different hydrogels, as shown in Figure 1.28. Nanogels are generally administered by systemic route, whereas microgels are delivered by pulmonary or oral route. In contrast, macroscopic hydrogels can be delivered in the human body by local injection, or in the form of transdermal patch, epicardial patch, etc. Macroscopic hydrogels made from alginate or chitosan have been widely used for wound dressing. Adaptivity of these hydrogels have been explored for transdermal drug delivery to deliver proteins [188, 189], such as, bovine serum albumin (BSA) and diclofenac sodium (DS). Some of them are being examined in clinical trials [183]. Furthermore, great efforts have been devoted to develop injectable hydrogels, especially in-situ gelling hydrogels since surgical implantation is invasive and could result in patient's resistance [190]. It is worthy to note that the manufacture of macroscopic hydrogels can be upscaled, and the approaches involved are more eco-friendly as compared with some special nanogels [191]. Therefore, in this thesis, a series of injectable macroscopic hydrogels are synthesized and investigated for drug delivery.

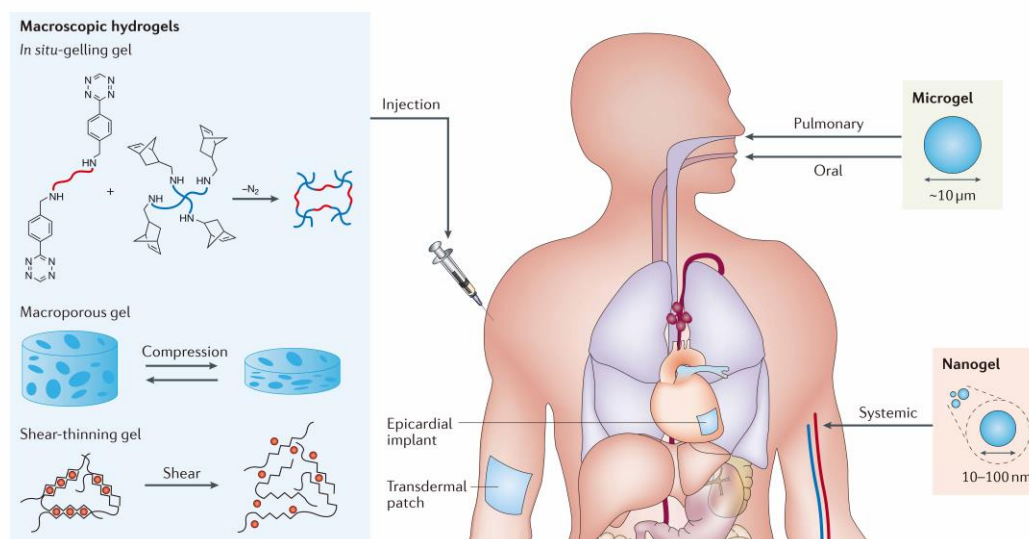


Figure 1.28 Macroscopic design determines the delivery route [183].

1.4.2.2 Anti-cancer drugs

Chemotherapy has been used to treat cancer since the 1940s. From then on, a number of anticancer drugs has been developed, including paclitaxel (PTX), curcumin, 5-Fluorouracil (5-Fu), doxorubicin (DOX), thymopentin (TP5), etc.

Paclitaxel (PTX) is a natural anti-cancer drug extracted from the bark of the pacific yew tree *Taxus brevifolia*. Since its approval by the U.S. Food and Drug Administration (FDA) for advanced ovarian cancer treatment in 1992, the clinical applications of PTX have been continuously growing [192]. Nowadays, PTX is considered as one of the most efficient anti-cancer drugs for the treatment of a variety of tumors, especially ovarian cancer, acellular lung cancer and metastatic breast cancer. It is noteworthy that PTX is a highly hydrophobic drug. The commonly used drug formulations of PTX are Taxol® and Abraxane®. The former is a co-solvent formulation composed of 50:50 Cremophor EL and dehydrated alcohol which allows to improve the bioavailability of PTX. And Abraxane® is an injectable formulation of albumin-bound paclitaxel nanoparticles which gained more and more importance in the past years, largely exceeding Taxol® in clinical uses [193].

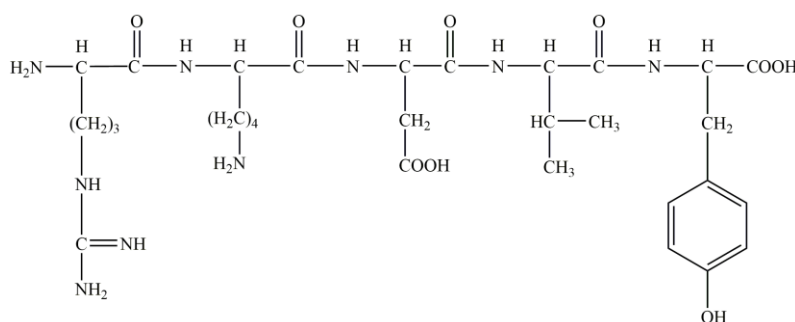


Figure 1.29 Structural formula of thymopentin (TP5).

Thymopentin (TP5) is a highly hydrophilic immunostimulant largely used in chemotherapy. TP5 is a synthetic pentapeptide (Arg-Lys-Asp-Val-Tyr, Mw = 679.77) comprising the residual sequence (32-36) of thymic hormone thymopoietin [194]; Its chemical structure is shown in Figure 1.29. TP5

conserves most of the biological activities of thymopoietin [195]. Therefore, as an approved drug, TP5 has been clinically used in immune enhancement [196], and in treatment of immune-related diseases such as cancers [197], acquired immunodeficiency syndrome (AIDS) [198], and autoimmune diseases [199]. Additionally, it has already been proven that TP5 can recover antibody production in old mice [200], enhance the antibody response in humans when it is used percutaneously 3 times a week at doses of 50 mg [201], and act as an assistant therapy for non - responders or hypo-responders to hepatitis B vaccination [202]. Therefore, TP5 presents great potential in anticancer, antitumor, and autoimmune diseases.

Noticeably, due to the existence of active amino groups TP5 can react with other functional groups such as carboxylic or aldehydes groups, which allows covalent attachment of TP5 to drug carriers. Hence, TP5 was selected in this thesis to evaluate the potential of dynamic hydrogels as carrier of hydrophilic drugs.

1.5 Summary and work plan

To sum up, hydrogels are three-dimensional networks consisting of hydrophilic polymeric chains, which have the ability to up-take a large quantity of water up to hundreds of times of their dry weight while maintaining their structural integrity. With the booming development of hydrogels in recent decades, dynamic hydrogels are appealing and have received much attention. Dynamic hydrogels are obtained by dynamic covalent bonds (DCBs), including Diels-Alder reaction, hydrazide-acylhydrazone bond, imine bond, etc. Among the various dynamic bonds, imine bond is most attractive because the reaction to generate imines is one of the oldest and most ubiquitous reactions in organic chemistry. Additionally, the reaction conditions of imine chemistry are mild and simply controllable. To the best of our knowledge, dynamic hydrogel based on imine bonds between O-carboxymethyl chitosan (O-CMCS), Jeffamine and

benzene-1,3,5-tricarbaldehyde (BTA) have never been reported.

O-CMCS is a typical derivative of chitosan which exhibits prominent biological properties such as enhanced moisture retention capability, high antimicrobial ability, antitumor ability, anticancer ability, antioxidant ability, antifungal activities, non-toxicity, biodegradability and biocompatibility. Moreover, O-CMCS is easily soluble in aqueous medium. Benzene-1,3,5-tricarbaldehyde (BTA) is a promising cross-linker for the formulation of dynamic hydrogels based on imine bonding as it can act as a tri-topic center for three-dimensional cross-linking with di-amino polymers. However, BTA is insoluble in water, which prevents its applications in aqueous medium. Fortunately, Schiff-base reaction of BTA with Jeffamine, a water soluble and biocompatible polyetheramine consisting of PPO and PEO blocks terminated with primary amino groups, yields a water-soluble 3D dynamer which can be further used to synthesize dynamic hydrogels by similar Schiff-base reaction.

The aim of this work was to synthesize dynamic O-CMCS based hydrogel by crosslinking through dual imine bonding and to apply the resultant hydrogels in three different fields, *i.e.*, cartilage cell encapsulation and culture, antibacterial membrane design, and hydrophilic anticancer drug release. Three CMCS with different molar masses were involved, including original CMCS and two CMCS oligomers obtained by depolymerization of CMCS in the presence of H₂O₂. Three commercial Jeffamine products were used, *i.e.*, Jeffamine ED 600, Jeffamine ED900, and Jeffamine ED2003. Typically, Jeffamine first reacts with BTA in methanol under reflux conditions at 70 °C. Methanol is then removed via rotary evaporation, followed by addition of Milli-Q water to form a homogeneous dynamer (Dy) aqueous solution. Finally, the CMCS and Dy aqueous solutions were mixed with gentle stirring at 37 °C to form a three-dimensional hydrogel network through imine bonding., also known as Schiff-base reaction. All the as-prepared dynamic hydrogels and precursors were characterized by FT-IR, NMR, SEM, rheometer, etc. The influence of molar ratio of CMCS/Dy, Jeffamine

molar mass, and CMCS molar mass on the physico-chemical properties were examined and discussed. Two kinds of human cells, namely human mesenchymal stromal cells (MSCs) isolated from subcutaneous adipose tissue (AT-MSCs) and from bone-marrow (BM-MSCs), were encapsulated inside the as-prepared hydrogel. The cell viability was investigated to evaluate the potential of dynamic hydrogel in cartilage engineering. The antibacterial activity of membranes prepared from as-prepared hydrogels against a non-pathogenic strain of *Escherichia coli* was assessed using liquid test and agar test. Finally, a novel drug delivery system was developed from the dynamic hydrogel by encapsulation of a hydrophilic anti-cancer drug, TP5, by both physical mixing and covalent bonding. The drug release properties were comparatively studied by considering various factors. Furthermore, the density functional theory (DFT) of computational chemistry was applied to calculate the energy barriers of the different imine bonds in the drug loaded hydrogel system so as to confirm the experimental data.

References

- [1] O. Wichterle, D. Lim, Hydrophilic gels for biological use, *Nature* 185(4706) (1960) 117-118.
- [2] E. Lee, S. Kim, S. Kim, J. Cardinal, H. Jacobs, Drug release from hydrogel devices with ratecontrolling barriers, *J. Membr. Sci.* 7(3) (1980) 293-303.
- [3] S.-H. Hyon, W.-I. Cha, Y. Ikada, Preparation of transparent poly (vinyl alcohol) hydrogel, *Polymer bulletin* 22(2) (1989) 119-122.
- [4] T. Miyata, N. Asami, T. Uragami, A reversibly antigen-responsive hydrogel, *Nature* 399(6738) (1999) 766-769.
- [5] F. Ullah, M.B.H. Othman, F. Javed, Z. Ahmad, H.M. Akil, Classification, processing and application of hydrogels: A review, *Materials Science Engineering: C* 57 (2015) 414-433.
- [6] Z. Sun, C. Song, C. Wang, Y. Hu, J. Wu, Hydrogel-based controlled drug

delivery for cancer treatment: a review, *Mol. Pharm.* (2019).

[7] K. Varaprasad, G.M. Raghavendra, T. Jayaramudu, M.M. Yallapu, R. Sadiku, A mini review on hydrogels classification and recent developments in miscellaneous applications, *Materials Science Engineering: C* 79 (2017) 958-971.

[8] M. Hamidi, A. Azadi, P. Rafiei, Hydrogel nanoparticles in drug delivery, *Adv. Drug Del. Rev.* 60(15) (2008) 1638-1649.

[9] B.V. Slaughter, S.S. Khurshid, O.Z. Fisher, A. Khademhosseini, N.A. Peppas, Hydrogels in regenerative medicine, *Adv. Mater.* 21(32 - 33) (2009) 3307-3329.

[10] Z. Feng, H. Zuo, W. Gao, N. Ning, M. Tian, L. Zhang, A Robust, Self - Healable, and Shape Memory Supramolecular Hydrogel by Multiple Hydrogen Bonding Interactions, *Macromolecular rapid communications* 39(20) (2018) 1800138.

[11] Y. Guo, X. Zhou, Q. Tang, H. Bao, G. Wang, P. Saha, A self-healable and easily recyclable supramolecular hydrogel electrolyte for flexible supercapacitors, *Journal of Materials Chemistry A* 4(22) (2016) 8769-8776.

[12] S. Liu, M. Jin, Y. Chen, H. Gao, X. Shi, W. Cheng, L. Ren, Y. Wang, High internal phase emulsions stabilised by supramolecular cellulose nanocrystals and their application as cell-adhesive macroporous hydrogel monoliths, *Journal of Materials Chemistry B* 5(14) (2017) 2671-2678.

[13] Q. Ding, X. Xu, Y. Yue, C. Mei, C. Huang, S. Jiang, Q. Wu, J. Han, Nanocellulose-mediated electroconductive self-healing hydrogels with high strength, plasticity, viscoelasticity, stretchability, and biocompatibility toward multifunctional applications, *ACS applied materials & interfaces* 10(33) (2018) 27987-28002.

[14] N.A. Peppas, S.R. Stauffer, Reinforced uncrosslinked poly (vinyl alcohol) gels produced by cyclic freezing-thawing processes: a short review, *J. Controlled Release* 16(3) (1991) 305-310.

[15] S.R. Stauffer, N.A. Peppast, Poly (vinyl alcohol) hydrogels prepared by

freezing-thawing cyclic processing, *Polymer* 33(18) (1992) 3932-3936.

[16] N. Vrana, A. O'Grady, E. Kay, P. Cahill, G. McGuinness, Cell encapsulation within PVA - based hydrogels via freeze - thawing: a one - step scaffold formation and cell storage technique, *Journal of tissue engineering regenerative medicine* 3(7) (2009) 567-572.

[17] H. Tsuji, F. Horii, M. Nakagawa, Y. Ikada, H. Odani, R. Kitamaru, Stereocomplex formation between enantiomeric poly (lactic acid) s. 7. Phase structure of the stereocomplex crystallized from a dilute acetonitrile solution as studied by high-resolution solid-state carbon-13 NMR spectroscopy, *Macromolecules* 25(16) (1992) 4114-4118.

[18] H. Tsuji, Poly (lactide) stereocomplexes: formation, structure, properties, degradation, and applications, *Macromol. Biosci.* 5(7) (2005) 569-597.

[19] S. Li, M. Vert, Synthesis, characterization, and stereocomplex-induced gelation of block copolymers prepared by ring-opening polymerization of L (D)-lactide in the presence of poly (ethylene glycol), *Macromolecules* 36(21) (2003) 8008-8014.

[20] S. Tang, L. Zhao, J. Yuan, Y. Chen, Y. Leng, Physical hydrogels based on natural polymers, *Hydrogels Based on Natural Polymers*, Elsevier2020, pp. 51-89.

[21] A.F. Thünemann, M. Müller, H. Dautzenberg, J.-F. Joanny, H. Löwen, Polyelectrolyte complexes, *Polyelectrolytes with defined molecular architecture II*, Springer2004, pp. 113-171.

[22] V.S. Meka, M.K. Sing, M.R. Pichika, S.R. Nali, V.R. Kolapalli, P. Kesharwani, A comprehensive review on polyelectrolyte complexes, *Drug Discovery Today* 22(11) (2017) 1697-1706.

[23] C.-J. Lee, H. Wu, Y. Hu, M. Young, H. Wang, D. Lynch, F. Xu, H. Cong, G. Cheng, Ionic Conductivity of Polyelectrolyte Hydrogels, *ACS applied materials & interfaces* 10(6) (2018) 5845-5852.

[24] L.-A. Tziveleka, N. Pippa, P. Georgantea, E. Ioannou, C. Demetzos, V.

Roussis, Marine sulfated polysaccharides as versatile polyelectrolytes for the development of drug delivery nanoplateforms: Complexation of ulvan with lysozyme, *Int. J. Biol. Macromol.* 118 (2018) 69-75.

[25] A.S. Michaels, Polyelectrolyte complexes, *Industrial Engineering Chemistry* 57(10) (1965) 32-40.

[26] S.N. Pawar, K.J. Edgar, Alginate derivatization: a review of chemistry, properties and applications, *Biomaterials* 33(11) (2012) 3279-3305.

[27] R. LogithKumar, A. KeshavNarayan, S. Dhivya, A. Chawla, S. Saravanan, N. Selvamurugan, A review of chitosan and its derivatives in bone tissue engineering, *Carbohydr. Polym.* 151 (2016) 172-188.

[28] A. Fallacara, E. Baldini, S. Manfredini, S. Vertuani, Hyaluronic acid in the third millennium, *Polymers* 10(7) (2018) 701.

[29] J. Zhang, Y. Zhu, J. Song, J. Yang, C. Pan, T. Xu, L. Zhang, Novel balanced charged alginate/PEI polyelectrolyte hydrogel that resists foreign-body reaction, *ACS applied materials & interfaces* 10(8) (2018) 6879-6886.

[30] M. Ishihara, S. Kishimoto, S. Nakamura, Y. Sato, H. Hattori, Polyelectrolyte complexes of natural polymers and their biomedical applications, *Polymers* 11(4) (2019) 672.

[31] J. Van der Gucht, E. Spruijt, M. Lemmers, M.A.C. Stuart, Polyelectrolyte complexes: Bulk phases and colloidal systems, *Journal of colloid interface science* 361(2) (2011) 407-422.

[32] J. You, S. Xie, J. Cao, H. Ge, M. Xu, L. Zhang, J. Zhou, Quaternized chitosan/poly (acrylic acid) polyelectrolyte complex hydrogels with tough, self-recovery, and tunable mechanical properties, *Macromolecules* 49(3) (2016) 1049-1059.

[33] M.B. Oliveira, H.X. Bastos, J.F. Mano, Sequentially moldable and bondable four-dimensional hydrogels compatible with cell encapsulation, *Biomacromolecules* 19(7) (2018) 2742-2749.

[34] S. Cohen, C. Bano, K.B. Visscher, M. Chow, H.R. Allcock, R.S. Langer,

Ionic cross-linked polymeric microcapsules, Google Patents, 1992.

[35] Y. Li, Y. Han, X. Wang, J. Peng, Y. Xu, J.J.A.a.m. Chang, Multifunctional hydrogels prepared by dual ion cross-linking for chronic wound healing, *ACS applied materials & interfaces* 9(19) (2017) 16054-16062.

[36] X. Li, H. Wang, D. Li, S. Long, G. Zhang, Z. Wu, Dual ionically cross-linked double-network hydrogels with high strength, toughness, swelling resistance, and improved 3D printing Processability, *ACS applied materials & interfaces* 10(37) (2018) 31198-31207.

[37] J. Yang, F. Xu, C. Han, Metal ion mediated cellulose nanofibrils transient network in covalently cross-linked hydrogels: mechanistic insight into morphology and dynamics, *Biomacromolecules* 18(3) (2017) 1019-1028.

[38] M. Wang, L. Luo, L. Fu, H. Yang, Ion responsiveness of polyacrylamide/sodium alginate (PAM/SA) shape memory hydrogel, *Soft Materials* 17(4) (2019) 418-426.

[39] M. Bruchet, A. Melman, Fabrication of patterned calcium cross-linked alginate hydrogel films and coatings through reductive cation exchange, *Carbohydr. Polym.* 131 (2015) 57-64.

[40] L. Li, J. Zhao, Y. Sun, F. Yu, J. Ma, Ionically cross-linked sodium alginate/k-carrageenan double-network gel beads with low-swelling, enhanced mechanical properties, and excellent adsorption performance, *Chemical Engineering Journal* 372 (2019) 1091-1103.

[41] J. Wang, T. Li, F. Chen, D. Zhou, B. Li, X. Zhou, T. Gan, S. Handschuh - Wang, X. Zhou, Softening and Shape Morphing of Stiff Tough Hydrogels by Localized Unlocking of the Trivalent Ionically Cross - Linked Centers, *Macromolecular rapid communications* 39(12) (2018) 1800143.

[42] F. Chen, D. Zhou, J. Wang, T. Li, X. Zhou, T. Gan, S. Handschuh - Wang, X. Zhou, Rational Fabrication of Anti - Freezing, Non - Drying Tough Organohydrogels by One - Pot Solvent Displacement, *Angew. Chem., Int. Ed.* 130(22) (2018) 6678-6681.

- [43] P. Lin, S. Ma, X. Wang, F.J.A.m. Zhou, Molecularly engineered dual - crosslinked hydrogel with ultrahigh mechanical strength, toughness, and good self - recovery, *Adv. Mater.* 27(12) (2015) 2054-2059.
- [44] Y. Yang, X. Wang, F. Yang, L. Wang, D. Wu, Highly elastic and ultratough hybrid ionic-covalent hydrogels with tunable structures and mechanics, *Adv. Mater.* 30(18) (2018) 1707071.
- [45] M. Rinaudo, Chitin and chitosan: properties and applications, *Progress in polymer science* 31(7) (2006) 603-632.
- [46] R. Nigmatullin, V. Gabrielli, J.C. Muñoz-García, A.E. Lewandowska, R. Harniman, Y.Z. Khimyak, J. Angulo, S.J. Eichhorn, Thermosensitive supramolecular and colloidal hydrogels via self-assembly modulated by hydrophobized cellulose nanocrystals, *Cellulose* 26(1) (2019) 529-542.
- [47] K.T. Dicker, L.A. Gurski, S. Pradhan-Bhatt, R.L. Witt, M.C. Farach-Carson, X. Jia, Hyaluronan: a simple polysaccharide with diverse biological functions, *Acta Biomater.* 10(4) (2014) 1558-1570.
- [48] A.K. Mahanta, P. Maiti, Injectable Hydrogel through Hydrophobic Grafting on Chitosan for Controlled Drug Delivery, *ACS Applied Bio Materials* 2(12) (2019) 5415-5426.
- [49] T. Jayaramudu, G.M. Raghavendra, K. Varaprasad, R. Sadiku, K.M. Raju, Development of novel biodegradable Au nanocomposite hydrogels based on wheat: For inactivation of bacteria, *Carbohydr. Polym.* 92(2) (2013) 2193-2200.
- [50] R. Tong, G. Chen, D. Pan, H. Qi, R.a. Li, J. Tian, F. Lu, M. He, Highly stretchable and compressible cellulose ionic hydrogels for flexible strain sensors, *Biomacromolecules* 20(5) (2019) 2096-2104.
- [51] C. Jiang, X. Wang, G. Wang, C. Hao, X. Li, T. Li, Adsorption performance of a polysaccharide composite hydrogel based on crosslinked glucan/chitosan for heavy metal ions, *Composites Part B: Engineering* 169 (2019) 45-54.
- [52] A. Sehlinger, M.A. Meier, Passerini and Ugi multicomponent reactions in polymer science, *Multi-component and sequential reactions in polymer*

synthesis, Springer2014, pp. 61-86.

[53] Y. Zeng, Y. Li, G. Liu, Y. Wei, Y. Wu, L. Tao, Antibacterial Self-Healing Hydrogel via the Ugi Reaction, *ACS Applied Polymer Materials* 2(2) (2019) 404-410.

[54] R. Jin, L.S.M. Teixeira, P. Dijkstra, V.B. Clemens A, K. Marcel, F. Jan, Enzymatically-crosslinked injectable hydrogels based on biomimetic dextran–hyaluronic acid conjugates for cartilage tissue engineering, *Biomaterials* 31(11) (2010) 3103-3113.

[55] Y. Zhong, J. Wang, Z. Yuan, Y. Wang, Z. Xi, L. Li, Z. Liu, X. Guo, A mussel-inspired carboxymethyl cellulose hydrogel with enhanced adhesiveness through enzymatic crosslinking, *Colloids Surfaces B: Biointerfaces* 179 (2019) 462-469.

[56] Q. Wei, J. Duan, G. Ma, W. Zhang, Q. Wang, Z. Hu, Enzymatic crosslinking to fabricate antioxidant peptide-based supramolecular hydrogel for improving cutaneous wound healing, *Journal of Materials Chemistry B* 7(13) (2019) 2220-2225.

[57] M. Zhai, F. Yoshii, T. Kume, K. Hashim, Syntheses of PVA/starch grafted hydrogels by irradiation, *Carbohydr. Polym.* 50(3) (2002) 295-303.

[58] R. Singh, D. Singh, Radiation synthesis of PVP/alginate hydrogel containing nanosilver as wound dressing, *J. Mater. Sci. Mater. Med.* 23(11) (2012) 2649-2658.

[59] R. Lozano, L. Stevens, B.C. Thompson, K.J. Gilmore, R. Gorkin III, E.M. Stewart, M. in het Panhuis, M. Romero-Ortega, G.G. Wallace, 3D printing of layered brain-like structures using peptide modified gellan gum substrates, *Biomaterials* 67 (2015) 264-273.

[60] T. Zhu, J. Mao, Y. Cheng, H. Liu, L. Lv, M. Ge, S. Li, J. Huang, Z. Chen, H. Li, Recent Progress of Polysaccharide - Based Hydrogel Interfaces for Wound Healing and Tissue Engineering, *Advanced Materials Interfaces* 6(17) (2019) 1900761.

- [61] S.J. Rowan, S.J. Cantrill, G.R. Cousins, J.K. Sanders, J.F. Stoddart, Dynamic covalent chemistry, *Angew. Chem., Int. Ed.* 41(6) (2002) 898-952.
- [62] J.N. Cambre, B.S. Sumerlin, Biomedical applications of boronic acid polymers, *Polymer* 52(21) (2011) 4631-4643.
- [63] Y. Chen, W. Qian, R. Chen, H. Zhang, X. Li, D. Shi, W. Dong, M. Chen, Y. Zhao, One-pot preparation of autonomously self-healable elastomeric hydrogel from boric acid and random copolymer bearing hydroxyl groups, *ACS Macro Lett.* 6(10) (2017) 1129-1133.
- [64] Z. Wang, F. Tao, Q. Pan, A self-healable polyvinyl alcohol-based hydrogel electrolyte for smart electrochemical capacitors, *Journal of Materials Chemistry A* 4(45) (2016) 17732-17739.
- [65] J.-M. Lehn, Dynamers: dynamic molecular and supramolecular polymers, *Progress in polymer science* 30(8-9) (2005) 814-831.
- [66] D.E. Apostolides, C.S. Patrickios, Dynamic covalent polymer hydrogels and organogels crosslinked through acylhydrazone bonds: synthesis, characterization and applications, *Polym. Int.* 67(6) (2018) 627-649.
- [67] G. Deng, C. Tang, F. Li, H. Jiang, Y. Chen, Covalent cross-linked polymer gels with reversible sol– gel transition and self-healing properties, *Macromolecules* 43(3) (2010) 1191-1194.
- [68] H. Yang, J. Tang, C. Shang, R. Miao, S. Zhang, K. Liu, Y. Fang, Calix [4] arene - Based Dynamic Covalent Gels: Marriage of Robustness, Responsiveness, and Self - Healing, *Macromolecular rapid communications* 39(4) (2018) 1700679.
- [69] X. Yang, G. Liu, L. Peng, J. Guo, L. Tao, J. Yuan, C. Chang, Y. Wei, L. Zhang, Highly efficient self - healable and dual responsive cellulose - based hydrogels for controlled release and 3D cell culture, *Adv. Funct. Mater.* 27(40) (2017) 1703174.
- [70] F. Klepel, B.J. Ravoo, Dynamic covalent chemistry in aqueous solution by photoinduced radical disulfide metathesis, *Org. Biomol. Chem.* 15(18) (2017)

3840-3842.

[71] A. Tobolsky, W. MacKnight, M. Takahashi, Relaxation of disulfide and tetrasulfide polymers, *The Journal of Physical Chemistry* 68(4) (1964) 787-790.

[72] U.F. Fritze, M. von Delius, Dynamic disulfide metathesis induced by ultrasound, *Chem. Commun.* 52(38) (2016) 6363-6366.

[73] M. Arisawa, M. Yamaguchi, Rhodium-catalyzed disulfide exchange reaction, *J. Am. Chem. Soc.* 125(22) (2003) 6624-6625.

[74] G.S. Garusinghe, S.M. Bessey, A.E. Bruce, M.R. Bruce, The influence of gold (I) on the mechanism of thiolate, disulfide exchange, *Dalton Transactions* 45(28) (2016) 11261-11266.

[75] L. Li, W. Feng, A. Welle, P.A. Levkin, UV - Induced Disulfide Formation and Reduction for Dynamic Photopatterning, *Angew. Chem.* 128(44) (2016) 13969-13973.

[76] M.T.I. Mredha, J.Y. Na, J.-K. Seon, J. Cui, I. Jeon, Multifunctional poly (disulfide) hydrogels with extremely fast self-healing ability and degradability, *Chemical Engineering Journal* (2020) 124941.

[77] P. Chakma, D. Konkolewicz, Dynamic covalent bonds in polymeric materials, *Angew. Chem., Int. Ed.* 58(29) (2019) 9682-9695.

[78] X. Chen, M.A. Dam, K. Ono, A. Mal, H. Shen, S.R. Nutt, K. Sheran, F. Wudl, A thermally re-mendable cross-linked polymeric material, *Science* 295(5560) (2002) 1698-1702.

[79] P.J. Boul, P. Reutenauer, J.-M. Lehn, Reversible Diels–Alder reactions for the generation of dynamic combinatorial libraries, *Org. Lett.* 7(1) (2005) 15-18.

[80] B. Gacal, H. Durmaz, M. Tasdelen, G. Hizal, U. Tunca, Y. Yagci, A. Demirel, Anthracene–maleimide-based Diels–Alder “click chemistry” as a novel route to graft copolymers, *Macromolecules* 39(16) (2006) 5330-5336.

[81] C. Shao, M. Wang, H. Chang, F. Xu, J.J.A.S.C. Yang, A self-healing cellulose nanocrystal-poly (ethylene glycol) nanocomposite hydrogel via Diels–Alder click reaction, *ACS Sustainable Chemistry Engineering & Mining Journal*

5(7) (2017) 6167-6174.

[82] B. Bi, M. Ma, S. Lv, R. Zhuo, X. Jiang, In-situ forming thermosensitive hydroxypropyl chitin-based hydrogel crosslinked by Diels-Alder reaction for three dimensional cell culture, *Carbohydr. Polym.* 212 (2019) 368-377.

[83] H. Schiff, The syntheses and characterization of Schiff base, *Ann. Chem. Suppl* 3 (1864) 343-349.

[84] M.E. Belowich, J.F. Stoddart, Dynamic imine chemistry, *Chem. Soc. Rev.* 41(6) (2012) 2003-2024.

[85] A. Chao, I. Negulescu, D. Zhang, Dynamic Covalent Polymer Networks Based on Degenerative Imine Bond Exchange: Tuning the Malleability and Self-Healing Properties by Solvent, *Macromolecules* 49(17) (2016) 6277-6284.

[86] K. Fukuda, M. Shimoda, M. Sukegawa, T. Nobori, J.-M. Lehn, Doubly degradable dynamers: dynamic covalent polymers based on reversible imine connections and biodegradable polyester units, *Green Chem.* 14(10) (2012) 2907-2911.

[87] C. Godoy - Alcántar, A.K. Yatsimirsky, J.M. Lehn, Structure - stability correlations for imine formation in aqueous solution, *J. Phys. Org. Chem.* 18(10) (2005) 979-985.

[88] Y. Zhang, L. Tao, S. Li, Y. Wei, Synthesis of multiresponsive and dynamic chitosan-based hydrogels for controlled release of bioactive molecules, *Biomacromolecules* 12(8) (2011) 2894-901.

[89] Z. Wei, J. Yang, Z. Liu, F. Xu, J. Zhou, M. Zrínyi, Y. Osada, Y. Chen, Novel Biocompatible Polysaccharide-Based Self-Healing Hydrogel, *Adv. Funct. Mater.* 25 (2015) 1352-1359.

[90] Y. Li, L. Yang, Y. Zeng, Y. Wu, Y. Wei, L. Tao, Self-Healing Hydrogel with a Double Dynamic Network Comprising Imine and Borate Ester Linkages, *chemical of materials* 31 (2019) 5576-5583.

[91] M.C. Roberts, M.C. Hanson, A.P. Massey, E.A. Karren, P.F. Kiser, Dynamically restructuring hydrogel networks formed with reversible covalent

crosslinks, *Adv. Mater.* 19(18) (2007) 2503-2507.

[92] G. Deng, F. Li, H. Yu, F. Liu, C. Liu, W. Sun, H. Jiang, Y. Chen, Dynamic hydrogels with an environmental adaptive self-healing ability and dual responsive sol–gel transitions, *ACS Macro Lett.* 1(2) (2012) 275-279.

[93] P. Reutenauer, E. Buhler, P.J. Boul, S.J. Candau, J.M. Lehn, Room temperature dynamic polymers based on Diels–Alder chemistry, *Chem. Eur. J.* 15(8) (2009) 1893-1900.

[94] J. Yu, H. Deng, F. Xie, W. Chen, B. Zhu, Q. Xu, The potential of pH-responsive PEG-hyperbranched polyacylhydrazone micelles for cancer therapy, *Biomaterials* 35(9) (2014) 3132-3144.

[95] A. Herrmann, Dynamic combinatorial/covalent chemistry: a tool to read, generate and modulate the bioactivity of compounds and compound mixtures, *Chem. Soc. Rev.* 43(6) (2014) 1899-1933.

[96] Y. Zhang, B. Yang, X. Zhang, L. Xu, L. Tao, S. Li, Y. Wei, A magnetic self-healing hydrogel, *Chem. Commun.* 48(74) (2012) 9305-9307.

[97] B. Yang, Y. Zhang, X. Zhang, L. Tao, S. Li, Y. Wei, Facilely prepared inexpensive and biocompatible self-healing hydrogel: a new injectable cell therapy carrier, *Polymer Chemistry* 3(12) (2012) 3235-3238.

[98] K. Halake, H.J. Kim, M. Birajdar, B.S. Kim, H. Bae, C. Lee, Y.J. Kim, S. Kim, S. Ahn, S.Y. An, Recently developed applications for natural hydrophilic polymers, *Journal of industrial engineering chemistry* 40 (2016) 16-22.

[99] H. Hamed, S. Moradi, S.M. Hudson, A.E. Tonelli, Chitosan based hydrogels and their applications for drug delivery in wound dressings: A review, *Carbohydr. Polym.* 199 (2018) 445-460.

[100] M.C.G. Pella, M.K. Lima-Tenorio, E.T. Tenorio-Neto, M.R. Guilherme, E.C. Muniz, A.F. Rubira, Chitosan-based hydrogels: From preparation to biomedical applications, *Carbohydr. Polym.* 196 (2018) 233-245.

[101] C. Cui, C. Shao, L. Meng, J. Yang, High-Strength, Self-Adhesive, and Strain-Sensitive Chitosan/ Poly(acrylic acid) Double-Network Nanocomposite

Hydrogels Fabricated by Salt-Soaking Strategy for Flexible Sensors, *ACS applied materials & interfaces* (2019).

[102] J. Qu, X. Zhao, Y. Liang, T. Zhang, P.X. Ma, B. Guo, Antibacterial adhesive injectable hydrogels with rapid self-healing, extensibility and compressibility as wound dressing for joints skin wound healing, *Biomaterials* 183 (2018) 185-199.

[103] T. Wu, J. Huang, Y. Jiang, Y. Hu, X. Ye, D. Liu, J. Chen, Formation of hydrogels based on chitosan/alginate for the delivery of lysozyme and their antibacterial activity, *Food Chem.* (2018).

[104] C. Qin, J. Zhou, Z. Zhang, W. Chen, Q. Hu, Y. Wang, Convenient one-step approach based on stimuli-responsive sol-gel transition properties to directly build chitosan-alginate core-shell beads, *Food Hydrocolloids* 87 (2019) 253-259.

[105] K.Y. Lee, D.J. Mooney, Alginate: properties and biomedical applications, *Progress in polymer science* 37(1) (2012) 106-126.

[106] W.R. Gombotz, S. Wee, Protein release from alginate matrices, *Adv. Drug Del. Rev.* 31(3) (1998) 267-285.

[107] M. Zhang, X. Zhao, Alginate hydrogel dressings for advanced wound management, *Int. J. Biol. Macromol.* 162 (2020) 1414-1428.

[108] D.S. Lima, E.T. Tenório-Neto, M.K. Lima-Tenório, M.R. Guilherme, D.B. Scariot, C.V. Nakamura, E.C. Muniz, A.F. Rubira, pH-responsive alginate-based hydrogels for protein delivery, *J. Mol. Liq.* 262 (2018) 29-36.

[109] X. Chen, M. Fan, H. Tan, B. Ren, G. Yuan, Y. Jia, J. Li, D. Xiong, X. Xing, X. Niu, Magnetic and self-healing chitosan-alginate hydrogel encapsulated gelatin microspheres via covalent cross-linking for drug delivery, *Materials Science Engineering: C* 101 (2019) 619-629.

[110] N.C. Hunt, D. Hallam, A. Karimi, C.B. Mellough, J. Chen, D.H. Steel, M. Lako, 3D culture of human pluripotent stem cells in RGD-alginate hydrogel improves retinal tissue development, *Acta Biomater.* 49 (2017) 329-343.

[111] T. Heinze, T. Liebert, B. Heublein, S. Hornig, Functional polymers based

on dextran, Polysaccharides li, Springer2006, pp. 199-291.

[112] R. Zhang, M. Tang, A. Bowyer, R. Eienthal, J. Hubble, A novel pH-and ionic-strength-sensitive carboxy methyl dextran hydrogel, *Biomaterials* 26(22) (2005) 4677-4683.

[113] J. Qu, Y. Liang, M. Shi, B. Guo, Y. Gao, Z. Yin, Biocompatible conductive hydrogels based on dextran and aniline trimer as electro-responsive drug delivery system for localized drug release, *Int. J. Biol. Macromol.* 140 (2019) 255-264.

[114] N. Riahi, B. Liberelle, O. Henry, G. De Crescenzo, Impact of RGD amount in dextran-based hydrogels for cell delivery, *Carbohydr. Polym.* 161 (2017) 219-227.

[115] S. Barkhordari, M. Yadollahi, Carboxymethyl cellulose capsulated layered double hydroxides/drug nanohybrids for Cephalexin oral delivery, *Applied Clay Science* 121 (2016) 77-85.

[116] H. Namazi, R. Rakhshaei, H. Hamishehkar, H.S. Kafil, Antibiotic loaded carboxymethylcellulose/MCM-41 nanocomposite hydrogel films as potential wound dressing, *Int. J. Biol. Macromol.* 85 (2016) 327-334.

[117] Y. Shahbazi, Application of carboxymethyl cellulose and chitosan coatings containing *Mentha spicata* essential oil in fresh strawberries, *Int. J. Biol. Macromol.* 112 (2018) 264-272.

[118] J. Shang, Z. Shao, X. Chen, Electrical behavior of a natural polyelectrolyte hydrogel: chitosan/carboxymethylcellulose hydrogel, *Biomacromolecules* 9(4) (2008) 1208-1213.

[119] G. Abatangelo, V. Vindigni, G. Avruscio, L. Pandis, P. Brun, Hyaluronic acid: redefining its role, *Cells* 9(7) (2020) 1743.

[120] K. Meyer, J.W. Palmer, The polysaccharide of the vitreous humor, *J. Biol. Chem.* 107(3) (1934) 629-634.

[121] E. Hachet, H. Van Den Berghe, E. Bayma, M.R. Block, R. Auzély-Velty, Design of Biomimetic Cell-Interactive Substrates Using Hyaluronic Acid

Hydrogels with Tunable Mechanical Properties, *Biomacromolecules* 13(6) (2012) 1818-1827.

[122] G. Huang, H. Huang, Application of hyaluronic acid as carriers in drug delivery, *Drug Delivery* 25(1) (2018) 766-772.

[123] Y. Luo, K.R. Kirker, G.D. Prestwich, Cross-linked hyaluronic acid hydrogel films: new biomaterials for drug delivery, *J. Controlled Release* 69(1) (2000) 169-184.

[124] M.N. Sayed Aly, Intra-articular drug delivery: a fast growing approach, *Recent patents on drug delivery formulation* 2(3) (2008) 231-237.

[125] F. Quero, C. Padilla, V. Campos, J. Luengo, L. Caballero, F. Melo, Q. Li, S.J. Eichhorn, J. Enrione, Stress transfer and matrix-cohesive fracture mechanism in microfibrillated cellulose-gelatin nanocomposite films, *Carbohydr. Polym.* 195 (2018) 89-98.

[126] M. Norziah, A. Al-Hassan, A. Khairulnizam, M. Mordi, M. Norita, Characterization of fish gelatin from surimi processing wastes: Thermal analysis and effect of transglutaminase on gel properties, *Food Hydrocolloids* 23(6) (2009) 1610-1616.

[127] Y. Zeng, L. Zhu, Q. Han, W. Liu, X. Mao, Y. Li, N. Yu, S. Feng, Q. Fu, X. Wang, Preformed gelatin microcryogels as injectable cell carriers for enhanced skin wound healing, *Acta Biomater.* 25 (2015) 291-303.

[128] S. Thakur, P.P. Govender, M.A. Mamo, S. Tamulevicius, V.K. Thakur, Recent progress in gelatin hydrogel nanocomposites for water purification and beyond, *Vacuum* 146 (2017) 396-408.

[129] P. Jaipan, A. Nguyen, R.J. Narayan, Gelatin-based hydrogels for biomedical applications, *Mrs Communications* 7(3) (2017) 416-426.

[130] E. Karadağ, S. Kundakçı, Application of highly swollen novel biosorbent hydrogels in uptake of uranyl ions from aqueous solutions, *Fibers and Polymers* 16(10) (2015) 2165-2176.

[131] P. Sahariah, M. Masson, Antimicrobial chitosan and chitosan derivatives:

a review of the structure–activity relationship, *Biomacromolecules* 18(11) (2017) 3846-3868.

[132] J.-K.F. Suh, H.W. Matthew, Application of chitosan-based polysaccharide biomaterials in cartilage tissue engineering: a review, *Biomaterials* 21(24) (2000) 2589-2598.

[133] H. Fukuda, Polyelectrolyte complexes of chitosan with sodium carboxymethylcellulose, *Bull. Chem. Soc. Jpn.* 53(4) (1980) 837-840.

[134] H.S. Kas, Chitosan: properties, preparations and application to microparticulate systems, *J. Microencapsulation* 14(6) (1997) 689-711.

[135] G. Geisberger, E.B. Gyenge, D. Hinger, A. Käch, C. Maake, G.R. Patzke, Chitosan-thioglycolic acid as a versatile antimicrobial agent, *Biomacromolecules* 14(4) (2013) 1010-1017.

[136] V. Mourya, N.N. Inamdar, A. Tiwari, Carboxymethyl chitosan and its applications, *Advanced Materials Letters* 1(1) (2010) 11-33.

[137] K. Inouye, M. Kurokawa, S. Nishikawa, M. Tsukada, Use of Bombyx mori silk fibroin as a substratum for cultivation of animal cells, *Journal of biochemical and biophysical methods* 37(3) (1998) 159-164.

[138] T. Yamaoka, Y. Takebe, Y. Kimura, Surface modification of poly (L-lactic acid) film with bioactive materials by a novel direct alkaline treatment process, *Kobunshi ronbunshu* 55(6) (1998) 328-333.

[139] X. Liu, Y. Guan, D. Yang, Z. Li, K. Yao, Antibacterial action of chitosan and carboxymethylated chitosan, *Journal of applied polymer science* 79(7) (2001) 1324-1335.

[140] J. Wang, J. Chen, J. Zong, D. Zhao, F. Li, R. Zhuo, S. Cheng, Calcium carbonate/carboxymethyl chitosan hybrid microspheres and nanospheres for drug delivery, *The Journal of Physical Chemistry C* 114(44) (2010) 18940-18945.

[141] T.L. Hill, A. Fundamental studies. On the theory of the Donnan membrane equilibrium, *Discuss. Faraday Soc.* 21 (1956) 31-45.

- [142] S.S. Vaghani, M.M. Patel, C. Satish, Synthesis and characterization of pH-sensitive hydrogel composed of carboxymethyl chitosan for colon targeted delivery of ornidazole, *Carbohydr. Res.* 347(1) (2012) 76-82.
- [143] C. Lou, X. Tian, H. Deng, Y. Wang, X. Jiang, Dialdehyde- β -cyclodextrin-crosslinked carboxymethyl chitosan hydrogel for drug release, *Carbohydr. Polym.* 231 (2020) 115678.
- [144] X. Yin, J. Chen, W. Yuan, Q. Lin, L. Ji, F. Liu, Preparation and antibacterial activity of Schiff bases from O-carboxymethyl chitosan and para-substituted benzaldehydes, *Polymer bulletin* 68(5) (2012) 1215-1226.
- [145] P.A. Gunatillake, R. Adhikari, Biodegradable synthetic polymers for tissue engineering, *European Cells and Materials* 5(1) (2003) 1-16.
- [146] E. Marin, J. Rojas, Y. Ciro, A review of polyvinyl alcohol derivatives: Promising materials for pharmaceutical and biomedical applications, *African Journal of Pharmacy and Pharmacology* 8(24) (2014) 674-684.
- [147] M.I. Baker, S.P. Walsh, Z. Schwartz, B.D. Boyan, A review of polyvinyl alcohol and its uses in cartilage and orthopedic applications, *Journal of Biomedical Materials Research Part B: Applied Biomaterials* 100(5) (2012) 1451-1457.
- [148] G. Paradossi, F. Cavalieri, E. Chiessi, C. Spagnoli, M.K. Cowman, Poly (vinyl alcohol) as versatile biomaterial for potential biomedical applications, *J. Mater. Sci. Mater. Med.* 14(8) (2003) 687-691.
- [149] S.-H. Hyon, W.-I. Cha, Y. Ikada, M. Kita, Y. Ogura, Y. Honda, Poly (vinyl alcohol) hydrogels as soft contact lens material, *J. Biomater. Sci. Polym. Ed.* 5(5) (1994) 397-406.
- [150] M. Kobayashi, Y.-S. Chang, M. Oka, A two year in vivo study of polyvinyl alcohol-hydrogel (PVA-H) artificial meniscus, *Biomaterials* 26(16) (2005) 3243-3248.
- [151] A. Takamura, F. Ishii, H. Hidaka, Drug release from poly (vinyl alcohol) gel prepared by freeze-thaw procedure, *J. Controlled Release* 20(1) (1992) 21-27.

- [152] C. Weis, E.K. Odermatt, J. Kressler, Z. Funke, T. Wehner, D. Freytag, Poly (vinyl alcohol) membranes for adhesion prevention, *Journal of Biomedical Materials Research Part B: Applied Biomaterials* 70(2) (2004) 191-202.
- [153] X. Xu, Y. Liu, W. Fu, M. Yao, Z. Ding, J. Xuan, D. Li, S. Wang, Y. Xia, M. Cao, Poly (N-isopropylacrylamide)-based thermoresponsive composite hydrogels for biomedical applications, *Polymers* 12(3) (2020) 580.
- [154] M. Oak, R. Mandke, J. Singh, Smart polymers for peptide and protein parenteral sustained delivery, *Drug Discovery Today: Technologies* 9(2) (2012) e131-e140.
- [155] M. Cao, Y. Wang, X. Hu, H. Gong, R. Li, H. Cox, J. Zhang, T.A. Waigh, H. Xu, J. Lu, Reversible thermoresponsive peptide–PNIPAM hydrogels for controlled drug delivery, *Biomacromolecules* 20(9) (2019) 3601-3610.
- [156] Z. Atoufi, S.K. Kamrava, S.M. Davachi, M. Hassanabadi, S.S. Garakani, R. Alizadeh, M. Farhadi, S. Tavakol, Z. Bagher, G.H. Motlagh, Injectable PNIPAM/Hyaluronic acid hydrogels containing multipurpose modified particles for cartilage tissue engineering: Synthesis, characterization, drug release and cell culture study, *Int. J. Biol. Macromol.* 139 (2019) 1168-1181.
- [157] D. Wu, J. Zhu, H. Han, J. Zhang, F. Wu, X. Qin, J. Yu, Synthesis and characterization of arginine-NIPAAm hybrid hydrogel as wound dressing: In vitro and in vivo study, *Acta Biomater.* 65 (2018) 305-316.
- [158] J. Wang, L. Lin, Q. Cheng, L. Jiang, A Strong Bio - Inspired Layered PNIPAM–Clay Nanocomposite Hydrogel, *Angew. Chem., Int. Ed.* 51(19) (2012) 4676-4680.
- [159] M.A. Haq, Y. Su, D. Wang, Mechanical properties of PNIPAM based hydrogels: A review, *Materials Science Engineering: C* 70 (2017) 842-855.
- [160] M. Karimi, A. Ghasemi, P.S. Zangabad, R. Rahighi, S.M.M. Basri, H. Mirshekari, M. Amiri, Z.S. Pishabad, A. Aslani, M. Bozorgomid, Smart micro/nanoparticles in stimulus-responsive drug/gene delivery systems, *Chem. Soc. Rev.* 45(5) (2016) 1457-1501.

- [161] A.A. D'souza, R. Shegokar, Polyethylene glycol (PEG): a versatile polymer for pharmaceutical applications, *Expert opinion on drug delivery* 13(9) (2016) 1257-1275.
- [162] Y. Zhang, C. Pham, R. Yu, E. Petit, S. Li, M. Barboiu, Dynamic hydrogels based on double imine connections and application for delivery of fluorouracil, *Frontiers in Chemistry* 8 (2020) 739.
- [163] Y. Lei, M. Rahim, Q. Ng, T. Segura, Hyaluronic acid and fibrin hydrogels with concentrated DNA/PEI polyplexes for local gene delivery, *J. Controlled Release* 153(3) (2011) 255-261.
- [164] J.B. Leach, C.E. Schmidt, Characterization of protein release from photocrosslinkable hyaluronic acid-polyethylene glycol hydrogel tissue engineering scaffolds, *Biomaterials* 26(2) (2005) 125-135.
- [165] A. Lu, E. Petit, S. Li, Y. Wang, F. Su, S. Monge, Novel thermo-responsive micelles prepared from amphiphilic hydroxypropyl methyl cellulose-block-JEFFAMINE copolymers, *Int. J. Biol. Macromol.* 135 (2019) 38-45.
- [166] W. Agut, A. Brûlet, D. Taton, S. Lecommandoux, Thermoresponsive micelles from Jeffamine-b-poly (L-glutamic acid) double hydrophilic block copolymers, *Langmuir* 23(23) (2007) 11526-11533.
- [167] N.B. Javan, H. Montazeri, L.R. Shirmard, N.J. Omid, G.R. Barbari, M. Amini, M.H. Ghahremani, M. Rafiee-Tehrani, F.A. Dorkoosh, Preparation, characterization and in vivo evaluation of a combination delivery system based on hyaluronic acid/jeffamine hydrogel loaded with PHBV/PLGA blend nanoparticles for prolonged delivery of Teriparatide, *Eur. J. Pharm. Sci.* 101 (2017) 167-181.
- [168] A.S. Ertürk, M. Tülü, A.E. Bozdoğan, T. Parali, Microwave assisted synthesis of Jeffamine cored PAMAM dendrimers, *Eur. Polym. J.* 52 (2014) 218-226.
- [169] Q. Chai, Y. Jiao, X. Yu, Hydrogels for biomedical applications: their characteristics and the mechanisms behind them, *Gels* 3(1) (2017) 6.

- [170] S. Cascone, G. Lamberti, Hydrogel-based commercial products for biomedical applications: A review, *International Journal of Pharmaceutics* 573 (2020) 118803.
- [171] A.S. Hoffman, Hydrogels for biomedical applications, *Adv. Drug Del. Rev.* 64 (2012) 18-23.
- [172] M. Liu, X. Zeng, C. Ma, H. Yi, Z. Ali, X. Mou, S. Li, Y. Deng, N. He, Injectable hydrogels for cartilage and bone tissue engineering, *Bone Reserch* 5 (2017) 17014.
- [173] W.T. Green Jr, Articular cartilage repair: behavior of rabbit chondrocytes during tissue culture and subsequent allografting, *Clin. Orthop. Relat. Res.* 124 (1977) 237-250.
- [174] M. Brittberg, A. Lindahl, A. Nilsson, C. Ohlsson, O. Isaksson, L. Peterson, Treatment of deep cartilage defects in the knee with autologous chondrocyte transplantation, *New england journal of medicine* 331(14) (1994) 889-895.
- [175] T.G. Kim, H. Shin, D.W. Lim, Biomimetic scaffolds for tissue engineering, *Adv. Funct. Mater.* 22(12) (2012) 2446-2468.
- [176] J.L. Drury, D.J. Mooney, Hydrogels for tissue engineering: scaffold design variables and applications, *Biomaterials* 24(24) (2003) 4337-4351.
- [177] D. Seliktar, Designing cell-compatible hydrogels for biomedical applications, *Science* 336(6085) (2012) 1124-1128.
- [178] B. Choi, S. Kim, B. Lin, B.M. Wu, M.J.A.a.m. Lee, Cartilaginous extracellular matrix-modified chitosan hydrogels for cartilage tissue engineering, *ACS applied materials & interfaces* 6(22) (2014) 20110-20121.
- [179] S. Van Vlierberghe, P. Dubruel, E. Schacht, Biopolymer-based hydrogels as scaffolds for tissue engineering applications: a review, *Biomacromolecules* 12(5) (2011) 1387-1408.
- [180] F. Bray, J. Ferlay, I. Soerjomataram, R.L. Siegel, L.A. Torre, A. Jemal, Global cancer statistics 2018: GLOBOCAN estimates of incidence and mortality worldwide for 36 cancers in 185 countries, *CA Cancer J. Clin.* 68(6) (2018) 394-

424.

- [181] M. Sepantafar, R. Maheronnaghsh, H. Mohammadi, F. Radmanesh, M.M. Hasani-Sadrabadi, M. Ebrahimi, H. Baharvand, Engineered hydrogels in cancer therapy and diagnosis, *Trends Biotechnol.* 35(11) (2017) 1074-1087.
- [182] Q. Wu, Z. He, X. Wang, Q. Zhang, Q. Wei, S. Ma, C. Ma, J. Li, Q. Wang, Cascade enzymes within self-assembled hybrid nanogel mimicked neutrophil lysosomes for singlet oxygen elevated cancer therapy, *Nat. Commun.* 10(1) (2019) 1-14.
- [183] J. Li, D. Mooney, Designing hydrogels for controlled drug delivery, *Nature Reviews Materials* 1(12) (2016) 1-17.
- [184] H. Bodugoz-Senturk, C.E. Macias, J.H. Kung, O.K. Muratoglu, Poly (vinyl alcohol)–acrylamide hydrogels as load-bearing cartilage substitute, *Biomaterials* 30(4) (2009) 589-596.
- [185] J. Li, W.R. Illeperuma, Z. Suo, J.J. Vlassak, Hybrid hydrogels with extremely high stiffness and toughness, *ACS Macro Lett.* 3(6) (2014) 520-523.
- [186] J. Su, B. Hu, W.L. Lowe Jr, D.B. Kaufman, P.B. Messersmith, Anti-inflammatory peptide-functionalized hydrogels for insulin-secreting cell encapsulation, *Biomaterials* 31(2) (2010) 308-314.
- [187] A. Kikuchi, T. Okano, Pulsatile drug release control using hydrogels, *Adv. Drug Del. Rev.* 54(1) (2002) 53-77.
- [188] N. Bhattarai, J. Gunn, M. Zhang, Chitosan-based hydrogels for controlled, localized drug delivery, *Adv. Drug Del. Rev.* 62(1) (2010) 83-99.
- [189] S. Chen, Y. Wu, F. Mi, Y. Lin, L. Yu, H. Sung, A novel pH-sensitive hydrogel composed of N, O-carboxymethyl chitosan and alginate cross-linked by genipin for protein drug delivery, *J. Controlled Release* 96(2) (2004) 285-300.
- [190] L. Yu, J. Ding, Injectable hydrogels as unique biomedical materials, *Chem. Soc. Rev.* 37(8) (2008) 1473-1481.
- [191] F. Sultana, M. Manirujjaman, M.A. Imran-Ul-Haque, S. Sharmin, An overview of nanogel drug delivery system, *Journal of Applied Pharmaceutical*

Science 3(8) (2013) 95-105.

[192] V.A. de Weger, J.H. Beijnen, J.H. Schellens, Cellular and clinical pharmacology of the taxanes docetaxel and paclitaxel—a review, *Anti-Cancer Drugs* 25(5) (2014) 488-494.

[193] Q. Chen, X. Wang, C. Wang, L. Feng, Y. Li, Z. Liu, Drug-induced self-assembly of modified albumins as nano-theranostics for tumor-targeted combination therapy, *ACS nano* 9(5) (2015) 5223-5233.

[194] G. Goldstein, T.K. Audhya, Thymopoietin to thymopentin: experimental studies, *Surv. Immunol. Res.* 4(1) (1985) 1.

[195] V.K. Singh, S. Biswas, K.B. Mathur, W. Haq, S.K. Garg, S.S. Agarwal, Thymopentin and splenopentin as immunomodulators, *Immunol. Res.* 17(3) (1998) 345-368.

[196] S. Lin, B. Cai, G. Quan, T. Peng, G. Yao, C. Zhu, Q. Wu, H. Ran, X. Pan, C. Wu, Novel strategy for immunomodulation: Dissolving microneedle array encapsulating thymopentin fabricated by modified two-step molding technology, *Eur. J. Pharm. Biopharm.* 122 (2018) 104-112.

[197] J. Li, Y. Cheng, X. Zhang, L. Zheng, Z. Han, P. Li, Y. Xiao, Q. Zhang, F. Wang, The in vivo immunomodulatory and synergistic anti-tumor activity of thymosin α 1–thymopentin fusion peptide and its binding to TLR2, *Cancer Lett.* 337(2) (2013) 237-247.

[198] N. Clumeck, S. Cran, P. Van de Perre, F. Mascart-Lemone, J. Duchateau, K. Bolla, Thymopentin treatment in AIDS and pre-AIDS patients, *Surv. Immunol. Res.* 4(1) (1985) 58-62.

[199] T. Zhang, X. Qin, X. Cao, W. Li, T. Gong, Z. Zhang, Thymopentin-loaded phospholipid-based phase separation gel with long-lasting immunomodulatory effects: in vitro and in vivo studies, *Acta Pharmacologica Sinica* 40(4) (2019) 514-521.

[200] J. Duchateau, G. Servais, R. Vreyens, G. Delespesse, K. Bolla, Modulation of immune response in aged humans through different

administration modes of thymopentin, *Surv. Immunol. Res.* 4(1) (1985) 94.

[201] J. Duchateau, G. Delespesse, K. Bolla, Phase variation in the modulation of the human immune response, *Immunol. Today* 4(8) (1983) 213.

[202] K. Zaruba, M. Rastorfer, P. Grob, H. Joller-Jemelka, K. Bolla, Thymopentin as adjuvant in non-responders or hyporesponders to hepatitis B vaccination, *The Lancet* 322(8361) (1983) 1245.

Chapter 2 Biobased pH-responsive and self-healing hydrogels prepared from O-carboxymethyl chitosan and a 3-dimensional dynamer as cartilage engineering scaffold

Abstract: Novel dynamic hydrogels were prepared from O-carboxymethyl chitosan (CMCS) and a water soluble dynamer Dy via crosslinking by imine bond formation using an environmentally friendly method. Dy was synthesized by reaction of Benzene-1,3,5-tricarbaldehyde with Jeffamine. The resulting soft hydrogels exhibit a porous and interconnected morphology, storage modulus up to 1400 Pa, and excellent pH-sensitive swelling properties. The swelling ratio is relatively low at acidic pH due to electrostatic attraction, and becomes exceptionally high up to 7000% at pH 8 due to electrostatic repulsion. Moreover, hydrogels present outstanding self-healing properties as evidenced by closure of split pieces and rheological measurements. This study opens up a new horizon in the preparation of dynamic hydrogels with great potential for applications in drug delivery, wound dressing, and in particular in tissue engineering as the hydrogels present excellent cytocompatibility.

Keywords: O-carboxymethyl chitosan; Imine chemistry; Dynamic hydrogel; Self-healing; pH responsive; Cytocompatibility

2.1 Introduction

In the past decades, hydrogels have been widely studied as biomaterials for various applications in drug delivery, wound dressing and tissue engineering due to their outstanding properties such as biocompatibility [1], biodegradability [2], mechanical [3] and stimuli-responsive [4] properties.

Hydrogels [5, 6] consist of a cross-linked network, which can absorb large amounts of water [7] or physiological fluids [8], while keeping their three-dimensional structural integrity. Generally, according to the preparation approach, hydrogels can be classified into two categories: chemical gels or irreversible gels, and physical gels or reversible gels [9, 10]. Chemical gels are formed by irreversible covalent bonding, whereas in physical gels, the polymeric chains are held together by chain entanglements and/or supramolecular hydrophobic, ion-pair or hydrogen bonding interactions.

From our previous studies has emerged the definition of “dynamic gels” (i.e., *dynagels*) [11] which are dynamic on both the molecular and supramolecular levels, reversibly exchanging their components [12], responding to external stimuli, such as pH [13], ions [14, 15] and temperature [16]. Among the various reversible covalent bonds involved in dynamic constitutional design [17], the amino-carbonyl/imine chemistry is considered as the most promising strategy to generate dynamic materials with modifiable properties. It may implement adaptive reversible rearrangements of the components toward a high level of correlativity which may embody the flow of structural information from molecular level to multivalent materials which can bind bioactive molecules, cells on their nanosurface, or present self-healing properties [18]. This concerns the use of Dynamic Constitutional Frameworks - DCF [17] composed of linear and/or cross-linked components reversibly interconnected *via* imine bonds to core connectors and containing functional groups synergistically interacting with external stimuli [19].

Chitosan (CS), a polysaccharide obtained from alkaline hydrolysis of chitin found in the exoskeleton/shell of crustaceans, presents remarkable properties such as biocompatibility, biodegradability, low toxicity, low cost or immune-stimulatory activity [20]. Chitosan is a good candidate for in-situ dynamic reversible crosslinking via its amino groups present along the polymer chain with aldehydes [21], alginate [22], gelatin [23], resulting in the formation of pH-

responsive and biodegradable hydrogels. However, chitosan is soluble only in acidic media due to strong internal hydrogen bonding, which greatly limits its potential biomedical or pharmaceutical applications. The carboxymethylation of D-glucosamines of chitosan generates carboxymethyl chitosan (CMCS) which is readily soluble in water at neutral pH, thus allowing uses in tissue engineering, drug delivery, wound dressing and food industry.

Crosslinking of CS/CMCS with aldehydes *via* the imine-bond formation along polymeric backbones occurs with very low yields in aqueous solutions and we have previously shown that it is significantly improved in hydrogels or in solid state films with dynamic properties [24]. It is well known that no continuous cross-linked networks are formed when monoaldehydes [10, 21] and dialdehydes [25] are used for cross-linking. The resulting hydrogels exhibit good swelling behaviors, but disordered micro-structure and weak mechanical strength. Increasing the cross-linking by using 3-armed [26] or 4-armed [27] aldehydes, dynamic hydrogels exhibiting pH and temperature-responsive swelling ratios, strong mechanical performance, and self-healing behavior have been obtained. Nevertheless, the toxicity of aldehydes, and especially of glutaraldehyde related to the human body restricts their use for biomedical applications and imposes the necessity of finding new biocompatible crosslinking agents.

Toward this aim herein, a constitutional dynamer Dy was prepared from 1,3,5-benzenetri-aldehyde and water-soluble Jeffamine, providing a network that can be used as a biomimetic cross-linking component. CMCS based hydrogels were further prepared by using an original strategy and a double linked framework obtained through a “green” synthetic route in water and supposed to specifically target peptides and proteins as well as cells *via* biomimetic encapsulation. The chemical and supramolecular structures of the CMCS based hydrogels, their morphology, their rheological and swelling properties, as well as their unexpected strong self-healing behaviors were evaluated and

discussed. Cytotoxicity of the hydrogels was assessed by co-culture in the presence of human mesenchymal stromal cells (MSCs) to evaluate their potential as scaffold in cartilage engineering.

2.2 Experimental section

2.2.1 Materials

Benzene-1,3,5-tricarbaldehyde (BTA) from Manchester Organics and O,O'-Bis(2-aminopropyl) PPO-*b*-PEO-*b*-PPO (Jeffamine® ED-2003, M_n 1.9×10^3) from Sigma Aldrich were used without purification. CMCS (M_n 2×10^5 Da, degree of deacetylation 90 %, degree of carboxymethylation 80 %) was purchased from Golden-shell Biochemical Co., Ltd. Methanol (96%), citric acid ($\geq 99.5\%$), disodium hydrogen phosphate dodecahydrate ($\geq 99\%$), boric acid ($\geq 99.5\%$), borax($\geq 99\%$) were of analytical grade, and obtained from Sigma Aldrich.

2.2.2 Synthesis of dynamer Dy

Typically, BTA (162 mg, 1 mmol), Jeffamine (1.90 g, 1 mmol) are added in 30 mL methanol, and the reaction mixture was stirred at 70 °C for 4 h. After evaporation of the solvent, 20 mL Milli Q water was added, yielding a homogeneous dynamer solution of 5×10^{-2} M as calculated from the remaining aldehyde groups.

2.2.3 Preparation of CMCS-Dy hydrogels

CMCS (1.06 g, 5 mmol calculated from D-glucosamine units) was dissolved in 50 mL Milli-Q water at room temperature, yielding a transparent solution of 1×10^{-1} M. CMCS and dynamer solutions were mixed at different ratios to a total volume of 12 mL, followed by ultra-sonication for 1 min to remove trapped bubbles. Gelation then proceeded at 37 °C for 24 h, yielding a CMCS-based

hydrogel.

Freeze-drying was performed as follows so as to conserve the original structure. As-prepared hydrogels were placed in small vials and immersed in liquid nitrogen ($-196\text{ }^{\circ}\text{C}$) for instantaneous freezing. The vials were then placed in a 500 mL round-bottomed flask which was fixed on LABCONCO® freeze dryer. The hydrogels were freeze-dried for 24 h before analyses.

2.2.4 Characterization

^1H NMR spectroscopy was carried out using Bruker NMR spectrometer (AMX500) of 300 MHz. CDCl_3 or D_2O was used as the solvent. 5 mg of sample were dissolved in 0.5 mL of solvent for each analysis. Chemical shifts were recorded in ppm using tetramethylsilane (TMS) as internal reference. The morphology of freeze-dried hydrogels was examined using scanning electron microscopy (SEM, Hitachi S4800). The samples were subjected to gold coating prior to analysis. Fourier-transform infrared spectroscopy (FT-IR) was performed with Nicolet Nexus FT-IR spectrometer, equipped with ATR diamant Golden Gate.

2.2.5 Structural stability of Dy

The stability of the dynamer Dy was evaluated in D_2O under neutral and acidic conditions since imine bond formation is reversible at low pH. D_2O solutions at pH of 1, 3, and 5 were prepared by addition of trifluoroacetic acid. NMR spectra were registered just after dynamer dissolution and after 7 days.

2.2.6 Rheology

The rheological properties of hydrogels were examined with Physical MCR 301 Rheometer (Anton Paar). Hydrogels prepared in Milli-Q water were placed on a cone plate (diameter of 4 cm, apex angle of 2° , and clearance 56 μm).

Measurements were made in the linear visco-elastic range as a function of time, strain, or frequency.

2.2.7 Swelling

The swelling behavior of hydrogels was evaluated in buffer solutions at various pH values. Solutions from pH 1 to pH 7 were prepared using 0.1×10^{-3} M citric acid solution and 0.2×10^{-3} M disodium hydrogen phosphate solution, whereas solutions of pH 8 and 9 were prepared using 0.2×10^{-3} M boric acid solution and 0.5×10^{-4} M borax solution. Freeze-dried gels were immersed in a buffer, and taken out at different time intervals. The swollen hydrogels were weighed after wiping surface water with filter paper, freeze-dried for 24 h, and weighed again. The swelling ratio and mass loss ratio of hydrogel were calculated according to equation (1) and equation (2), respectively:

$$\text{Swelling ratio \%} = \frac{(M_s - M_d)}{M_d} \times 100 \quad (1)$$

$$\text{Loss ratio \%} = \frac{(M_0 - M_d)}{M_0} \times 100 \quad (2)$$

Where M_0 is the initial mass of xerogel, M_s is the wet mass of the swollen hydrogel, and M_d is the dried mass of the swollen hydrogel after lyophilization

2.2.8 Self-healing experiments

Various hydrogel samples were prepared in Milli-Q water, and in pH = 7 and pH = 8 buffers. Some of them were dyed yellow with 5 μ L of lucigenin, or dyed red with Rhodamine. 3 different approaches were applied to examine the self-healing behavior of hydrogels: 1) a hole with diameter around 3 mm was punched at the circle center of the sample; 2) samples were split into two pieces, and then a yellow piece was put together with a transparent piece immediately at 37 °C ; 3) injection of transparent and red samples on the surface of a Petri dish to observe color changes.

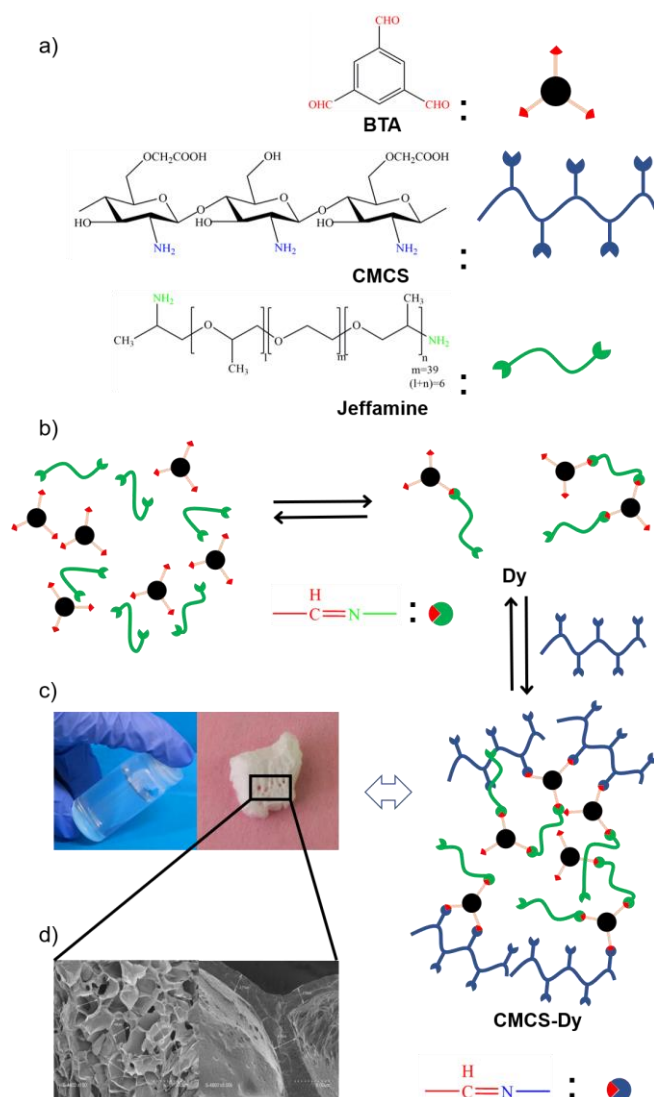
2.2.9 Cell cultures and Cytotoxicity

2 mL of CMCS at 100 mmol and 1 mL of dynamer at 50 mmol were mixed. Human MSCs isolated from adipose tissue (AT-MSCs) or from bone marrow (BM-MSCs) were added at a concentration of 1×10^6 cells / mL. As control, AT-MSCs or BM-MSCs were seeded on 96-wells TCPS (Tissue Culture Polystyrene System) plates at 5×10^3 cells per well, or were embedded in 3 mg / mL rat collagen type I hydrogel (Corning) at 1×10^6 cells / mL. 50 μ L of cell laden solution were loaded in each well of 96 wells ultra-low adhesion plates (Corning). After 2 h gelation in an atmosphere at 37 °C, 5 % CO₂ and 95 % of humidity, 100 μ L of proliferative medium (α MEM containing 10% fetal calf serum, 100 μ g/mL penicillin/streptomycin, 2×10^{-3} M glutamine, 1 ng / mL of basic fibroblast growth factor) were added on the top of the hydrogel. MSCs were cultured for 7 days with medium change at day 3. After 1- or 7-days culture, the cell viability was analyzed by confocal microscopy (Leica) after staining the live cells in green and the dead cells in red using the live/dead assay kit (Invitrogen).

2.3 Results and discussion

2.3.1 Synthesis of dynamer

A water soluble dynamer Dy was first synthesized by reaction of BTA as the core structure and bifunctional diamine, Jeffamine[®] ED-2003 (Mn=1900) as the water-soluble linker at a molar ratio of 1:1 via reversible imine bond formation, as shown in Scheme 2.1. Thus, it remains in average one aldehyde group per molecule of BTA for further cross-linking reaction with the amine groups of CMCS.



Scheme 2.1 Synthesis route of CMCS-based dynamic hydrogel: a) chemical structures of BTA, CMCS and Jeffamine; b) synthesis of the dyanmer Dy by reaction of equimolar BTA and Jeffamine, and synthesis of hydrogel by imine formation between Dy and CMCS; c) images of as prepared hydrogel and freeze-dried hydrogel; and d) SEM images of freeze-dried hydrogel.

^1H NMR spectroscopy was used to monitor the formation and stability of imine bonds during the synthesis of the dyanmer. Figure 2.1 presents the ^1H NMR spectrum of the dyanmer mixture obtained after 4 h reaction at 70 °C. Three signals of aldehyde groups are observed in the 10.1-10.3 ppm range, corresponding to different degrees of substitution in trialdehyde. Signals **a** at 10.21 ppm, **b** at 10.15 ppm, and **c** at 10.09 ppm belong to non-substituted, mono-substituted, and di-substituted trialdehydes, respectively. The molar ratio

of signals **a**, **b** and **c** is 1:6.6:11.5, as determined from the peak integrations. These findings indicate formation of a dyanmer with various free aldehyde groups, which is beneficial for subsequent crosslinking with amino groups of CMCS by imine formation. Signal **d** in the range of 8.0-8.7 ppm is assigned to the imine and aromatic protons, signal **e** around 3.7 ppm to the methylene and methine protons, and signal **f** around 1.2 ppm to the methyl protons of Jeffamine, respectively [28]. The presence of residual CHCl_3 and H_2O is detected at 7.3 and 1.8 ppm, respectively.

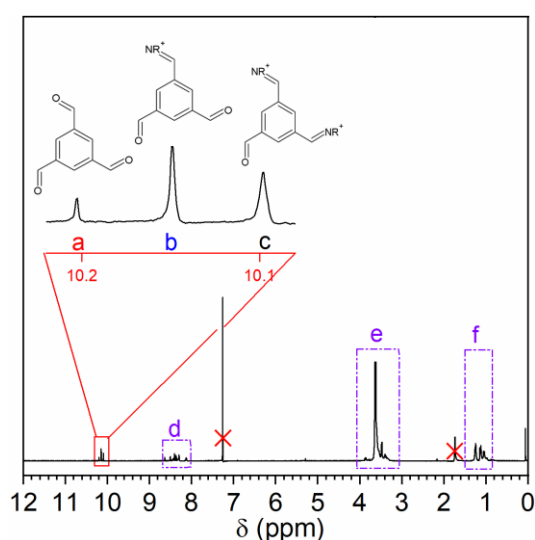


Figure 2.1 ^1H NMR spectrum of the dyanmer **Dy** obtained by reaction of BTA and Jeffamine in CDCl_3 .

The effect of reaction time on the formation of dyanmer was investigated. No difference was observed on the ^1H NMR spectra of samples up to 72 h reaction (Figure S2.1, Supporting Information), thus implying that equilibrium was reached after 4 h reaction. Therefore, the dyanmer obtained after 4 h reaction was selected for further studies. Moreover, the dyanmer apparently remained unchanged for a week in pure D_2O and in acidic D_2O at pH 3 and 5, while became highly hydrolyzed in strongly acidic medium at pH 1 (Figure 2.2). The spectra obtained in D_2O and at pH 3 and 5 remain unchanged even after 7 days (Figure S2.2, Supporting Information). In contrast, major changes are observed on the spectrum of dyanmer at pH 1. The signal **a** (10.21 ppm) belonging to

free aldehydes becomes much more intense, indicating that imine bonds are hydrolyzed back to aldehydes. Therefore, the dynamer Dy seems stable at neutral and slightly acidic pH, but unstable at strongly acidic pH. As previously observed for PEGylated networks, Jeffamine chains could have a protecting effect against the hydrolysis of imine bonds, favoring the imine formation in slightly acidic or neutral media [28].

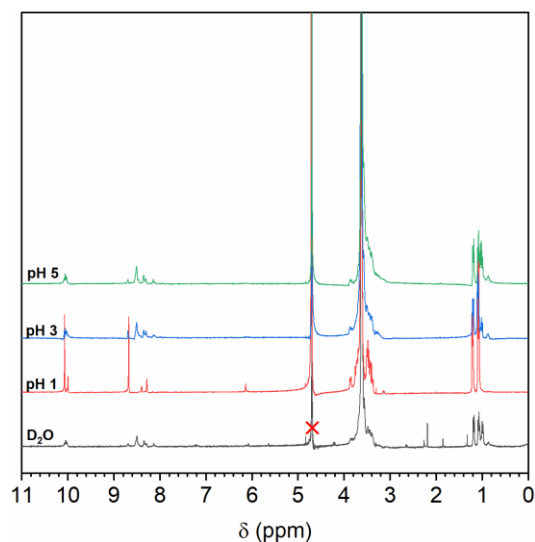


Figure 2.2 ^1H NMR spectra of the dynamer Dy in pure D_2O and acidic D_2O at pH = 1, 3, and 5.

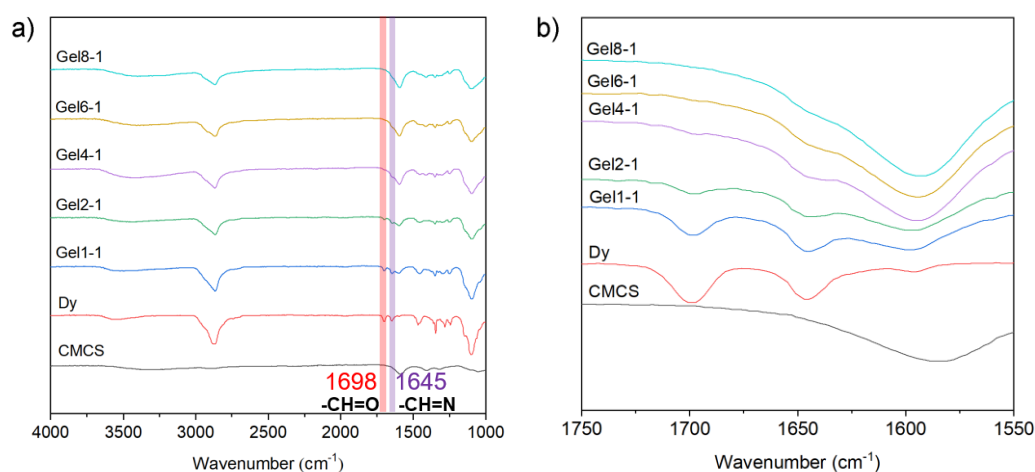
2.3.2 Synthesis of CMCS-Dy hydrogels

CMCS based hydrogels were prepared via a ‘green’ and environmentally friendly method, as shown in Scheme 2.1. The free aldehyde groups of Dy react with the amine groups of CMCS to form imine bonds in water, leading to a three-dimensional network of CMCS based hydrogel. A series of hydrogels were obtained by mixing 1×10^{-1} M CMCS and 5×10^{-2} M dynamer aqueous solutions to a total volume of 12 mL. Gelation proceeded at 37 °C for 24 h. The D-glucosamine to dynamer molar ratio varied from 1:1 to 8:1, as shown in Table 2.1.

Table 2.1 Molar and mass composition of CMCS-Dy hydrogels ^{a)}.

Sample	D-glucosamine/Dy molar ratio	CMCS ^{b)}			Dy			Total polymer concentration [w/v %]
					[mmol]	[mg]		
		[mmol]	[mg]	[w/v %]	^{c)}	^{d)}	[w/v %]	
Gel1-1	1:1	0.4	85	0.7	0.4	810	6.8	7.5
Gel2-1	2:1	0.6	127	1.1	0.3	608	5.0	6.1
Gel4-1	4:1	0.8	170	1.4	0.2	405	3.4	4.8
Gel6-1	6:1	0.9	191	1.6	0.15	304	2.5	4.1
Gel8-1	8:1	0.96	204	1.7	0.12	243	2.0	3.7

^{a)} Hydrogels are prepared by mixing CMCS and dynamer solutions at different ratios to a total volume of 12 mL; ^{b)} The concentration of CMCS solution is 100 mM. Calculations are made on the basis of the average molar mass of 212 g/mol obtained for D-glucosamine, taking into account the degree of deacetylation of 90 % and the degree of carboxymethylation of 80 %; ^{c)} The concentration of Dy solution is 50 mM calculated from the remaining aldehyde groups. In a typical reaction, 1 mmol BTA (162 mg) reacts with 1 mmol Jeffamine (1900 mg) to form a dynamer. As BTA has 3 aldehydes and Jeffamine 2 amines, there remains theoretically 1 mmol of aldehydes in the dried dynamer. Addition of 20 mL water yields a dynamer solution of 50 mM; ^{d)} The amount of Dy in solution is obtained from the initial quantities of BTA and Jeffamine.

**Figure 2.3 a) FT-IR spectra and b) enlarged view of the 1550-1750 cm⁻¹ wavelength range of CMCS, dynamer Dy and freeze-dried CMCS-Dy hydrogels.**

FTIR was used to confirm the formation of imine bonds during the synthesis of

the dynamer Dy and CMCS based hydrogel. As shown in Figure 2.3, the characteristic bands of aldehyde and imine bonds are observed at 1698 and 1645 cm^{-1} on the spectra of Dy, respectively. The dried gels present all the characteristic bands of CMCS and dynamer: a large band in the 3200-3500 cm^{-1} assigned to free OH and NH_2 groups, an intense band at 1595 cm^{-1} assigned to carboxyl groups of CMCS, and two strong signals at 2850 and 1100 cm^{-1} attributed to C-H and C-O stretching in the dynamer, respectively. With increasing D-glucosamine to dynamer molar ratio, the aldehyde band progressively disappears at ratios above 4:1, while the imine band merges with that of carboxyl groups at 1595 cm^{-1} which turns more intense. These findings confirm that hydrogels are formed because of imine formation between aldehyde and amine groups.

2.3.3 Rheological studies

The rheological properties of hydrogels were investigated under various conditions. CMCS and Dy aqueous solutions were mixed in situ on the plate of rheometer, and changes of the storage modulus (G') and loss modulus (G'') were followed as a function of time at 37 °C (Figure 2.4a). For all samples, at the beginning of experiment the storage modulus is lower than the loss modulus ($G' < G''$), which illustrates a liquid-like behavior of the starting mixture. After an induction time, both G' and G'' begin to increase, G' increasing faster than G'' . A cross-over point between G' and G'' is detected, indicating sol-gel transition. As shown in Figure 2.4a, the gelation time decreases from 600 s for Gel1-1 to a minimum of 360 s for Gel4-1, and then increases to 660 s for Gel8-1. In fact, gelation occurs by crosslinking via imine bonds formation and is thus dependent on the ratio between amine groups of CMCS and aldehyde groups of the dynamer. In Gel1-1, there are less amine groups than aldehyde ones, as calculated by taking into account the degree of deacetylation of 90 %. Thus, gelation is relatively slow. Gelation is progressively improved for Gel2-1 and

Gel4-1, as the concentration of amine groups increases. Gelation is not optimal for Gel2-1, since unreacted aldehyde groups are detected by FTIR after 24 h at 37 °C (Figure 2.3). In contrast, optimal imine bond formation is achieved for Gel4-1 as aldehyde groups are no longer detectable. Nevertheless, with further increase of D-glucosamine/dynamer ratio to 6:1 and 8:1, the gelation becomes longer as there are less aldehyde groups available for imine formation.

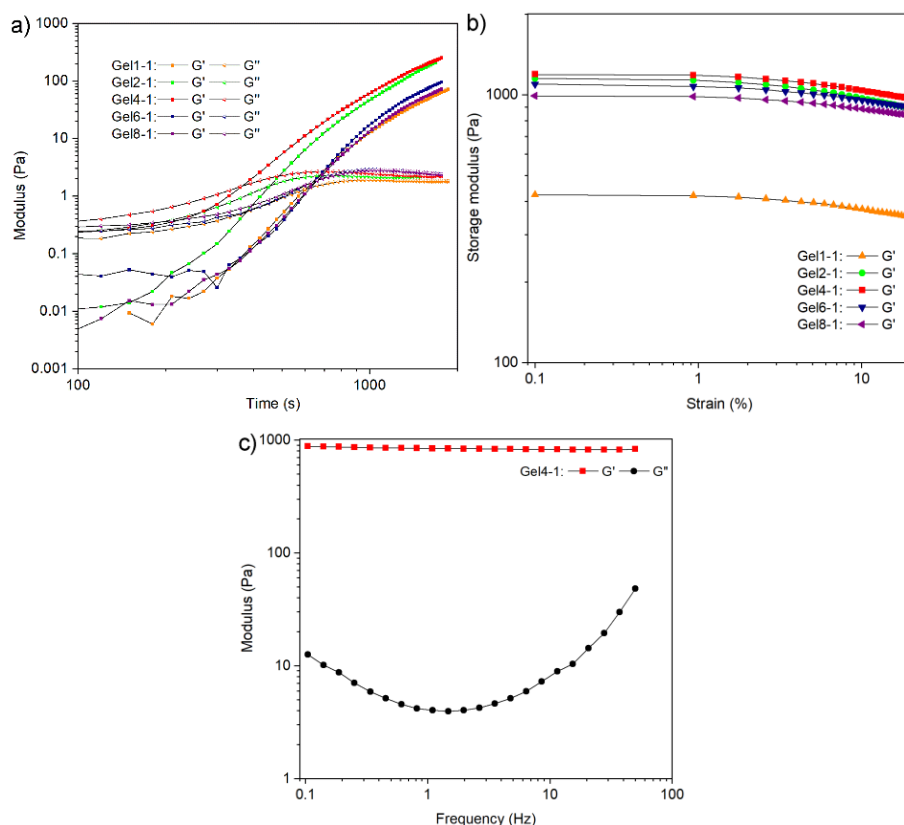


Figure 2.4 a) Storage modulus (G') and loss modulus (G'') changes as a function of time after mixing CMCS and Dy aqueous solutions at various ratios at 37 °C, strain of 1%, and frequency of 1 Hz; b) G' changes as a function of applied strain for all hydrogels at 25 °C, and frequency of 1 Hz; and c) G' and G'' changes of Gel4-1 as a function of frequency at 25 °C, and strain of 1%. All hydrogels are prepared in Milli-Q water.

Rheological measurements performed at 25 °C illustrate the viscoelastic behaviors of as prepared hydrogels. The storage modulus of all gels slightly decreases (less than 20 % of the initial value) when increasing the strain up to 20 % (Figure 2.4b), indicating that the hydrogels are stable in this strain range with viscoelastic behavior. On the other hand, the modulus increases with

increasing D-glucosamine to dynamer molar ratio from 1:1 to 4:1, reaching a maximum value of c.a. 1200 Pa at 4:1. In contrast, higher D-glucosamine to dynamer ratios of 6:1 and 8:1 result in decrease in modulus because there are less aldehydes available for crosslinking in Gel6-1 and Gel8-1 compared to Gel4-1. These findings well agree with storage modulus (G') and loss modulus (G'') changes versus time in Fig. 4a, confirming that optimal crosslinking is achieved with Gel4-1. In order to investigate the stability of the hydrogels, a frequency sweep over a range from 0.01 to 50 Hz was carried out at a fixed strain of 1 %. Taking Gel4-1 as an example (Figure 2.4c), the storage modulus G' is always much higher than the loss modulus G'' . G' remains nearly unchanged, whereas G'' exhibits some fluctuations with increasing frequency. The other hydrogels exhibit similar behaviors (Figure S2.3, Supporting Information). These rheological results well corroborate with the formation of highly stable covalent networks, in contrast to physical hydrogels whose storage and loss moduli are dependent on the frequency [29-30]. It is generally admitted that hydrogels with G' below 2000 Pa are 'soft' materials suitable for specific tissue engineering applications (brain, cartilage, muscle, etc).

2.3.4 Morphology and swelling studies

Scanning electron microscopy (SEM) was used to qualitatively assess the microstructure of the freeze-dried hydrogels. As shown in Figure 2.5, all samples exhibit a sponge-like structure with open and interconnected pores. Gel4-1 apparently exhibits the most uniform porous structure with mean pore size around 150 μm and mean wall thickness of c.a 3 μm , whereas the other samples, in particular Gel1-1 and Gel8-1, present larger and irregular pore size and larger wall thickness. These findings well agree with the optimal imine formation or crosslinking of Gel4-1 since higher crosslinking leads to smaller pore size and wall thickness.

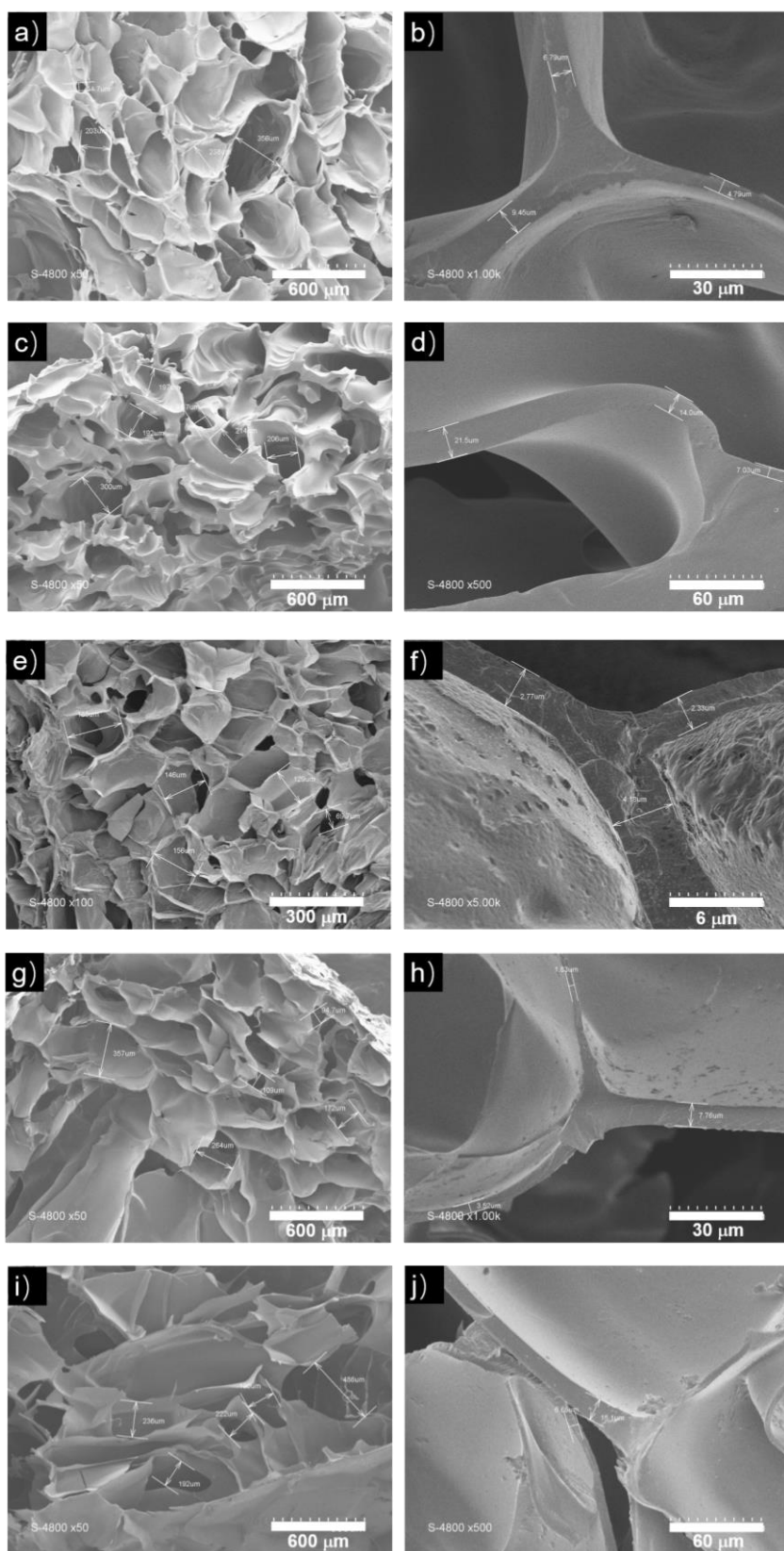


Figure 2.5 SEM images of freeze-dried hydrogels: (a, b) Gel1-1; (c, d) Gel2-1; (e, f) Gel4-1; (g, h) Gel6-1; (i, j) Gel8-1.

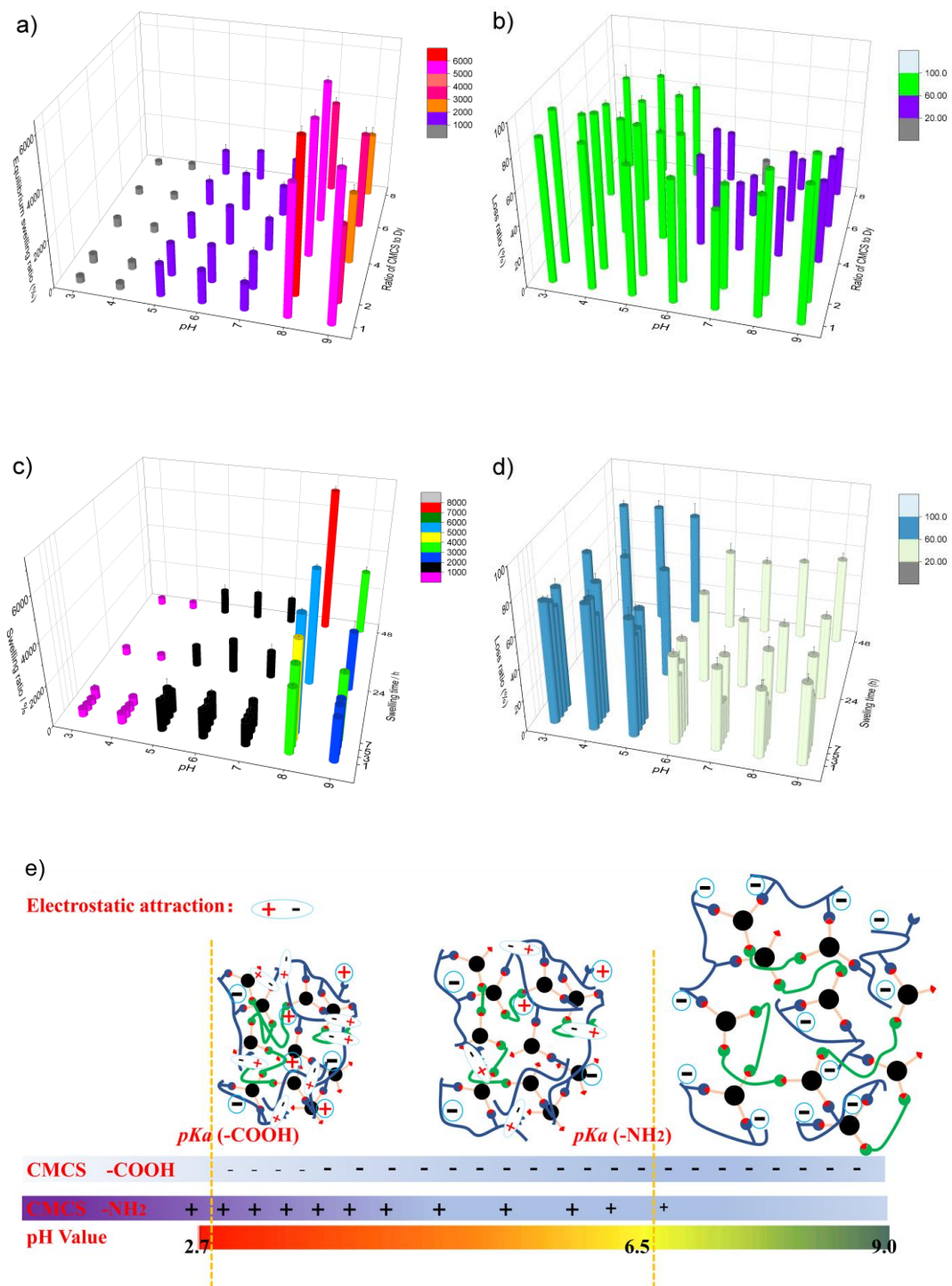


Figure 2.6 a) Equilibrium swelling ratios, and b) Mass loss ratios of Gel1-1, Gel2-1, Gel4-1, Gel6-1, and Gel8-1 at various pH values for 24 h, c) Swelling ratios, and d) Mass loss ratios of Gel4-1 at different pH values as a function of immersion time, e) Schematic presentation of the swelling behavior of freeze-dried hydrogels immersed in buffers at various pH values.

The swelling behaviors of hydrogels are of major importance for the

applications as drug carrier or as tissue engineering scaffold. The five samples exhibit similar swelling behaviors at a given pH value in the pH range from 3 to 9. The highly pH-sensitive swelling ratios are below 1000 % for acidic media (gray bar, pH 3/4), between 1000 % and 2000 % for neutral media (violet bar, pH 5/6/7), above 2000 % and up to 6000 % for alkaline media (orange bar, pink bar, reddish orange bar, magenta bar, and red bar, pH 8/9) as shown in Figure 2.6a. Interestingly, when immersed in slightly alkaline medium at pH 8, the swelling ratio of Gel4-1 dramatically depends on the immersion time (Figure 2.6c). It increases from 3130 % (green bar) after 1 h to 7050 % (red bar) after 48 h immersion. In more alkaline medium at pH 9, the variation of the swelling ratio is attenuated, from 2500 % (blue bar) after 1 h to 3500 % (green bar) after 48 h immersion (Figure 2.6c). In contrast, this exceptional time dependent swelling behavior of Gel4-1 rapidly reaches an equilibrium at 1 h for pH 3-7.

Mass loss could occur after swelling of hydrogels at various pH values, resulting from the diffusion and washing away of non-crosslinked species, including those initially present or formed by hydrolysis of imine bonds under acidic conditions. Thus, the mass loss ratio reflects the crosslinking degree and the stability of hydrogels. Obviously, when immersed in acidic media at $\text{pH} \leq 5$ for all hydrogels or in the whole pH range for Gel1-1 and Gel2-1 with low CMCS and high Dy contents (Figure 2.6b), the mass loss ratio is above 60 % (green bar). Loss ratios below 60 % (violet and gray bars) are obtained only in neutral or alkaline media ($\text{pH} \geq 6$) for Gel4-1 with optimal crosslinking, and Gel6-1 and Gel8-1 with decreasing Dy content (Table 1). These findings indicate that higher Dy content and acidic medium are conducive to the mass loss of hydrogels during swelling. It is thus supposed that unconnected or incompletely connected Dy is predominant in the soluble fraction. Dy rings or homopolymers could be formed during reaction of BTA and Jeffamine (Scheme 2.1). These species may escape coupling with CMCS in the hydrogel preparation procedure. This assumption is consistent with IR analysis showing the presence of the

aldehyde band for Gel1-1 and Gel2-1, and its absence for Gel4-1, Gel6-1 and Gel8-1 samples (Figure 2.3). The reaction conditions could be improved by reducing the time and/or lowering the temperature to minimize the formation of these species.

The mass loss ratio of Gel4-1 also varies with immersion time at different pH values: in the range of 20-60 % (milk white bar) up to 48 h in neutral / alkaline media at $\text{pH} \geq 6$, and above 60% (dusty blue bar) in acidic media at $\text{pH}=3-5$ probably because of the partial hydrolysis of imine bonds (Figure 2.6d). These results indicate that freeze dried hydrogels could be interesting for uses in physiological environment owing to higher swelling and better stability.

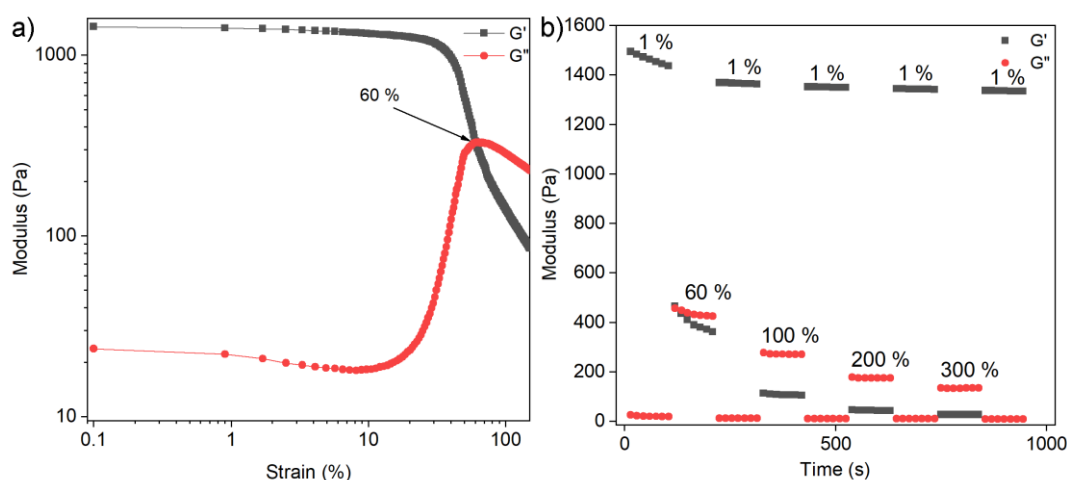
The pH dependent swelling behaviors of hydrogels could be explained by the electrostatic interactions due to the presence of amino and carboxyl groups along CMCS chains. In fact, the pK_a of amino and carboxyl groups is 6.5 and 2.7 [6], respectively. Thus, at acidic pH 3 and 4, there is strong electrostatic attraction between negatively charged $-\text{COO}^-$ and positively charged $-\text{NH}_3^+$ groups, which results in shrinkage or low swelling ratio of hydrogels (Figure 2.6e). With increasing pH up to 7, there are less protonated NH_3^+ and ionized $-\text{COO}^-$ groups, leading to lower electrostatic attraction and higher swelling. In contrast, at pH 8, the NH_2 groups are not charged, while the electrostatic repulsion between the charged $-\text{COO}^-$ groups along CMCS chains leads to strong swelling. However, at pH 9, the electrostatic repulsion between the $-\text{COO}^-$ groups is counterbalanced by the OH^- ions in solution. Consequently, the swelling is attenuated as compared to that observed at pH 8.

Changes of the micro-structure of hydrogels were observed by using SEM after 24 h swelling at two pH values. At pH 4, all freeze-dried hydrogels strongly shrink with reduced pore size and pore number (Figure S2.4, Supporting Information). Noticeably, the pore size of Gel4-1 decreases from c.a 150 to 100 μm , and the wall thickness increases from c.a 3.5 μm to 15 μm , reminiscent with the contraction of hydrogels due to electrostatic attraction at acidic pH

(Figure 2.6e). In contrast, expansion of the porous structure is observed at pH 8 (Figure S2.5, Supporting Information). The pores wall shows a cracked structure, with the thickness strongly decreasing from c.a 3.5 μm to 200-600 nm due to strong swelling of hydrogels provoked by electrostatic repulsion at basic pH (Figure 2.6e).

2.3.5 Self-healing

CMCS-based hydrogels present interesting self-healing behaviors as evidenced by rheological recovery tests at fixed frequency of 1 Hz and at 37 °C. Gel4-1 hydrogels were prepared in Milli-Q water, and in pH 7 and pH 8 buffers in order to examine the self-healing behavior under different swollen conditions. Gelation was realized at 37°C for 24 h. As shown in Figure 2.7a, both the storage modulus (G') and loss modulus (G'') of Gel4-1 in Milli-Q water slightly decreases until a strain of 20%. Beyond, G' dramatically decreases, whereas G'' rapidly increases. A crossover point of G' and G'' values is observed at a strain of 60%. Similar profiles are observed for Gel4-1 at pH 7 with a crossover point at 35% (Figure S2.6a, Supporting Information). In contrast, Gel4-1 at pH 8 exhibits lower storage modulus because of its highly swollen state as shown in Figure 2.6a. The crossover points of G' and G'' is detected at 55% at pH 8 (Figure S2.6c, Supporting Information).



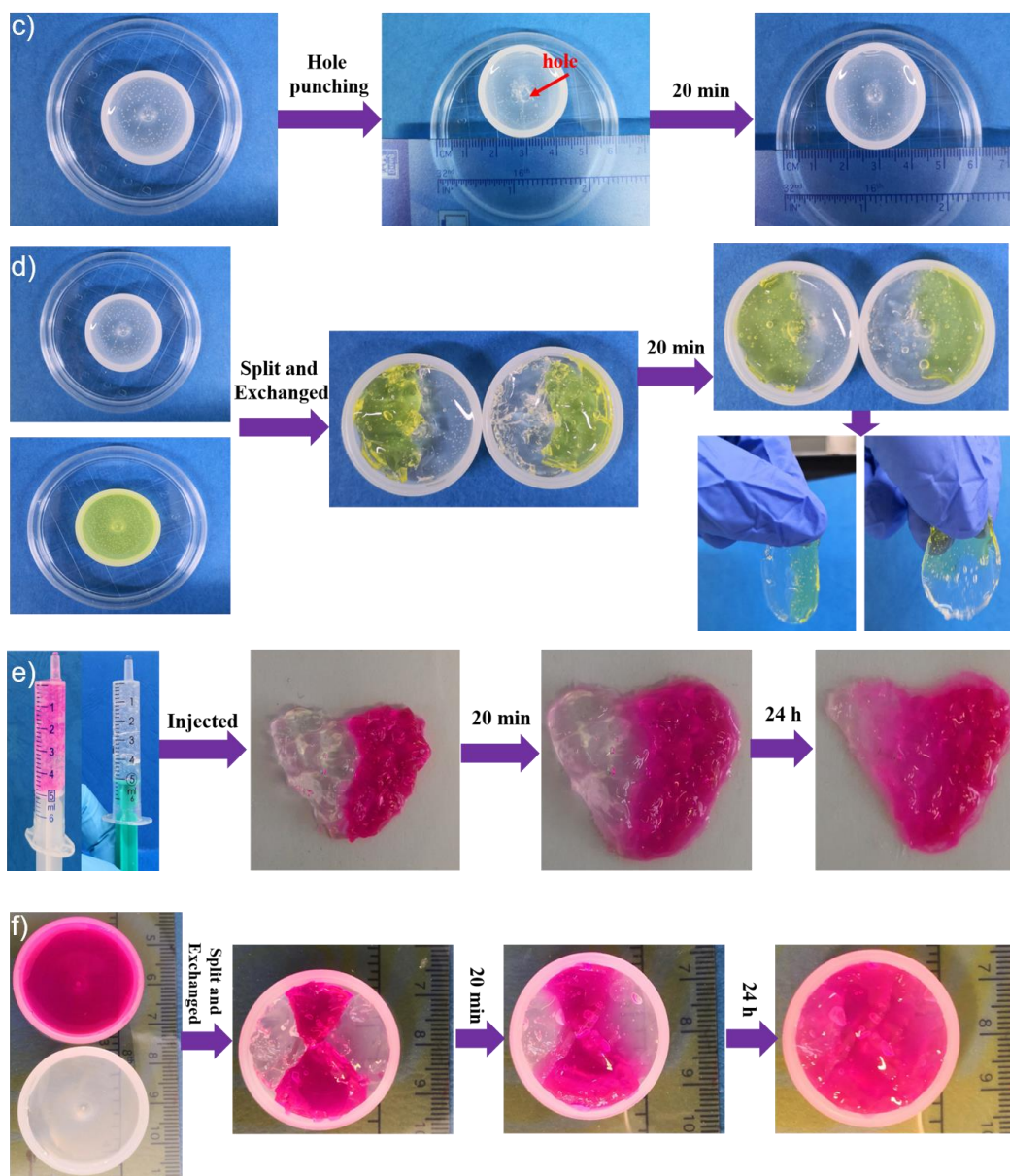


Figure 2.7 a) Modulus changes as a function of strain of Gel4-1 prepared in Milli-Q water; b) Modulus changes of Gel4-1 prepared in Milli-Q water with alternatively applied high and low oscillatory shear strains at 37°C; c-f) Self-healing macroscopic approaches using hydrogel samples prepared in Milli-Q water (c-d), at pH 7 (e) and at pH 8 (f) , see text for details.

Based on the strain amplitude sweep results, continuous step strain measurements were performed to examine the rheological recovery behavior of Gel4-1. At 1 %, Gel4-1 in Milli-Q water behaves as a hydrogel since G' is largely superior to G'' . As the oscillatory shear strain increases from 1% to 60% and is maintained at 60% for 105 s (Figure 2.7b), G' becomes lower than G'' ,

indicating the destruction of hydrogel structure. Both G' and G'' immediately recover their initial values when the strain is back to 1%. Modulus recovery is observed when larger strains (100, 200, and 300%) and small strain (1%) are alternatively applied. Similar phenomena are also observed for Gel4-1 prepared in pH 7 and 8 buffers (Figure S2.6b, S2.6d, Supporting Information). Therefore, it could be concluded that dynamic hydrogels exhibit rapid recovery (self-healing) behavior probably due to the reconstruction of reversible imine bond linkage when they are subjected to alternatively applied high and low oscillatory shear strains.

The self-healing behavior of Gel4-1 was further evidenced with four different macroscopic approaches using one transparent hydrogel sample and another one incorporating yellow lucigenin or red Rhodamine B dyes. First, a hole with diameter of 3 mm was punched at the center of a hydrogel sample prepared in Milli-Q water, and the hole disappeared after 20 min at 37°C (Figure 2.7c). In a second approach, transparent and yellow hydrogel samples prepared in Milli-Q water were cut into two semicircular pieces. They became integrated after only 20 min contact at 37°C. The merged piece could be then taken off and support its own weight (Figure 2.7d).

In a third approach, one transparent hydrogel and another one containing red Rhodamine B dye prepared in pH 7 buffer were crushed via injection onto a Petri dish using a syringe, and became integrated 20 min later (Figure 2.7e). Almost the whole hydrogel was dyed red after 24 h. Similar phenomena were observed in a fourth approach for transparent and dyed red hydrogels prepared in pH 8 buffer (Figure 2.7f), demonstrating that the color exchange may be observed via diffusion at the restored self-healed interfaces between different dynagels at pH 7 or pH 8.

These tests strongly demonstrate the outstanding self-healing properties of the dynamic hydrogels - dynagels via reconstruction of reversible imine bond crosslinking, and migration of components or constituent exchanges between

different hydrogels. Importantly, the use of these hydrogels with distinct and interchangeable states at different pH conditions would be advantageous for biomedical applications such as drug delivery and tissue engineering.

2.3.6 Cytocompatibility of hydrogels

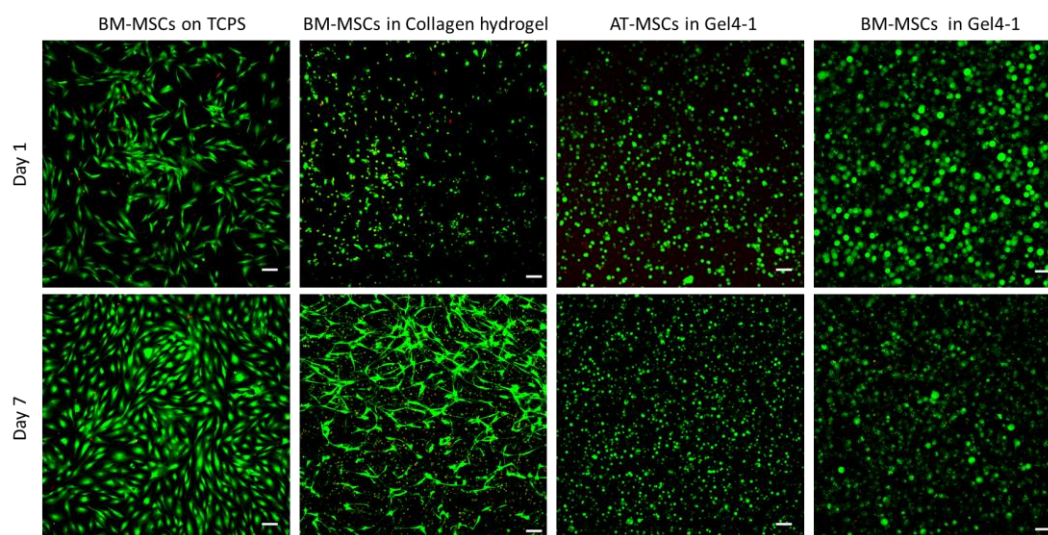


Figure 2.8 Cell viability of human AT-MSCs or BM-MSCs in Gel4-1, in comparison with BM-MSCs in collagen hydrogel or plated on TCPS as control. Cells were labelled using the Live/Dead assay after 1 or 7 days in culture and imaged using confocal microscopy. Viable cells were stained in green and dead cells in red. Images are maximal projections of z-axis and scale bars represent 100 μm (TCPS: Tissue Culture Polystyrene Surface; AT-MSCs: Adipose Tissue-MSCs; BM-MSCs: Bone Marrow-MSCs).

Human mesenchymal stromal cells (MSCs) isolated from subcutaneous adipose tissue (AT-MSCs) or from bone-marrow (BM-MSCs) were encapsulated inside Gel4-1 (1×10^6 cells/mL), and cultured up to 7 days in proliferative medium at 37 °C to evaluate the cytocompatibility. Compared to control conditions in 2D on TCPS plate or encapsulated in a type I collagen hydrogel, AT-MSCs and BM-MSCs exhibited a round shape in Gel4-1 and not a fibroblastic phenotype (Figure 2.8). One day after inclusion in the hydrogel, the large majority of AT-MSCs (95%) and BM-MSCs (99%) were alive as indicated by the green color in confocal microscopy using live/dead assay, whereas only 66% of viability was observed in type I collagen hydrogel (Figure

2.8). The two cell types survived for at least 7 days, as only 1 and 4% of dead cells were quantified for AT-MSCs and BM-MSCs, respectively (Figure 2.8). These findings demonstrate the excellent cytocompatibility of the hydrogel. It is noteworthy that the size of AT-MSCs and BM-MSCs after 7 days was smaller than that at day 1, suggesting that the pore size was reduced without affecting cell viability. Three-D reconstruction clearly shows the homogeneous distribution of MSCs in the whole hydrogel volume, indicating that the gelation time was compatible with homogenous distribution of the cells without sedimentation (Video file, Supporting Information, data not shown).

2.4 Conclusions

Multistate pH-sensitive hydrogels were synthesized via dynamic covalent imine bonding from two water soluble polymers, i.e., O-carboxymethyl chitosan (CMCS) and a cross-linking dynamer obtained by reaction of amine terminated Jeffamine as connector and Benzene-1,3,5-tricarbaldehyde as core center. The hydrogel Gel4-1 with D-glucosamine to dynamer molar ratio of 4:1 exhibits the shortest gelation time and the highest storage modulus, in agreement with optimal cross-linking or imine bond formation. Freeze-dried gels exhibit interconnected porous structures and pH-dependent swelling behavior. The swelling ratio is relatively low at acidic pH 3-5 due to electrostatic attraction, while became very high, up to 7000 % at pH 8 due to electrostatic repulsion. Moreover, hydrogels present outstanding self-healing properties as evidenced by closure of split pieces and rheological studies. Self-healing occurs autonomously for different pH-dependent states, being able to reshape or to regenerate a strong chemical gel from various situations. Last but not least, MSCs encapsulated in hydrogels are all alive after 7 days, in agreement with the excellent cytocompatibility of hydrogels.

This concept, exploiting different physical swelling states depending on pH values, results in the definition of stimuli-responsive dynagels which self-adapt

their structure in response to environmental conditions. These ‘two-in-one’ dynagels may find potential uses in biomedical applications in particular as scaffold in tissue engineering

Supporting information

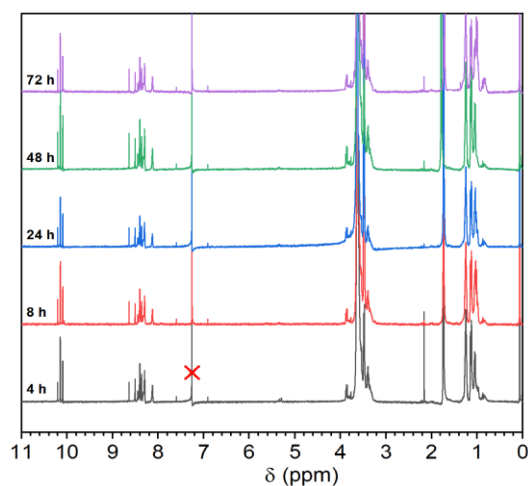


Figure S2.1 ^1H NMR spectra of the dynamer Dy obtained After 4, 8, 24, 48 and 72 h reaction recorded in CDCl_3 .

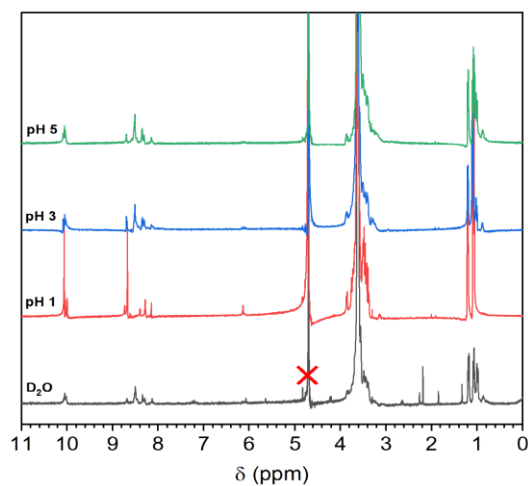


Figure S2.2 ^1H NMR spectra of the dynamer Dy recorded after 7 days in D_2O and at pH = 1, 3, and 5.

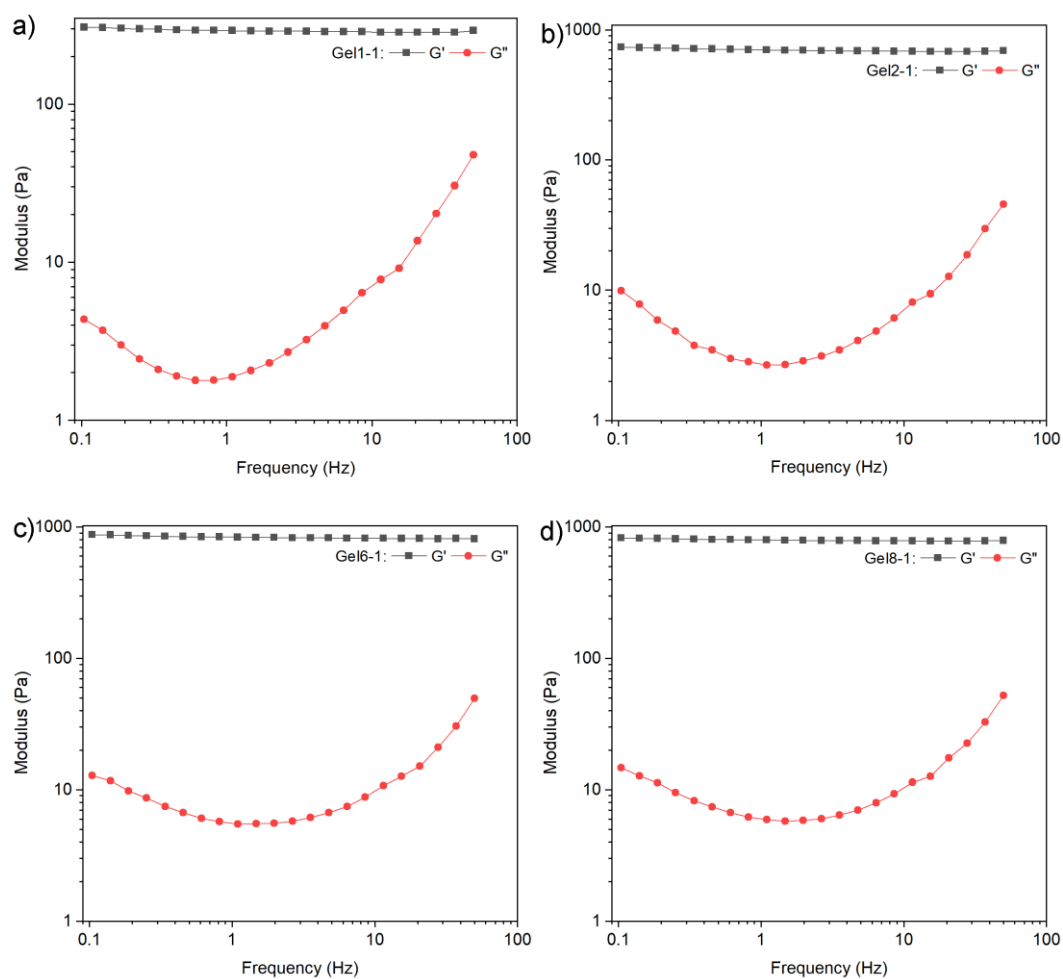


Figure S2.3 Storage modulus (G') and loss modulus (G'') changes as function of frequency for samples: Gel1/1, Gel2/1, Gel6/1, Gel8/1.

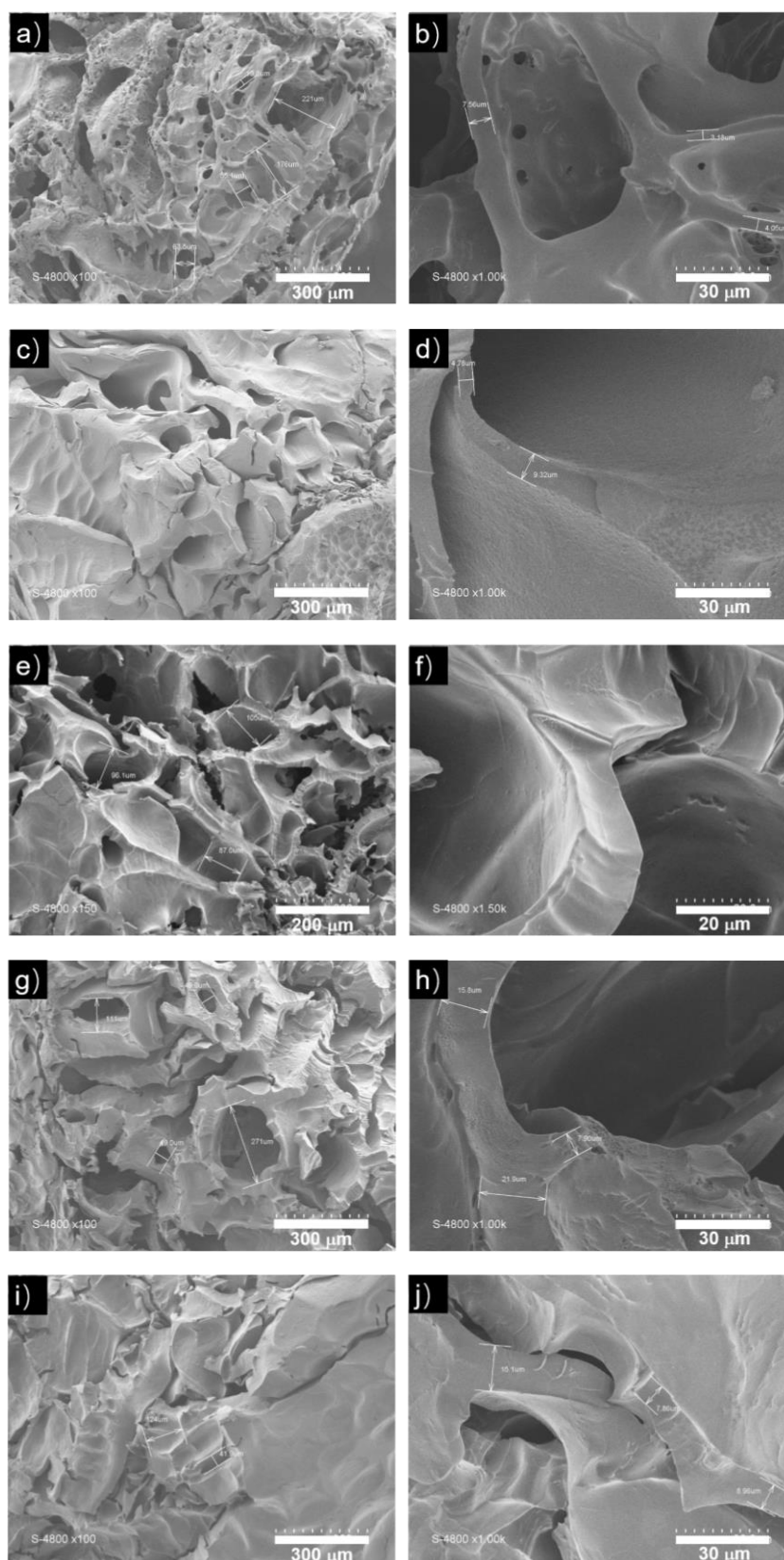


Figure S2.4 SEM images of freeze-dried hydrogels (a, b) Gel1-1; (c, d) Gel2-1; (e, f) Gel4-1; (g, h) Gel6-1; (i, j) Gel8-1 after 24 h swelling at pH 4.

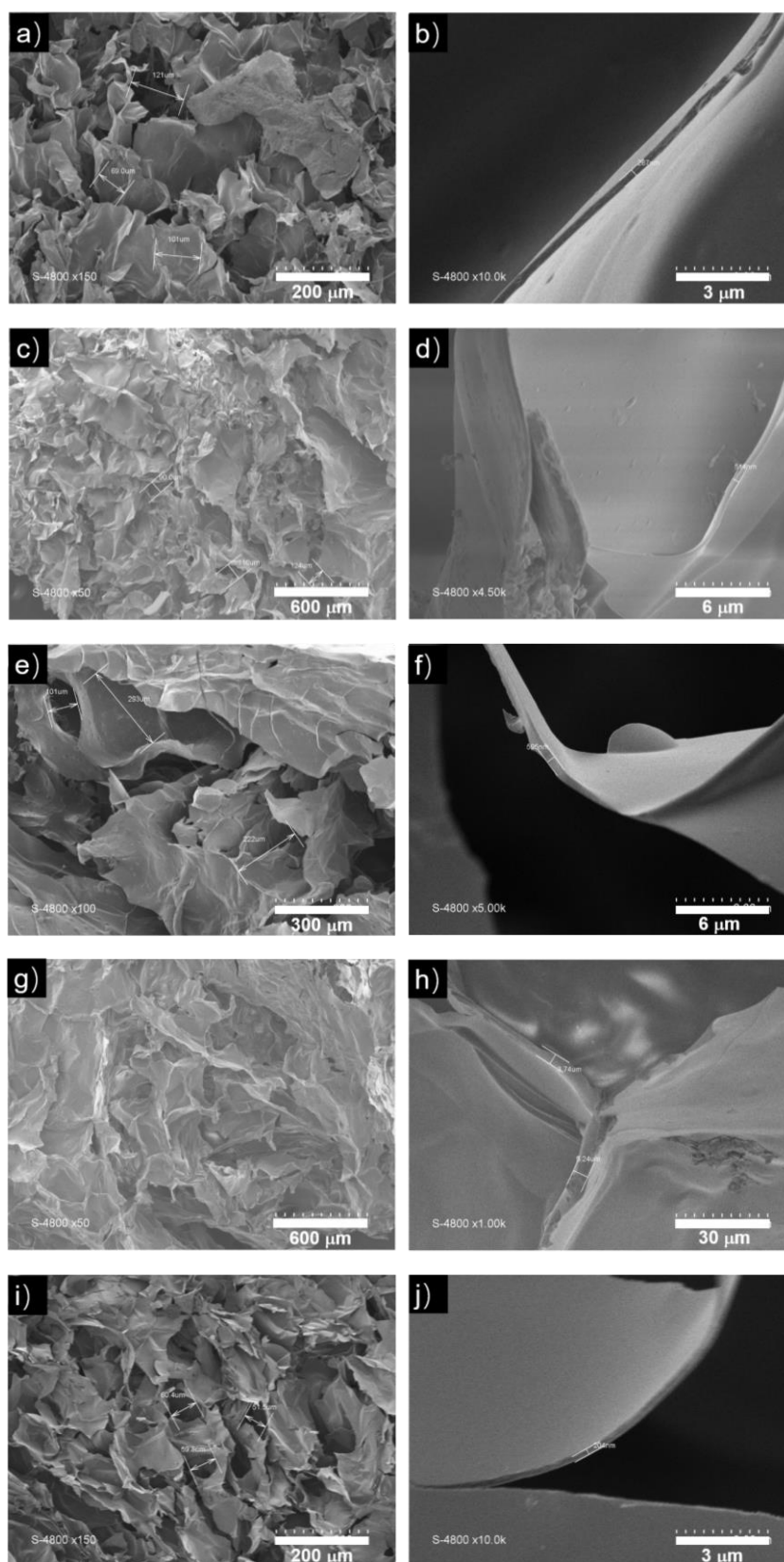


Figure S2.5 SEM images of freeze-dried hydrogels (a, b) Gel1-1; (c, d) Gel2-1; (e, f) Gel4-1; (g, h) Gel6-1; (i, j) Gel8-1 after 24 h swelling at pH=8.

A rheological recovery test was performed on hydrogels by following modulus changes and switching the strain from a small one ($\gamma=1\%$) to a large one up to 300% at 105 s intervals.

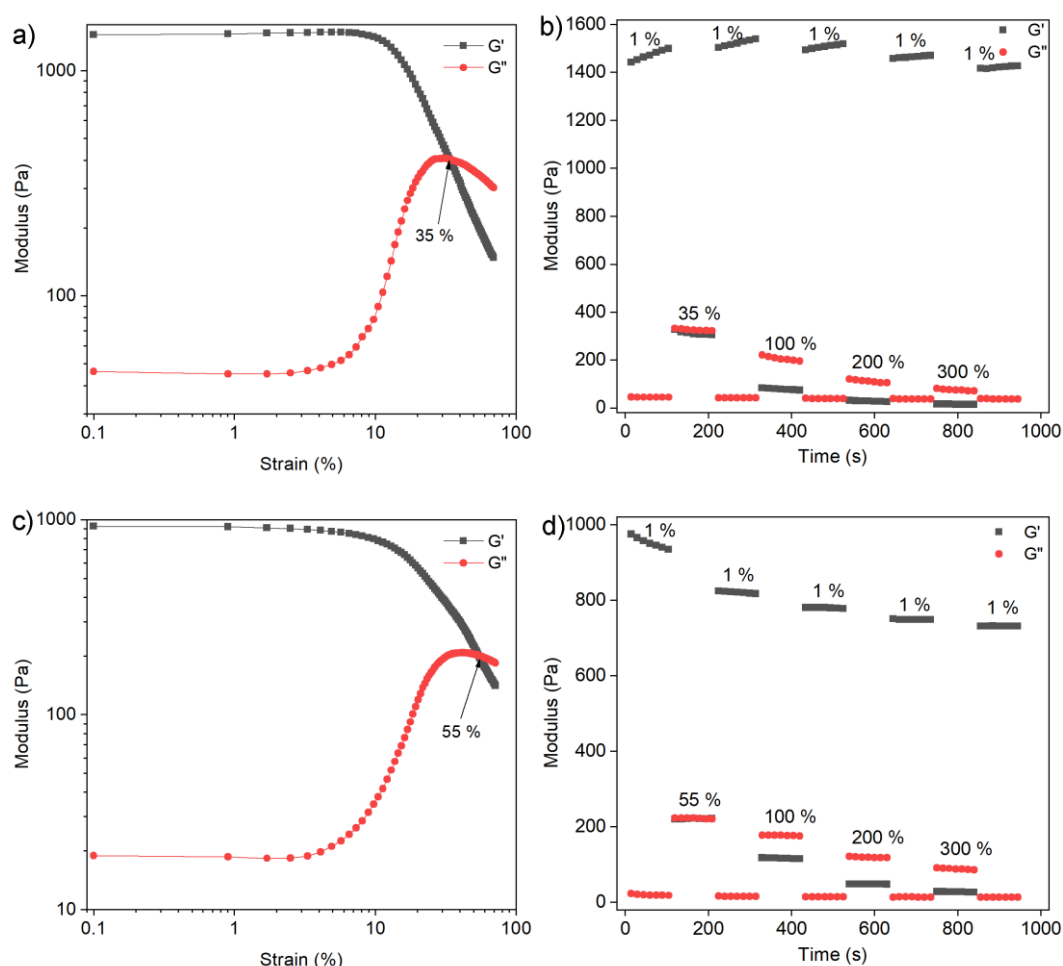


Figure S2.6 Modulus changes as a function of strain of Gel4-1 prepared at pH=7 (a) and pH=8 (c); modulus changes with alternatively applied low and high oscillatory shear strains at 37 °C for Gel4-1 prepared at pH=7 (b) and pH=8 (d).

References

- [1] J. Qu, X. Zhao, Y. Liang, T. Zhang, P.X. Ma, B. Guo, Antibacterial adhesive injectable hydrogels with rapid self-healing, extensibility and compressibility as wound dressing for joints skin wound healing, *Biomaterials* 183 (2018) 185-199.
- [2] C. Ghobril, M. Grinstaff, *The chemistry and engineering of polymeric*

hydrogel adhesives for wound closure: a tutorial, *Chem. Soc. Rev.* 44(7) (2015) 1820-1835.

[3] S. Van Vlierberghe, P. Dubruel, E. Schacht, Biopolymer-based hydrogels as scaffolds for tissue engineering applications: a review, *Biomacromolecules* 12(5) (2011) 1387-1408.

[4] Y. Zhang, L. Tao, S. Li, Y. Wei, Synthesis of multiresponsive and dynamic chitosan-based hydrogels for controlled release of bioactive molecules, *Biomacromolecules* 12(8) (2011) 2894-901.

[5] F. Su, J. Wang, S. Zhu, S. Liu, X. Yu, S. Li, Synthesis and characterization of novel carboxymethyl chitosan grafted polylactide hydrogels for controlled drug delivery, *Polym. Adv. Technol.* 26(8) (2015) 924-931.

[6] X. Lv, W. Zhang, Y. Liu, Y. Zhao, J. Zhang, M. Hou, Hygroscopicity modulation of hydrogels based on carboxymethyl chitosan/Alginate polyelectrolyte complexes and its application as pH-sensitive delivery system, *Carbohydr. Polym.* 198 (2018) 86-93.

[7] Y. Yang, X. Wang, F. Yang, L. Wang, D. Wu, Highly elastic and ultratough hybrid ionic-covalent hydrogels with tunable structures and mechanics, *Adv. Mater.* 30(18) (2018) 1707071.

[8] R. Dimatteo, N.J. Darling, T. Segura, In situ forming injectable hydrogels for drug delivery and wound repair, *Adv. Drug Del. Rev.* 127 (2018) 167-184.

[9] D. Stewart, D. Antypov, M.S. Dyer, M.J. Pitcher, A.P. Katsoulidis, P.A. Chater, F. Blanc, M. Rosseinsky, Stable and ordered amide frameworks synthesised under reversible conditions which facilitate error checking, *Nat. Commun.* 8(1) (2017) 1102.

[10] M.M. Iftime, S. Morariu, L. Marin, Salicyl-imine-chitosan hydrogels: Supramolecular architecturing as a crosslinking method toward multifunctional hydrogels, *Carbohydr. Polym.* 165 (2017) 39-50.

[11] L. Marin, S. Moraru, M.C. Popescu, A. Nicolescu, C. Zgardan, B.C. Simionescu, M. Barboiu, Out - of - Water Constitutional Self - Organization of

Chitosan – Cinnamaldehyde Dynagels, *Chem. Eur. J.* 20(16) (2014) 4814-4821.

[12] N. Sreenivasachary, J.-M. Lehn, Gelation-driven component selection in the generation of constitutional dynamic hydrogels based on guanine-quartet formation, *Proc. Natl. Acad. Sci. U. S. A.* 102(17) (2005) 5938-5943.

[13] X. Zeng, G. Liu, W. Tao, Y. Ma, X. Zhang, F. He, J. Pan, L. Mei, G. Pan, A drug - self - gated mesoporous antitumor nanoplatfrom based on pH - sensitive dynamic covalent bond, *Adv. Funct. Mater.* 27(11) (2017) 1605985.

[14] A. Rotaru, G. Pricope, T.N. Plank, L. Clima, E.L. Ursu, M. Pinteala, J.T. Davis, M. Barboiu, G-Quartet hydrogels for effective cell growth applications, *Chem. Commun.* 53(94) (2017) 12668-12671.

[15] C. Arnal Hérault, A. Banu, M. Barboiu, M. Michau, A. van der Lee, Amplification and transcription of the dynamic supramolecular chirality of the guanine quadruplex, *Angew. Chem., Int. Ed.* 46(23) (2007) 4268-4272.

[16] W. Zhang, X. Jin, H. Li, R. Zhang, C. Wu, Injectable and body temperature sensitive hydrogels based on chitosan and hyaluronic acid for pH sensitive drug release, *Carbohydr. Polym.* 186 (2018) 82-90.

[17] Y. Zhang, M. Barboiu, Constitutional Dynamic Materials Toward Natural Selection of Function, *Chem. Rev.* 116(3) (2015) 809-834.

[18] A. Chao, I. Negulescu, D. Zhang, Dynamic covalent polymer networks based on degenerative imine bond exchange: tuning the malleability and self-healing properties by solvent, *Macromolecules* 49(17) (2016) 6277-6284.

[19] Y. Zhang, M. Barboiu, Dynameric asymmetric membranes for directional water transport, *Chem. Commun.* 51(88) (2015) 15925-15927.

[20] A. Ali, S. Ahmed, A review on chitosan and its nanocomposites in drug delivery, *Int. J. Biol. Macromol.* 109 (2018) 273-286.

[21] L. Marin, B. Simionescu, M. Barboiu, Imino-chitosan biodynamers, *Chem. Commun.* 48(70) (2012) 8778-8780.

[22] C. Qin, J. Zhou, Z. Zhang, W. Chen, Q. Hu, Y. Wang, Convenient one-step approach based on stimuli-responsive sol-gel transition properties to directly

build chitosan-alginate core-shell beads, *Food Hydrocolloids* 87 (2019) 253-259.

[23] C. Qiao, X. Ma, J. Zhang, J. Yao, Molecular interactions in gelatin/chitosan composite films, *Food Chem.* 235 (2017) 45-50.

[24] Y. Xu, Y. Li, Q. Chen, L. Fu, L. Tao, Y. Wei, Injectable and self-healing chitosan hydrogel based on imine bonds: design and therapeutic applications, *Int. J. Mol. Sci.* 19(8) (2018) 2198.

[25] S. Yu, X. Zhang, G. Tan, L. Tian, D. Liu, Y. Liu, X. Yang, W. Pan, A novel pH-induced thermosensitive hydrogel composed of carboxymethyl chitosan and poloxamer cross-linked by glutaraldehyde for ophthalmic drug delivery, *Carbohydr. Polym.* 155 (2017) 208-217.

[26] G. Deng, Q. Ma, H. Yu, Y. Zhang, Z. Yan, F. Liu, C. Liu, H. Jiang, Y. Chen, Macroscopic organohydrogel hybrid from rapid adhesion between dynamic covalent hydrogel and organogel, *ACS Macro Lett.* 4(4) (2015) 467-471.

[27] W. Huang, Y. Wang, Y. Chen, Y. Zhao, Q. Zhang, X. Zheng, L. Chen, L. Zhang, Strong and Rapidly Self - Healing Hydrogels: Potential Hemostatic Materials, *Adv. Healthcare Mater.* 5(21) (2016) 2813-2822.

[28] R. Catana, M. Barboiu, I. Moleavin, L. Clima, A. Rotaru, E.L. Ursu, M. Pinteala, Dynamic constitutional frameworks for DNA biomimetic recognition, *Chem. Commun.* 51(11) (2015) 2021-2024.

[29] Y. Zhang, X. Wu, Y. Han, F. Mo, Y. Duan, S. Li, Novel thymopentin release systems prepared from bioresorbable PLA–PEG–PLA hydrogels, *Int. J. Pharm.* 386(1-2) (2010) 15-22.

[30] S. Li, A. El Ghzaoui, E. Dewinck, Rheology and drug release properties of bioresorbable hydrogels prepared from polylactide/poly (ethylene glycol) block copolymers, *Macromol. Symp.*, Wiley Online Library, 2005, pp. 23-36.

Chapter 3 Anti-bacterial dynamic hydrogels prepared from O-carboxymethyl chitosan by dual imine bond crosslinking for biomedical applications

Abstract: Imine dynamic hydrogels are synthesized via dual-imine bond crosslinking from O-carboxymethyl chitosan (CMCS) and a water soluble dynamer using a 'green' approach. Three dynamers are prepared through reaction of benzene-1,3,5-tricarbaldehyde and di-amino Jeffamine with molar mass of 500, 800 and 1900, respectively. Hydrogels, namely H500, H800 and H1900 are then obtained by mixing CMCS and dynamer aqueous solutions. FT-IR confirms the formation of hydrogels via imine bonding. H1900 presents larger pore size and higher storage modulus as compared to H500 and H800 due to the higher molar mass of Jeffamine linker. The hydrogels exhibit pH sensitive swelling behavior due to electrostatic attraction or repulsion in the pH range from 3 to 10. The highest swelling ratio is obtained at pH 8, reaching 7500 % for H800. Self-healing of hydrogels is evidenced by rheological measurements with alternatively applied low and high strains, and by using a macroscopic approach with re-integration of injected filaments. Furthermore, the H1900 membrane exhibits significant antibacterial activity against an *E. coli* suspension at 10^8 CFU mL⁻¹. Therefore, dynamic hydrogels synthesized from CMCS and Jeffamine present outstanding rheological, swelling, self-healing and antibacterial properties, and are most promising as healthcare material in wound dressing, drug delivery and tissue engineering.

Keywords: O-carboxymethyl chitosan, Jeffamine, Imine bonding; pH-sensitive, Self-healing, Antibacterial property

3.1 Introduction

Hydrogels are soft materials which are capable of absorbing large amount of water without dissolution [1]. They are generally composed of a 3-dimensional hydrophilic polymer network linked together either by covalent bonds [2], or by physical interactions via chain entanglements, hydrophobic association, electrostatic interactions, van der Waals forces, etc. [3]. In the past decades, hydrogels have been most widely studied for applications in drug delivery [4], wound dressing [5], tissue engineering [6], and in agriculture [7], owing to their prominent properties such as flexibility, ductility, and biocompatibility.

Dynamic hydrogels are a new generation of hydrogels which are crosslinked by dynamic covalent bonding via SN2-type nucleophilic substitution [8], imine chemistry [9], Diels-Alder reaction [10], etc. Generally, they are responsive to external stimuli, such as light, temperature, and pH [11-13]. A dynamic hydrogel was formed by specific benzoxaborole-carbohydrate interactions between benzoxaborole-modified hyaluronic acid and fructose-based glycopolymer. Release of doxorubicin from the hydrogel can be precisely switched on/off by near-infrared light as a trigger [11]. A thermos-sensitive hydrogel was generated by dynamic chemical oxime bonding from alkoxyamine-terminated Pluronic F127 and oxidized hyaluronic acid, as well as hydrophobic association. The hydrogel exhibits much higher modulus and higher stability than the Pluronic F127 hydrogel, and could be used as a promising postoperative anti-adhesion material in clinical practice [12]. On the other hand, soft hydrogels based on alginate-boronic acid were obtained from reversible inter- and intramolecular interactions by dynamic equilibrium of boronic acid–diol complexation and dissociation. The hydrogels present pH- and glucose-sensitivities, [13] and could be promising for applications as biological glues that require stretchability, self-healing, and multi-responsive behavior. Although these dynamic hydrogels exhibit versatile stimuli-responsive properties compared to common hydrogels,

the approaches involved in the hydrogel fabrication is rather complex. Thereby, among the various dynamic bonds, imine bonding attracted great interest because of mild reaction conditions [14], the efficient reversibility of imine bonds, tunable properties and stimuli-responsive performance of resulted materials [15].

Chitosan (CS) is a polysaccharide widely used to prepare hydrogels for various applications because of its biocompatibility [16], biodegradability [17], and anti-bacterial activities [18]. Recently, chitosan received much attention as a hydrophilic biopolymer for reversible crosslinking via reaction between the amino groups along the backbone and other polymers [19], including hyaluronic acid [20], alginate [21], and gelatin [22]. Nevertheless, high molar mass chitosan is poorly soluble in water at neutral or basic pH due to intermolecular hydrogen bonding [23], which is not beneficial for its utilization in the biomedical field.

Carboxymethyl chitosan (CMCS) is a water-soluble derivative of chitosan which presents outstanding biological properties [24]. Crosslinking of CS or CMCS with different aldehydes has been reported, including monoaldehydes [25], dialdehydes [26], and derivatives of aldehydes [27]. The resulting hydrogels present good mechanical strength [26, 28], and have been studied for applications in tissue engineering. However, these hydrogels present some disadvantages such as low swelling ratio, tedious preparation procedure, disordered micro-structure, etc.

Benzene-1,3,5-tricarbaldehyde (BTA) is a promising cross-linker for the formulation of dynamic hydrogels based on imine bonding. In fact, BTA can serve as a tri-topic center for three-dimensional cross-linking with diamino polymers, thus yielding nonlinear and continuous network structures [29]. Nevertheless, BTA is not soluble in water, which prevents its uses in aqueous medium. Jeffamine is a biocompatible polyetheramine consisting of poly(propylene oxide) (PPO) and poly(ethylene oxide) (PEO) blocks terminated

with primary amino groups. It has been largely used in the synthesis of amphiphilic block copolymers [30], hydrogels [31], and dynamic frameworks [32].

Currently, with the appearance of new medical equipments and technologies, the prevention of bacteria and fungi becomes a key issue in different medical therapies. The development of antimicrobial materials attracted much interest [33], especially hydrogels possessing intrinsic antibacterial properties. For example, hydrogels based on CS or CMCS have been largely investigated as wound dressing [34].

In our previous work, a dual-imine dynamic hydrogel was prepared using a two steps procedure [35]. Difunctional Jeffamine ED2003 (Mn 1900) first reacts with BTA to form a water soluble dynamer (Dy), followed by crosslinking of the dynamer and CMCS in water to yield a 3-dimensional network, both based on Schiff base reaction. The resulting hydrogels present high storage modulus, pH-sensitive swelling behavior, outstanding self-healing performance and excellent cytocompatibility. In this work, dynamic hydrogels were prepared using the same procedure from three Jeffamines of different molar masses, *i.e.*, ED600 (Mn 500), ED900 (Mn 800) and ED2003 (Mn 1900). The resulting hydrogels were characterized by Fourier-transform infrared spectroscopy (FT-IR) and rheological measurements. The pH dependent swelling and self-healing behaviors were evaluated to evidence the effect of Jeffamine molar mass on hydrogel properties. Mild and “green” preparation of the hydrogel and the antibacterial properties determine the potential of dynamic hydrogels in biomedical applications, such as wound dressing or tissue engineering scaffold.

3.2 Experimental section

3.2.1 Materials

O,O'-Bis (2-aminopropyl) poly(propylene glycol)-block-poly(ethylene glycol)-

block-poly(propylene glycol) (Jeffamine[®]) ED-600 (Mn 500), ED900 (Mn 800) and ED-2003 (Mn 1900) from Sigma-Aldrich, benzene-1,3,5-tricarbaldehyde (BTA) from Manchester Organics (Purity 98 %) were used without further purification. O-carboxymethyl chitosan (CMCS) with degree of carboxymethylation of 80%, degree of deacetylation of 90%, and Mw of 200000 Da was supplied by Golden-shell Biochemical Co., Ltd. Methanol (96%), citric acid (99.5%), disodium hydrogen phosphate dodecahydrate (99%), boric acid (99.5%), and borax (99%) were of analytical grade, and obtained from Sigma-Aldrich. All chemicals were used without further purification. *Escherichia coli* (K12 DSM 423) was purchased from DSMZ, Germany.

3.2.2 Synthesis of dynamers Dy500, Dy800 and Dy1900

BTA (162.14 mg, 1 mmol), Jeffamine[®] ED-600 (0.5 g, 1 mmol) were added in 30 mL methanol. The reaction mixture was stirred at 70 °C under reflux for 4 h. The solvent was then evaporated using rotary evaporator. 20 mL Milli-Q water was added to yield a homogeneous Dy500 solution of 50 mM, as calculated from remaining aldehyde groups. Dy800 and Dy1900 were prepared from Jeffamine[®] ED-900 or ED-2003 under the same conditions.

3.2.3 Synthesis of hydrogels

100 mM CMCS solution was prepared by dissolving 1.06 g CMCS (5 mmol, calculated from D-glucosamine units) in 50 mL Milli-Q water at room temperature. CMCS and dynamer aqueous solutions were mixed at a glucosamine/Dy molar ratio of 4/1 to a total volume of 3 mL. The mixture was ultra-sonicated for 1 min to remove trapped bubbles. Gelation then proceeded at 37 °C for 24 h to yield a hydrogel, namely H500, H800 or H1900.

3.2.4 Preparation of H1900 membranes

8 mL of 100 mM CMCS and 4 mL of 50 mM Dy1900 solutions were mixed in a flask. The mixture was ultra-sonicated for 1 min to remove trapped bubbles, and poured into a round PTFE mold of 8 cm diameter. Gelation then proceeded at 37 °C for 24 h. The resulting hydrogel was air dried under natural ventilation to yield a H1900 membrane. The membrane was recovered and vacuum dried up to constant weight before antibacterial tests. H1900^a membrane stands for H1900 membrane subjected to only thermal treatment for sterilization, H1900^b membrane stands for H1900 membrane subjected to both thermal treatment and UVc exposure for sterilization (section 2.8.2), unless otherwise stated.

3.2.5 Characterization

¹H NMR spectroscopy was carried out using Bruker NMR spectrometer (400-LS) of 400 MHz. Chloroform-d₂ was used as the solvent. 5 mg of sample were dissolved in 0.5 mL of solvent for each analysis. Chemical shifts were recorded in ppm using tetramethylsilane (TMS) as internal reference.

Fourier-transform infrared (FT-IR) spectroscopy of freeze-dried hydrogels was conducted on Nicolet Nexus FT-IR spectrometer, equipped with ATR diamant Golden Gate.

The morphology of freeze-dried hydrogels was examined by using Hitachi S4800 scanning electron microscopy (SEM). As-prepared hydrogels were placed in small vials, and immersed in liquid nitrogen (-196 °C) in order to conserve the original structure. The frozen samples were then lyophilized using LABCONCO[®] freeze dryer for 24 h. The samples were sputter coated prior to analysis.

Physical MCR 301 Rheometer (Anton Paar) was utilized to determine the rheological properties of hydrogels, using a cone plate geometry (diameter of 4 cm, apex angle of 2 °, and clearance 56 µm). The storage modulus (G') and

loss modulus (G'') were measured as a function of time, strain or frequency.

3.2.6 Swelling of freeze-dried gels

The swelling performance of freeze-dried gels was evaluated by immersion in buffer solutions at different pH values. Buffers from pH 1 to pH 7 were prepared from 0.1 M citric acid and 0.2 M disodium hydrogen phosphate dodecahydrate solutions, buffers at pH 8 and pH 9 from 0.2 M boric acid and 0.05 M borax solutions, and buffer at pH 10 from 0.05 M borax and 0.2 M sodium hydroxide solutions. Freeze-dried gels were immersed in a buffer solution, and taken out after 24 h. The swollen hydrogels were weighed after wiping surface water with filter paper, and weighed again after 24 h lyophilization. The swelling and mass loss ratios of hydrogels were calculated according to the following equations, respectively:

$$\text{Swelling ratio } \% = \frac{(M_s - M_d)}{M_d} \times 100 \quad (\text{Eq. 1})$$

$$\text{Mass loss ratio } \% = \frac{(M_0 - M_d)}{M_0} \times 100 \quad (\text{Eq. 2})$$

Where M_0 is the initial mass of dried gel, M_s is the wet mass of the swollen hydrogel, and M_d is the dried mass of the swollen hydrogel after lyophilization.

3.2.7 Self-healing properties of hydrogels

Hydrogel samples were prepared in Milli-Q water. One of them was dyed red with Rhodamine B for better observation. 2 different approaches were applied to examine the self-healing behavior of hydrogels: 1) Modulus changes of hydrogels were followed with alternatively applied high and low oscillatory shear strains at 37 °C; 2) hydrogels were injected in a petri dish to observe integration of filaments at 37 °C.

3.2.8 Antibacterial activity of membranes

3.2.8.1 Bacterium and preparation of the bacterial suspension

A non-pathogenic strain of *Escherichia coli* (K12 DSM 423, DSMZ, Germany) was selected as a model for bacterial contamination. A culture medium Lysogeny Broth (LB) Miller was used for growth and counting. LB agar and soft agar were obtained by adding microbiological agar (Sigma, France) into LB solution at concentrations of 15 g L⁻¹ and 5 g L⁻¹, respectively. For each experiment, a new bacterial culture was prepared from frozen aliquots of *E. coli* stored at -20 °C. The aliquots were inoculated into fresh LB medium (2 %, v/v), and incubated 18 h at 30 °C under constant stirring at 150 rpm until the optical density at 600 nm of the bacterial culture reached about 5 (which corresponds approximately to 10⁹ CFU mL⁻¹). Bacteria were in a stationary phase in these conditions. Once prepared, the bacterial culture was centrifuged at 15 000 g for 5 min at 4 °C to discard the culture medium, followed by washing with the same volume of 9 g L⁻¹ NaCl solution in the same conditions. Finally, the washed bacteria were diluted with 9 g L⁻¹ NaCl solution to yield suspensions at bacterial concentrations ranging from 10⁸ to 10⁵ CFU mL⁻¹ for antibacterial activity tests. The bacterial concentration of the suspensions was stabilized, *i.e.*, no growth could occur due to the absence of nutrients.

3.2.8.2 Antibacterial tests

Each HM1900 membrane piece was first sterilized by a thermal treatment, *i.e.* incubated for 24 h at 100 °C wrapped in an aluminum foil. In addition to the thermal treatment, some membrane pieces were also exposed to UVc (30 min for each side) with the neon of the microbiological safety cabinet (Bioair, Safemate 1.2).

A liquid test was firstly performed to assess the total bacterial removal, including

both bacterial adsorption and inactivation. The membrane piece was immersed 3 h at ambient temperature (20 °C) in the bacterial suspension prepared in Section 2.8.1. The bacterial concentration was measured before and after contact with the membrane. An initial bacterial concentration C_0 of about 10^8 CFU mL⁻¹ was used for this test. A concentration decrease was correlated to bacterial removal. The bacterial log-removal value was defined as the logarithm (base 10) ratio of the initial bacterial concentration C_0 (CFU mL⁻¹) to the bacterial concentration C (CFU mL⁻¹) measured after 3 h contact with the membrane. A log-removal value of $\log(C_0)$ was attributed to the particular case of total bacterial removal. A log-removal value of 1 corresponds to a decrease of 90% of the bacterial population, and a log-removal value of 2 corresponds to a decrease of 99% bacterial population.

The antibacterial effect of the membrane was then assessed by a soft agar test. 50 µL of the bacterial suspension (at about 10^5 CFU mL⁻¹) was deposited onto a membrane piece (between 2 and 3 cm²) placed individually in an empty petri dish. After 3 h contact at ambient temperature (20 °C), 10 mL of nutritive LB soft agar were added, embedding the membrane in a 2 mm thick soft agar. The plates were then incubated 72 h at 30 °C to let the colonies grow. This soft agar test allows the growth of bacteria adsorbed on the membrane without damaging the membrane.

For each antibacterial test, a positive control was realized under the same conditions without membranes. All tests were duplicated.

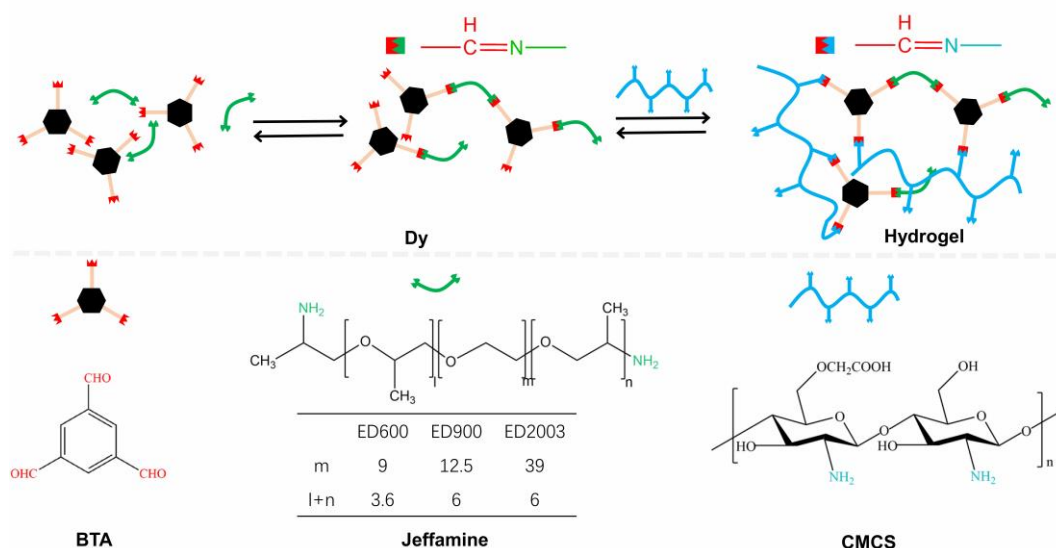
3.2.8.3 Counting of viable cells

The bacteria were counted by using the conventional plaque assay method. For the liquid test, each sample was diluted in decades in a 9 g L⁻¹ NaCl solution; six successive dilutions were done. Then, 400 µL of each dilution were spread onto a LB agar plate, and incubated for 72 h at 30 °C. Once the cultivable bacteria had grown on plates, the colonies were counted, keeping in mind that

each colony stemmed from one initial bacterium. For the soft agar test, the colonies grown in the soft agar were directly counted. For all tests, the concentration of bacteria was calculated as the average of the counted colony number divided by the inoculated volume, taking into account the dilution factor. The quantification limit was 3 CFU mL⁻¹. Each counting was duplicated. Negative control (*i.e.*, without bacteria) was always performed in parallel to check the sterility.

3.3 Results and discussion

3.3.1 Preparation of hydrogels



Scheme 3.1 Synthesis route of dynamic hydrogel by imine bond formation between CMCS and a dynamer obtained from BTA and Jeffamine.

Imine dynamic hydrogels were prepared through a two steps approach as previously reported [35]. A water soluble dynamer Dy500, Dy800 or Dy1900 was first synthesized by reaction of BTA as the core structure and bifunctional Jeffamine[®] ED-600 (Mn = 500), ED-900 (Mn=800) or ED-2003 (Mn=1900) as the water-soluble linker via reversible imine chemistry (Scheme 3.1). The BTA to Jeffamine[®] molar ratio was 1:1. In other words, one aldehyde group per BTA molecule remains available for further cross-linking with the amine groups of

CMCS since each BTA molecule has three aldehydes and each Jeffamine[®] molecule has two amines.

Figure 3.1 presents the ¹H NMR spectra of the as-prepared dynamers obtained after 4 h reaction in methanol at 70 °C. Three signals of aldehyde groups are observed in the 10.1-10.3 ppm range (**a**), and attributed to different degrees of substitution in tri-aldehyde. Signals (**b**) between 8.0 and 8.7 ppm are assigned to the imine and aromatic protons, signals (**c**) around 3.5 ppm to the methylene and methine protons, and signals (**d**) around 1.0 ppm to the methyl protons of Jeffamine. The presence of residual H₂O is detected between 2.0 and 1.8 ppm. Signals at 5.24 ppm and 0 ppm are attributed to the chloroform-d₂ and internal standard, respectively.

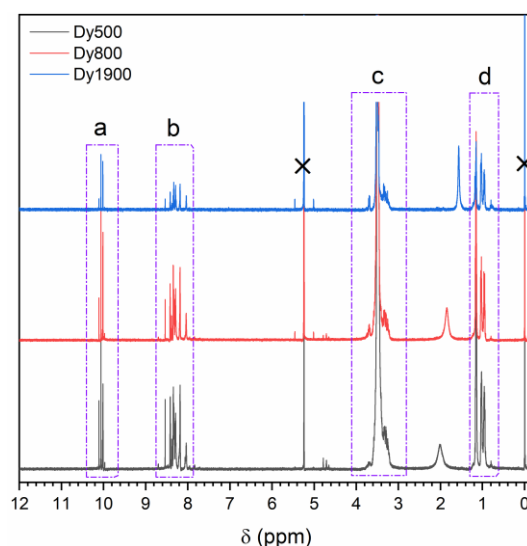


Figure 3.1 ¹H NMR spectra of the dynamers Dy500, Dy800 and Dy1900 obtained by reaction of BTA and Jeffamine.

In the second step, the remaining aldehyde groups of the dynamer react with the amines of CMCS, resulting in a dynamic hydrogel composed of a double imine bonding framework. This double imine crosslinking in aqueous medium is facile and eco-friendly as compared to CMCS-based hydrogel prepared by amide bond crosslinking using 1-ethyl-3(3-dimethylaminopropyl) carbodiimide and N-hydroxysuccinimide [36].

Three series of hydrogels were prepared via a mixture of aqueous solutions of

100 mM CMCS and 50 mM Dy500, Dy800 or Dy1900 at a D-glucosamine to Dy molar ratio of 4. This ratio was used because it leads to optimal crosslinking as previously reported [35]. Gelation proceeded at 37 °C for 24 h to yield H500, H800 or H1900 hydrogels. Table 3.1 summarizes the molar compositions and total polymer concentrations of the three hydrogels. The total polymer concentration increases from 2.4% for H500 to 2.9 % for H800, and to 4.8 % for H1900.

Table 3.1 Molar and mass compositions of dynamic hydrogels ^{a)}.

Sample	CMCS		Dy500 ^b		Dy800 ^b		Dy1900 ^b		Total polymer concentration
	[mmol]	[w/v %]	[mmol]	[w/v %]	[mmol]	[w/v %]	[mmol]	[w/v %]	[w/v %]
H500	0.2	1.4	0.05	1.0	-	-	-	-	2.4
H800	0.2	1.4	-	-	0.05	1.5	-	-	2.9
H1900	0.2	1.4	-	-	-	-	0.05	3.4	4.8

^{a)} Hydrogels are prepared by mixing CMCS and Dy solutions at a D-glucosamine/Dy ratio of 4/1 to a total volume of 3 mL. The concentration of CMCS solution is 100 mM. Calculations are made on the basis of the average molar mass of 212 g / mol obtained for D-glucosamine, taking into account the degree of deacetylation of 90 % and the degree of carboxymethylation of 80 %; ^b The concentration of Dy solution is 50 mM obtained from the remaining aldehyde groups. In a typical reaction, 1 mmol BTA (162 mg) reacts with 1 mmol Jeffamine ED600 (500 mg) or Jeffamine ED900 (800 mg) or Jeffamine ED2003 (1900 mg) to form a dynamer. As BTA has 3 aldehydes and Jeffamine 2 amines, there remains theoretically 1 mmol of aldehydes in the dried dynamer. Addition of 20 mL water yields a dynamer solution of 50 mM.

3.3.2 FT-IR

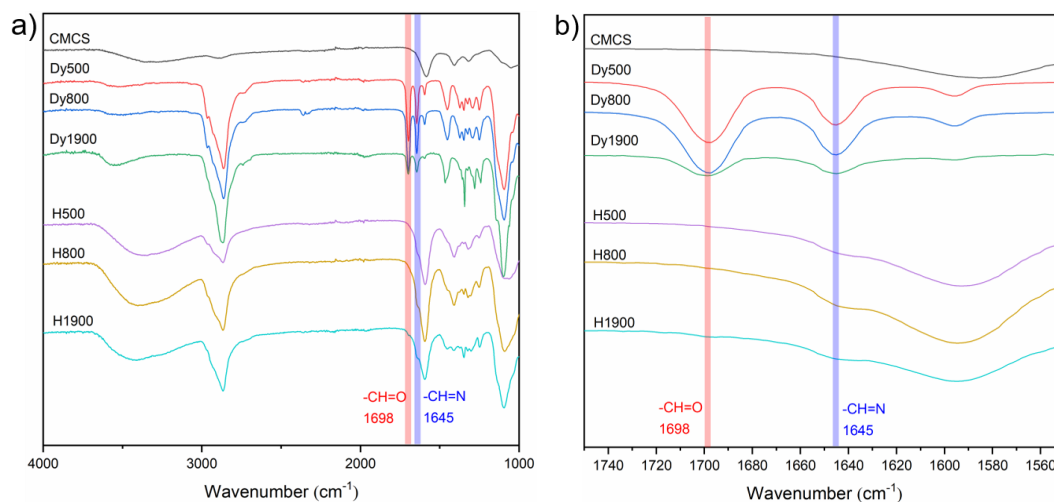


Figure 3.2 a) FT-IR spectra, and b) enlarged view of the 1550-1750 cm^{-1} wavenumber range of CMCS, Dy500, Dy800, Dy1900, H500, H800 and H1900.

Figure 3.2 shows the FTIR spectra of CMCS, the dynamers and the dried gels. The large band around 3500 cm^{-1} is attributed to free OH and NH_2 groups, and the intense band at 1595 cm^{-1} to carbonyl groups of CMCS. The dynamers present large bands at 2850 and 1100 cm^{-1} belonging to C-H and C-O stretching, and two characteristic bands at 1698 and 1645 cm^{-1} corresponding to aldehyde and imine bonds, respectively. All the characteristic bands of CMCS and Dy are observed on the spectra of dried gels. Nevertheless, the enlarged view in the 1750-1550 cm^{-1} wavenumber range shows that the aldehyde band almost disappears, while the imine band merges with that of carbonyl groups at 1595 cm^{-1} . These results indicate that hydrogels are formed owing to imine formation through aldehyde and amine groups.

3.3.3 Rheology

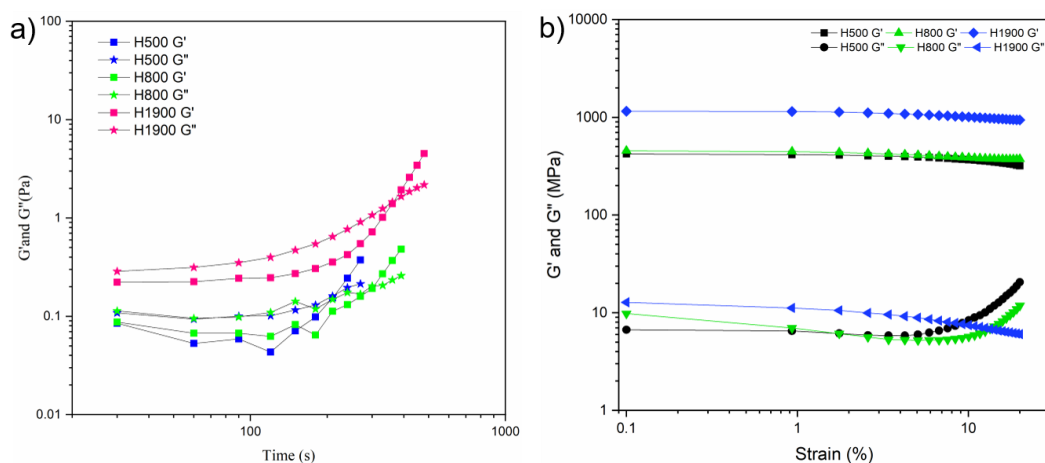


Figure 3.3 a) Storage modulus (G') and loss modulus (G'') changes as a function of time after mixing CMCS with Dy solutions at 37 °C, at strain of 1% and frequency of 1 Hz; b) Storage modulus (G') and loss modulus (G'') changes of H500, H800 and H1900 as a function of strain at 25 °C and 1 Hz.

The gelation of dynamic hydrogels was investigated by rheological measurements. CMCS and Dy aqueous solutions were mixed in situ on the plate of the rheometer, and changes of the storage modulus (G') and loss modulus (G'') were followed as a function of time at 37°C (Figure 3.3a). For all samples, G' is initially lower than G'' , which illustrates a liquid-like behavior of the starting mixture. After an induction time, both G' and G'' begin to increase, G' increasing faster than G'' . A crossover point of G' and G'' is detected, indicating sol-gel transition. The gelation time of H500, H800 and H1900 is 210 s, 300 s, and 360 s, respectively, with corresponding modulus of 0.15 Pa, 0.20 Pa, and 1.46 Pa at the gelation point. Thus, low molar mass of Jeffamine is beneficial for rapid gelation, but leads to lower modulus of as-prepared hydrogels.

Figure 3.3b presents the modulus changes of as prepared hydrogels as a function of applied strain at 25 °C and at 1 Hz. G' is nearly stable over the whole strain range up to 20% although a slight G' decrease is detected at high strains. On the other hand, the loss modulus G'' is much lower than the storage

modulus G' in all cases, indicating viscoelastic behavior rather than liquid behavior of hydrogels. In fact, a linear viscoelastic range is generally observed for chemically or physically crosslinked hydrogels [36-38].

When the Jeffamine molar mass increases from 500 to 800, the storage modulus slightly increases from 422 Pa for H500 to 453 Pa for H800 at 1% strain. In contrast, much higher G' of 1190 Pa is obtained for H1900. This finding indicates that the molar mass of Jeffamine strongly influences the mechanical properties of hydrogels. Higher molar mass of Jeffamine leads to higher modulus of hydrogels. In fact, although there are more amine groups than aldehyde ones in the mixture, the amines are less available for imine chemistry than aldehydes due to their lower chain mobility and steric effect as they are present along the CMCS backbone with a M_w of 200,000. Thus, a D-glucosamine to Dy molar ratio of 4 was used for optimal crosslinking. The optimal ratio 4 is further confirmed by the measurement of the modulus changes of as prepared hydrogels as a function of applied frequency at 25 °C and at 1 % strain, as shown in Figure S3.1 (Supporting Information). It is noteworthy that the as-prepared hydrogels present better mechanical performance than CMCS-based hydrogel by amide bond crosslinking [36].

3.3.4 Morphology and swelling performance

The inner structure of freeze-dried hydrogels was examined using SEM. As shown in Figure 3.4, H500, H800 and H1900 exhibit a sponge-like porous structure with regularly distributed and interconnected pores, which is beneficial for utilization in drug delivery or tissue engineering as compared to chaotic microstructure of other chitosan hydrogels [39].

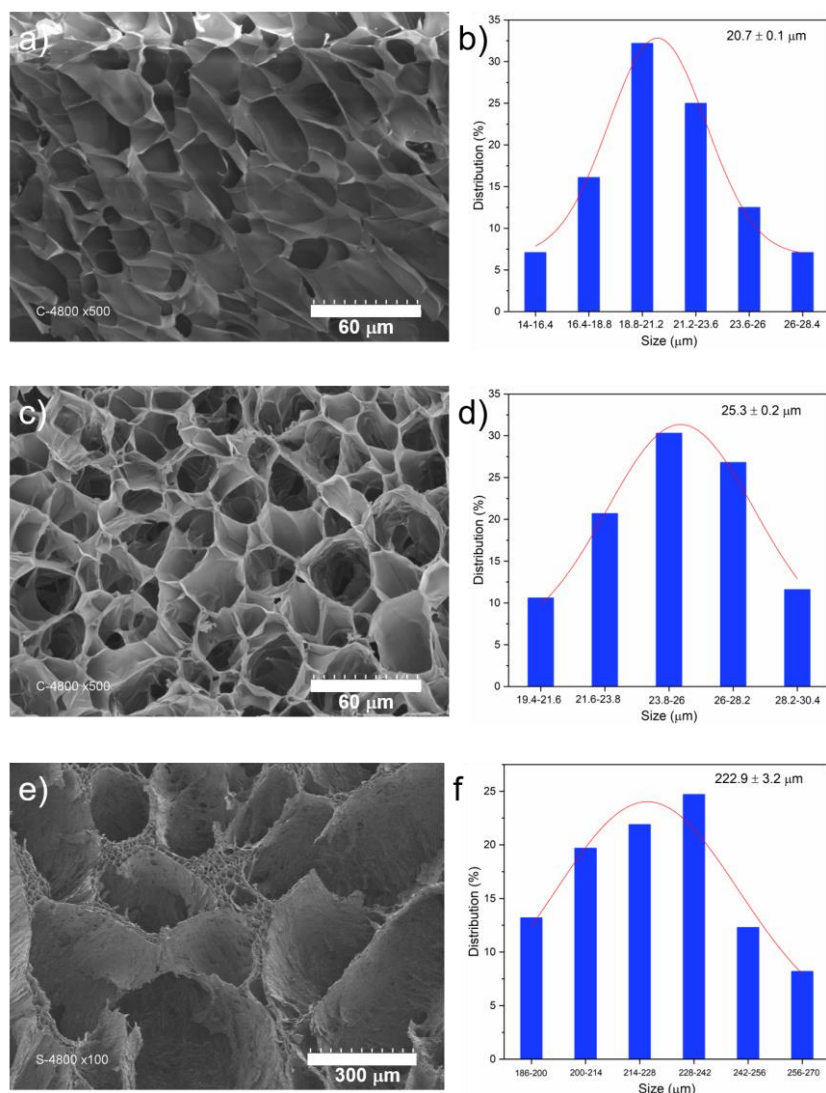


Figure 3.4 SEM images and pore size distributions of freeze-dried gels: (a, b) H500; (c, d) H800; (e, f) H1900.

Noticeably, the average pore size varies from $20.7 \pm 0.1 \mu\text{m}$ for H500, to $25.3 \pm 0.2 \mu\text{m}$ for H800, and to $222.9 \pm 3.2 \mu\text{m}$ for H1900. This finding suggests that the molar mass of Jeffamine significantly affect the three-dimensional architecture of hydrogels, especially on the pore size. Higher Jeffamine molar mass leads to larger pore size because Jeffamine molecules serve as linkers in the hydrogel network.

The swelling behavior of hydrogels is of major importance for medical applications in wound dressing, drug delivery or tissue engineering. It is thus of interest to compare the swelling of hydrogels prepared from different

Jeffamines.

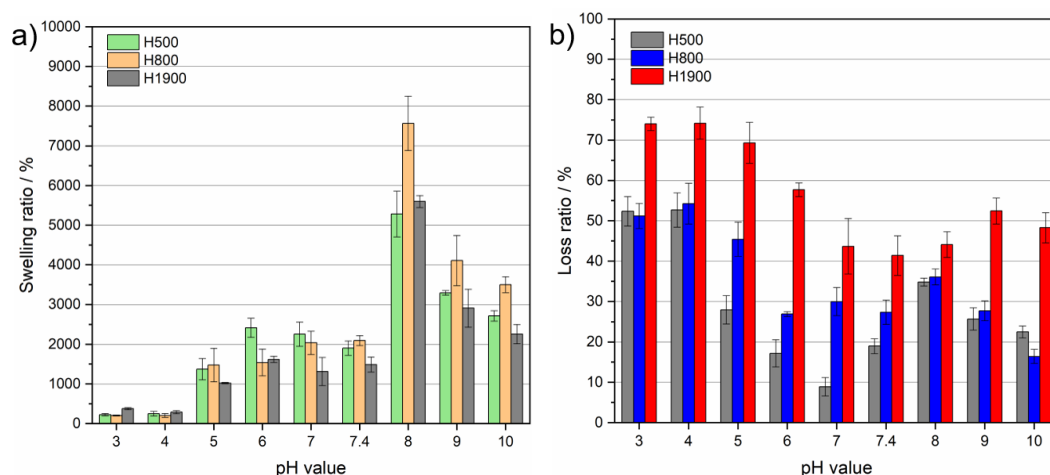


Figure 3.5 a) Equilibrium swelling ratios, and b) Mass loss ratios of H500, H800 and H1900 after 24 h immersion in buffers at various pH values.

As shown in Figure 3.5a, the swelling ratio is strongly pH dependent as previously reported [35]. In acidic media at pH 3 and 4, the swelling ratio is rather low (between 200 - 300%). In slightly acidic and neutral media (pH 5, 6, 7 and 7.4), the swelling ratio progressively increases to reach c.a 2000%. Maximal swelling is observed in slightly basic media at pH 8, with a swelling ratio of 5280%, 7560% and 5590 % for H500, H800, and H1900, respectively. With further increase to pH 9 and 10, however, the swelling ratio decreases, reaching 2710%, 3500% and 2250 % for H500, H800, and H1900 at pH 10, respectively. The pH dependence of the swelling of hydrogels is attributed to electrostatic interactions resulted from the presence of amino and carboxyl groups along CMCS chains [35]. In fact, strong electrostatic attraction occurs between negatively charged -COO^- and positively charged -NH_3^+ groups in strong acidic media (pH 3 and 4), leading to shrinkage of hydrogels and low swelling ratio. Electrostatic attraction becomes weaker at slightly acidic or neutral pH, and thus the swelling ratio increases. In contrast, strong electrostatic repulsion occurs between negatively charged -COO^- groups in slightly alkaline medium at pH 8, resulting in strong swelling. With further increase of alkalinity, however, the electrostatic repulsion between the -COO^-

groups is counterbalanced by the OH^- ions in solution. Hence, the swelling of hydrogels at pH 9 and 10 diminishes compared to that at pH 8. No major difference was observed between the three hydrogels in acidic and neutral media, although H800 seems to present higher swelling ratio than H500 and H1900 in alkaline media. Additionally, compared to the other chitosan-based hydrogel [36], the excellent swelling ability of the as-prepared hydrogels should be beneficial to absorption of interstitial fluid or wound exudate, and thus enlarging their biomedical utilization, especially as wound dressing [40].

Mass loss often occurs during swelling of hydrogels due to the solubilization of non-crosslinked species. Thus, the mass loss ratio is an indicator of the crosslinking degree and the stability of hydrogels. Figure 3.5b presents the mass loss ratio of hydrogels at different pH values. Noticeably, the mass loss of hydrogels is strongly pH dependent. High mass loss above 50% is obtained in acidic buffers at pH 3 and 4. From pH 5 to pH 7.4, the mass loss ratio progressively decreases. And in alkaline media, a slight increase of mass loss is observed. These findings suggest that the imine bonds in the hydrogel network are partly hydrolyzed in acidic media, especially at pH 3 and 4. In contrast, they are stable in neutral and alkaline media. The slight increase of mass loss in alkaline media could be assigned to the high swelling which facilitated the washing away of uncross-linked species. Among the three hydrogels, H1900 exhibits the highest mass loss in the whole pH range, in agreement with lower crosslinking degree due to the higher molar mass of Jeffamine ED2003. In fact, better crosslinking could be achieved between CMCS and Dy500 or Dy800 based on Jeffamine ED600 and ED900 of lower molar masses. This hypothesis is supported by the fact that H500 exhibits the lowest mass loss ratio in the range from pH 5 to 9, with a minimum mass loss ratio of 8% at pH 7.

3.3.5 Self-healing

The prepared dynamic hydrogel exhibits self-healing behavior as evidenced by rheological measurements at fixed frequency of 1 Hz and at 37 °C. Figure 3.6a shows modulus changes of H1900 as a function of applied strain. With increasing strain, the storage modulus of H1900 remains stable till a strain of 30%. Beyond, G' rapidly decreases. On the other hand, the loss modulus begins to increase beyond 10% strain. A crossover point is detected at a strain of 62 %, indicating the collapse of the hydrogel structure.

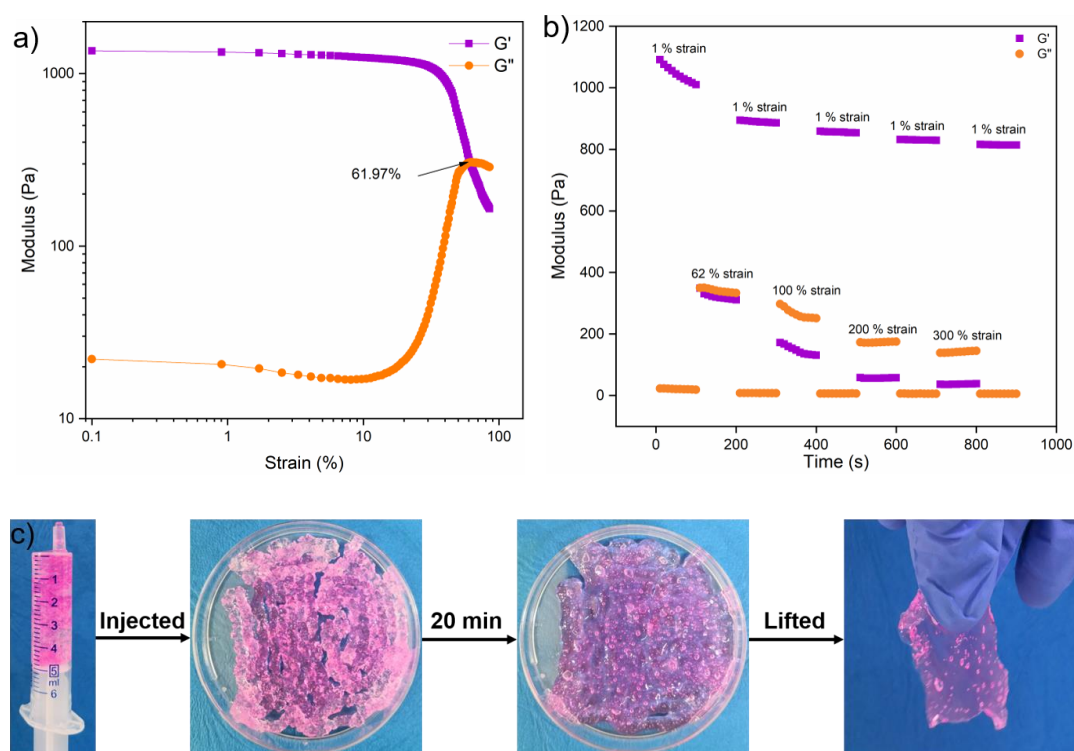


Figure 3.6 a) Modulus changes as a function of strain of H1900 prepared in Milli-Q water; b) Modulus changes of H1900 prepared in Milli-Q water with alternatively applied high and low oscillatory shear strains at 37 °C; c) Macroscopic observation of self-healing of H1900 at 37 °C.

Continuous step strain measurements were then performed to verify the rheological self-recovery of H1900 with alternatively applied low and high strains. As shown in Figure 3.6b, at a strain of 1%, H1900 behaves as a hydrogel since G' is highly superior to G'' in spite of some G' decrease. Then

the oscillatory shear strain was increased to 62% and maintained for 100 s. Both G' and G'' almost overlap. With the shear strain back to 1%, H1900 behaves again like a hydrogel with both G' and G'' remaining stable. Similar measurements were made by alternatively applying higher strains (100, 200 and 300%) and low strain (1%). At high strains, G' is lower than G'' due to collapse of the hydrogel structure. And at 1% strain, G' almost recovers its initial value. Similar behaviors are observed for H500 and H800 with alternatively applied low and high strains. Therefore, rheological measurements clearly evidence the self-recovery properties of dynamic hydrogels owing to the reconstruction of reversible crosslinking in the hydrogel network, which makes them promising for applications in cell therapy, tumor therapy and even in bone repairing [41].

A macroscopic approach was used to further illustrate the self-healing of imine dynamic hydrogels, by using a hydrogel sample dyed red with Rhodamine B for better visualization (Figure 3.6c). The sample was injected onto a plastic petri dish through a syringe and placed as filaments side by side. The filaments became almost integrated only after 20min, and was easily peeled from the petri dish and lifted by hand.

3.3.6 *In vitro* antibacterial assay

Chitosan based materials present intrinsic antimicrobial properties due to the presence of amino groups [42]. Considering the overall properties of the three hydrogels, H1900 was selected for *in vitro* antibacterial activity studies by using *E. coli* (Gram-negative bacterium). H1900 membranes were first subjected to two sterilization treatments, i.e., H1900^a exposed to thermal treatment only and H1900^b exposed to thermal treatment followed by UVc exposure so as to examine the effect of UV on the membrane properties [43]. The membranes were characterized by FT-IR analysis in comparison with pristine H1900 (Figure S3.2, Supporting Information). The results show that the thermal treatment and

the UVc exposure have no major impact on the chemical structure of membrane since the main functional groups remained the same without apparent peak shift, implying the good stability of H1900 membranes. UVc treatment for sterilization of CMCS-based biomaterials is therefore acceptable after thermal treatment.

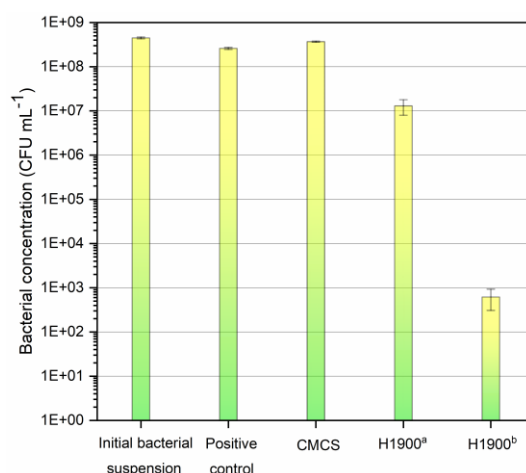


Figure 3.7 Bacterial concentrations (CFU mL⁻¹) obtained for positive control, CMCS, H1900^a, and H1900^b in liquid tests. (H1900^a: dealt with only thermal treatment for sterilization; H1900^b: dealt with both thermal treatment and UVc exposure for sterilization)

Figure 3.7 shows the bacterial concentrations obtained in liquid tests for H1900^a and H1900^b in comparison with CMCS membrane and positive control. After 3 h contact at ambient temperature (20 °C) with a bacterial suspension at 10⁸ CFU mL⁻¹, the positive control and CMCS membrane present small log-removal values, *i.e.*, 0.2 and 0.1, respectively (Table 3.2, entries 2 and 5). On the contrary, the H1900 membranes exhibit significant log-removal values, *i.e.*, 1.5 for H1900^a and 5.6 for H1900^b (Table 3.2, entries 3 and 4). In other words, 97.11% and 99.9999% of bacteria were removed by H1900^a and H1900^b, respectively, suggesting outstanding antibacterial properties of H1900. The antibacterial activity of the hydrogel could be assigned to the positively charged amino groups along the CMCS chains which could bind to the negatively charged phospholipid groups present on the bacterial membranes, thus inducing

membrane permeabilization, release of the intracellular fluids and finally cell death [42, 44]. Additionally, the Schiff-base containing a benzene ring could also play a significant role in the antimicrobial activity since Schiff-base bonds in the hydrogel network have been demonstrated as a promising candidate for designing more efficient antimicrobial agents [45]. Hence, the Schiff bases and protonated amino groups are supposed to impart outstanding antibacterial activity to H1900 membrane.

Table 3.2 Antibacterial activity of H1900 membrane (entry 1-5: liquid test; entries 6-9: soft agar tests)

Entry	Sample	C _{bacteria} [CFU mL ⁻¹]	Log-removal value [-]
1	Initial bacterial suspension	$4.5 \pm 0.2 * 10^8$	-
2	Positive control	$2.6 \pm 0.1 * 10^8$	0.2
3	H1900 ^a	$1.3 \pm 0.5 * 10^7$	1.5
4	H1900 ^b	$6.2 \pm 3.1 * 10^2$	5.6
5	CMCS	$3.7 \pm 0.1 * 10^8$	0.1
6	Positive control	$2.1 \pm 0.7 * 10^5$	-
7	H1900 ^a	$5.0 \pm 3.0 * 10^1$	4.0
8	H1900 ^b	0	5.3
9	CMCS	nd	nd

nd: not determined (too many bacteria)

H1900^a: only thermal treatment for sterilization

H1900^b: both thermal treatment and UVc exposure for sterilization

The biocidal activity of H1900^b appears better than H1900^a in liquid tests (Figure 3.7 and Table 3.2), even though UVc exposure seemed not to induce major changes in the chemical structure of H1900 membrane (Figure S3.2,

Supporting Information). Nevertheless, it has been reported that UV radiation could decrease the degree of deacetylation of chitosan [46]. On the other hand, the antibacterial activity of CMCS based materials is dependent on the amount of NH_3^+ groups [42, 44], and thus on the degree of deacetylation. Therefore, it can be assumed that the antibacterial activity of H1900^b is improved by UVc exposure as compared to H1900^a exposed to thermal treatment only.

Soft agar tests were carried out in order to make sure that bacteria were effectively deactivated rather than adsorbed on the membrane. Indeed, if present, adsorbed bacteria would form colonies onto the membrane that could be observed after 72 h incubation at 30 °C. As shown in Table 3.2 (entries 6 and 8) and Figure 3.8, the bacterial concentration is zero CFU mL⁻¹ for H1900^b with corresponding log-removal value of 5.3. In other words, no colonies grew onto the H1900^b membrane, in contrast to the positive control (Figure 3.8). Besides, the log-removal value is very close to that obtained in the liquid test (Table 3.2, entry 4). It is thus concluded that the bacterial removal observed in the liquid test mainly results from the antibacterial action of H1900^b membrane, not from adsorption. In the same way, the H1900^a membrane exhibits a significant log-removal value of 4.0 (Table 3.2, entry 7), thus confirming the intrinsic and strong bactericidal activity of H1900 membranes. On the contrary, the CMCS membrane exhibits too many bacteria on a small surface for bacterial counting (Table 3.2), suggesting that CMCS does not have any biocidal action in these conditions probably due to membrane dissolution. It is also worth noticing that the log-removal value obtained for H1900^a in soft agar test (Table 3.2, entry 7) is much higher than that obtained in the liquid test (Table 3.2, entry 3). This result is consistent with the assumption that the physical structure of H1900^a allows a limited contact with bacteria when it is in suspension in a liquid, while in soft agar test, bacteria are directly deposited onto the membrane surface.

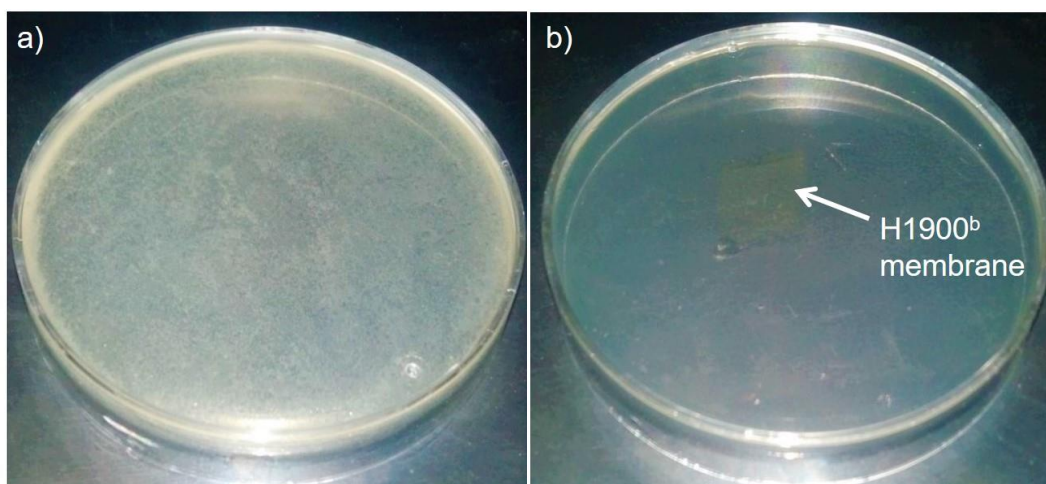


Figure 3.8 Soft agar tests: a) picture of the positive control plate and b) picture of the plate with H1900^b membrane. (H1900^b: dealt with both thermal treatment and UV exposure for sterilization).

3.4 Conclusions

In this work, three pH-sensitive dynamic hydrogels, namely, H500, H800 and H1900, are prepared by dual-imine bond crosslinking: a dynamer is first synthesized from BTA with Jeffamine ED600, ED900 or ED2003 of different molar masses, and then the remaining aldehydes of dynamer react with the amines of CMCS to yield a hydrogel network. The gelation process is environmental-friendly without involving any organic solvent. The hydrogels present a highly porous structure with regularly distributed pores, the pore size increasing with the molar mass of Jeffamine which serves as the linker in the hydrogel network. H1900 also exhibits higher storage and loss moduli as compared to H500 and H800. The swelling and mass loss of hydrogels are highly pH sensitive due to electrostatic attraction or repulsion in buffers at various pH values. H1900 exhibits the highest mass loss probably due to the lower crosslinking degree because of the higher molar mass of Jeffamine linker. The hydrogels are more stable in neutral and alkaline media than in acidic media which facilitate the cleavage of imine bonds. The hydrogels also present excellent self-healing and antibacterial properties, and are thus most promising for biomedical applications in wound dressing, drug delivery and tissue

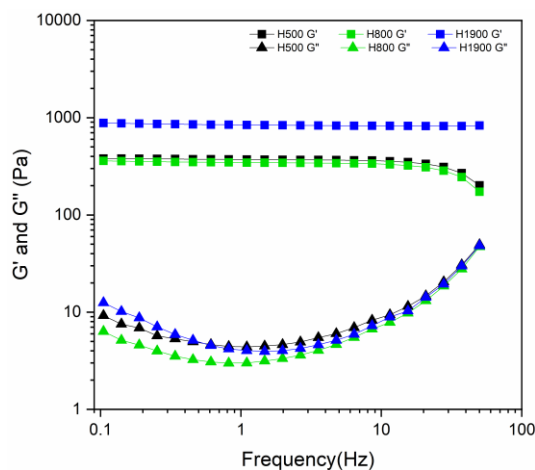


Figure S3.1 Storage modulus (G') and loss modulus (G'') changes of H500, H800 and H1900 as a function of frequency at 25 °C and 1% strain.

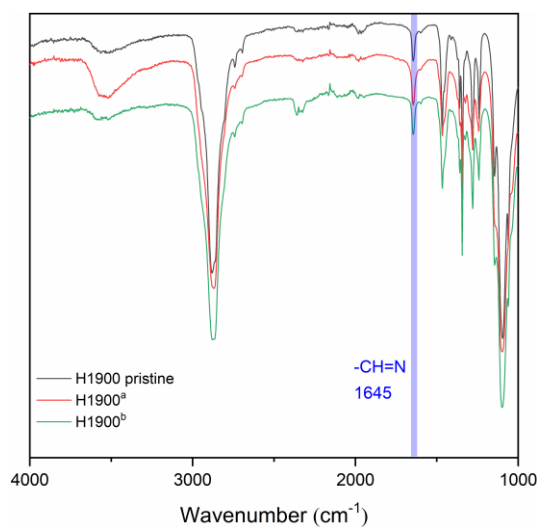


Figure S3.2 FT-IR spectra of the pristine H1900 membrane, H1900^a and H1900^b. (H1900^a: dealt with only thermal treatment for sterilization; H1900^b: dealt with both thermal treatment and UV exposure for sterilization).

References

- [1] S. Van Vlierberghe, P. Dubruel, E. Schacht, Biopolymer-based hydrogels as scaffolds for tissue engineering applications: a review, *Biomacromolecules* 12(5) (2011) 1387-1408.

- [2] N.A. Peppas, J.Z. Hilt, A. Khademhosseini, R. Langer, Hydrogels in biology and medicine: from molecular principles to bionanotechnology, *Adv. Mater.* 18(11) (2006) 1345-1360.
- [3] N. Bhattarai, J. Gunn, M. Zhang, Chitosan-based hydrogels for controlled, localized drug delivery, *Adv. Drug Del. Rev.* 62(1) (2010) 83-99.
- [4] M. Norouzi, B. Nazari, D.W. Miller, Injectable hydrogel-based drug delivery systems for local cancer therapy, *Drug Discovery Today* 21(11) (2016) 1835-1849.
- [5] H. Hamed, S. Moradi, S.M. Hudson, A.E. Tonelli, Chitosan based hydrogels and their applications for drug delivery in wound dressings: A review, *Carbohydr. Polym.* 199 (2018) 445-460.
- [6] M. Liu, X. Zeng, C. Ma, H. Yi, Z. Ali, X. Mou, S. Li, Y. Deng, N. He, Injectable hydrogels for cartilage and bone tissue engineering, *Bone research* 5(1) (2017) 1-20.
- [7] B. Qu, Y. Luo, Chitosan-based hydrogel beads: Preparations, modifications and applications in food and agriculture sectors—A review, *Int. J. Biol. Macromol.* (2020).
- [8] S. Kulchat, J.M. Lehn, Dynamic covalent chemistry of nucleophilic substitution component exchange of quaternary ammonium salts, *Chemistry—An Asian Journal* 10(11) (2015) 2484-2496.
- [9] L. Marin, B. Simionescu, M. Barboiu, Imino-chitosan biodynamers, *Chem. Commun.* 48(70) (2012) 8778-8780.
- [10] N. Roy, J.M. Lehn, Dynamic Covalent Chemistry: A Facile Room - Temperature, Reversible, Diels - Alder Reaction between Anthracene Derivatives and N - Phenyltriazolinedione, *Chemistry-An Asian Journal* 6(9) (2011) 2419-2425.
- [11] P. Sun, T. Huang, X. Wang, G. Wang, Z. Liu, G. Chen, Q. Fan, Dynamic-Covalent Hydrogel with NIR-Triggered Drug Delivery for Localized Chemo-Photothermal Combination Therapy, *Biomacromolecules* 21(2) (2019) 556-565.

- [12] Z. Li, L. Liu, Y. Chen, Dual dynamically crosslinked thermosensitive hydrogel with self-fixing as a postoperative anti-adhesion barrier, *Acta Biomater.* (2020).
- [13] S.H. Hong, S. Kim, J.P. Park, M. Shin, K. Kim, J.H. Ryu, H. Lee, Dynamic bonds between boronic acid and alginate: hydrogels with stretchable, self-healing, stimuli-responsive, remoldable, and adhesive properties, *Biomacromolecules* 19(6) (2018) 2053-2061.
- [14] M.G. Dekamin, M. Azimoshan, L. Ramezani, Chitosan: a highly efficient renewable and recoverable bio-polymer catalyst for the expeditious synthesis of α -amino nitriles and imines under mild conditions, *Green Chem.* 15(3) (2013) 811-820.
- [15] Y. Zhang, M. Barboiu, Constitutional Dynamic Materials Toward Natural Selection of Function, *Chem. Rev.* 116(3) (2015) 809-834.
- [16] F.-L. Mi, Y.-C. Tan, H.-F. Liang, H.-W. Sung, In vivo biocompatibility and degradability of a novel injectable-chitosan-based implant, *Biomaterials* 23(1) (2002) 181-191.
- [17] R. Dong, X. Zhao, B. Guo, P.X. Ma, Self-healing conductive injectable hydrogels with antibacterial activity as cell delivery carrier for cardiac cell therapy, *ACS applied materials & interfaces* 8(27) (2016) 17138-17150.
- [18] N. Sudarshan, D. Hoover, D. Knorr, Antibacterial action of chitosan, *Food Biotechnol.* 6(3) (1992) 257-272.
- [19] N. Bhattarai, J. Gunn, M. Zhang, Chitosan-based hydrogels for controlled, localized drug delivery, *Advanced drug delivery reviews* 62(1) (2010) 83-99.
- [20] H. Tan, C.R. Chu, K.A. Payne, K.G. Marra, Injectable in situ forming biodegradable chitosan–hyaluronic acid based hydrogels for cartilage tissue engineering, *Biomaterials* 30(13) (2009) 2499-2506.
- [21] Y.-H. Lin, H.-F. Liang, C.-K. Chung, M.-C. Chen, H.-W. Sung, Physically crosslinked alginate/N, O-carboxymethyl chitosan hydrogels with calcium for

oral delivery of protein drugs, *Biomaterials* 26(14) (2005) 2105-2113.

[22] Y. Li, J. Rodrigues, H. Tomas, Injectable and biodegradable hydrogels: gelation, biodegradation and biomedical applications, *Chem. Soc. Rev.* 41(6) (2012) 2193-2221.

[23] L. Pighinelli, M. Kucharska, Chitosan–hydroxyapatite composites, *Carbohydr. Polym.* 93(1) (2013) 256-262.

[24] R.A. Muzzarelli, Chitins and chitosans for the repair of wounded skin, nerve, cartilage and bone, *Carbohydr. Polym.* 76(2) (2009) 167-182.

[25] M.M. Iftime, G.L. Ailiesei, E. Ungureanu, L. Marin, Designing chitosan based eco-friendly multifunctional soil conditioner systems with urea controlled release and water retention, *Carbohydr. Polym.* 223 (2019) 115040.

[26] W. Huang, Y. Wang, Z. Huang, X. Wang, L. Chen, Y. Zhang, L. Zhang, On-demand dissolvable self-healing hydrogel based on carboxymethyl chitosan and cellulose nanocrystal for deep partial thickness burn wound healing, *ACS applied materials & interfaces* 10(48) (2018) 41076-41088.

[27] A.R. Karimi, M. Tarighatjoo, G. Nikraves, 1, 3, 5-Triazine-2, 4, 6-tribenzaldehyde derivative as a new crosslinking agent for synthesis of pH-thermo dual responsive chitosan hydrogels and their nanocomposites: Swelling properties and drug release behavior, *Int. J. Biol. Macromol.* 105 (2017) 1088-1095.

[28] W.J. Huang, Y.X. Wang, L.M. McMullen, M.T. McDermott, H.B. Deng, Y.M. Du, L.Y. Chen, L.N. Zhang, Stretchable, tough, self-recoverable, and cytocompatible chitosan/cellulose nanocrystals/polyacrylamide hybrid hydrogels, *Carbohydr. Polym.* 222 (2019) 12.

[29] Y. Zhang, Y. Qi, S. Ulrich, M. Barboiu, O. Ramström, Dynamic covalent polymers for biomedical applications, *Materials Chemistry Frontiers* 4(2) (2020) 489-506.

[30] A. Lu, E. Petit, S. Li, Y. Wang, F. Su, S. Monge, Novel thermo-responsive micelles prepared from amphiphilic hydroxypropyl methyl cellulose-block-

- JEFFAMINE copolymers, *Int. J. Biol. Macromol.* 135 (2019) 38-45.
- [31] G. Chen, L.V.D. Does, A. Bantjes, Investigations on vinylene carbonate. VI. Immobilization of alkaline phosphatase onto poly (vinylene carbonate) - jeffamine® hydrogel beads, *Journal of applied polymer science* 48(7) (1993) 1189-1198.
- [32] Y. Zhang, Y. Qi, S. Ulrich, M. Barboiu, O. Ramström, Dynamic covalent polymers for biomedical applications, *Materials Chemistry Frontiers* (2020).
- [33] S. Li, S. Dong, W. Xu, S. Tu, L. Yan, C. Zhao, J. Ding, X. Chen, Antibacterial hydrogels, *Advanced science* 5(5) (2018) 1700527.
- [34] M. Kong, X.G. Chen, K. Xing, H.J. Park, Antimicrobial properties of chitosan and mode of action: a state of the art review, *Int. J. Food Microbiol.* 144(1) (2010) 51-63.
- [35] R. Yu, Y. Zhang, M. Barboiu, M. Maumus, D. Noël, C. Jorgensen, S. Li, Biobased pH-responsive and self-healing hydrogels prepared from O-carboxymethyl chitosan and a 3-dimensional dynamer as cartilage engineering scaffold, *Carbohydr. Polym.* (2020) 116471.
- [36] F. Su, J. Wang, S. Zhu, S. Liu, X. Yu, S. Li, Synthesis and characterization of novel carboxymethyl chitosan grafted polylactide hydrogels for controlled drug delivery, *Polym. Adv. Technol.* 26(8) (2015) 924-931.
- [37] F. Li, S. Li, A. El Ghzaoui, H. Nouailhas, R. Zhuo, Synthesis and gelation properties of PEG- PLA- PEG triblock copolymers obtained by coupling monohydroxylated PEG- PLA with adipoyl chloride, *Langmuir* 23(5) (2007) 2778-2783.
- [38] F. Li, S. Li, M. Vert, Synthesis and rheological properties of polylactide/poly (ethylene glycol) multiblock copolymers, *Macromol. Biosci.* 5(11) (2005) 1125-1131.
- [39] M. Hamdi, R. Nasri, S. Li, M. Nasri, Bioinspired pH-sensitive riboflavin controlled-release alkaline hydrogels based on blue crab chitosan: Study of the effect of polymer characteristics, *Int. J. Biol. Macromol.* 152 (2020) 1252-1264.

- [40] R. Jayakumar, M. Prabakaran, P.S. Kumar, S. Nair, H. Tamura, Biomaterials based on chitin and chitosan in wound dressing applications, *Biotechnol. Adv.* 29(3) (2011) 322-337.
- [41] Y. Xu, Y. Li, Q. Chen, L. Fu, L. Tao, Y. Wei, Injectable and self-healing chitosan hydrogel based on imine bonds: design and therapeutic applications, *Int. J. Mol. Sci.* 19(8) (2018) 2198.
- [42] J. Qu, X. Zhao, Y. Liang, T. Zhang, P.X. Ma, B. Guo, Antibacterial adhesive injectable hydrogels with rapid self-healing, extensibility and compressibility as wound dressing for joints skin wound healing, *Biomaterials* 183 (2018) 185-199.
- [43] L. Huang, J. Peng, M. Zhai, J. Li, G. Wei, Radiation-induced changes in carboxymethylated chitosan, *Radiation Physics Chemistry & Biodiversity* 76(11-12) (2007) 1679-1683.
- [44] K.A. Brogden, Antimicrobial peptides: pore formers or metabolic inhibitors in bacteria?, *Nature reviews microbiology* 3(3) (2005) 238-250.
- [45] M. Mohy Eldin, E. Soliman, A. Hashem, T. Tamer, Antimicrobial activity of novel aminated chitosan derivatives for biomedical applications, *Adv. Polym. Tech.* 31(4) (2012) 414-428

Chapter 4 Biobased dynamic hydrogels by reversible imine bonding for controlled release of thymopentin

Abstract: A dynamic hydrogel was developed by reversible imine bond crosslinking for sustained release of thymopentin (TP5), a hydrophilic immunostimulant. Blank and TP5 loaded hydrogels were synthesized *in situ* by Schiff-base reaction of water-soluble O-carboxymethyl chitosan (CMCS) with a dynamer made from Jeffamine and benzene-1,3,5-tricarbaldehyde. Various factors, including the molar mass of CMCS, drug loading conditions, and drug content, were considered to figure out their effects on hydrogel properties and drug release behaviors. The structural, rheological, morphological and swelling characteristics of the hydrogels were investigated. All hydrogels showed regular and interpenetrating porous architecture, and extraordinary pH-sensitive swelling which could reach over 10,000 % at pH 8. The dynamic nature of imine bonds endows hydrogels with good rheological stability in the strain range from 0.1-20 % or in the frequency change from 0.1 to 50 Hz. Importantly, TP5 encapsulation affects the rheological properties of hydrogels as TP5 is partially attached to the network via imine bonding between the amino groups of TP5 and aldehyde groups of the dynamer. *In vitro* release of TP5 was performed in phosphate buffered saline at 37 °C. In all cases, an initial burst is observed, followed by slower release to reach a plateau. Higher TP5 loading content led to higher initial and final release rates. TP5 was not totally released because of attachment to the hydrogel network via imine bonding. Faster release is observed at pH 5.5 than at pH 7.4 due to lower stability of imine bonds in acidic media. Fitting of release data by using Higuchi model showed that the initial TP5 release is essentially diffusion controlled. Density functional theory (DFT) computation was applied to theoretically confirm the chemical connections between TP5 and CMCS with Dy. All these findings proved that CMCS based

dynamic hydrogels are promising carriers for controlled delivery of hydrophilic drugs, and shed new light on the design of drug release systems by both physical mixing and reversible covalent bonding.

Keywords: O-carboxymethyl chitosan; Imine bonding; Dynamic hydrogel; Thymopentin; Drug release; Density functional theory

4.1 Introduction

Thymopentin (TP5) is a synthetic pentapeptide (Arg-Lys-Asp-Val-Tyr, $M_n = 679.77$) associated with the residual sequence (32-36) of thymic hormone thymopoietin [1, 2]. It possesses the biological properties characteristic of thymopoietin [3], and has been widely used for immunomodulation [4], and for treatments of autoimmune diseases [5], including cancer immunodeficiency [6], rheumatoid arthritis [7], tuberculosis [8], chronic heart failure [9], and chronic lymphocytic leukemia [10]. TP5 can facilitate the differentiation of thymocytes and affect the function to induce maturation of T-cells [11, 12] and bone marrow dendritic cells [13]. Nevertheless, due to the short half-life (≤ 30 s in plasma) and massive metabolism in the gastrointestinal tract [14], TP5 is generally applied as a freeze-dried powder by intramuscular or percutaneous injection [5]. Chronic autoimmune diseases require long therapies and repetitive injections of TP5 which could provoke complications. These disadvantages highly limit the clinical utilization of TP5.

Controlled drug delivery systems have attracted much interest in recent decades, including nanoparticles [15], micelles [16], liposomes [17], and hydrogels [18, 19]. These various systems present many advantages such as prolonged drug release, constant drug concentration, reduced side effects, protection of drugs from degradation, etc. Micelles, liposomes and nanoparticles have been used to encapsulate TP5, but the encapsulation efficiency is quite low because of its high hydrophilicity [16, 20]. Dissolving microneedle array was studied as a new strategy for TP5 delivery by

transdermal injection [4]. However, customized microneedle arrays and daily administration are needed, leading to high cost and low bioavailability. In contrast, hydrogel delivery systems appear most interesting for sustained delivery of hydrophilic drugs, and have been used clinically [21]. Hydrogels can easily encapsulate a variety of hydrophilic therapeutic agents, including small-molecule drugs [22], macromolecular drugs [23] and cells [24]. Furthermore, the high-water up taking capacity endows hydrogels with the physical features similar to tissues, and excellent biocompatibility. Besides, the crosslinked framework of hydrogels can hinder penetration of proteins [25], and thus protecting vulnerable bioactive drugs from degradation by inwardly diffusing enzymes [26].

Hydrogels have been investigated for the encapsulation of TP5. Zhang et al. developed a physical hydrogel from polylactide-poly(ethylene glycol) (PLA-PEG) block copolymers via stereo-complexation between poly(L-lactide) and poly(D-lactide) blocks [18]. High drug loading and rapid drug release were obtained. Nevertheless, PLA degradation leads to acidic by-products which could provoke inflammatory reactions, and such physical hydrogels exhibit low stability and mechanical strength. Su et al. synthesized a hydrogel by crosslinking PLA grafted O-carboxymethyl chitosan (CMCS) using 1-(3-dimethylaminopropyl)-3-ethylcarbodiimide and N-hydroxysuccinimide as crosslinking agents [27]. The resulting hydrogel was used to encapsulate TP5 by immersion of dried gel in a TP5 solution. More than 80% of TP5 was released in 48 h. However, the presence of residual chemicals or solvents could compromise the biocompatibility of the system [28]. Therefore, it becomes a major challenge to develop a delivery system of TP5 which exhibits good biocompatibility, stability and high encapsulation efficiency.

CMCS is a water-soluble derivative of chitosan, the second most abundant polysaccharide in nature. It has been studied as a promising carrier for the delivery of peptides and proteins [29]. On the other hand, Jeffamine is a

biocompatible polyetheramine containing poly(propylene oxide) and poly(ethylene oxide) blocks, as well as primary amino groups at chain ends. It has been used in drug delivery because of its water solubility and cytocompatibility [30]. Recently, our group has developed a CMCS and Jeffamine based dynamic hydrogel that could be potentially used for drug delivery [31], cartilage engineering [32], and antibacterial materials [33]. The hydrogel was prepared via dual imine bond crosslinking between the amino groups of CMCS and the aldehyde ones of a dynamer (Dy). Dy was first obtained by Schiff-base reaction of 1,3,5-benzenetri-aldehyde (BTA) and di-amino Jeffamine, followed by Schiff-base reaction of Dy and CMCS in aqueous solution to yield a 3D network. Trifunctional BTA served as a core to ensure 3D crosslinking, and Jeffamine as a linker to endow Dy with aqueous solubility. The whole process is environmentally friendly as no toxic solvents or catalysts are used, which should be beneficial for encapsulation of fragile drugs such as proteins or peptides [21]. Interestingly, the hydrogel network contains free aldehyde and amino groups which are able to react with the functional groups of drugs or other bioactive molecules.

In this work, CMCS and Jeffamine based dynamic hydrogels are used to conceive a novel delivery system of TP5 by both physical mixing and reversible covalent bonding. *In situ* incorporation of TP5 within the dynamic hydrogel allows to achieve 100 % encapsulation efficiency, and to protect TP5 from organic solvents. The rheological properties, internal morphology and swelling performance of dynamic hydrogels and TP5-loaded hydrogels were comparatively investigated. *In vitro* drug release of TP5-loaded hydrogels was studied under different conditions, and fitted using Higuchi's model. Finally, density functional theory (DFT) was applied to model the different imine bonds in the hydrogel network.

4.2 Experimental section

4.2.1 Materials

O,O'-bis(2-aminopropyl) poly(propylene glycol)-block-poly(ethylene glycol)-block-poly(propylene glycol), namely Jeffamine[®] ED-2003 with M_n of 1900, methanol (96%), hydrogen peroxide solution (H_2O_2 , 30%) citric acid (99.5%), disodium hydrogen phosphate dodecahydrate (99%), boric acid (99.5 %), and borax (99%) were all of analytical grade, and obtained from Sigma-Aldrich. Benzene-1,3,5-tricarbaldehyde (BTA, purity 98%) was purchased from Manchester Organics. O-carboxymethyl chitosan (CMCS) with degree of carboxymethylation of 80 %, degree of deacetylation of 90 % was supplied by Golden-shell Biochemical Co., Ltd. TP5 (99%) was purchased from Soho-Yiming Pharmaceutical Co., LTD (Shanghai, China). All chemicals were used as received without further purification.

4.2.2 Synthesis of dynamer

A dynamer (Dy) was synthesized from Jefamine and BTA. Typically, BTA (81 mg, 0.5 mmol) and Jeffamine (0.95 g, 0.5 mmol) were dissolved in 20 mL methanol. The mixture was then heated to 70 °C and allowed to react for 4 h under gentle stirring. The solvent was totally removed by using rotary evaporator. 10 mL Milli Q water was added to yield a homogeneous Dy solution at a concentration of 0.05 M, as calculated from the remaining aldehyde groups.

4.2.3 Depolymerization of CMCS

Low molar mass CMCS was prepared via degradation of original CMCS in the presence of H_2O_2 . Typically, CMCS (1 g) was dissolved in 30 mL Milli-Q water under stirring at 25 °C. 0.15 mL H_2O_2 was then dropped in the solution. After 30 min degradation, the solution was immediately freezed by immersing in

liquid nitrogen, and transferred onto a freeze dryer. After 24 h lyophilization, a white powder was obtained. The product was dissolved in 10 mL Milli-Q water, followed by precipitation in 200 mL absolute ethanol. Finally, the product was obtained by vacuum drying at 40 °C for 24 h. Another product was obtained after 60 min degradation using the same process. The original CMCS and depolymerized ones for 30 and 60 min are 80 000, 30 000 and 25 000, respectively, as determined by GPC in aqueous medium. They are accordingly named as CMCS80K, CMCS30K and CMCS25K.

4.2.4 Preparation of dynamic hydrogels

Dynamic hydrogels were prepared from CMCS, Jeffamine and BTA as previously reported. Typically, CMCS solution (0.15 M) was prepared by dissolving 0.318 g CMCS (1.5 mmol, calculated from D-glucosamine units) in 10 mL Milli-Q water at room temperature. The CMCS solution (0.15 M) was then mixed with the Dy solution (0.05 M) with a 4/1 molar ratio of glucosamine/Dy. After removal of trapped bubbles by using ultra-sound, gelation was allowed to proceed at 37 °C for 24 h to yield a transparent hydrogel named as Gel80K, Gel30K or Gel25K according to the Mn of CMCS.

4.2.5 Preparation of TP5 loaded hydrogels

TP5 loaded hydrogels were prepared through in-situ encapsulation. In brief, 2.625 mg TP5 was dissolved in 0.5 mL CMCS80K (0.15 M). The resulting solution was mixed with 0.375 mL Dy solution (0.05 M). The glucosamine of CMCS to Dy molar ratio was 4/1. After removal of trapped bubbles by ultra-sound, the mixture, namely Gel80K-TP5, was transferred into an oven at 37 °C for 24 h gelation. Another TP5 loaded hydrogel, named as Gel80K-TP5-3B, was prepared using the same procedure, but TP5 was dissolved in Dy solution before mixing with CMCS80K solution. TP5 was also loaded in Gel30K or Gel25K, and the corresponding samples were named as Gel30K-TP5 or

Gel25K-TP5, respectively. In addition, unless otherwise specified, the TP5 concentration in drug loaded hydrogels was 3 mg/mL.

4.2.6 Characterization

^1H NMR spectroscopy was carried out using Bruker NMR spectrometer (400-LS) at 400 MHz. D_2O was used as the solvent. 5 mg of sample were dissolved in 0.5 mL of solvent for each analysis.

Gel permeation chromatography (GPC) was performed on a Water 1515 multidetector GPC system equipped with Waters 410 differential detector and ultra-hydrogel 250 column. 0.1 M NaCl was used as the mobile phase with a flow velocity of 0.6 mL/min. The column temperature was set at 40 °C, and the sample concentration was 5.0 mg/mL. Poly(ethylene glycol) standards were used for calibration.

Fourier-transform infrared (FT-IR) spectroscopy of freeze-dried hydrogels was conducted on Nicolet Nexus FT-IR spectrometer, equipped with ATR diamant Golden Gate.

The morphology of freeze-dried hydrogels was examined by using Hitachi S4800 scanning electron microscopy (SEM). As-prepared hydrogels were placed in small vials, and immersed in liquid nitrogen (-196 °C) in order to conserve the original structure. The frozen samples were lyophilized with LABCONCO® freeze dryer for 24 h, and sputter coated prior to analysis.

Physical MCR 301 Rheometer (Anton Paar) was utilized to determine the rheological properties of hydrogels, using a cone plate geometry (diameter of 4 cm, apex angle of 2°, and clearance of 56 μm). The storage modulus (G') and loss modulus (G'') were measured as a function of time, strain or frequency.

4.2.7 Swelling of freeze-dried hydrogels

The swelling performance of freeze-dried gels was evaluated by immersion in buffer solutions at different pH values. Buffers from pH 3 to pH 7.4 were

prepared from 0.1 M citric acid and 0.2 M disodium hydrogen phosphate dodecahydrate solutions, buffers at pH 8 and pH 9 from 0.2 M boric acid and 0.05 M borax solutions, and buffer at pH 10 from 0.05 M borax and 0.2 M sodium hydroxide solutions. Freeze-dried gel samples were immersed in a buffer solution, and taken out after 24 h. The swollen hydrogels were weighed after wiping surface water with filter paper, and weighed again after 24 h lyophilization. The swelling and mass loss ratios of hydrogels were calculated according to the following equations:

$$\text{Swelling ratio \%} = \frac{(M_s - M_d)}{M_d} \times 100 \quad (\text{Eq. 1})$$

$$\text{Mass loss ratio \%} = \frac{(M_0 - M_d)}{M_0} \times 100 \quad (\text{Eq. 2})$$

Where M_0 is the initial mass of dried gel, M_s is the wet mass of the swollen hydrogel, and M_d is the dried mass of the swollen hydrogel after lyophilization.

4.2.8 *In-vitro* release of TP5

In-vitro drug release was realized in pH = 7.4 phosphate buffered saline (PBS) at 37 °C. TP5-containing hydrogel samples were placed in a centrifuge tube (50 mL) containing 10 mL pH 7.4 PBS. *In vitro* release was performed in shaking water bath at 37 °C. At preset time intervals, 3 mL of the buffer solution was taken out, and replaced by 3 mL fresh buffer. TP5 concentration of the release supernatant was determined by HPLC-UV. A calibration curve was previously established using TP5 solution with known concentrations. *In-vitro* release of TP5 was also conducted in acidic buffer (pH 5.5), using the same procedure.

The cumulative release of TP5 was calculated using equation 3:

$$\text{Release rate} = \frac{V_e \sum_{i=1}^{n-1} C_i + V_0 C_n}{m_{\text{drug}}} \times 100 \quad (\text{Eq. 3})$$

Where C_n and C_i represent the drug concentrations in the supernatant for n and i withdrawing steps, respectively; V_0 is initial total volume of PBS; V_e is collected volume of PBS; m_{drug} is the original loading amount of TP5. The drug loading efficiency is 100 % due to the in-situ encapsulation of TP5. All of the

experiments were performed in triplicate, and values were given in mean \pm SD for $n = 3$.

4.2.9 The release kinetics model

The release kinetics of the various TP5-loaded hydrogel drug release systems were studied by fitting the *in vitro* release data on the following one classic mathematic model [34, 35]:

Higuchi model: $Q_t = K_H \times t^{1/2}$, where Q_t is the quantity of drug released within the time t , K_H is the Higuchi dissolution constant.

4.2.10 Density functional theory (DFT) computation

All calculations were performed using the Dmol3 code [36] in the Materials Studio 7.0 package. The GGA/PBE functional was selected, and double numerical plus polarization (DNP) [37] was used as the basis set. Convergence tolerances for the total energy, maximum force, and maximum displacement were set to 1.0×10^{-5} Hartree, 2.0×10^{-3} Hartree/Å, and 5.0×10^{-3} Hartree/Å, respectively. The self-consistent field convergence was 1.0×10^{-6} Hartree. To accelerate the self-consistent field (SCF) convergence, the smearing was set to 0.005 Hartree. The solvent effect was simulated by conductor-like screening model (COSMO) [38], using the dielectric constant of 78.54 (water). The transition states were calculated by using the synchronous method with conjugated gradient refinements. This method involves linear synchronous transit (LST) maximization, followed by repeated conjugated gradient (CG) minimizations and then quadratic synchronous transit (QST) maximizations and repeated CG minimizations until a transition state is located [39]. The energy barrier (EBarrier) was calculated using equation 4:

$$E_{Barrier} = E_{TS} - E_{IN} \quad (\text{Eq. 4})$$

where E_{TS} is the energy of the transition state and E_{IN} is the energy of the intermediate that is connected to the transition state.

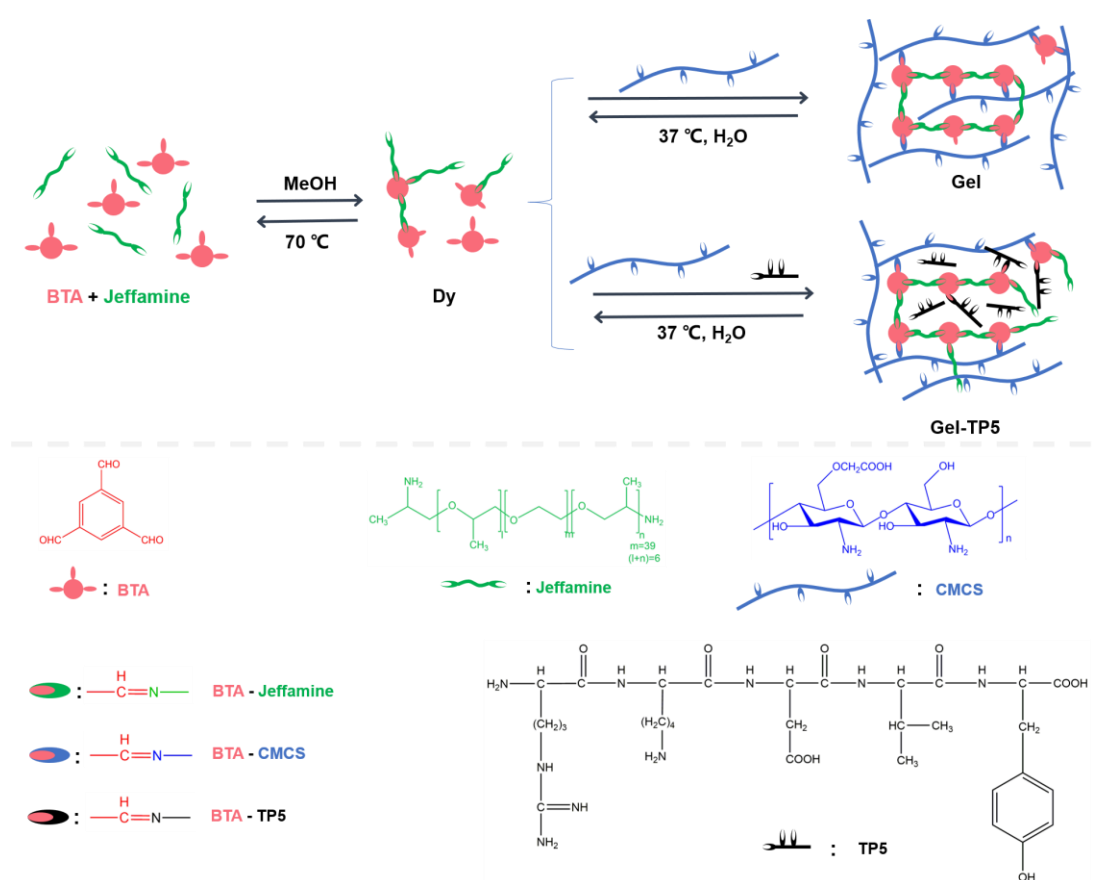
The reaction energy (ERE) of the elementary steps was calculated using equation 5:

$$E_{RE} = E_P - E_R \quad (\text{Eq. 5})$$

where E_P is the energy of the elementary reaction product and E_R is the initial energy of the elementary reaction reactant.

4.3 Results and discussion

4.3.1 Preparation of hydrogels



Scheme 4.1 Synthesis of dynamic hydrogels via Schiff-base reaction between CMCS and Dy, and in-situ loading of TP5 in hydrogels.

Dynamic hydrogels were synthesized via Schiff-base reaction between CMCS and the dynamer, as shown in Scheme 4.1. Upon mixing CMCS and Dy aqueous solutions, the amino groups along the CMCS backbone react with the remaining aldehyde groups of Dy, resulting in formation of a 3D network by dual

imine bonding. The CMCS to Dy molar ratio of 4:1 was adopted since it allows optimal crosslinking, as demonstrated in our previous work [32]. Additionally, the in-situ TP5 encapsulation in hydrogels is shown in Scheme 4.1 as well. Table 4.1 summarizes all the details of preparation of blank and drug loaded hydrogels.

Table 4.1 Molar and mass compositions of blank and TP5 loaded hydrogels ^{a)}.

Sample	CMCS80K		CMCS30K		CMCS25K		Dy ^{c)}		TP5 ^{d)}
	[mmol]	[w/v%]	[mmol]	[w/v%]	[mmol]	[w/v%]	[mmol]	[w/v%]	
	b)		b)		b)				
Gel80K	0.3	1.8	-	-	-	-	0.075	4.3	-
Gel30K	-	-	0.3	1.8	-	-	0.075	4.3	-
Gel25K	-	-	-	-	0.3	1.8	0.075	4.3	-
Gel80K-TP5-0.1	0.3	1.8	-	-	-	-	0.075	4.3	0.1
Gel80K-TP5-3	0.3	1.8	-	-	-	-	0.075	4.3	3
Gel80K-TP5-3B	0.3	1.8	-	-	-	-	0.075	4.3	3
Gel80K-TP5-9	0.3	1.8	-	-	-	-	0.075	4.3	9
Gel30K-TP5-3	-	-	0.3	1.8	-	-	0.075	4.3	3
Gel25K-TP5-3	-	-	-	-	0.3	1.8-	0.075	4.3	3

^{a)} Hydrogels are prepared by mixing CMCS80K/CMCS30K/CMCS25K and Dy aqueous solutions at a D-glucosamine/Dy molar ratio of 4/1 to a total volume of 3.5 mL. The concentration of CMCS solution is 0.15 M, and that of Dy solution is 0.05 M; ^{b)} Moles of glucosamine units of CMCS. Calculations are made on the basis of the average molar mass of 212 g/mol obtained for D-glucosamine, taking into account the degree of deacetylation of 90% and the degree of carboxymethylation of 80%; ^{c)} The concentration of Dy solution is obtained from the remaining aldehyde groups. In a typical reaction, 0.5 mmol BTA (81 mg) reacts with 0.5 mmol Jeffamine ED2003 (950 mg) to form a Dy solution. As BTA has 3 aldehydes and Jeffamine 2 amines, there remains theoretically 0.5 mmol of aldehydes in the dried Dy. Addition of 10 mL water yields a dynamer solution of 0.05 M. ^{d)} The addition concentration of TP5 in hydrogel is 0.1 mg/ml or 3 mg/ml or 9 mg/ml, and values were expressed as mean \pm SD for n = 3.

4.3.2 FT-IR and NMR

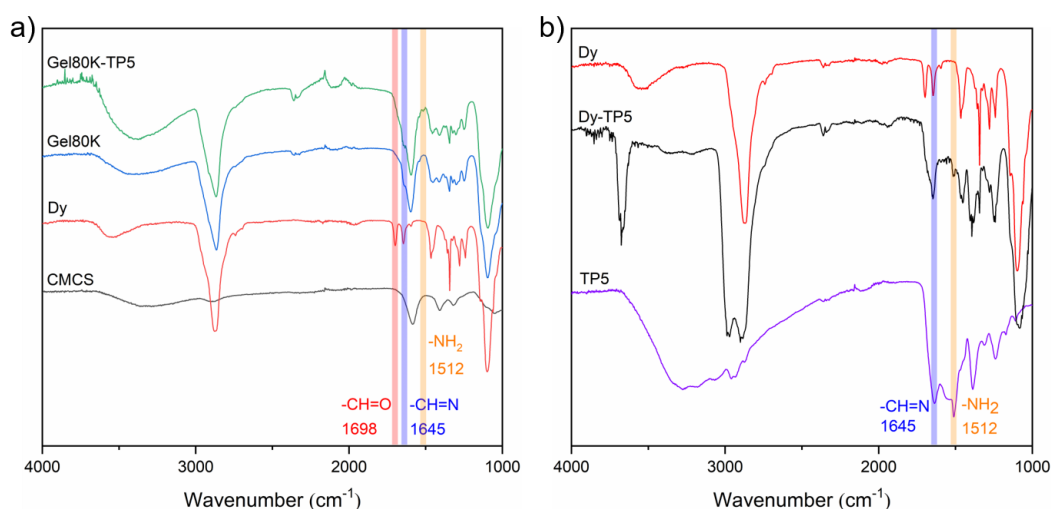


Figure 4.1 a) FT-IR spectra of freeze-dried CMCS, Dy, Gel80K and Gel80K-TP5-3; b) FT-IR spectra of Dy, TP5, and Dy-TP5 which is an obtained by mixing TP5 in Dy solution at a molar ratio of 1/1, reaction at 37 °C for 24h, and 24 h lyophilization.

Figure 4.1a shows the FTIR spectra of CMCS, Dy, and freeze dried Gel80K and TP5 loaded Gel80K-TP5-3. CMCS presents a large band around 3350 cm^{-1} which is attributed to free OH and NH_2 groups, and an intense band at 1595 cm^{-1} due to carbonyl groups. The dynamer exhibits two intense bands at 2850 and 1100 cm^{-1} assigned to C-H and C-O stretching, and two characteristic bands at 1698 and 1645 cm^{-1} corresponding to aldehyde and imine bonds, respectively. All the characteristic bands of CMCS and Dy are observed on the spectrum of freeze dried Gel80K. Nevertheless, the band of aldehyde groups at 1698 cm^{-1} is almost invisible, but the band at 1645 cm^{-1} corresponding to newly formed imine bonds is clearly distinguished. These results illustrate that hydrogels are formed due to imine formation between aldehydes of Dy and amine groups of CMCS. On the spectrum of Gel80K-TP5-3, a band is detected at 2100 cm^{-1} , which is assigned to the O-H stretching of water [40]. In fact, the freeze-dried samples rapidly absorbed water due to the high hygroscopicity of TP5 [41, 42]. In addition, a small new band is detected at 1512 cm^{-1} which is attributed to N-H pending of amine groups of TP5 [16], suggesting the efficient

combination of TP5 in the hydrogel. Similar findings are obtained for other blank and TP5 loaded hydrogels (Figure S4.1, Supporting Information).

Figure 4.1b presents the FT-IR spectra of TP5 and a Dy-TP5 mixture. The latter was prepared in order to figure out the interactions between the aldehydes of Dy and the amines of TP5. It was obtained by dissolving TP5 in Dy solution at a molar ratio of 1/1, followed by 24 h reaction at 37 °C and finally 24 h lyophilization. TP5 presents characteristic bands at 1630 and 1512 cm^{-1} which are assigned to the C=O stretching of amides and N-H pending of amines, together with a large band around 3300 cm^{-1} due to the presence of water. Interestingly, the band of aldehydes at 1698 cm^{-1} is not detected on the spectrum of Dy-TP5, suggesting that the aldehydes have reacted with the amine groups of TP5 via Schiff-base reaction.

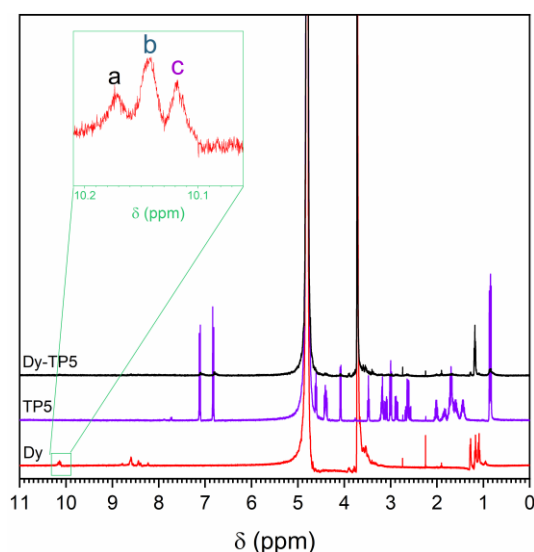


Figure 4.2 ^1H NMR spectra of the Dy, TP5, and Dy-TP5 in D_2O .

Figure 4.2 shows the ^1H NMR spectra of the Dy, TP5, and Dy-TP5. TP5 presents numerous signals associated to its various protons. On the spectrum of Dy, the three small signals in the 10.1-10.2 ppm range are assigned to aldehyde groups of BTA with different degrees of substitution, including non-substituted (a), mono-substituted (b), and di-substituted aldehydes (c). Signals between 8.2 and 8.7 ppm are assigned to the imine and aromatic protons,

signals around 3.7 ppm to the methylene and methine protons, and signals between 1.0 and 1.3 ppm to the methyl protons of Jeffamine. The presence of residual H₂O is detected at 4.8 ppm [32, 33]. Obviously, no signals in the range of 10.1-10.2 ppm are observed on the spectrum of Dy-TP5, implying that all the remaining aldehydes of Dy have reacted with the amine groups of TP5, in agreement with FTIR data (Figure 4.1b).

The morphology of CMCS, Dy, their mixtures with TP5 (CMCS-TP5 and Dy-TP5) was examined by using SEM (Fig. S2). No obvious difference is observed between pristine CMCS (Figure S4.2a, b, Supporting Information) and CMCS-TP5 (Figure S4.2e, f, Supporting Information). Both samples display a lamellar structure with the presence of holes of c.a 10 μ m, suggesting the absence of interactions between the two components. In contrast, some difference is detected between pristine Dy (Figure S4.2c, d, Supporting Information) and the mixture Dy-TP5 (Figure S4.2g, h, Supporting Information). Both samples exhibit a highly porous structure. The surface of Dy appears rugged, whereas that of Dy-TP5 appears smooth. These findings seem to indicate the occurrence of interactions between TP5 and the Dy.

4.3.3 Rheology

Rheological measurements were conducted on the various hydrogels at 25 °C to evidence the effect of CMCS molar mass on the rheological properties as well as the interaction between TP5 and Dy in the hydrogel network. Firstly, the storage modulus (G') and loss modulus (G'') changes of blank hydrogels (Gel80K, Gel30K and Gel25K) were determined as a function of strain at a frequency of 1 Hz and at 25 °C, as shown in Figure 4.3a. As the strain increases from 0.1 % to 20 %, G' remains almost constant for all the blank hydrogels, whereas G'' slightly decreases, indicating a linear viscoelastic (LVE) behavior of hydrogels in the 0.1 to 20 % strain range.

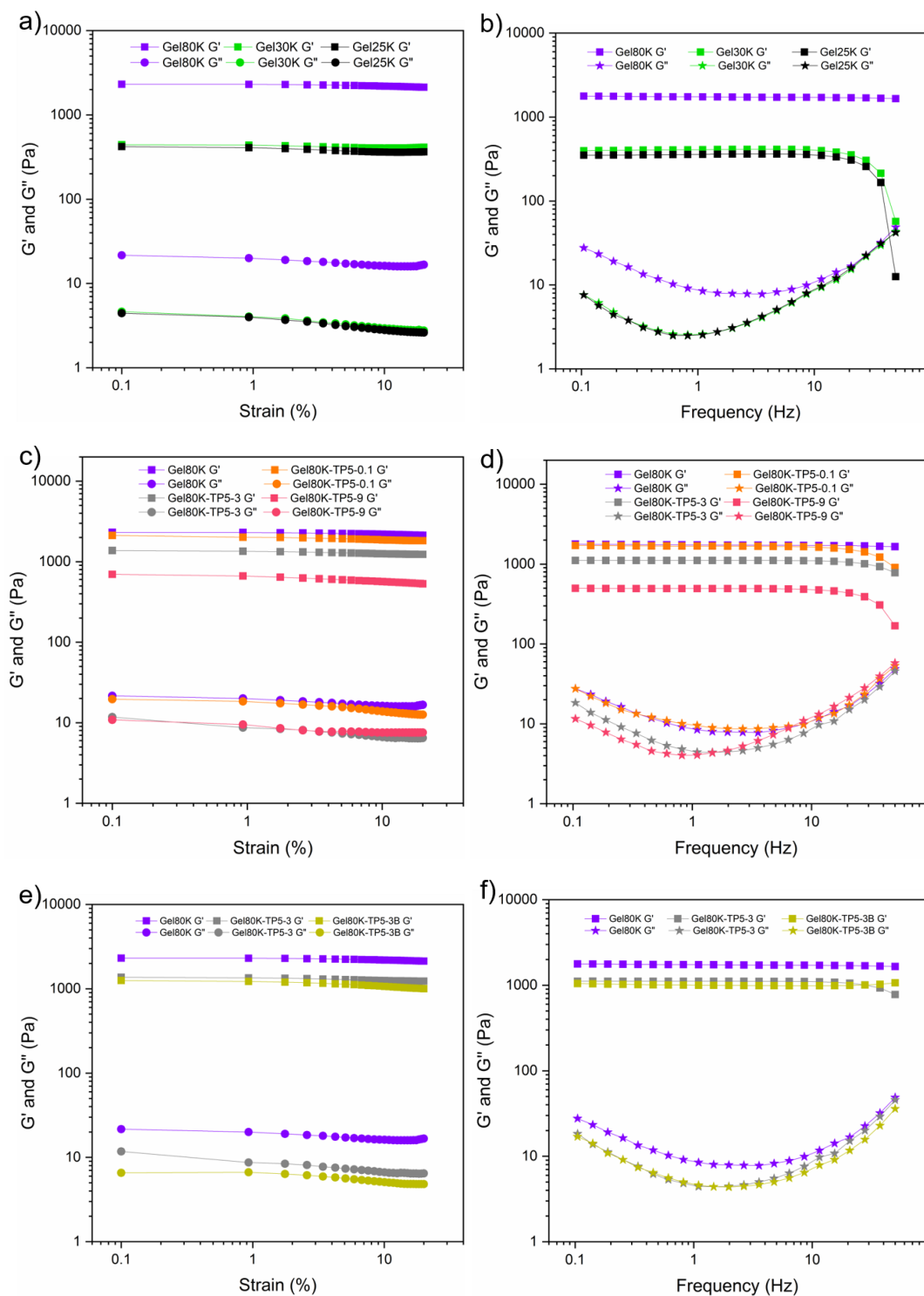


Figure 4.3 Storage modulus (G') and loss modulus (G'') changes of Gel80K, Gel30K and Gel25K as a function of strain at 25 °C and at 1 Hz (a) and as a function of frequency at 25 °C and at a strain of 1 % (b); G' and G'' changes of Gel80K, , Gel80K-TP5-0.1, Gel80K-TP5-3 and Gel80K-TP5-9 as a function of strain at 25 °C and at 1 Hz (c) and as a function of frequency at 25 °C and at a strain of 1% (d); G' and G'' changes of Gel80K, Gel80K-TP5-3, and Gel80K-TP5-3B as a function of strain at 25 °C and at 1 Hz (e) and as a function of frequency at 25 °C and at a strain of 1 % (f).

Meanwhile, the moduli of blank hydrogels are highly dependent on the molar mass of CMCS. With the decrease of molar mass of CMCS from 80,000 to 30,000 and to 25,000, G' at a strain of 1% decreases from 2300 Pa for Gel80K to 440 Pa for Gel30K, and to 420 Pa for Gel25K, respectively. Similar phenomena are observed for G'' changes. In fact, higher molar mass chains have more amino groups, which allows to enhance the crosslinking density thus resulting in higher modulus of hydrogels.

Figure 4.3b shows the modulus changes of blank hydrogels as a function of frequency from 0.1 Hz to 50 Hz at a constant strain (1%) and at 25 °C. G' remains constant in the whole frequency range for Gel80K, whereas a sharp decrease of G' is observed beyond 30 Hz in the cases of Gel30K and Gel25K. On the other hand, G'' exhibits some fluctuations with increasing frequency. These rheological results well corroborate with the formation of highly stable covalent networks, in contrast to physical hydrogels whose storage and loss moduli increase with increasing frequency due to chain entanglements [18, 43]. It is also noteworthy that Gel80K exhibit higher stability than Gel30K and Gel25K due to higher crosslinking density as mentioned above.

Figure 4.3c presents G' and G'' changes *versus* strain of Gel80K hydrogels containing various amounts of TP5 (0, 0.1, 3, and 9 mg/mL). Obviously, with addition of TP5 in hydrogels, G' decreases from 2310 Pa for Gel80K to 2222 Pa for Gel80K-TP5-0.1, to 1374 Pa for Gel80K-TP5-3, and to 697 Pa for Gel80K-TP5-9. These results illustrate that in-situ TP5 encapsulation affects the rheological properties of drug loaded hydrogels. In fact, the amine groups of TP5 can react with the free aldehyde groups of Dy, as shown in Figure 4.1b and Figure 4.2. Hence, there is competition between TP5 and CMCS after mixing aqueous solution of Dy with that of CMCS and TP5, leading to decreased imine bonding between CMCS and Dy. On the other hand, attachment of TP5 to the network does not contribute to the crosslinking because TP5 is a small molecule compared to CMCS. Therefore, the

crosslinking density decreases with increase of TP5 content, and consequently the modulus of hydrogels decreases. A frequency sweep of hydrogels was performed over a range from 0.01 to 50 Hz at a fixed strain of 1 %. G' remains constant for Gel80K, and slightly decreases beyond 30 Hz for TP5 loaded hydrogels, indicating that TP5 encapsulation affects the stability of hydrogels. A hydrogel (Gel80K-TP5-3B) was prepared by dissolving TP5 in Dy solution, followed by mixing with CMCS solution before gelation. As TP5 is supposed to react with Dy, dissolving TP5 in Dy solution should favor imine formation between them. G' and G'' changes of Gel80K, Gel80K-TP5-3, and Gel80K-TP5-3B were examined as a function of strain and frequency (Figure 4.3e, f). Noticeably, G' of Gel80K-TP5-3 is higher than that of Gel80K-TP5-3B in nearly the whole strain and frequency ranges, which confirms that mixing TP5 and Dy first decreased the crosslinking density of hydrogels.

A strain sweep and a frequency sweep were also performed on blank and TP5 loaded Gel30K and Gel25K hydrogels (Figure S4.3, Supporting Information). Similar phenomena were observed, illustrating the stability of hydrogels and interactions between TP5 and the dynamer.

4.3.4 Morphology and swelling

The morphology of as-prepared hydrogels after lyophilization was observed by SEM. All hydrogels, and especially Gel80K, exhibit a porous structure with regularly distributed and interconnected pores (Figure 4.4). The interconnected porous structure enables hydrogels to mimic the extracellular matrix, which is beneficial for biomedical applications in drug delivery [44], and in tissue engineering [32, 45]. The average pore diameter of Gel80K, Gel30K and Gel25K is $82.9 \pm 0.5 \mu\text{m}$ (Figure 4.4c), $76.1 \pm 1.8 \mu\text{m}$ (Figure 4.4f), and $59.5 \pm 0.4 \mu\text{m}$ (Figure 4.4i), respectively. Thus, it seems that the pore diameter slightly decreases with decrease of the molar mass of CMCS. In a previous work, it is shown that the pore diameter of hydrogels is dependent on the molar mass of

Jeffamine which serves as linker [33]. Therefore, the porous structure of dynamic hydrogels can be tailored by varying the molar mass of the components.

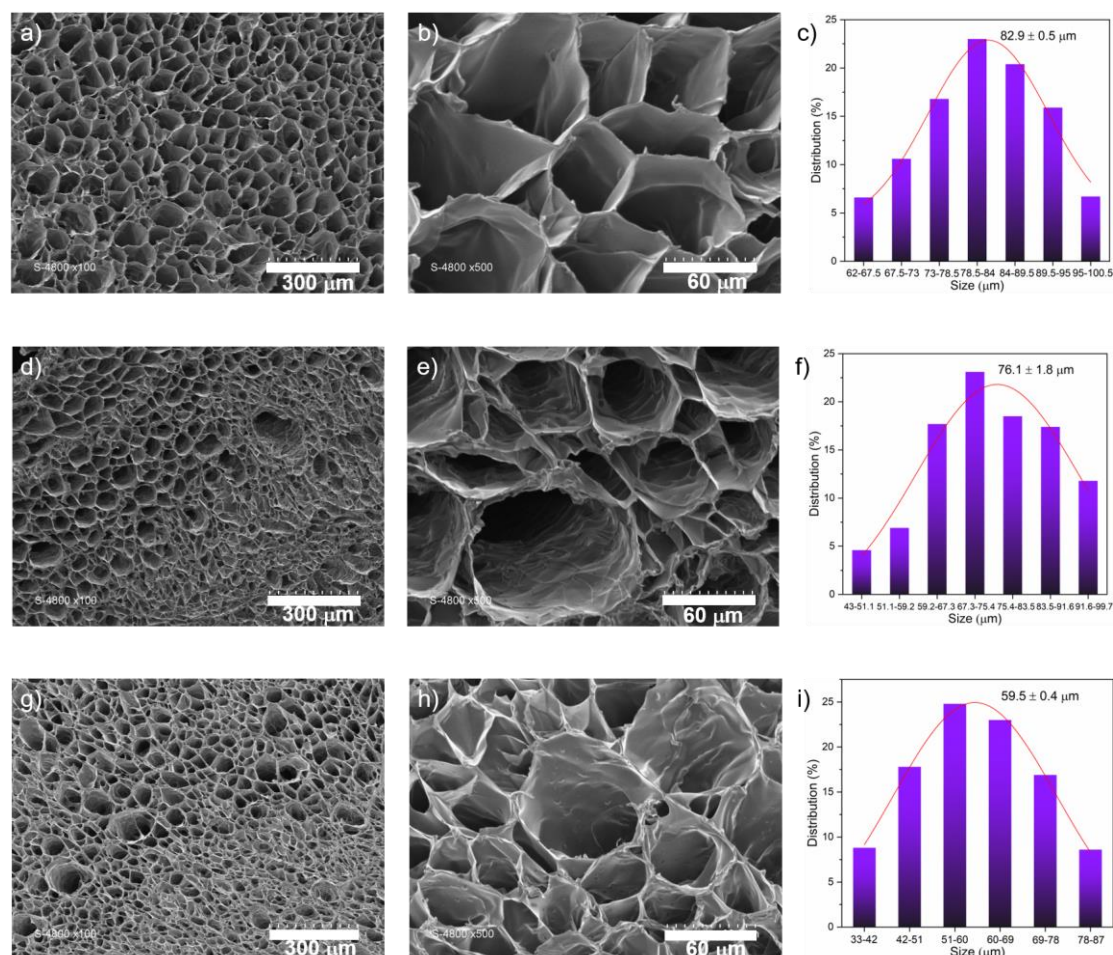


Figure 4.4 SEM images and pore size distributions of freeze-dried gels: (a, b, c) Gel80K; (d, e, f) Gel30K; (g, h, i) Gel25K.

As aforementioned, the most important characteristic of hydrogels is their capability to retain large amount of water in the polymeric network, which is beneficial for controlling the release profiles of drugs and the absorption of wound exudate [46]. Figure 4.5a presents the swelling performance of freeze-dried hydrogels in buffers at various pH values. All the hydrogels exhibit a highly pH-dependent swelling behavior. The swelling degree is low (< 1000 %) in strong acid buffers (pH 3/4), and increases to around 2000 % from pH 4 to 6. It remains at the same level around 2000 % in the pH 6 to 7.4 range. All hydrogels

exhibit a maximum swelling at pH 8, 6600 % for Gel80K, 10000 % for Gel30K, and 11000 % for Gel25K. As the alkalinity continues to increase to pH 9 and 10, the swelling degree of hydrogel decreases dramatically to a level around 3000 %. In addition, there is no major difference between the swelling ratios of the three samples except at pH 8.

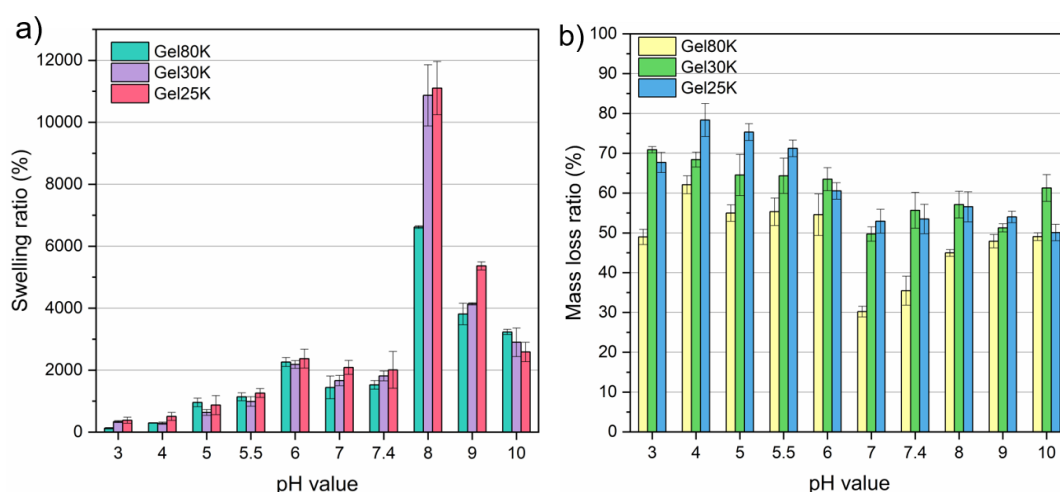


Figure 4.5 a) Swelling ratios, and b) Mass loss ratios of Gel80K, Gel30K and Gel25K after 24 h immersion in buffers at various pH values. Data are expressed as mean \pm SD for n = 3.

The pH sensitivity of the swelling of hydrogels is assigned to electrostatic interactions between the amino and carboxyl groups along CMCS chains [32, 47]. In fact, the pK_a of amino and carboxyl groups is 6.5 and 2.7, respectively. Contraction of hydrogels occurs because of strong electrostatic attraction between negatively charged $-\text{COO}^-$ and positively charged $-\text{NH}_3^+$ groups which result from protonation in strong acidic media (pH 3 and 4), thus, leading to low swelling ratio. Electrostatic attraction diminishes with the decrease of the H^+ concentration (pH 5, 5.5, and 6), and thus to the swelling gradually increases. At pH 6, 7 and 7.4 which are around the pK_a of amino groups, the swelling remains almost constant as the electrostatic interactions are weak due to low concentrations of charges. In contrast, high swelling of hydrogels occurs because of strong repulsion between negatively charged $-\text{COO}^-$ groups at pH 8. Nevertheless, with further enhancement of alkalinity at pH 9 and 10, OH^- ions

in solution would counterbalance the electrostatic repulsion between -COO^- groups [32], thus resulting in decrease of the swelling degree. The pH sensitive swelling of hydrogels could be of great importance for the design of drug delivery systems because of large variation in physiological pH at various body sites in normal and pathological conditions [48].

Mass loss of hydrogels occurs during the swelling process due to the solubilization and washing away of non-crosslinked species, as shown in Figure 4.5b. Overall, the mass loss ratio of all the hydrogels varies between 30 % and 80 % in the whole pH range. The hydrogels show higher mass loss in acid conditions than in neutral and alkaline conditions. Noticeably, the mass loss ratio of Gel80K is lower than those of Gel30K and Gel25K in the whole pH range. This finding could be attributed to the higher cross-linking density of Gel80K as compared to Gel30K and Gel25K, in agreement with rheological data. The lowest mass loss ratio is 30 and 36 % obtained for Gel80K at pH 7 and 7.4, respectively, in agreement with the better stability of Gel80K. Thus, Gel80K is used for a comprehensive study of TP5 release from hydrogels under various conditions.

The swelling and mass loss behaviors of Gel80K were investigated under drug release conditions in pH 7.4 PBS at 37 °C up to 168 h (Fig. S4, Information supplementary). The swelling ratio rapidly increases to 750 % and 1200 % after immersion for 10 and 20 min, respectively, whereas the mass loss ratio increases 25 % and 32 % in the meantime. Thereafter, the swelling and mass loss ratios remain almost at the same level up to 168 h, fluctuating around 1300 % and 34 %, respectively. These findings indicate that an equilibrium is rapidly reached after immersion of dried gels in PBS, and that the hydrogels are stable after initial mass loss.

4.3.5 *In vitro* release of the TP5

TP5 is an immuno-modulating drug, and is widely applied in the treatment of

autoimmune diseases such as chronic lymphocytic leukemia [10], Sezary's syndrome [49, 50], etc. Besides, TP-5 is able to induce the differentiation of T-cells and accelerate the development of T lymphocytes [11]. Therefore, a series of TP5-loaded hydrogels were prepared, including Gel80K-TP5-0.1, Gel80K-TP5-3, Gel80K-TP5-9, Gel80K-TP5-3B, Gel30K-TP5-3, and Gel25K-TP5-3 so as to evaluate the effects of various factors.

The morphology of the various TP5-loaded hydrogels was examined by using SEM (Figure S4.5, Supporting Information). It appears that TP5 encapsulation affects the regularity of the porous structure of hydrogels. In fact, Gel80K-TP5-0.1 exhibits a porous structure similar to that of Gel80K (Figure 4.4a,b), but the surface appears rougher. With increase of TP5 content from 0.1 mg/mL (Figure S4.5a, b, Supporting Information) to 3 mg/mL (Figure S4.5c, d, Supporting Information), and to 9 mg/mL (Figure S4.5e, f, Supporting Information), the three-dimensional architecture becomes more and more irregular as compared with that of Gel80K (Figure 4.4a,b). Similarly, TP5 encapsulation also affects the structure of Gel30K-TP5-3 and Gel25K-TP5-3 as compared to corresponding blank hydrogels. On the other hand, difference is also noticed between the morphology of Gel80K-TP5-3 and Gel80K-TP5-3B. Both have exactly the same compositions, but different mixing orders. Gel80K-TP5-3B exhibits a smoother surface compared to Gel80K-TP5-3. When TP5 is first mixed with Dy solution as in the case of Gel80K-TP5-3B, some TP5 molecules can be attached to the dynamer Dy and thus the structure of the hydrogel is more affected.

TP5 release from the various TP5-loaded hydrogels was monitored to evaluate the potential of dynamic hydrogels as drug carrier in cancer therapy [35]. Figure 4.6 shows the release profiles of TP5 from Gel80K-TP5-3, Gel30K-TP5-3, and Gel25K-TP5-3 in pH 7.4 PBS at 37 °C. Overall, all samples displayed release profile in two stages, namely a burst release in the first 7 h followed by a slowly and continuous release during 7 days. After 1 h in the medium, significant

release rates are recorded, 28.0% for Gel25K-TP5, 13.0% for Gel30K-TP5 and 10.5 % for Gel80K-TP5. TP5 release increases almost linearly to reach 53.17%, 35.14% and 29.68% after 7 h for the 3 samples, respectively. Thereafter, TP5 release slows down, reaching a plateau after 96 h. The total TP5 release is 63.37, 67.99, and 57.13% after 168 h for Gel25K-TP5, Gel30K-TP5 and Gel80K-TP5, respectively. Gel80K-TP5 exhibits slower and more sustainable release as compared to Gel25K-TP5 and Gel30K-TP5 due to its higher crosslinking density which disfavors drug diffusion. Therefore, Gel80K is used as drug carrier in further studies.

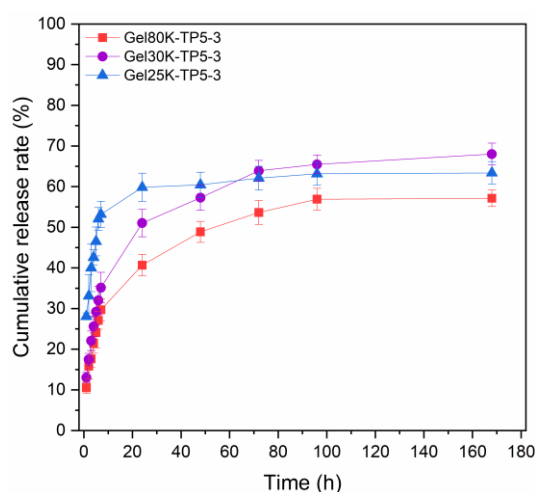


Figure 4.6 Cumulative release of TP5 from Gel80K-TP5-3, Gel30K-TP5-3, and Gel25K-TP5-3; Values were expressed as mean \pm SD for $n = 3$.

Figure 4.7 show the TP5 release curves from various hydrogels and different medium. No difference is noticed between the release profiles 25 °C-Gel80K-TP5-3 and Gel80K-TP5-3 (Figure 4.7a), indicating the gelation temperature (25 or 37 °C) of Gel80K-TP5 has little impact on the release of TP5. On the other hand, although the samples Gel80K-TP5-3, Gel80K-TP5-3-pH5.5 and 25 °C-Gel80K-TP5-3 present similar equilibrium release ratios around 60% (Figure 4.7a-b), the initial release rate of Gel80K-TP5-3-pH5.5 is much faster than those of Gel80K-TP5-3 and 25 °C-Gel80K-TP5-3. This difference can be assigned to the fact that the imine bonds are prone to hydrolysis under acidic condition [51], which leads to partial disassociation of the three-dimensional

network thus favoring diffusion of trapped TP5. It is also of interest to evaluate the effect of initial drug load on the release rate by comparing the release performance of Gel80K-TP5-0.1, Gel80K-TP5-3, Gel80K-TP5-9, as shown in Figure 4.7c. Apparently, the latter shows the highest equilibrium rate, reaching 90 % after 168 h, which is much higher than that of Gel80K-TP5-0.1 (22.5%) and Gel80K-TP5-3 (57 %). This difference well corroborates with the partial attachment of TP5 to the hydrogel network by imine bonding. It can be assumed that the amount of covalently bonded TP5 is the same for the 3 samples and only non-bonded TP5 is released. Thus, hydrogels with higher drug loading have higher proportion of free drug, and consequently higher drug release ratio [35]. Finally, TP5 release behaviors from Gel80K-TP5-3 and Gel80K-TP5-3B are compared to examine the effect of the mixing order (Figure 4.7d). Gel80K-TP5-3B presents a total release ratio of 38%, which is much lower than that of Gel80K-TP5-3 (60%). This finding also confirms the covalent attachment of TP5 to the hydrogel network by imine bonding. As TP5 is first mixed with Dy before mixing with CMCS in the case of Gel80K-TP5-3B, more TP5 is covalently attached to the network, leading to lower TP5 release as compared to Gel80K-TP5-3. Therefore, only physically encapsulated TP5 can be released under in vitro conditions. The release rate of TP5 from hydrogels depends on many factors such as the molar mass of CMCS, the pH of the medium, the drug load, the mixing order during hydrogel preparation.

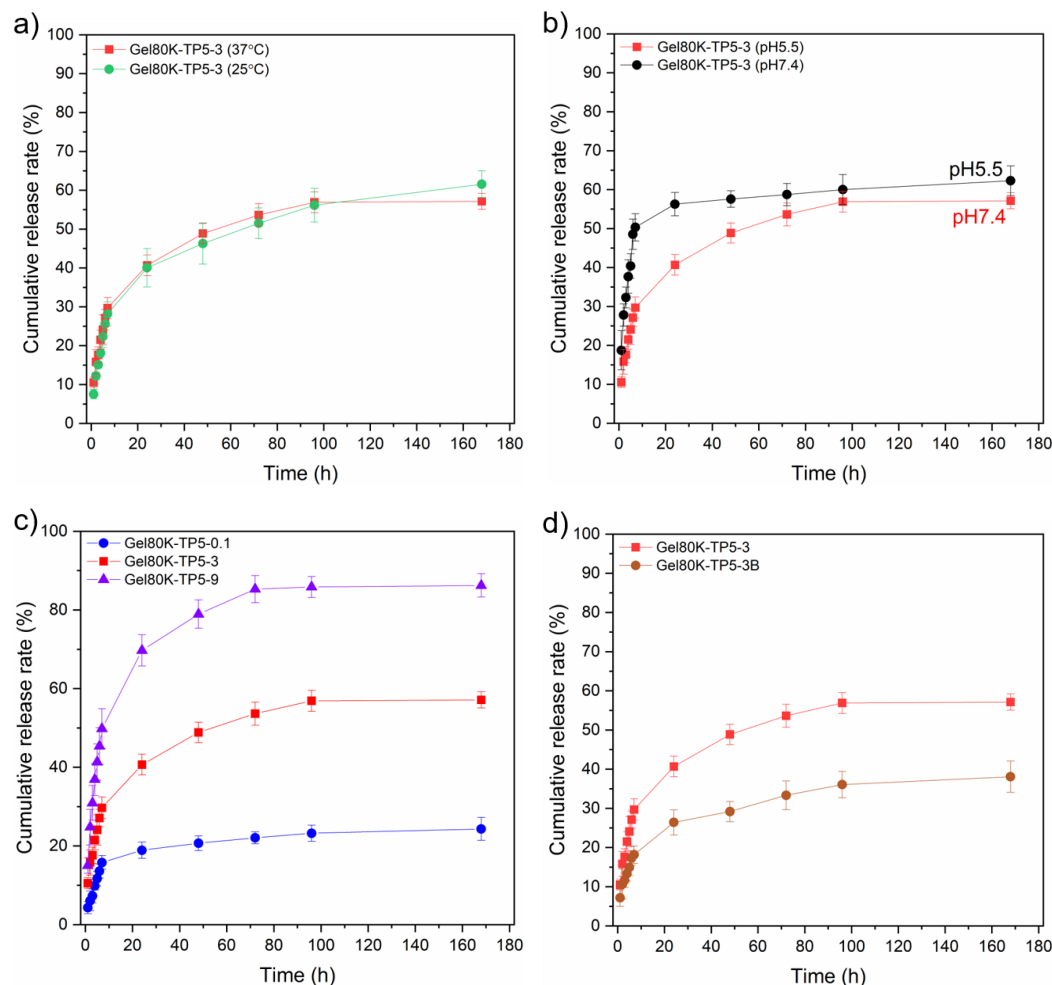


Figure 4.7 a) Cumulative release of TP5 from Gel80K-TP5-3 synthesized at 25 °C and 37 °C, namely, Gel80K-TP5-3 (25 °C) and Gel80K-TP5-3 (37 °C); b) Cumulative release of TP5 from Gel80K-TP5-3 under PBS medium (pH 7.4, 37 °C) and acid buffer medium (pH 5.5, 37 °C), respectively; c) Cumulative release of TP5 from Gel80K loaded with various TP5 content: Gel80K-TP5-0.1, Gel80K-TP5-3, and Gel80K-TP5-9; d) Cumulative release of TP5 from Gel80K-TP5-3 with different TP5 addition sequence, namely, Gel80K-TP5-3 and Gel80K-TP5-3B. Values were expressed as mean \pm SD for n = 3.

4.3.6 Drug release kinetics

It is widely admitted that the release of a hydrophilic drug mainly depends on the diffusion process. Other factors such as physical forces between the drug and the hydrogel matrix and swelling of bulk hydrogel affect the release profile as well. In order to better understand the release mechanism of TP5 from dynamic hydrogels, the release kinetics were investigated through fitting of

experimental data in the first 6 h using Higuchi model [35], as shown in Figure S4.6 (Supporting Information) and Table 4.2.

Table 4.2 Parameters obtained from fitting of experimental data using Higuchi model
a).

Sample	R ²	K _H
Gel80K-TP5-0.1	0.967	6.477
Gel80K -TP5-3	0.990	11.110
Gel80K -TP5-9	0.998	20.897
Gel80K-TP5-3B	0.978	6.502
Gel80K-TP5 (pH5.5)	0.982	19.141
Gel80K-TP5 (25 °C)	0.985	12.271
Gel30k -TP5	0.997	13.315
Gel25k -TP5	0.986	16.172

a) Experimental data in Figure 4.6-7.

Data in Table 2 show that the correlation coefficient is above 0.98 in all cases except Gel80K-TP5-0.1, suggesting that the TP5 release was mainly controlled by diffusion process [52]. In fact, the maximum concentration of TP5 after total release in the release medium is well below its saturation concentration (> 10 mg/mL) even for Gel80K-TP5-9 [18]. Thus, it could be considered that the dissolution is the ruling force of TP5 release from the hydrogels as drug release was conducted under immersion conditions [35]. It is also of interest to compare the K_H values of the different systems. Gel80K-TP5-9 and Gel80K-TP5-0.1 present the highest and the lowest K_H values, respectively, in agreement with the fastest and the slowest release rates. Intermediate K_H values were obtained for other TP5 loaded hydrogels.

4.3.7 Density functional theory (DFT) insights

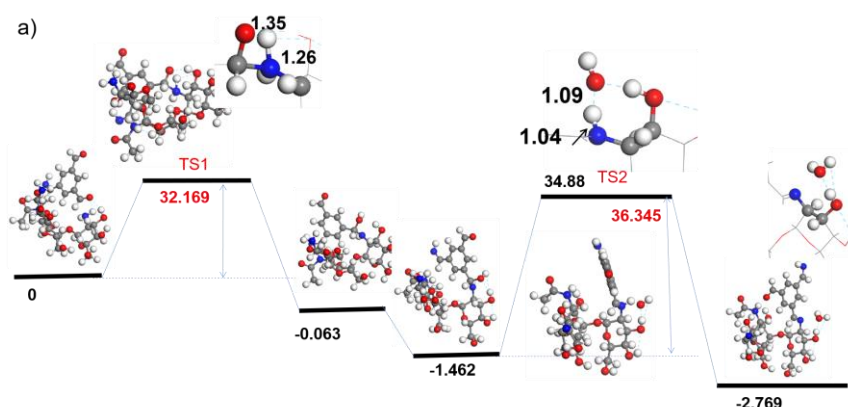
Density Functional Theory (DFT) was used to determine the reaction energy

and energy barrier of imine linkages between TP5 and Dy (TP5-I-Dy, 'I' represents for linkage, similarly hereinafter) as well as those between CMCS and Dy (CMCS-I-Dy. The simplified models of CMCS, Dy and TP5 are shown in Figure S4.7a-c (Supporting Information). Only one reaction site was considered taking into account the repeatability of the amino groups in CMCS and the symmetry of Dy. The lowest energy pathway of the Schiff-base reaction between CMCS and Dy is shown in Figure 4.8a. The first step of the reaction is the dehydrogenation from the amino group of Dy, namely, the formation of hemiamines (exothermic process [53]), which requires overcoming an energy barrier of 32.2 kcal/mol. The formation of CH-NH bond is thermodynamically favorable. This is followed by the cleavage of the oxhydryle group, namely, imine formation (endothermic process [54]), which needs higher energy than the first step, reaching 36.3 kcal/mol. Thus, the rate-limiting step of the reaction between CMCS and Dy is the cleavage of oxhydryle with an energy barrier of 36.3 kcal/mol.

There are three kinds of amino groups in TP5 which have different chemical environments (Figure S4.7c, Supporting Information). Thus, there are three -NH₂ sites that can be involved in the Schiff-base reaction, which are marked as TP5(1)-I-Dy (Figure 4.8b), TP5(2)-I-Dy (Figure 4.8c) and TP5(3)-I-Dy (Figure 4.8d), respectively. The Schiff-base reactions of TP5(1)-I-Dy and TP5(3)-I-Dy are similar. The rate-limiting step of both reactions is the dehydrogenation from the amino groups of TP5 (the first step), which needs to overcome an energy barrier of 53.15 and 53.24 kcal/mol, respectively. The reaction process to yield TP5(2)-I-Dy is more complex than those of the two other reactions. The reaction begins with dehydrogenation from the amino group of TP5, but the H atom tends to bond with the adjacent oxygen atom (O2), and the process needs to overcome an energy barrier of 37.2 kcal/mol. In the second step, the hydrogen proton transfers from O2 to O1, which needs 10.7 kcal/mol and the formation of -C-NH bond is thermodynamically favorable. Subsequently, the cleavage of

oxyhydryle needs to overcome a barrier of 26.4 kcal/mol. Thus, the rate-limiting step of the reaction needs to overcome a barrier of 37.2 kcal/mol, which is only 0.9 kcal/mol higher than that of the Schiff-base reaction between CMCS and Dy. Thus, the -C=O group adjacent to the -NH₂ of TP5 could promote the Schiff-base reaction between TP5 and Dy to form TP5(2)-I-Dy. Moreover, the two other -NH₂ sites of TP-5 may also participate in the Schiff-base reaction in spite of higher energy barrier. Hence, although the energy barrier of TP5-I-Dy is higher than that of CMCS-I-Dy, both reactions proceed concomitantly in a competitive way.

Furthermore, it is worth noting that the gelation time of blank hydrogel without TP5 (e.g., Gel80K) is shorter than that of hydrogel containing TP5 (e.g., Gel80K-TP5) (data not shown). Therefore, the presence of TP5 affects the crosslinking between CMCS and Dy because TP5 reacts competitively with Dy and that formation of TP5-I-Dy does not contribute to the crosslinking due to steric effect. When TP5 is mixed with Dy, it can theoretically and experimentally react with Dy via Schiff base reaction, which is in full agreement with the results obtained by FT-IR (Figure 4.1), NMR (Figure 4.2), and SEM (Figure S4.4, Supporting Information), and TP5 release (Figure 4.6 and Figure 4.7).



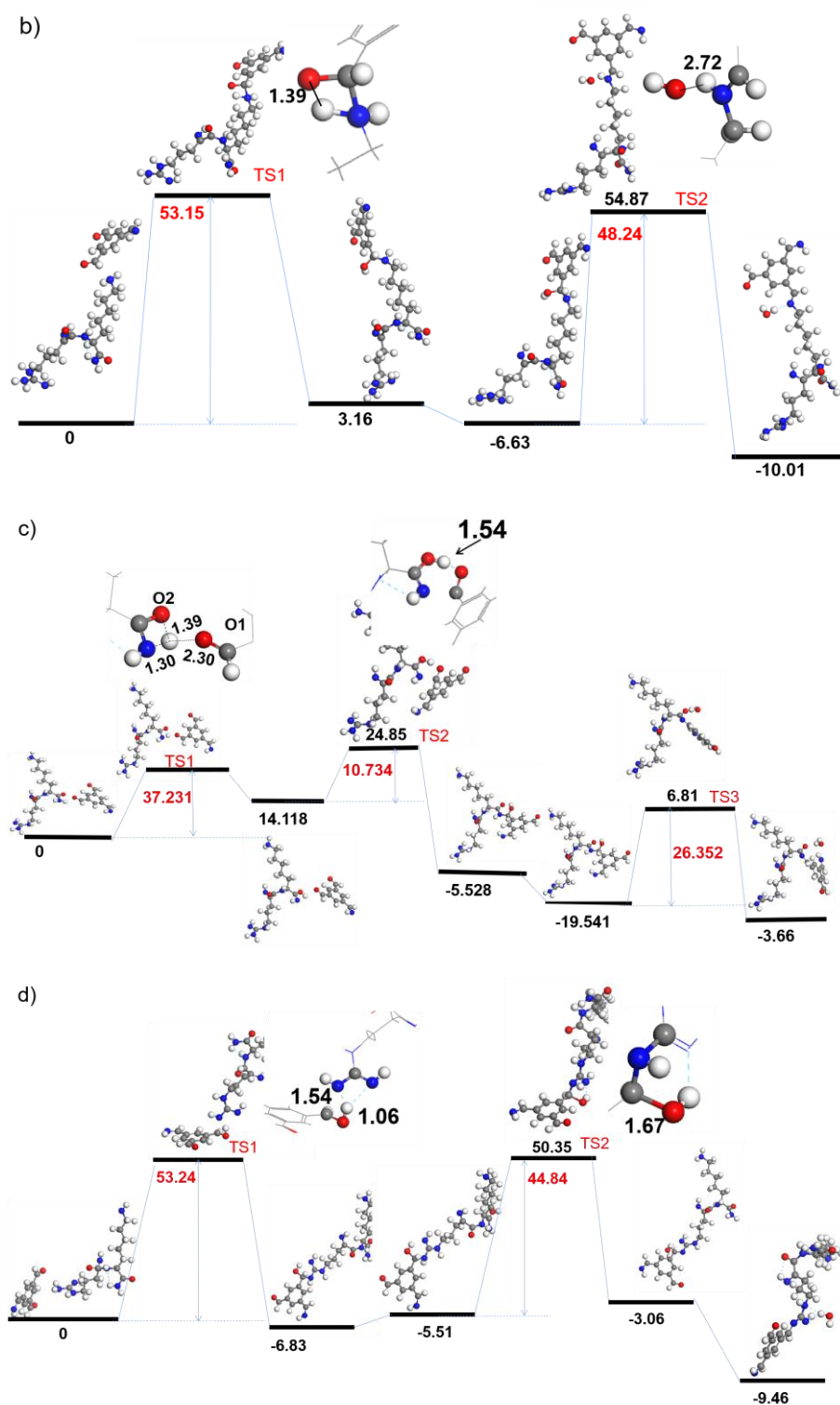


Figure 4.8 Computation by Density Functional Theory (DFT) to determine the lowest reaction pathways between : a) CMCS-I-Dy; b) TP5(1)-I-Dy (TP5 site 1); c) TP5(2)-I-Dy (TP5 site 2); and d) TP5(3)-I-Dy (TP5 site 3). The reaction energy and energy barrier are calculated by Eq. 4 and Eq. 5 in kcal/mol.

4.4 Conclusion

This work focused on the synthesis and characterization of a novel drug delivery system based on dynamic hydrogels for the sustainable release of an immunostimulant – thymopentin (TP5). The hydrogels were prepared via *in situ* gelation of O-carboxymethyl chitosan with a dynamer made from Jeffamine and BTA in aqueous solution by imine bonding, in the presence or absence of TP5. These hydrogels display a porous structure, outstanding rheological properties and excellent pH-sensitive swelling performance. Analyses showed that TP5 is partly attached to the hydrogel network by imine bonding, together with free TP5 molecules adsorbed by physical forces into the hydrogel pore walls. *In vitro* release showed a burst release in the first 24 h, followed by a slower release to reach a plateau up to 168 h. The maximum release rate depends on various factors such as drug content, drug loading and release conditions. Data show that only free TP5 is released under *in vitro* conditions. Covalently attached TP5 is not released due to the stability of imine bonds at pH 7.4. Density functional theory study allowed to better understand the chemical combination between the hydrogel's components and the drug. All these findings suggest that *in situ* gelation of water soluble CMCS with a 3D dynamer is a means of choice to design efficient release systems of hydrophilic drugs, in particular those containing amino groups which can be covalently attached to the hydrogel network. Last but not least, this study offers a simple and environmentally friendly strategy to prepare bioactive and biodegradable hydrogels for drug delivery systems.

Supporting materials

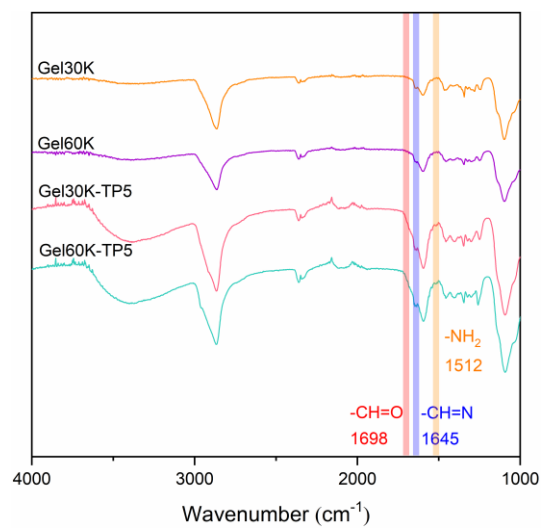


Figure S4.1 FT-IR spectra of freeze-dried Gel30K, Gel25K, Gel30K-TP5, and Gel25K-TP5.

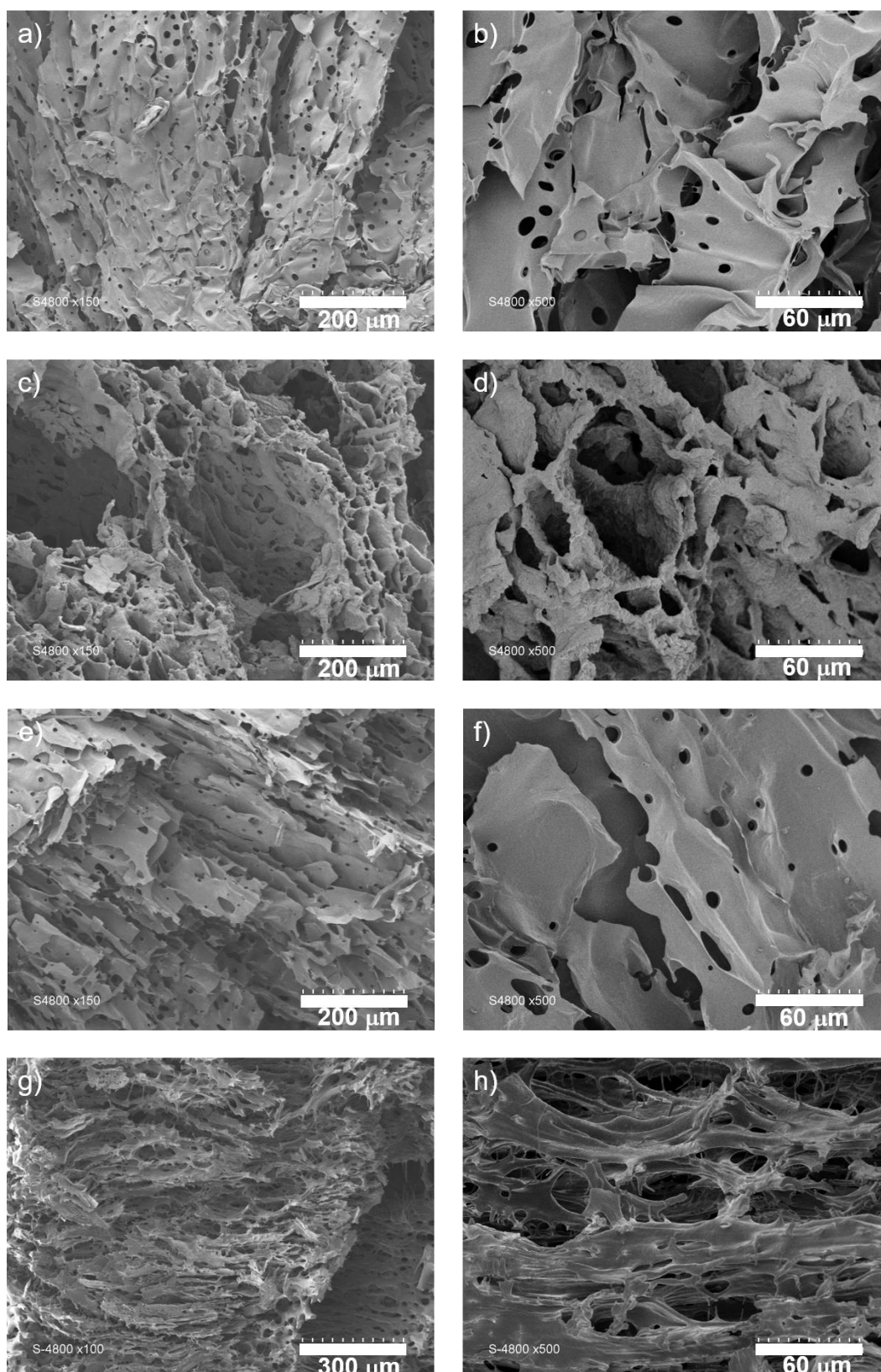


Figure S4.2 SEM images of freeze-dried CMCS (a, b) Dy (c,d), CMCS-TP5 (e,f) and Dy-TP5 (g, h). The samples CMCS-TP5 and Dy-TP5 are obtained by mixing CMCS and TP5 or Dy and TP5 in water with a molar ratio of 1/1, and freeze dried after 24 h at 37°C.

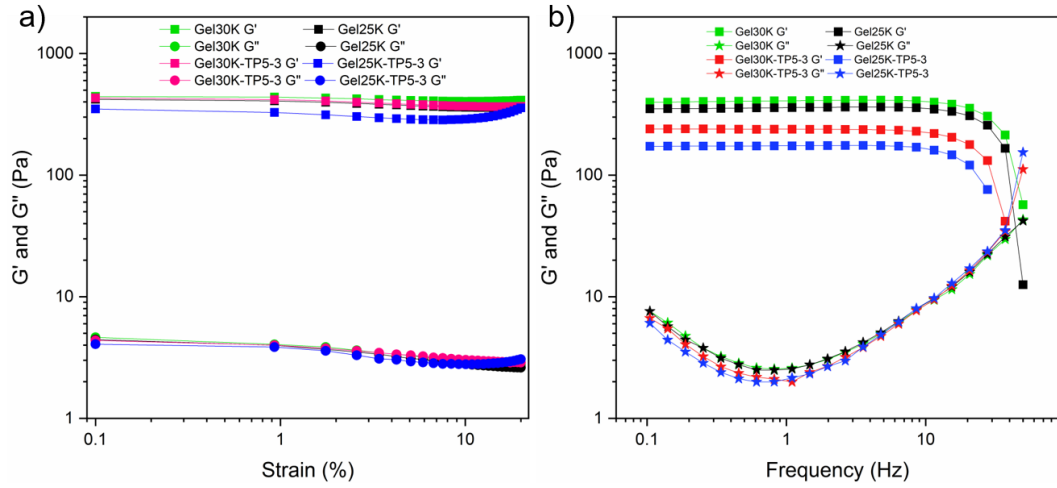


Figure S4.3 Storage modulus (G') and loss modulus (G'') changes of Gel30K, Gel30K-TP5-3, Gel25K, and Gel25K-TP5-3 as a function of strain a); or as a function of frequency b) at 25 °C.

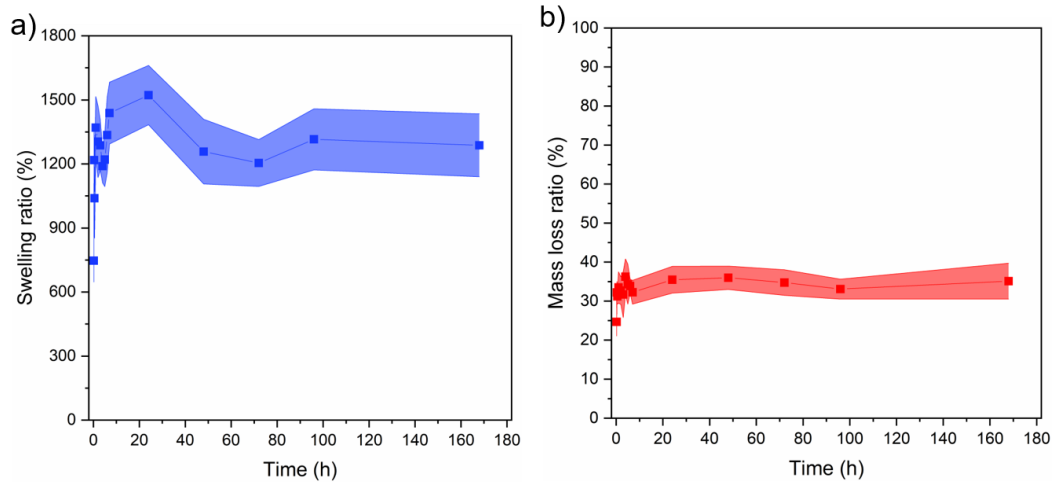
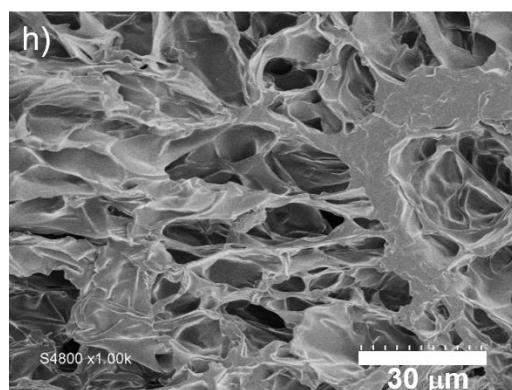
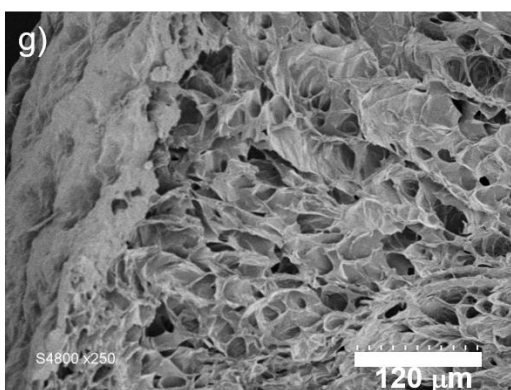
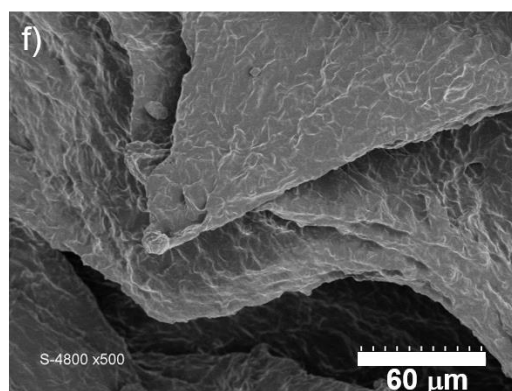
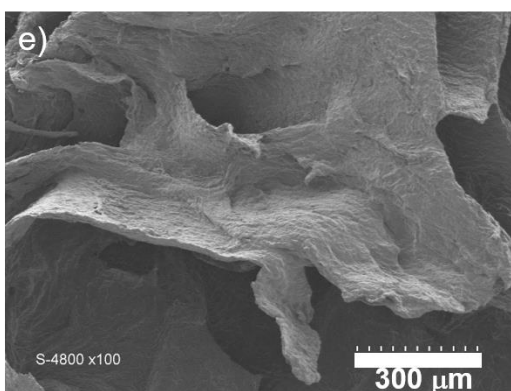
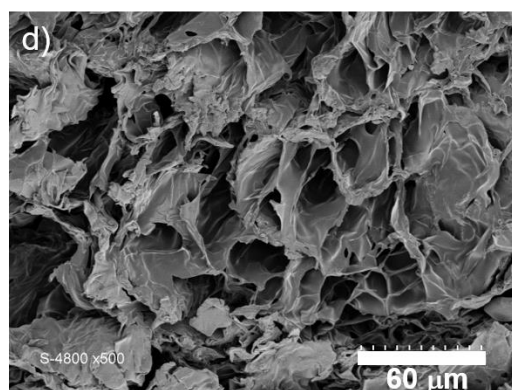
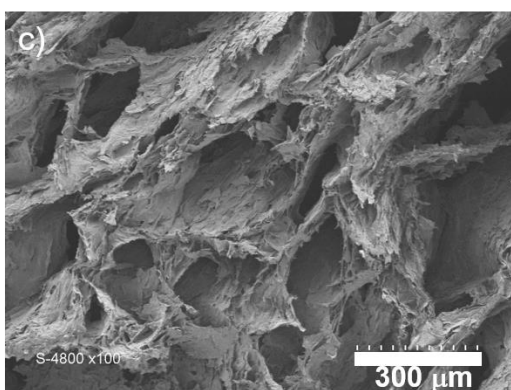
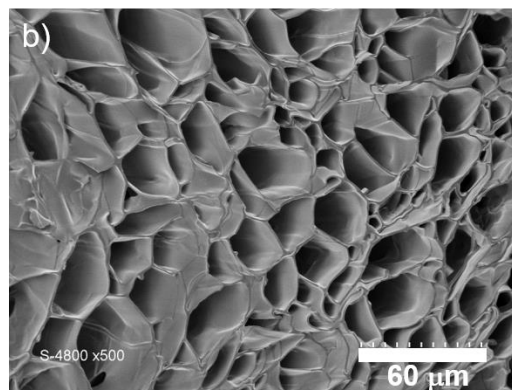
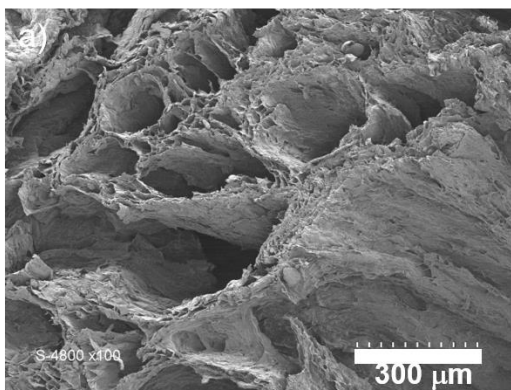


Figure S4.4 a) Swelling ratio, and b) mass loss ratio of Gel80K versus immersion time in pH 7.4 PBS at 37 °C. Values were expressed as mean \pm SD for $n = 3$, and presented by error band.



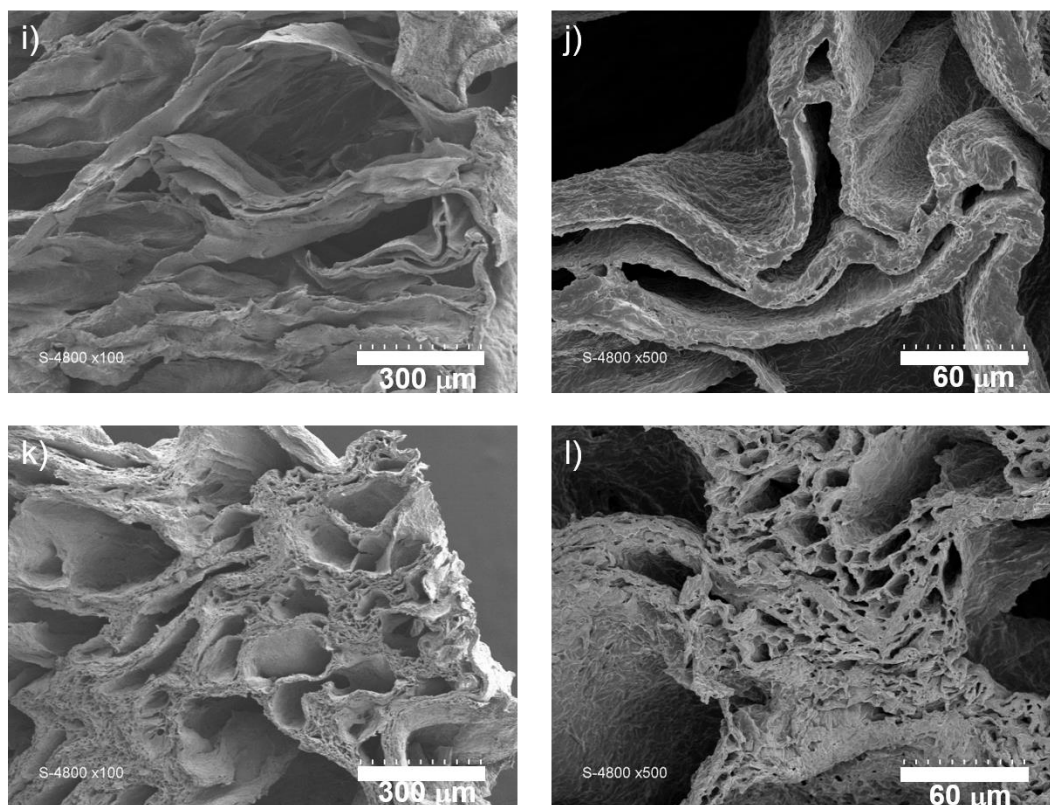


Figure S4.5 SEM images of TP5-loaded hydrogels: a, b) Gel80K-TP5-0.1; c, d) Gel80K-TP5-3; e, f) Gel80K-TP5-9; g, h) Gel80K-TP5-3B; i, j) Gel30KTP5-3; and k, l) Gel25K-TP5-3.

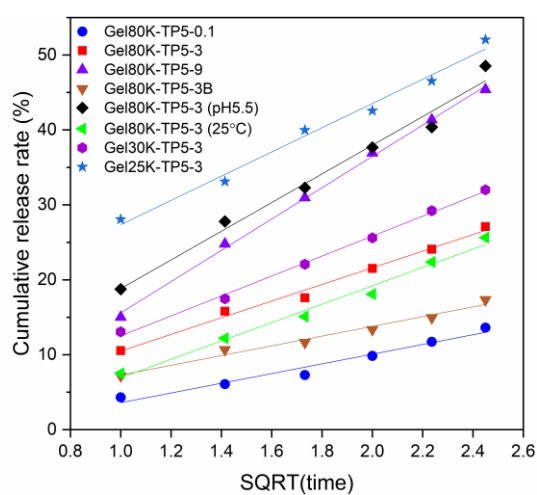


Figure S4.6 Graphical representation of the model fitting on the TP5 release data using Higuchi model.

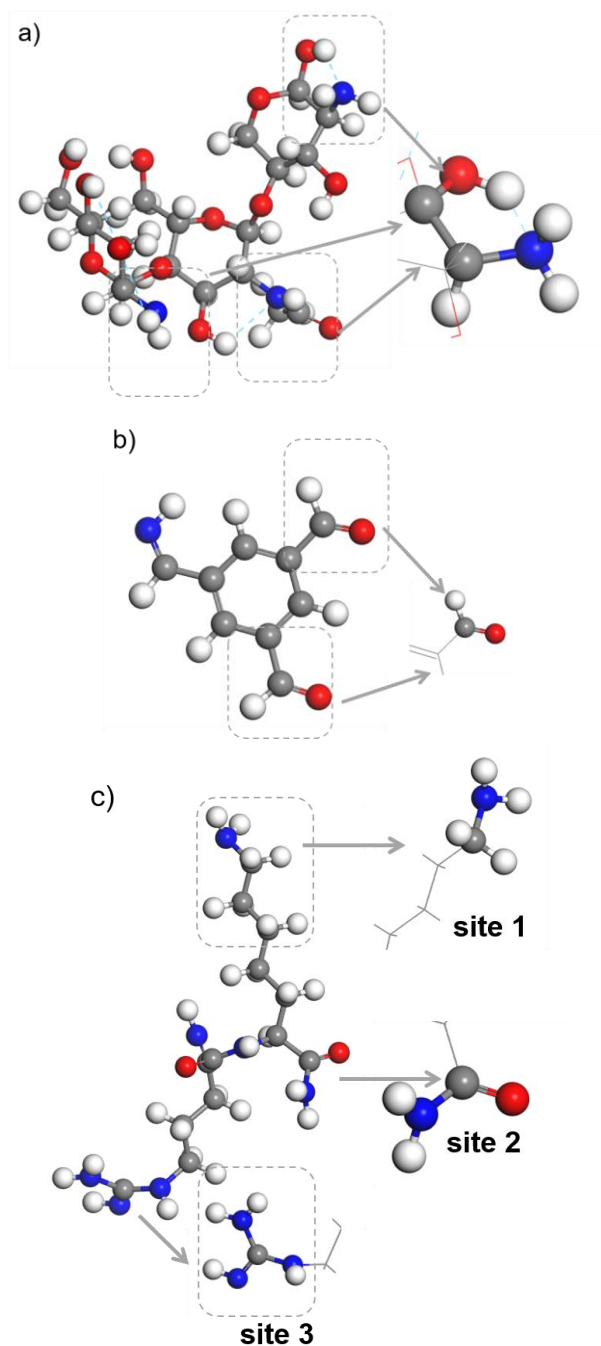


Figure S4.7 Typical geometries of a) CMCS; b) Dy, and c) TP5. TP5(1), TP5(2), and TP5(3) stand for site 1, site 2, and site 3 in TP5, respectively.

References

- [1] G. Goldstein, T.K. Audhya, Thymopoietin to thymopentin: experimental studies, *Surv. Immunol. Res.* 4(1) (1985) 1.
- [2] D.H. Schlesinger, G. Goldstein, The amino acid sequence of thymopoietin

II, Cell 5(4) (1975) 361-365.

[3] G. Goldstein, M.P. Scheid, E.A. Boyse, D.H. Schlesinger, J. Van Wauwe, A synthetic pentapeptide with biological activity characteristic of the thymic hormone thymopoietin, Science 204(4399) (1979) 1309-1310.

[4] S. Lin, B. Cai, G. Quan, T. Peng, G. Yao, C. Zhu, Q. Wu, H. Ran, X. Pan, C. Wu, Novel strategy for immunomodulation: Dissolving microneedle array encapsulating thymopentin fabricated by modified two-step molding technology, Eur. J. Pharm. Biopharm. 122 (2018) 104-112.

[5] T. Zhang, X. Qin, X. Cao, W. Li, T. Gong, Z. Zhang, Thymopentin-loaded phospholipid-based phase separation gel with long-lasting immunomodulatory effects: in vitro and in vivo studies, Acta Pharmacologica Sinica 40(4) (2019) 514-521.

[6] B. Bodey, B. Bodey Jr, S.E. Siegel, H.E. Kaiser, Review of thymic hormones in cancer diagnosis and treatment, Int. J. Immunopharmacol 22(4) (2000) 261-273.

[7] B. Kantharia, N. Goulding, N. Hall, J. Davies, P. Maddison, P. Bacon, M. Farr, J. Wojtulewski, K. Englehart, S. Liyanage, Thymopentin (TP-5) in the treatment of rheumatoid arthritis, Rheumatology 28(2) (1989) 118-123.

[8] Y. Wang, X. Ke, J.S. Khara, P. Bahety, S. Liu, S.V. Seow, Y. Yang, P.L.R. Ee, Synthetic modifications of the immunomodulating peptide thymopentin to confer anti-mycobacterial activity, Biomaterials 35(9) (2014) 3102-3109.

[9] X. Cao, Y. Li, Y. Guo, F. Cao, Thymopentin improves cardiac function in older patients with chronic heart failure, Anatolian journal of cardiology 17(1) (2017) 24.

[10] R. Colle, T. Ceschia, A. Colatutto, F. Biffoni, Use of thymopentin in autoimmune hemolytic anemia due to chronic lymphocytic leukemia, Current therapeutic research 44(6) (1988) 1045-1049.

[11] M. Zhu, W. Wan, H. Li, J. Wang, G. Chen, X. Ke, Thymopentin enhances the generation of T-cell lineage derived from human embryonic stem cells in

vitro, Exp. Cell Res. 331(2) (2015) 387-398.

[12] M.S. Kondratyev, S.M. Lunin, A.V. Kabanov, A.A. Samchenko, V.M. Komarov, E.E. Fesenko, E.G. Novoselova, Structural and dynamic properties of thymopoietin mimetics, J. Biomol. Struct. Dyn. 32(11) (2014) 1793-1801.

[13] Y. Wang, Y. Cao, Y. Meng, Z. You, X. Liu, Z. Liu, The novel role of thymopentin in induction of maturation of bone marrow dendritic cells (BMDCs), Int. Immunopharmacol. 21(2) (2014) 255-260.

[14] J.P. Tischio, J.E. Patrick, H.S. Weintraub, M. Chasin, G. Goldstein, Short in vitro half - life of thymopoietin 32 - 36 pentapeptide in human plasma, Int. J. Pept. Protein Res. 14(5) (1979) 479-484.

[15] X. Jin, Y. Xu, J. Shen, Q. Ping, Z. Su, W. You, Chitosan–glutathione conjugate-coated poly (butyl cyanoacrylate) nanoparticles: promising carriers for oral thymopentin delivery, Carbohydr. Polym. 86(1) (2011) 51-57.

[16] Y. Xu, G. Li, W. Zhuang, H. Yu, Y. Hu, Y. Wang, Micelles prepared from poly (N-isopropylacrylamide-co-tetraphenylethene acrylate)-b-poly [oligo (ethylene glycol) methacrylate] double hydrophilic block copolymer as hydrophilic drug carrier, Journal of Materials Chemistry B 6(45) (2018) 7495-7502.

[17] J. Zuo, T. Gong, X. Sun, Y. Huang, Q. Peng, Z. Zhang, Multivesicular liposomes for the sustained release of thymopentin: stability, pharmacokinetics and pharmacodynamics, Die Pharmazie-An International Journal of Pharmaceutical Sciences 67(6) (2012) 507-512.

[18] Y. Zhang, X. Wu, Y. Han, F. Mo, Y. Duan, S. Li, Novel thymopentin release systems prepared from bioresorbable PLA–PEG–PLA hydrogels, Int. J. Pharm. 386(1-2) (2010) 15-22.

[19] Y. Hu, Y. Liu, X. Qi, P. Liu, Z. Fan, S. Li, Novel bioresorbable hydrogels prepared from chitosan - graft - polylactide copolymers, Polym. Int. 61(1) (2012) 74-81.

[20] Y. Yin, D. Chen, M. Qiao, Z. Lu, H. Hu, Preparation and evaluation of lectin-conjugated PLGA nanoparticles for oral delivery of thymopentin, J. Controlled

Release 116(3) (2006) 337-345.

[21] J. Li, D. Mooney, Designing hydrogels for controlled drug delivery, *Nature Reviews Materials* 1(12) (2016) 1-17.

[22] J. Zhao, X. Zhao, B. Guo, P.X. Ma, Multifunctional interpenetrating polymer network hydrogels based on methacrylated alginate for the delivery of small molecule drugs and sustained release of protein, *Biomacromolecules* 15(9) (2014) 3246-3252.

[23] S. Peers, A. Montembault, C. Ladavière, Chitosan hydrogels for sustained drug delivery, *J. Controlled Release* 326 (2020) 150-163.

[24] X. Yang, G. Liu, L. Peng, J. Guo, L. Tao, J. Yuan, C. Chang, Y. Wei, L. Zhang, Highly efficient self - healable and dual responsive cellulose - based hydrogels for controlled release and 3D cell culture, *Adv. Funct. Mater.* 27(40) (2017) 1703174.

[25] J. Su, B. Hu, W.L. Lowe Jr, D.B. Kaufman, P.B. Messersmith, Anti-inflammatory peptide-functionalized hydrogels for insulin-secreting cell encapsulation, *Biomaterials* 31(2) (2010) 308-314.

[26] J.M. Reichert, Trends in development and approval times for new therapeutics in the United States, *Nature Reviews Drug Discovery* 2(9) (2003) 695-702.

[27] F. Su, J. Wang, S. Zhu, S. Liu, X. Yu, S. Li, Synthesis and characterization of novel carboxymethyl chitosan grafted polylactide hydrogels for controlled drug delivery, *Polym. Adv. Technol.* 26(8) (2015) 924-931.

[28] S.T.K. Raja, T. Prakash, A. Gnanamani, Redox responsive albumin autogenic nanoparticles for the delivery of cancer drugs, *Colloids Surf. B. Biointerfaces* 152 (2017) 393-405.

[29] Y. Lin, H. Liang, C. Chung, M. Chen, H. Sung, Physically crosslinked alginate/N, O-carboxymethyl chitosan hydrogels with calcium for oral delivery of protein drugs, *Biomaterials* 26(14) (2005) 2105-2113.

[30] A. Lu, E. Petit, S. Li, Y. Wang, F. Su, S. Monge, Novel thermo-responsive

micelles prepared from amphiphilic hydroxypropyl methyl cellulose-block-JEFFAMINE copolymers, *Int. J. Biol. Macromol.* 135 (2019) 38-45.

[31] Y. Zhang, C. Pham, R. Yu, E. Petit, S. Li, M. Barboiu, Dynamic hydrogels based on double imine connections and application for delivery of fluorouracil, *Frontiers in Chemistry* 8 (2020) 739.

[32] R. Yu, Y. Zhang, M. Barboiu, M. Maumus, D. Noël, C. Jorgensen, S. Li, Biobased pH-responsive and self-healing hydrogels prepared from O-carboxymethyl chitosan and a 3-dimensional dynamer as cartilage engineering scaffold, *Carbohydr. Polym.* 244 (2020) 116471.

[33] R. Yu, L. Cornette de Saint-Cyr, L. Soussan, M. Barboiu, S. Li, Anti-bacterial dynamic hydrogels prepared from O-carboxymethyl chitosan by dual imine bond crosslinking for biomedical applications, *Int. J. Biol. Macromol.* 167 (2020) 1146-1155.

[34] S. Dash, P.N. Murthy, L. Nath, P. Chowdhury, Kinetic modeling on drug release from controlled drug delivery systems, *Acta Pol. Pharm.* 67(3) (2010) 217-223.

[35] A.M. Craciun, L.M. Tartau, M. Pinteala, L. Marin, Nitrosalicyl-imine-chitosan hydrogels based drug delivery systems for long term sustained release in local therapy, *Journal of Colloid and Interface Science* 536 (2019) 196-207.

[36] B. Delley, From molecules to solids with the DMol 3 approach, *The Journal of chemical physics* 113(18) (2000) 7756-7764.

[37] S. Grimme, J. Antony, S. Ehrlich, H. Krieg, A consistent and accurate ab initio parametrization of density functional dispersion correction (DFT-D) for the 94 elements H-Pu, *The Journal of chemical physics* 132(15) (2010) 154104.

[38] A. Klamt, G. Schüürmann, COSMO: a new approach to dielectric screening in solvents with explicit expressions for the screening energy and its gradient, *Journal of the Chemical Society, Perkin Transactions 2* (5) (1993) 799-805.

[39] N. Govind, M. Petersen, G. Fitzgerald, D. King-Smith, J. Andzelm, A generalized synchronous transit method for transition state location,

Computational materials science 28(2) (2003) 250-258.

[40] H.R. Rizvi, M.J. Khattak, A.A. Gallo, Rheological and mechanistic characteristics of Bone Glue modified asphalt binders, *Construction Building Materials* 88 (2015) 64-73.

[41] R. Singh, K. Rao, A. Anjaneyulu, G. Patil, Moisture sorption properties of smoked chicken sausages from spent hen meat, *Food Res. Int.* 34(2-3) (2001) 143-148.

[42] P. Xue, N. Sun, Y. Li, S. Cheng, S. Lin, Targeted regulation of hygroscopicity of soybean antioxidant pentapeptide powder by zinc ions binding to the moisture absorption sites, *Food Chem.* 242 (2018) 83-90.

[43] S. Li, A. El Ghzaoui, E. Dewinck, Rheology and drug release properties of bioresorbable hydrogels prepared from polylactide/poly (ethylene glycol) block copolymers, *Macromol. Symp.*, Wiley Online Library, 2005, pp. 23-36.

[44] N. Bhattarai, J. Gunn, M. Zhang, Chitosan-based hydrogels for controlled, localized drug delivery, *Adv. Drug Del. Rev.* 62(1) (2010) 83-99.

[45] S.V. Madihally, H.W. Matthew, Porous chitosan scaffolds for tissue engineering, *Biomaterials* 20(12) (1999) 1133-1142.

[46] Y. Liang, X. Zhao, T. Hu, Y. Han, B. Guo, Mussel-inspired, antibacterial, conductive, antioxidant, injectable composite hydrogel wound dressing to promote the regeneration of infected skin, *Journal of colloid interface science* 556 (2019) 514-528.

[47] X. Lv, W. Zhang, Y. Liu, Y. Zhao, J. Zhang, M. Hou, Hygroscopicity modulation of hydrogels based on carboxymethyl chitosan/Alginate polyelectrolyte complexes and its application as pH-sensitive delivery system, *Carbohydr. Polym.* 198 (2018) 86-93.

[48] P. Gupta, K. Vermani, S. Garg, Hydrogels: from controlled release to pH-responsive drug delivery, *Drug Discovery Today* 7(10) (2002) 569-579.

[49] M.G. Bernengo, A. Appino, M. Bertero, M. Novelli, M.T. Fierro, G.C. Doveil, F. Lisa, Thymopentin in Sezary syndrome, *JNCI: Journal of the National Cancer*

Institute 84(17) (1992) 1341-1346.

[50] A. Patruno, P. Tosco, E. Borretto, S. Franceschelli, P. Amerio, M. Pesce, S. Guglielmo, P. Campiglia, M.G. Bernengo, R. Fruttero, Thymopentin down-regulates both activity and expression of iNOS in blood cells of Sézary syndrome patients, *Nitric Oxide* 27(3) (2012) 143-149.

[51] S. Zhao, M.M. Abu-Omar, Recyclable and malleable epoxy thermoset bearing aromatic imine bonds, *Macromolecules* 51(23) (2018) 9816-9824.

[52] J. Siepmann, N.A. Peppas, Higuchi equation: derivation, applications, use and misuse, *Int. J. Pharm.* 418(1) (2011) 6-12.

[53] S. Berski, L.Z. Ciunik, The mechanism of the formation of the hemiaminal and Schiff base from the benzaldehyde and triazole studied by means of the topological analysis of electron localisation function and catastrophe theory, *Mol. Phys.* 113(8) (2015) 765-781.

[54] K. Wajda-Hermanowicz, D. Pieniążczak, A. Zatajska, R. Wróbel, K. Drabent, Z. Ciunik, A study on the condensation reaction of 4-amino-3, 5-dimethyl-1, 2, 4-triazole with benzaldehydes: structure and spectroscopic properties of some new stable hemiaminals, *Molecules* 20(9) (2015) 17109-17131.

Conclusion

In this work, novel dynamic hydrogels based on O-carboxymethyl chitosan (O-CMCS) were synthesized via 'Schiff-base' reaction between O-CMCS and a dynamer (Dy) which was previously prepared via 'Schiff-base' reaction between Jeffamine and Benzene-1,3,5-tricarbaldehyde (BTA). The as-prepared dual imine bond hydrogels were characterized by using various methods, including NMR, FT-IR, SEM, rheological and swelling measurements, self-healing tests, etc. The effect of CMCS/Dy molar ratio, Jeffamine molar mass, and CMCS molar mass on the physico-chemical properties of hydrogels was investigated. The potential of these dynamic hydrogels to serve as cartilage engineering scaffold, antibacterial membrane, and drug delivery system for hydrophilic anti-cancer drugs was evaluated. The following conclusions can be drawn from this work:

- a) Dynamic hydrogels were successfully synthesized via dual imine bonding by Schiff-base reaction of O-carboxymethyl chitosan (CMCS) and a 3D dynamer (Dy) in aqueous solution under mild conditions. The latter was previously obtained by Schiff-base reaction between amine terminated Jeffamine as linker and benzene-1,3,5-tricarbaldehyde (BTA) as core center. The hydrogel Gel4-1 with D-glucosamine to dynamer molar ratio of 4:1 exhibits the shortest gelation time and the highest storage modulus, in agreement with optimal cross-linking or imine bond formation. In fact, gelation occurs by crosslinking via imine bond formation and is thus dependent on the ratio between amine groups of CMCS and aldehyde groups of Dy. With lower D-glucosamine/Dy ratios, there are less amine groups available for crosslinking, whereas higher D-glucosamine/Dy ratios also disfavor crosslinking due to lack of aldehydes.

Freeze-dried gels exhibit interconnected porous structures with more or less regular pore distribution. The swelling behavior of dried gels is highly

pH-dependent, which is related to the pK_a values of the carboxylic and amino groups of CMCS. Electrostatic attraction between negatively charged $-\text{COO}^-$ and positively charged $-\text{NH}_3^+$ groups at low pH results in shrinkage or low swelling of hydrogels. In contrast, electrostatic repulsion between negatively charged $-\text{COO}^-$ groups at alkaline pH leads to very high swelling. Substantial mass loss occurs during swelling of hydrogels due to the dissolution of unconnected species, especially Dy rings which are formed during reaction of BTA and Jeffamine and which may escape coupling with CMCS in the hydrogel preparation procedure.

Hydrogels present outstanding self-healing properties as evidenced by closure of split pieces and rheological studies with alternatively applied high and low oscillatory shear strains. Self-healing occurs autonomously for different pH-dependent states, being able to reshape or to regenerate a strong chemical hydrogel from various situations via reconstruction of reversible imine bond crosslinking, and migration of components or constituent exchanges.

Human mesenchymal stromal cells (MSCs) were encapsulated in Gel4-1 and cultured in proliferative medium at 37 °C. Excellent cell viability was obtained up to 7 days. Moreover, MSCs were homogeneously distributed in the whole hydrogel volume, indicating that the dynamic hydrogels are most promising as scaffold in cartilage engineering.

- b) CMCS based dynamic hydrogels (H500, H800, and H1900) with different molar masses of Jeffamine ($M_n = 500, 800, \text{ and } 1900$) were prepared by Schiff-base reaction under the same conditions mentioned above. The gelation is faster with Jeffamine of lower molar mass. In fact, reaction of BTA with low molar mass Jeffamine yields Dy with higher mobility, which results in faster crosslinking and gelation. In contrast, the storage modulus of hydrogels increases with the increase of Jeffamine molar mass. SEM images show that H1900 presents larger pore size as compared to H500

and H800 due to the higher molar mass of Jeffamine linker. Similar swelling and self-healing behaviors are observed for the three hydrogels with different Jeffamines. Interestingly, H1900 exhibits the highest mass loss during swelling in the whole pH range from 3 to 10. This finding seems to confirm that mass loss during swelling of hydrogels results from the dissolution of unconnected Dy rings as H1900 contains larger amount of Dy rings due to the higher molar mass of Jeffamine ED2003.

The antibacterial properties of H1900 membranes were evaluated by liquid and soft agar tests. Both tests confirmed the excellent antibacterial properties against *E. coli* (Gram-negative bacterium), suggesting the potential of dynamic hydrogels in applications as antibacterial materials.

- c) Three dynamic hydrogels (Gel80K, Gel30K, and Gel25K) with different molar masses of CMCS ($M_n = 80K, 30K, \text{ and } 25K$) were formulated via Schiff-base reaction under the same conditions. In situ encapsulation of thymopentin (TP5) was successfully realized during hydrogel preparation. Rheological results show that the storage modulus of the obtained hydrogels is dependent on the molar mass of CMCS and the TP5 content. Higher molar mass of CMCS leads to higher storage modulus because there are more amines along polymeric chains for crosslinking. In contrast, higher TP5 content leads to lower storage modulus because the amine groups of TP5 can react with the free aldehyde groups of Dy leading to decreased imine bonding between CMCS and Dy. Moreover, attachment of TP5 to the network does not contribute to the crosslinking because TP5 is a small molecule. Therefore, the crosslinking density decreases with increase of TP5 content, and consequently the modulus of hydrogels decreases.

In vitro release showed a burst release in the first hours, followed by a slower release to reach a plateau. The maximum release rate depends on various factors such as drug content, drug loading and release conditions.

Data show that only free TP5 is released under *in vitro* conditions. Covalently attached TP5 is not released due to the stability of imine bonds at pH 7.4. Density functional theory study confirmed the covalent attachment of TP5 to the hydrogel network by imine bonding, and allowed to better understand the chemical combination between the hydrogel's components and the drug. All these findings suggest that *in situ* gelation of water soluble CMCS with a 3D dyanamer is a means of choice to design efficient release systems of hydrophilic drugs, in particular those containing amino groups which can be covalently attached to the hydrogel network. Last but not least, this study offers a simple and environmentally friendly strategy to prepare bioactive and biodegradable hydrogels for drug delivery systems.

Publications

- [1] **R. Yu**, Y. Zhang, M. Barboiu, M. Maumus, D. Noël, C. Jorgensen, S. Li, Biobased pH-responsive and self-healing hydrogels prepared from O-carboxymethyl chitosan and a 3-dimensional dynamer as cartilage engineering scaffold, *Carbohydr. Polym.* 244 (2020) 116471.
- [2] **R. Yu**, L. Cornette de Saint-Cyr, L. Soussan, M. Barboiu, S. Li, Anti-bacterial dynamic hydrogels prepared from O-carboxymethyl chitosan by dual imine bond crosslinking for biomedical applications, *Int. J. Biol. Macromol.* 167 (2020) 1146-1155.
- [3] **R. Yu**, E. Petit, M. Barboiu, S. Li, W. Sun, C. Chen, Biobased dynamic hydrogels by triple imine bonding for controlled release of thymopentin, *Journal of Controlled Release*, Submitted.
- [4] Y. Zhang, C. Pham, **R. Yu**, E. Petit, S. Li, M. Barboiu, Dynamic hydrogels based on double imine connections and application for delivery of fluorouracil, *Frontiers in Chemistry* 8 (2020) 739.

Communications

- [1] **R. Yu**, M. Barboiu, S. Li, Synthesis and characterization of dynamic CMCS-based hydrogel. **Oral Presentation** in session of frontiers in supramolecular materials, the 47th World Chemistry Congress of IUPAC 2019 organized by International Union of Pure and Applied Chemistry, 7-12 July 2019, Paris, France.
- [2] **R. Yu**, M. Barboiu, S. Li, Dynamic hydrogels as multivalent matrices for controlled drug delivery and tissue engineering. **Oral Presentation**, *the 6th edition of the Mediterranean young researchers' days (JMJC 2018)*, 18-19 October 2018, Marseille, France.
- [3] **R. Yu**, M. Barboiu, S. Li, Dynamic hydrogels as multivalent matrices for controlled drug delivery and tissue engineering. **Poster Presentation**, Journées 2018 de l'ED SCB ENSCM Amphithéâtre Mousseron, Montpellier, France.

Acknowledgements

Time flies and I have been studying in France for more than three years. I am now writing this final part with cheerful and complicated mood. Upon the completion of this thesis, I would like to convey my appreciation to those who have offered me guidance, encouragements and support during the course of my study.

First and foremost, my heartiest thanks flow to my supervisor Prof. Suming Li for his helpful guidance, valuable suggestions and constant encouragement both in my study and in my life. His profound insight and accurateness about my research taught me so much that they are engraved on my heart. He provided me with beneficial help and offered me precious comments during the whole process of my writing, without which the paper would not be what it is now. In addition, his rigorous research attitude, rigorous work ethic and efficient way of working encouraged me to actively engage in the challenging yet fascinating field of academic research.

I would like to express my great gratitude to my co-supervisor, Prof. Mihail Barboiu who have given me supervision and support for experiment implementations, the advices to revise the research articles. I have learned a lot after each discussion with him. Moreover, his research attitude and ideas also inspired me.

I would like to extend my deep gratefulness to my friends in France, thanks for their selfless help and companionship. Many thanks would go to my beloved parents for their loving considerations and great confidence in me all through these years. For so many years, they have always been supporting me and respecting me. I thank my girlfriend for her constant understanding, support and love for me. Their love and care are the greatest fortune of my life.

I also thank China Scholarship Council (CSC) for offering me the scholarship to study in Montpellier.

Last but not least, I would like to thank myself for never giving up through thick and thin and always moving forward.

26th, January, 2021

Montpellier, France

Nouveaux hydrogels à liaison imine double préparés à partir d'O-carboxyméthyl chitosane et de Jeffamine par chimie covalente dynamique pour applications biomédicales

Une série d'hydrogels dynamiques ont été synthétisés à partir de O-carboxyméthyl chitosane (CMCS) et de Jeffamine avec le benzène-1,3,5-tricarbaldéhyde (BTA) comme réticulant. Le BTA réagit d'abord avec la Jeffamine pour donner un dynamère (Dy) hydrosoluble, suivi de mélange avec le CMCS dans l'eau pour donner un hydrogel dynamique, tous deux basés sur une réaction de base de Schiff. Les hydrogels obtenus ont été caractérisés par la RMN, la FT-IR, la MEB et la rhéologie. Les effets du rapport molaire CMCS/Dy, de la masse molaire de la Jeffamine et du CMCS sur les propriétés physico-chimiques des hydrogels ont été étudiés. Les hydrogels présentent d'excellentes propriétés rhéologique et d'auto-guérison, et un comportement de gonflement dépendant du pH. Les cellules souches mésenchymateuses humaines chargées dans l'hydrogel montrent une excellente viabilité cellulaire, démontrant le grand potentiel de ces hydrogels dans l'ingénierie du cartilage. Les membranes préparées à partir d'hydrogels présentent une très bonne activité antibactérienne contre *E. coli* (bactérie à Gram négatif). Un immunostimulant hydrophile, la thymopentine (TP5) a été chargé dans l'hydrogel pendant la gélification. Les résultats montrent que la vitesse de libération dépend de divers facteurs tels que le contenu de la TP5, les conditions d'encapsulation et de libération. La théorie fonctionnelle de la densité a permis de mieux comprendre la combinaison chimique entre les composants de l'hydrogel et la TP5. Cette étude propose une nouvelle stratégie pour préparer des hydrogels dynamiques bioactifs pour diverses applications biomédicales.

Mots-clés: Chimie covalente dynamique ; Réaction de base de Schiff ; Carboxyméthyl chitosane ; Hydrogel ; Jeffamine ; Auto-guérison ; Ingénierie du cartilage ; Antibactérien ; Thymopentine ; Délivrance de principes actifs.

Novel dual imine bonding hydrogels prepared from O-carboxymethyl chitosan and Jeffamine by dynamic covalent chemistry for biomedical applications

A series of dynamic hydrogels were synthesized from O-carboxymethyl chitosan (CMCS) and Jeffamine using benzene-1,3,5-tricarbaldehyde (BTA) as crosslinker. BTA first reacted with Jeffamine to yield a water soluble dynamer (Dy), followed by mixing with CMCS in water to yield a dynamic hydrogel, both based on Schiff-base reaction. The as-prepared hydrogels were characterized by NMR, FT-IR, SEM and rheology. The effects of CMCS/Dy molar ratio, Jeffamine molar mass, and CMCS molar mass on the physico-chemical properties of hydrogels were investigated. The hydrogels exhibit outstanding rheological and self-healing properties, and pH dependent swelling behavior. Human mesenchymal stem cells loaded inside hydrogels showed excellent cell viability, demonstrating the great potential of these hydrogels in cartilage engineering. Membranes prepared from hydrogels exhibited high antibacterial activity against *E. coli* (Gram-negative bacterium). A hydrophilic immunostimulant, thymopentin (TP5) was loaded in hydrogels during gelation. Drug release data showed that the release rate depends on various factors such as drug content, drug loading and release conditions. Density functional theory allowed to better understand the chemical combination between the hydrogel's components and the drug. This study offers a new strategy to prepare bioactive dynamic hydrogels for various biomedical applications.

Keywords: Dynamic covalent chemistry; Schiff-base reaction; Carboxymethyl chitosan; Hydrogel; Jeffamine; Self-healing; Cartilage engineering; Antibacterial; Thymopentin; Drug delivery.